Characterisation of the Virulence and Determinants of Virulence of *C. Neoformans* var.*grubii* Genotypes from HIV Infected and Uninfected Patients in Vietnam

Thesis

CHARACTERIZATION OF *C. NEOFORMANS* VAR. *GRUBII* ISOLATES FROM HIV-INFECTED AND HIV-UNINFECTED PATIENTS FROM VIETNAM

by

Lam Tuan Thanh

A thesis submitted to the Open University U.K

For the degree of Doctor of Philosophy in the field of Life Sciences

Oxford University Clinical Research Unit

Hospital for Tropical Diseases

Ho Chi Minh City, Viet Nam

Mar, 2018

Abstract

C. neoformans var. *grubii* is the main cause of life-threatening cryptococcal meningitis worldwide, especially in individuals with underlying immunosuppressive conditions such as HIV infection. In contrast to its sister species *C. gattii* which is now considered a primary human pathogen, *C. neoformans* var. *grubii* does not commonly infect apparently healthy individuals. However, it is now clear that *C. neoformans* var. *grubii* infection also occurs in apparently healthy individuals in Vietnam, China and elsewhere in Southeast/East Asia. This could be explained by two possibilities: (i) disease in the immunocompetent is associated with strains with increased pathogenic potential, or (ii) there are unknown immune defect(s) that confers increased susceptibility in affected individuals. This thesis investigates the former hypothesis by systematically assessing and comparing genetic composition, virulence-associated phenotypes and transcriptomes of *C. neoformans* var. *grubii* isolates from Vietnam from HIV-infected and HIV-uninfected patients.

MLST-based interrogation of population structure of clinical *C. neoformans* var. *grubii* isolates from Vietnam and Laos reveal that the population from Vietnam is unique and intermediate in composition between that from Thailand/Laos to the West/Southwest and China to the East/Northeast. Almost all disease in HIV-uninfected patients is associated with the MLST ST5 lineage. Comparison of *in vitro* and *in vivo* (mouse and macrophage models) virulence-associated phenotypes reveals lineage-specific differences. Specifically, ST5 strains appear with more phenotypic variability, increased intracellular replication inside

macrophages, and induction of more robust immune responses but apparent decreased virulence in mice. RNAseq profiling under log-phase growth highlights genotype-specific differential expression of key processes which may contribute to virulence. My data suggest that higher ST5 prevalence in apparently immunocompetent patients in Vietnam are not necessarily associated with the ability to cause more severe in-host damage and mortality, but likely represent better adaptation to the innate immune system and establishing infection in immunocompetent hosts.

Co-authorship

The body of work presented in this thesis were primarily my own. However, parts of the results were obtained with assistance from my colleagues from the CNS/HIV group (OUCRU, Vietnam) and my international collaborators. Detailed authorship and acknowledgement is as follow:

Data Chapter 1:

- Clinical isolates from Vietnam were originated from 2 major clinical trials: the BK trial of combination antifungal therapy for HIV-infected patients with cryptococcal meningitis which recruited between 2004 and 2011 (PI: Prof. Jeremy Day from OUCRU, Vietnam) and the BMD study, a prospective, descriptive study of HIV-uninfected patients with central nervous system infections enrolled between 1998 and 2009 (PI: Dr. Tran Thi Hong Chau from OUCRU, Vietnam). Initial MLST typing of these isolates was performed by Ms. Hoang Nha Thu and Ms. Duong Van Anh (CNS/HIV group, OUCRU, Vietnam); I performed MLST of additional strains and data clean up along with my colleague Mr. Phan Hai Trieu (CNS/HIV group, OUCRU, Vietnam).
- Clinical isolates from Laos were from cryptococcosis patients consecutively admitted to Mahosot and associated hospitals in Vientiane, Laos PDR between 2003 and 2015 (PI: Dr. David Dance and Dr. Sayaphet Rattanavong from LOWRU, Laos). Dr. David

Dance and Dr. Sayaphet Rattanavong provided us with the isolates and corresponding patient's information for further characterization. MLST typing for these isolates were performed by Ms. Nguyen Mai Trinh and Ms. Cherelle Dacon from the CNS/HIV group (OUCRU, Vietnam) under my direction. I performed all analyses of sequence data.

Data Chapter 2:

- I set up and performed the phenotyping assays for the selected *C. neoformans* isolates and was assisted by Ms. Nguyen Mai Trinh (Research Assistant, CNS/HIV group, OUCRU, Vietnam).
- Mr. Charles Giamberardino (Duke University, USA) coordinated the extra cytokine profiling and histopathology works after I left the USA. Raw cytokine profiling data for was colelcted by Dr. Gregory Sempowski (Duke University, USA) which I used for downstream analysis of immune response. Dr. Yohannes Asfaw (Duke University, USA) performed the blinded histopathology scoring from paraffin-embedded lung specimens.

Data Chapter 4:

- Log-phase growth experiments and total RNA extraction from freshly grown yeasts were conducted by me, Mr. Phan Hai Trieu and Ms. Nguyen Mai Trinh (CNS/HIV group, OUCRU, Vietnam).

- RNAseq library preparation and Hiseq sequencing were performed commercially by Macrogen Inc.
- Raw RNAseq reads processing and cleaning were performed and generated by Dr. Philip Ashton (OUCRU, Vietnam). Dr. Philip Ashton provided the count matrices that I used for differential gene expression analysis and downstream interpretation of results.

Acknowledgements

Embarking on this PhD, to me, was a one-of-a-kind (academic) adventure that was full of unexpected twists, unprecedented frustration, sleepless nights and weird dreams (one of which was the one in which I running away from my supervisor who was merrily throwing dead mice at me) BUT was altogether a rewarding experience that brought me a step closer to the world of science and research. Equally important are the friends and colleagues I have had the pleasure of knowing and working with over the years. They and the memories I shared with them would be the treasures that I forever cherish.

Let me also take this opportunity to express my sincere appreciation to Professor. Jeremy Day for giving me a chance to participate in this project. As a mentor, he was considerate and was always there to listen, to support and to advise me on various aspects of the PhD project. I appreciate all the freedom and the insights he provided me to develop myself as an independent scientist. As a friend, he was always willing to crack a joke or two and was equally ready for a beer or two after work, thus making the PhD a more enjoyable journey. His enthusiasm in research surely gave me the inspiration to further my future career in science.

I also wish to thank Professor. John Perfect and his research team from Duke University, North Carolina, USA for accommodating me and for providing me with research guidance during the time I worked in the States. Professor John Perfect, together with Dena Toffaletti and Jennifer Tenor – his senior post-docs, provided invaluable support to a major part of my

project. Their expertise and insights were undoubtedly helpful to anyone who had the pleasure of working with and learning from them.

Next, I would also like to send my gratitude to the following individuals for their help with various aspects of the project. I would like to thank Professor Thomas Kozel (University of Nevada, Reno, USA) and Professor Arturo Casadevall (John Hopkins School of Medicine, USA) for providing the F12D2 and 18B7 monoclonal antibodies for the *in vitro* macrophage experiments. Many thanks to Mr. Charles Giamberardino (Duke University, USA) for coordinating the extra cytokine profiling and histopathology works after I left the USA. Also, I thank Dr. Yohannes Asfaw (Duke University, USA) for helping with the histopathology scoring and Dr. Gregory Sempowski (Duke University, USA) for the cytokine profiling work. My thanks to Dr. Philip Ashton (CNS/HIV, OUCRU, Vietnam) for advice and guidance on Bioinformatics and for restructuring my MLST manuscript. My acknowledgement to Dr. David Dance and Dr. Sayaphet Rattanavong (LOWRU, Laos) for providing the clinical *C. neoformans* var. *grubii* from Laos for MLST analyses. I am grateful to Ms. Nguyen Thi Mai Trinh (CNS/HIV, Vietnam) and Ms. Cherelle Dacon (University of Oxford, UK) for their help on extra phenotyping/genotyping works for the MLST chapter. Next, my appreciation to Ms. Le Thi Phuong Thao (Biostatistics, OUCRU, Vietnam) for the refreshment on statistics and the patience she took to explain basic stats to me. Last but not least, I would like to give my thanks and appreciation to members of the CNS/HIV group (OUCRU, Vietnam) and other members of OUCRU, Vietnam for all the good time and the endless fun. Justin - the beers and

sausages was a big help and encouragement whenever my whole week of experiment came to a dead end. Yours friendship and advice (good and bad) made my PhD endeavor a more pleasant one. Van Anh, Thu and Trieu – the road trips and retreats were great memories. We should do it more often!

Finally, I would like to acknowledge and parents and family for all the unconditional love and support for me. Without their many sacrifices I would not have been able to have a chance at a better future, for which I am forever in debt.

Abbreviations

&	And
µg	Microgram
µM	Micromole
µL	Microliter
7GFF	Solophenyl flavine
AF-542	Alexa-Fluor 542
AF-647	Alexa-Fluor 647
AFLP	Amplified Fragment Length Polymorphism
APC	Allophycocyanin
BAM	Binary alignment map
BLAST	Basic local alignment search tool
bp	Base pairs
CD4	Cluster of differentiation 4
CFU	Colony forming unit
CSF	Cerebral spinal fluid
CTAB	Cetyl-trimethylammonium bromide
ddNTP	Dideoxyribonucleotide triphosphate
DMEM	Dulbecco's Modified Eagle Medium
DNA	Deoxyribose nucleic acid
dNTP	Deoxyribonucleotide triphosphate

FBS	Fetal bovine serum
FC	Fold change
FDR	False discovery rate
FSC	Forward scattering
GalXM	Galactoxylomannan
GXM	Glucuronoxylomannan
HIV	Human Immunodeficiency Virus
ICL	Intracellular cryptococci load
IFNγ	Interferon gamma
IgG	Immunoglobulin G
IgM	Immunoglobulin M
IL	Interleukine
IPR	Intracellular Proliferation Rate
ISHAM	International Society for Human and Animal Mycology
kb	Kilobase pairs
L-DOPA	L-3,4-dihydroxyphenylalanine
lncRNA	Long non-coding RNA
Log2FC	Logarithm base 2 of fold change
MAD	Median absolute deviation
MDS	Multidimensional scaling
MLST	Multilocus sequence typing
Mbp	Million base pairs

ncRNA	Non coding RNA
PB	Pacific blue
PCA	Principal components analysis
PCR	Polymerase chain reaction
PE	R-phycoerythrin
PI	Phagocytic Index
PMA	Phorbol myristate acetate
PBS	Phosphate buffered saline
RAPD	Random Amplified Polymorphism DNA
RFLP	Random Fragment Length Polymorphism
RNA	Ribonucleic acid
RNAseq	RNA sequencing
SAM	Sequence alignment map
SFM	Serum-free medium
SSC	Side scattering
TF	Transcription factor
TNFα	Tumor necrosis factor alpha
YPD	Yeast peptone dextrose

Table of Contents

List of Figures

List of Tables

Chapter 1

INTRODUCTION

1.1. Overview of cryptococcosis

Cryptococcosis is disease caused by infection with *Cryptococcus* fungi, most notably *Cryptococcus neoformans* and its sister species *Cryptococcus gattii*. The disease impacts various patient groups including the apparently healthy as well as those immunosuppressed following solid organ transplantation, HIV infection, hematological and other malignancies, other iatrogenic immunosuppression, and immunosenescence related to aging [1–5]. Globally, *Cryptococcus neoformans* var. *grubii* is mostly associated with infection in immunosuppressed patients, although cases due to this species in otherwise healthy people are occasionally reported [5,6]. It is generally considered to be an opportunistic pathogen. This contrasts with *C. gattii*, now considered a primary human pathogen, which is mostly frequently reported causing disease in apparently healthy people [6,7]. Of note, a hypervirulent lineage of *C. gattii* has caused an outbreak of disease in immunocompetent individuals in Vancouver, Canada, over the last 20 years [8].

The most frequent presentation of cryptococcosis is a sub-acute or chronic meningitis [5,9]. This has a very poor prognosis, with 90 day mortality rates as high as 70% in low income countries, and even in rich well-resourced settings, in the order of 10 to 20% [2]. The best

treatment outcomes depend upon the use of the polyene Amphotericin B, which is associated with significant risk of renal and hematological toxicity. Moreover, it is expensive, requires a cold chain, and is frequently unavailable where the disease burden is most high. In wealthy countries, Amphotericin B is usually combined with flucytosine, both of which were developed over 50 years ago. There has been no significant advance in treatment since the development of the azole drugs in the 1980s. Of these, fluconazole is key in consolidation therapy and secondary prophylaxis [10]. Monotherapy with fluconazole is the only treatment available in many resource–poor areas; unfortunately this delivers significantly worse outcomes than combination therapy regiments.

1.2. The history of cryptococcosis

In 1894, the first cryptococcosis case in humans was observed and reported by Busse and Buschke, who cultured and isolated the etiologic agent from skin eruptions of the patient naming it *Saccharomyces*, and the disease *Saccharomycosis hominis* (*S. hominis*) [11,12]. In that same year, Francesco Sanfelice isolated an encapsulated yeast from peach juice and named it *Saccharomyces neoformans* (*S. neoformans*), marking the first description of an environmental isolate of the fungus [13]. The fact that the pathogen can persist in nature, infect and cause disease in both humans and animals was supported by isolation of *S.*

neoformans from the lymph node of an ox by Sanfelice in 1895 and from a pulmonary lesion from a horse by Frothingham in 1902 [14]. In 1896, another human case was described by the French pathologist, Curtis, who named the fungal pathogen *Saccharomyces subcutaneous tumefaciens* – distinguishable from *S. neoformans* in morphology and virulence in animal models [14]. In 1901, because of their lack of ascospore formation and carbon fermentation capability, cardinal characteristics of the genus *Saccharomyces*, Vuillemin reallocated *S. hominis* and *S. neoformans* (seemingly two different organism) into the genus *Cryptococcus* [15].

Cryptococcal meningitis was first described in 1914, although the causative agent was mistakenly named *Torula histolytica* and the disease named torulosis. Over the ensuing years *C. neoformans* came to have over 40 synonyms assigned under 7 different genera, including *S. neoformans*, *C. hominis*, *Torula neoformans* and *T. histolytica* [16]. It was not until 1950 that *Cryptococcus neoformans* became the official name, with torulosis and torula meningitis being replaced by cryptococcosis and cryptococcal meningitis and [16].

In 1970, a further varietal form was described following isolation from an African patient with leukemia by Gattii and Eeckels - *C. neoformans var*. *gattii*. Kwon-Chung *et al*. determined that this strain was the anamorph of *Filobasidiella bacillispora* and identical to the type strain of *Cryptococcus bacillisporus*. This variety, *C. neoformans* var. *gattii* has now been designated as

a separate species - *C. gattii* [17]. As causative agents for cryptococcosis and cryptococcal meningitis, *C. neoformans and C. gattii* are now officially established in the order Tremellales within the phylum Basidiomycota.

1.3. The *C. neoformans*/*C. gattii* species complex

In the 1950s it was discovered that rabbit serum could distinguish forms of *C. neoformans.* Serotyping by capsular antigen agglutination can define 5 serotypes: A, D, AD hybrid, B, and C [18]. In addition, it was demonstrated the biochemical characteristics including carbon and nitrogen assimilation, resistance to canavanine, urease production, and sporulation morphology could divide *C. neoformans* into the 2 varieties: var. *neoformans*, consisting of the serotypes A, D and the AD hybrid, and var. *gattii*, consisting of serotypes B and C [14,19–22]. Serotypes A and D were subsequently themselves classified as separate varieties of *C. neoformans* : var. *grubii* for serotype A and var. *neoformans* for serotype D[17]. The recent designation of *C. neoformans* and *C. gattii* as separate species is largely based upon the profound differences in key aspects of genetics, physiology and biochemistry between the *C. neoformans* and the *C. gattii* species complexes [23–26].

Besides serotyping by capsular antigen agglutination, various molecular typing methods have been employed to study the genealogy and molecular evolution of *Cryptococcus neoformans*

species complex. These include PCR fingerprinting methods that detect polymorphisms among microsatellites and similar repetitive DNA elements, RAPD (Random Amplified Polymorphic DNA), AFLP (Amplified Fragment Length Polymorphism), RFLP (Restriction Fragment Length Polymorphism), and direct DNA sequencing such as Multilocus Sequence Typing (MLST)[27–29]. A consensus MLST typing scheme has been established by the Cryptococcus Species Genotyping Working Group under the auspices of the International Society for Human and Animal Mycology (ISHAM), to facilitate data exchange and comparison between different research groups worldwide [30]. Isolates from serotype A belong to the VNI, VNII or VNB (so far unique to the southern Africa region) molecular types while serotype D isolates are molecular type VNIV [29]. Serotype B includes VGII, VGII and VGII molecular types while serotype C comprises a VGIII or VGIV pattern[31].

1.4. Ecology and environmental niches

Even though a main niche for *C. neoformans* in the environment has not been identified, it has been established that avian guano, especially from pigeons, is a frequent source of isolation in the environment [32–35]. *C. neoformans* cells are able to tolerate the high concentrations of urea, catecholamines and other nitrogenous compounds abundant in desiccated pigeon guano, suggesting the medium is a potential source for enrichment of

Cryptococcus cells [36]. Furthermore, pigeon guano may provide a survival advantage for *C. neoformans because* it is an inhospitable environment for competitive yeasts such as *Candida* and *Pichia*. These yeasts are known to produce anti-cryptococcal toxins[37]. While the association with pigeon guano in temperate climates is the most well-established, *C. neoformans* has also been isolated from the droppings of other birds species including chicken, duck, goose, parrot, owl, eagle and peacock [14,38]. *C. neoformans* has also been isolated from the beaks and feet of feral pigeons, suggesting that the birds have occupied and possibly foraged in *C. neoformans* -contaminated places [39]. Both serotypes A and D have been isolated from soil contaminated with pigeon droppings, air above avian guano-contaminated soil and tree swabs [40–42]. The demonstration of the presence of *C. neoformans* on the surface of pigeons, rather than solely in the guano, supports the notion that pigeons are implicated in the global spread of the organism, acting as carriers. Since the normal range of body temperature for pigeons is 41 – 42^{o}C, which is significantly higher than the optimal temperature for growth of *C. neoformans* , is unlikely that global dispersion is primarily attributed to infection of pigeons [43], but more likely due to its external carriage.

In addition to the well-documented association between *C. neoformans* and pigeon guano, *C. neoformans* can also be isolated from a variety of trees in many parts of the world, including South America, India and Thailand in Southeast Asia [44–48]. These arboreal niches are

considered to be in addition to the habitats associated with frequent exposure to avian feeding/guano.

1.5. Mating types in cryptococcal life cycle and their association with virulence

Two sexual phases (Mating Type – MAT) of *C. neoformans* and *C. gattii* have been identified and characterized: MATα and MATa [49,50]. The mating type is controlled by the *MAT* locus which is large (>100kb) and consists of more than 20 genes [51–53]. Many of these encode both regulators of sexual development and elements of the pheromone response pathway [53]. The *MAT* locus itself is a non-recombining chromosomal fragment from which an intact MATa or MATα allele is included in each segregated segment during meiosis [54]. The product of sexual mating between two isolates of opposite mating type is the basidiospore, which is proposed to be an important infectious propagule for cryptococcosis in human [55]. The role of mating types and the stages of the life cycle of *Cryptococcus neoformans* are summarized in **Figure 1.5-1.**

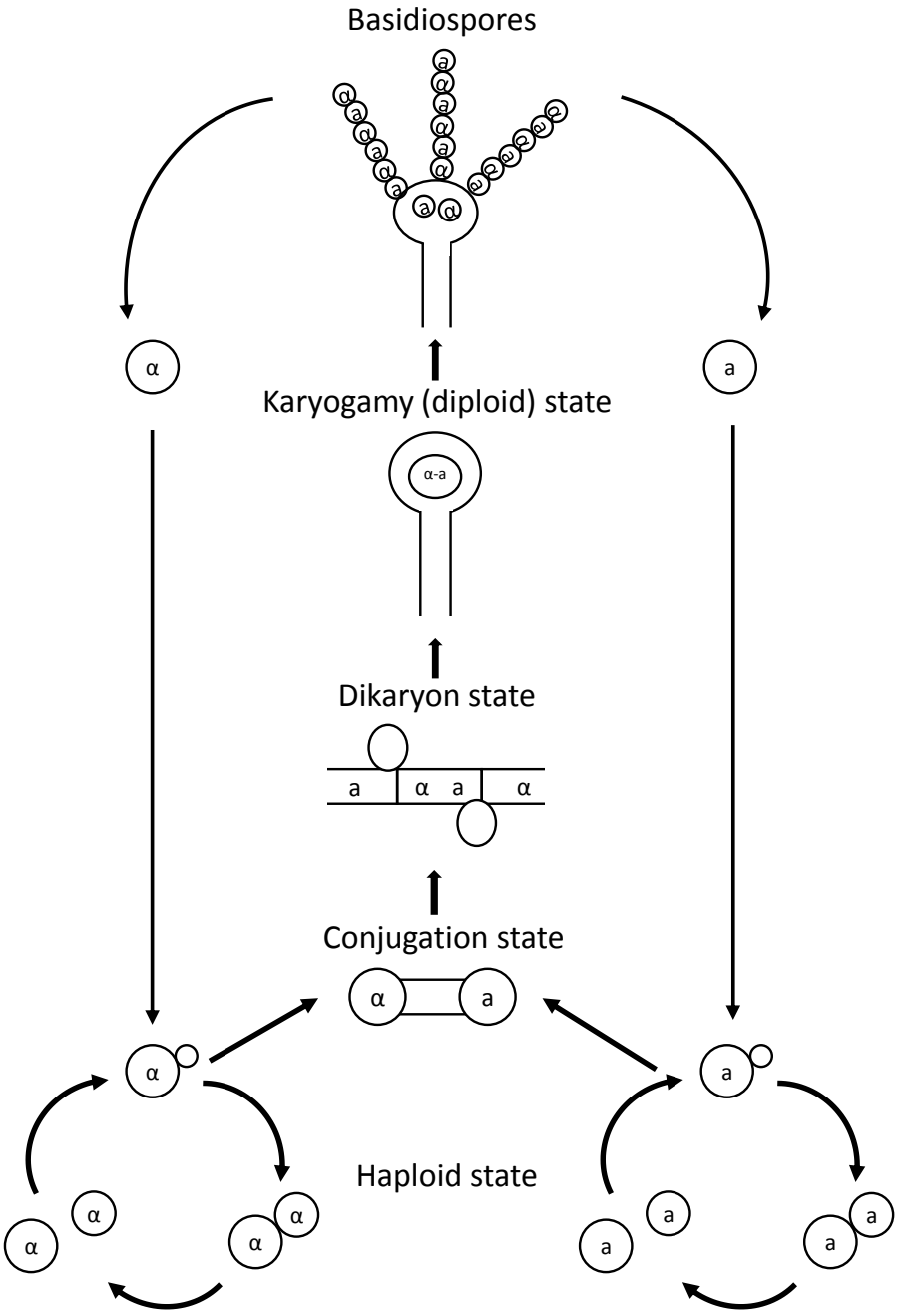

Figure 1.5-1. Life cycle of *Cryptococcus neoformans*

In a bipolar mating system such as that of *Cryptococcus* spp., an equal ratio of α:a mating types would be expected. However the majority of environmental and clinical isolates of *C. neoformans* were dominated by the MATα mating type [56]. In Sub-Saharan Africa, MATa isolates are found at a much higher frequency and population genetics analyses have revealed features of mating likely to involve both mating types [29,57].

The overall bias toward MATα in nature, given that there is no apparent physiological or fitness difference between α and a cells, remains unexplained. One possible explanation was provided by Wicker *et al*. (1996), who reported that only MATα cells were able to undergo haploid fruiting under nitrogen starvation conditions in the absence of a mating partner [58]. While this ability first appeared to be restricted to MATα strains, it has subsequently been described in MATa strains, and the phenomenon of haploid fruiting is clearly independent of mating type [59]. Haploid fruiting, while originally thought to be strictly mitotic, has been shown, *in vitro*, to share some of the features of sexual mating, including chromosomal diploidization and meiosis. This implies that α-α diploid cells can undergo independent chromosomal rearrangement and produce haploid basidiospore progenies [60]. Furthermore, fusion and meiosis has been shown to occur between non-isogenic alpha strains, enabling genetic exchange. The progenies of such 'same-sex mating' show high rates of recombination and have novel genotypes differing from the parental genotypes [60].

Phylogenetic studies of *C. gattii* strains form the Vancouver outbreak supports the idea that same sex mating also occurs in the environment [61]. It has been suggested that same sex mating occurring under specific environmental stresses confers an evolutionary advantage because the resultant recombinant basidiospores are easily aerosolized and dispersed to other geographical regions [61].

MATα has been considered the more virulent mating type based on animal studies [62,63]. MATα cells of *C. neoformans* var. *grubii* seemed to penetrate the CNS better during coinfection with congenic MATa *C. neoformans* var. *grubii* cells [63]. Notably, both bisexual and unisexual mating generate aneuploid progenies at similar rate [64]. This may be relevant because aneuploidy has been associated with variation in the expression of certain cryptococcal virulent factors, including melanin [65]. Aneuploidy has also previously been identified as a mechanism of drug resistance during normal growth on varying concentrations of fluconazole [66] and variable susceptibility to fluconazole could be seen in aneuploid progeny generated without selection by fluconazole [67]. Interestingly, there may be an important role for the MAT locus outside of mating. Transcriptional profiling of *C. neoformans* during murine macrophage infection reveals that almost the entire MATα locus has increased expression following ingestion by macrophages, suggesting the locus has a particular role during infection [68]. However, the sheer complexity of the MAT locus and the

diverse pleiotropic functions of its encoded products make it difficult to investigate the contribution of individual genes to virulence [38].

1.6. Infectious propagules for cryptococcosis in human

As with other fungal pathogens, inhalation of airborne spores has long been considered the most likely route of infection for cryptococcosis in human[69,70]. Cryptococcus spores (~1-2 µm in diameter) are significantly smaller than yeast cells or filamentous hyphal cells, which likely facilitates both their ability to become airborne and their entry into the alveoli following inhalation [71]. In addition, spores are potentially better able to persist in any given environment than yeast cells, being more resistant to desiccation and nutrient starvation conditions [58]. The ability of spores to establish successful infection has been demonstrated in a murine nasal infection model. Of note, spores from different varieties/lineages may have different virulence potential; serotype D spores have been reported to be more virulent than the corresponding yeast cells; this contrasts with serotype A spores which were not found to be as virulent as their yeast counterparts [72,73]. Interestingly, while serotype D strains were more potent in terms of establishing infection, this same model found spore-associated mortality in mice to be lower compared with that when a yeast cell inoculum was used [72].

The presence and infectivity of spores does not preclude the fact that infection may also occur following inhalation of desiccated yeast cells. The increased size of yeasts compared with spores may be mitigated by the fact that in nutrient deprived and low moisture environments there is considerable heterogeneity in capsule production and cell size. Under these circumstances cells may be as small as 3µm or less in diameter, thus facilitating their uptake by inhalation by the host [73]. However, the relative importance of yeasts versus spores in human infection remains unclear; the feasibility of such yeasts as infectious propagules must be considered in the context of their reduced viability and potential for dispersal in the environment [58]. However, the relative importance of spores in causing human infection must be considered in the light of the fact that while spore production has been demonstrated in the laboratory, due to at least 2 mechanisms - same-sex mating and opposite-sex mating - neither of these phenomena has been *directly* observed in nature, and population studies suggest that recombination appears to be a relatively infrequent event [74–77].

1.7. Population structure, genomic diversity and putative origin of the global *C. neoformans* var. *grubii* population

1.7.1. Global population structure of VNI *C. neoformans* var. *grubii*

C. neoformans var. *grubii* (serotype A) has a global distribution and is responsible for the vast majority of cryptococcal disease in immunocompromised hosts [78–80]. Molecular typing studies demonstrate that the greatest genetic diversity is found within African populations [23,29,81–83]. Both clinical and environmental populations are dominated by the MATα mating type [83–85]. The global *C. neoformans* var. *grubii* population can be divided into 3 main lineages: VNI, VNII and VNB[29,30,86]. While VNI and VNII are globally dispersed, the VNB lineage is largely restricted to southern Africa, having first been identified in Botswana [29]. Subsequently VNB has been sporadically reported from Brazil [22,25] and as an AD hybrid in China, Italy and the USA[87], though with much lower frequency. Current data suggest that the VNB lineage is largely geographically restricted to sub-Saharan Africa. The restriction of the VNB lineage to southern Africa may be explained by its adaptation to a particular ecological niche. While environmental isolates of VNI are often associated with pigeon excreta [40,88], environmental isolates from the VNB lineage are highly associated with a specific indigenous African Mopane tree species (*Colophospermum mopane)* [81,82].

Comparative genomics further divided the VNB lineage into 2 subgroups: VNB-I and VNB-II [82,89,90].

Xu *et al.,* (2000) investigated a set of strains from multiple geographical locations using a multi gene genealogies approach and reported high divergence among strains of different varieties/serotypes from the same geographical region but low divergence among strains of the same variety/serotype from different geographical regions, which supports the hypothesis of a relatively recent global dispersal of *C. neoformans* species [23]. The global VNI lineage, with its relatively low overall diversity, is proposed to have emerged from a small founder population that may have undergone repeated bottlenecks while spreading across different geographical regions [90].

A recent extensive phylogenetic study by Desjardins *et al*., using whole genome data (2017) further divided the VNI lineage into 3 distinct sub-clades with different geographical distributions (VNIa, VNIb and VNIc) [90]. VNIa and VNIb were globally distributed while VNIc was restricted to Sub-Saharan Africa [90] **(Figure 1.7-1)**. There appears to be active recombination events occurring between these individual sub-clades, as evidenced by faster rates of linkage disequilibrium decay in the major VNI lineage compared to the individual sub-clades [90] **(Figure 1.7-1)**. The finding of highly diverse progenitor African strains of *C. neoformans* var. *grubii* with the capacity for sexual as well as clonal reproduction, compared

to the largely clonal *C. neoformans* var. *grubii* strains elsewhere, suggests that the global population has been driven by an “out-of-Africa” dispersal [81]. The existence of the sub-Saharan Africa endemic VNIc sub-clade and the presence of African-origin VNIa and VNIb strains across the globe also support this “out-of-Africa” hypothesis [90]. These and previous findings suggest diversification of different VNI sub-clades occurred within Africa, with subsequent global expansion; the mechanisms through which this dispersion occurred are unknown mechanisms, but postulated to be facilitated by avian migrations and human activities [81,91,92].

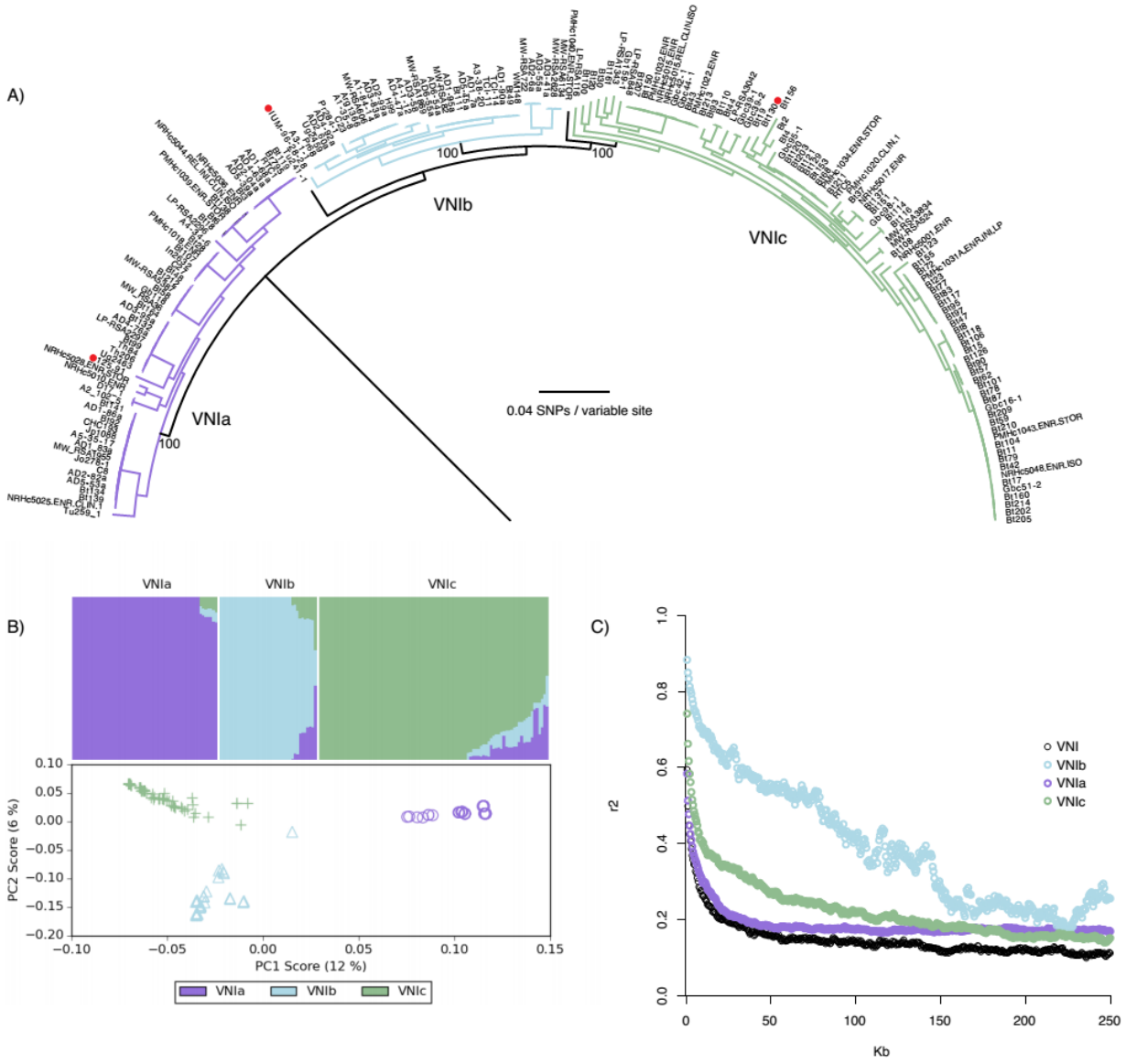

Figure 1.7-1. Sub-structures of the global *C. neoformans* var. *grubii* VNI population (adapted from Desjardins *et al.* (2017) [90]**.**

(A) Comparative genomics and phylogenetic analysis divide the global VNI population into 3 major sub-clades, the global VNIa and VNIb, and the Southeast African VNIc. (B) Clustering analysis in STRUCTURE and PCA reveal largely distinct sub-populations (VNIa, VNIb and VNIc) with a small degree of mixing between groups. (C) Linkage decays more rapidly in the global VNI population than in any individual sub-clade, suggesting the sub-populations are currently recombining with each other and do not represent reproductively isolated populations.

1.7.2. Genes under selection in *C. neoformans* var. *grubii*

Evaluation of genes under selection in all lineages of *C. neoformans* var. *grubii* revealed that the sugar transporters subset of the major facilitator superfamily (MFS) transporters, especially transporters for inositol, xylose, maltose, α-glucosides, lactose and galactose, are among those under extensive positive selection [90]. Other groups of genes under selection include monoxygenases in VNI and β-glucosidases in VNB [90]. This finding provides insights into the different adaptation of various lineages of *C. neoformans* var. *grubii* to environmental stress that also translate to pathogenicity in human in a "by-stander effect" fashion [93,94]. Specifically, enrichment of inositol and xylose transporters has been proposed to be involved in cryptococcal growth on different species of trees [90,95,96]. On the other hand, selection of inositol metabolism in the VNI lineage is evidently related to VNI pathogenicity in human since inositol is abundant in the human brain [97] and is a known stimulator for cryptococcal penetration of the Blood-Brain Barrier [98].

1.7.3. Population structure of *C. neoformans* var. *grubii* in Asia and Vietnam

Limited data exist on the population structure of *C. neoformans* var. *grubii* in Asia, including reports from India [99,100], Thailand [22,92,101,102], Vietnam [103], China [104–106] and Japan [107]. Pan-Asia MLST-based population structure analysis revealed clustering of *C. neoformans* var. *grubii* isolates according to their original geographical region: cluster 1

mostly consists of isolates from China, Japan and a number of isolates from Thailand; cluster 2 contains the remaining of the Thai isolates and a number of Indonesian isolates; cluster 3 included Indian isolates and the rest of the Indonesian isolates [101]. Widespread occurrence and overrepresentation of genotypes derived from clonal expansion of a few dominating parental genotypes was implicated, similar to what have been described for other pathogens including *Neisseria meningitides*, *Mycobacterium tuberculosis*, *Fusarium oxysporum*, and *Leishmania tropica* [108]. The overwhelming presence of the MATα mating type means that natural bisexual reproduction is rare among *C. neoformans* var. *grubii* populations in the environment and the fact that *C. neoformans* yeasts could undergo same sex mating, as well as the low rate of recombination which limits genetic divergence may have been one of the driving forces for the observed clonality in Asia.

Most reports of *C. neoformans* var. *grubii* population structure from Asia indicate there is limited population diversity compared to other parts of the world, as well as the expected domination of MATα in both environmental and clinical isolates [101]. For example, all the clinical isolates from a cohort of 120 Chinese patients were infected with the same MLST genotype, M5 [109], later identified as multilocus sequence type 5 (ST5) [104,106,110]. More than 90% of clinical *C. neoformans* var. *grubii* isolates from Japan and South Korea were also ST5 (designated as M5 or VNIc in the original studies) [107,111]. In contrast, most cases

reported from Thailand included *C. neoformans* var. *grubii* isolates from HIV-infected patients, which appeared to be more diverse than those from East Asia and included 3 main MLST genotypes: ST4, ST5 and ST6 [92,101,102]. Studies from the East Asian region (China, Japan, Korea), however, are complicated by a relative lack of isolates reported from patients with immunosuppression, in particular HIV infection. AFLP typing of the clinical population of VNI *C. neoformans* var. *grubii* from Vietnam separated the isolates into two distinct clusters with specific association with host immune type (HIV status) [103]. Specifically, the respective AFLP clusters were termed VNI-γ and VNI-δ, both of which were found in HIV-infected patients though with different proportions [103]. Intriguingly, VNI-γ accounted for over 80% of cases in HIV-uninfected patients with no known underlying diseases [103]. VNI-δ infection, when found in HIV-uninfected patients, was often accompanied by other serious immunosuppressive conditions [103]. While the genomic divergence between the two clusters was apparent, their implication to virulence potential and host preferences, i.e. paradoxical *C. neoformans* var. *grubii*-associated infection in apparently immunocompetent hosts, is still unknown.

1.8. Virulence in animal hosts results from adaptation for survival in the environment

Because cryptococcal infection is not contagious (i.e. no host-to-host transmission), it is widely held that the ability of *C. neoformans* to cause disease is due to the coincident or accidental acquisition of pathogenicity as it adapts to heterogeneous environmental conditions – so-called bystander pathogenicity [94,112]. A variety of virulence factors have been identified *in vitro,* including the polysaccharide capsule, the ability to grow at mammalian body temperatures, production of laccase and melanin, and a number of secreted factors important in countering the host immune response, including phospholipase B and urease [113][14]. Almost all these previously described cryptococcal virulence factors can be attributed to survival functionality in the environment. For instance, encapsulated yeast cells are more resistant to desiccation and predation by amoeba in the environment [114,115]; the ability to withstand and grow at high temperature is a desirable trait for fungal survival in niches with extreme temperature range [116,117]; and cell wall melanization is associated with protection from UV and other electromagnetic radiation [118,119].

Many virulence factors may play a role in protecting the yeast against environmental predation. Using *Acanthamoeba castellani* as an experimental host, it has been demonstrated that following ingestion *C. neoformans* undergoes intracellular replication.

This is accompanied by the accumulation of cytosolic vesicles containing shed capsular polysaccharide [115]. The intracellular growth rate of *C. neoformans* is impaired in mutants with deficient capsules or phospholipase; acapsular mutants are more readily killed following ingestion by the amoeba [120,121]. Interestingly, phagocytosis of *C. neoformans* cells by amoebas in the presence of divalent cations such as Mg^{2+} and Ca^{2+} enhanced yeasts killing, which suggests that *C. neoformans*-contaminated soil with increased concentration of divalent cations may harbor fewer number of cryptococci due to increased amoeba predatory activity [122]. On the other hand, melanin production may protect against predation by amoeba since, even in acapsular strains, melanized yeasts are more likely to survive ingestion [120,121]. These observations illustrate that virulence factors recognized in mammalian hosts, such as capsule and melanin, are likely derived from adaptations that have evolved to manage ecological risks. The development of such transferable intracellular survival skills may help to explain the broad host range of *C. neoformans* since all major mammalian immune responses rely on phagocytic effector cells.

Despite the fact that *Cryptococcus* spp. can infect a broad host range (from amoebae and worms to mammals) it is unlikely that a susceptible host is a pre-requisite for any stage of the Cryptococcus life cycle. While in-host environments could lead to microevolution of infecting *C. neoformans* yeasts [123–125], it is improbable that cryptococcal virulence is a result of *in*

vivo selective pressure because the disease is not passed from host to host. Rather, current data support the idea that selection pressures from environmental stress and predation have led to the acquisition of a unique set of cryptococcal survival strategies, which just happens to be confer the potential for mammalian infection.

1.9. Intracellular parasitism

The interactions of *C. neoformans* with amoeba and host macrophages are strikingly similar. In mammals *C. neoformans* is a facultative intracellular pathogen, and can survive phagocytosis by innate immune cells and proliferate intracellularly [14]. Recently it has been demonstrated that there can be subsequent non-lytic extrusion of yeast cells from macrophages to the extracellular space or adjacent host cells (vomocytosis) [120,126–131]. The intracellular parasitism of host monocytes and macrophages is a likely key in enabling *C. neoformans* to disseminate and cause brain infection [132–134]. This complex pattern of interaction with host innate immune cells is a key determinant of virulence - both Intracellular Proliferation Rate (IPR) and phagocytosis proclivity have been correlated with mortality and fungal clearance during antifungal treatment [133,135–137]. Cryptococcal interaction with phagocytic cells from the host's innate immune system is summarized in **Figure 1.8-1.**

Enhanced ability to survive and replicate inside macrophages has been shown to be associated with the spread of *C. gattii* in northwestern North America and may even have triggered the outbreak [130]. The strain associated with this outbreak – VGIIa - has a higher IPR than other *C. gattii* genotypes associated with a unique tubular mitochondrial morphology. It is postulated that this confers a protective effect by enabling repair of intra-phagosomal oxidative damage to mitochondrial DNA [130]. Such VGIIa yeasts with tubular mitochondrial morphology were found to be highly resistant to host Reactive Oxygen Species (ROS) [138]. In contrast to *C. gattii*, with *C. neoformans* it is yeast uptake by macrophages, rather than the IPR, which has been found to correlate with the patient's cerebrospinal fluid (CSF) fungal burden in HIV infected patients [135]. Furthermore, infection with high-laccase-activity, high-uptake *C. neoformans* correlates with both higher pre-treatment fungal burdens in patients' CSF and slower rates of CSF fungal clearance with antifungal treatment, which may lead to an increased risk of death[135]. Strains with smaller capsules, while more readily engulfed by macrophages, may possess mechanisms that confer improved intracellular survival and proliferation.

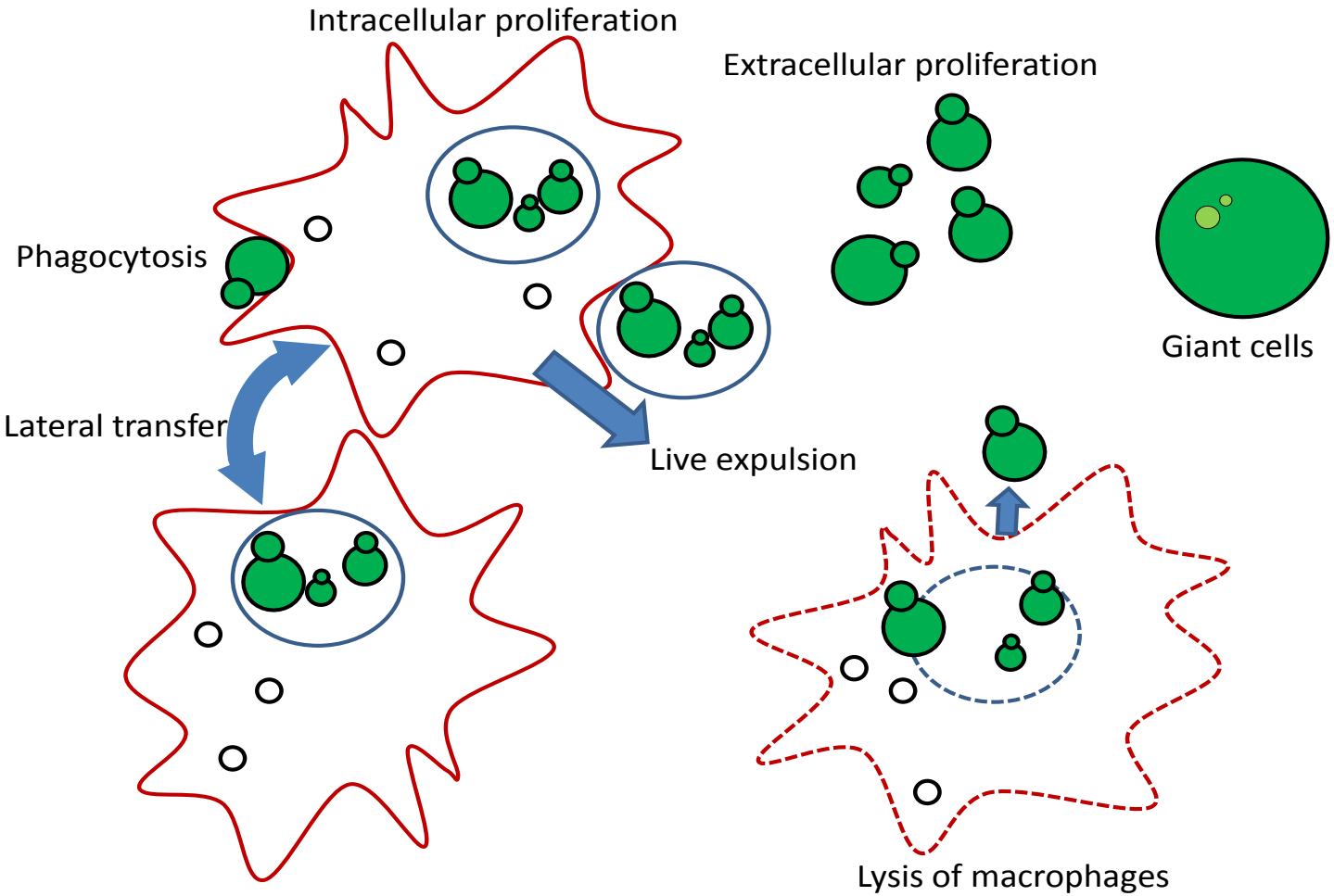

Figure 1.9-1. Interactions between infecting Cryptococcus yeasts and phagocytic cells from the host's innate immune system.

1.10. Acute infection versus latency in cryptococcosis

It is commonly held that active cryptococcosis in humans is largely the result of reactivation of latent, or dormant infection. Acute infection, following defined exposure incidents, has been reported, but seems to be a very rare event [139,140]. The evidence supporting latency prior to disease is derived from studies investigating *C. neoformans* -specific seroprevalence in adults [141–143]. Findings from a study in New York found serological evidence of previous exposure to *C. neoformans* infection from children as young as 2 years (over 50%), implying exposure is common and occur very early in life, resulting in long term latency [144]. The serological reactivity and prevalence in children differed according by geographical region, suggesting regional-associated differences in exposure [145].

Further evidence is derived from a study from France. In this study, AIDS-associated cryptococcosis patients, resident in France for a median period of 110 months, and without exposure to an African environment for at least 10 years, were found to be associated with infection by *C. neoformans* strains with African origins [146]. In another report, solid-organ-transplant patients were seropositive for cryptococcal antigens before the procedure, suggesting subsequent cryptococcal disease in these patients was reactivation from dormancy following immunosuppressive therapy [147]. Re-infection of the same strain(s) is

unlikely in this case because acute and progressive cryptococcal disease is only possible when patients are exposed to an unusually high inoculum of yeasts. Together, these data suggest that patients acquire and sequester initial infection with *C. neoformans* early in life. Active disease manifestation then occurs when patients acquire immunosuppression, most commonly HIV, resulting in loss of immune control and disease activation.

While in theory it would be possible to confirm the latency theory by comparing the latent strain with the disease strain, in practice this is impossible because the point of latent infection is (presumed) asymptomatic, and the strain cannot be obtained. However, most cases of recurring cryptococcosis are associated with persistence of the single original isolate, even after long periods of antifungal treatment, providing indirect evidence consistent with the latency hypothesis [148–150].

However, it is of course possible that 'relapse' in these cases in fact represents re-infection by a different isolate of the same genotype, given the ubiquitous distribution of *C. neoformans* in the environment and the largely clonal structure of the global *C. neoformans* population [92,101,151,152]. Conversely, relapse infection by a different genotype could represent either new infection or reactivation from a previous mixed infection with multiple strains [150]. Mixed infection by strains of different genotypes/serotypes may occur in up to 20% of all cryptococcosis cases [150].

1.11. Cryptococcal virulence factors

1.11.1. The polysaccharide capsule

Capsular structure

The cryptococcal capsule is unique amongst human pathogenic yeasts, and is comprised primarily of two polysaccharides, glucuronoxylomannan (GXM) and galactoxylomannan (GalXM), with a lesser proportion of mannoproteins (MP)[153]. GXM is a complex polysaccharide with a repeating structure of α-1,3-mannose with β-D-xylopyranosyl, β-D-glucuronosyl and 6-O-acetyl branching and accounts for 90-95% of capsular mass. GalXM is an α-(1→6)-galactan containing four short oligosaccharide branch structures and constitutes about 8% of the capsular mass. Mannoproteins constitutes less than 1% of capsular mass and share several structural features including N-terminal signal sequences, serine/threonine (S/T)–rich C-terminal regions, and glycosyl-phosphatidylinositol anchor motifs.

Heteropolymer branching is a notable conformation of the cryptococcal capsule. This is due to the fact that cryptococcal polysaccharides are synthesized intracellularly and transported to the extracellular space via vesicle-mediated secretion, with additional biochemical modification as they migrate through the cell-compartments to the cell surface [154–157]. The degree of branching and/or structural complexity influences the ability of capsular polysaccharides to interfere with phagocytosis, stimulate nitric oxide production by

macrophages, protect against reactive oxygen species (ROS) and antibody reactivity, as well as determining the half-life of capsular polysaccharide molecules in serum [158].

Capsule structure varies substantially depending on the strains and the surrounding environment, as well as during the course of infection [159]. Electron microscopy data reveal a heterogeneous structure consisting of an electron-dense inner layer and an electron-sparse outer layer [160–162]. With this configuration, the outer layer appears more permeable while the inner layer is more rigid, able to block larger macromolecules such as antibodies and complements proteins from reaching the cell wall [160,162,163].

Capsule size

Capsule size is highly variable, not only between different strains but also among individual cells from the same strain. Despite its importance in pathogenesis, the relationship between capsule size and virulence is not simple. In one study, HIV patients infected with strains producing large capsules were more likely to have higher intracranial pressures at presentation and lower fungal clearance rates upon treatment with amphotericin B and fluconazole [164]. Consistent with this, it has been demonstrated that acapsular *C. neoformans* strains have reduced pathogenicity in mice [165,166]. The fact that acapsular *C. neoformans* strains are only capable of causing prolonged brain infections in nude mice (mutants with an absent or deficient thymus resulting in T-cell failure) suggests that these

strains would only present virulence in severely immunocompromised hosts [167]. However, disease due to strains with small capsules in humans has been reported [167].

Role of the capsule in cryptococcal pathogenesis

The role of the capsule in cryptococcal survival and defense against hosts' immune response is well-established [153,164,168]. In the environment, the capsule protects yeast cells from dehydration and desiccation and contributes to survival in low humidity conditions [114]. In addition, encapsulated *C. neoformans* strains are less likely to be phagocytosed and killed by the amoeba *Acanthaamoeba castellani***,** [115]. Within mammalian hosts, the capsule protects un-opsonized yeasts from ingestion by phagocytes and impedes host immune response *in vitro* [169].

Capsular shedding may also have a role in pathogenesis *in vivo* [153]. Shed capsular polysaccharides are secreted into vesicles around the phagosome; the accumulation of these vesicles in the cytoplasm of the host cell results in macrophage dysfunction and lysis [170,171]. Capsular polysaccharide materials have also been found to induce proliferation and differentiation of normal CD4+ T cells into a (non-protective) Th2 phenotype, favoring intracellular parasitism and dissemination of *C. neoformans* [172].

In patients, data suggest that high levels of capsular antigen in CSF are associated with increased intracranial pressure, headaches and visual disturbance [173]. In addition, capsular

material impedes host neutrophil recruitment [174], interferes with cytokine response [175–179], induces macrophage apoptosis either via a Fas-ligand mediated pathway or nitric oxide production [180], and delays host dendritic cell maturation and activation [181].

1.11.2. Thermotolerance

The ability to grow at mammalian body temperatures (37^{o}C or higher) is an obvious yet essential attribute for any would-be invasive fungal human pathogen [182–185]. There are several proposed models for the origin and evolution of thermotolerance in *C. neoformans.* It has been hypothesized that a bolide collision 65 million years ago eliminated a vast proportion of the Earth's fauna and triggered a global chain reaction of volcanic and seismic activities, giving rise to a massive fungal bloom that fed on decaying vegetation [182]. Under these conditions, endothermy was a costly but effective adaptation for surviving mammals and birds species to offer protection against such a large fungal inoculum. Fungi would have to adapt too to successfully infect, colonize and cause disease in these new endothermic hosts [182] – however, since *Cryptococcus* spp. do not seem to require a mammalian host in any stage of its life cycle, adaptations to warmer environments seems a more plausible explanation for its thermotolerance.

While *C. neoformans* can grow in a wide range of temperatures (30^{o}C to 40^{o}C) [185], there is considerable variation in thermo-tolerance between different strains, and some evidence

that this is determined by geographic origin [186]. For instance, *C. neoformans* var. *neoformans* strains, which in general are more susceptible to high temperature than the globally distributed *C. neoformans* var. *grubii*, are more commonly found in temperate Europe [186]. Evidence suggesting that *Cryptococcus* spp. originated from Africa further supports the speculation that growth at higher temperatures, essential for pathogenicity, is a survival advantage that resulted from environmental selection pressures in regions with higher ambient temperatures [81,116].

1.11.3. Laccase and melanin production

Melanin is a brownish black pigment produced through the oxidative polymerization of phenolic compounds. *C. neoformans* produces melanin with an oxidative enzyme called laccase which synthesizes melanin from L-DOPA, dopamine, norepinephrine and epinephrine [187–189]. Given the fact that environmental isolates of *C. neoformans* are often melanized, melanization may have evolved as a survival strategy to protect cells from UV radiation and facilitate growth at extreme temperatures [118,190,191]. Defects in melanin production result in improved mouse survival in laboratory models, suggesting a role in virulence [189]. Melanin has various roles in cryptococcal viability and pathogenicity including protection against enzymatic degradation, antimicrobial peptides, oxidative stress and heavy metal toxicity [192–194]. Of note, melanin has been shown to decrease the efficacy of

amphotericin B *in vitro*[194]. Histopathological studies of lung tissue at different time points during the course of experimental mouse infection also reveal yeast cell enlargement due to melanin accumulation in the cell wall, a characteristic conferring resistance against oxidative stress and antimicrobials [195]. *C. neoformans* var. *grubii* isolates from HIV-infected patients with higher range laccase activity have higher *ex-vivo* CSF survival and are more resistant to antifungal treatment[135].

1.11.4. Titan/Giant cell formation

During the course of cryptococcal infection, yeast cells undergo various morphological transformations, depending on conditions. One such morphological change, first described in 2010, is titan cell formation [196]. These are giant cryptococcal cells, up to 100 µm in diameter, and may account for up to 20% of the lung fungal burden 24 hours after infection [197]. These larger cells are often polyploid (but uni-nucleated), suggesting an absence of cell fission following DNA replication [113].

In mouse models of infection, the giant cell subpopulation is typically 10% to 80% of the total pulmonary fungal population, depending on the duration of infection, degree of pulmonary inflammatory response and total fungal burden[121]. Mice infected with a lower dose of yeasts, and with less severe pulmonary symptoms, produce a higher proportion of giant cells[121]. DNA replication without the subsequent completion of mitosis and/or

cytokinesis results in the elevated chromosomal numbers (frequently tetraploidy or octaploidy) associated with giant cell formation. However, the daughter cells (produced by budding) from giant cells are usually haploid or diploid[121,197].

Pheromone and cyclic AMP-dependent signaling pathways have been shown to be major regulators of cryptococcal cell gigantism[113,121,198–200]. In addition temperature can be an important stimulus for giant cell formation. Yeast-cells from one brain tissue isolate were found to be of normal size (~5µm) at 25^{o}C *in vitro* but expanded to a diameter of 25µm when cultured at 35^{o}C[201].

The formation of giant cells may be part of a survival strategy facilitating evasion of host immune defenses to allow colonization and establishment of infection: giant cells are frequently found in extracellular spaces and are generally more resistant to phagocytosis than regular yeast cells, suggesting that the giant cells represent a more viable extracellular subpopulation, co-colonizing with the intracellular population of smaller cells which have taken advantage of being engulfed, to facilitate dissemination[196,202]. Lower CSF fungal burdens in patients with chronic or latent infections are in keeping with the observation that lower inoculum seem to induce more gigantism[113], whilst it is the smaller cells which hijack macrophages to gain access to the CSF. Morphological heterogeneity during the course of infection is an obstacle for the host immune response [195]. Specifically, giant cells appear

to be much more resistant to phagocytosis and antifungals, representing an extracellular population that are extremely fit; the normal sized cells, on the other hand, could be phagocytosed but can still survive, proliferate and readily disseminate [195]. This may explain some of the observed difficulties in cryptococcal disease therapy [195].

1.12. Genome "flexible stability" and survival-driven adaptability

1.12.1. Cryptococcal genomic stability versus flexibility

Early characterization of cryptococcal genomes employed electrophoretic karyotyping [203]. The size and number of cryptococcal chromosomes was highly variable in both clinical and environmental isolates, suggesting extensive chromosomal rearrangement and genomic flexibility [204]. Further investigation revealed the extent of variation within the population and suggested meiotic-driven karyotypic variation [205,206]. Karyotype changes also occur during the course of a single infection; this fact was observed in a series of human clinical cases, and confirmed in a mouse model of infection where karyotype was recorded before infection, and in organisms retrieved from body tissues [207]. Gross chromosomal rearrangement has been observed in closely related strains isolated from the same patient 77 days apart, further supporting host selective pressures as a driving force behind this genome flexibility [208].These results are in accordance with the notion that infecting yeasts

adapt to selective pressures within the host and the result may be a virulence-associated phenotype [159,209].

Large scale genomic studies employing comparative genomic hybridization reveal previously unobserved insertion and deletion type mutations (indels) within both var. *neoformans* and var. *grubii*, as well as a predisposition to aneuploidy which may confer resistance to fluconazole [66,210,211], a strategy also employed by *Candida albicans* where chromosomal rearrangement and duplication is proposed as a mechanism allowing populations to respond to selective pressures[212]. The term heteroresistance is used to refer to this situation, where a subpopulation of resistant organisms exists amongst a larger population of susceptible siblings, thanks to some degree of genomic plasticity.

Most reports linking antifungal drug resistance in *Cryptococcus* spp. with aneuploidy focus on azoles, particularly fluconazole[213]. Various studies on azole heteroresistance in *C. neoformans* have demonstrated disomy in chromosomes 1 and 4 occurring in resistant subpopulations selected from growth conditions containing high antifungal drug levels[66,214]. Resistant clones emerging in media with the highest drug levels were found to have disomies in 4 chromosomes : Chr1, 4, 10 and 14[66,214]. Amplification of ATP-transporter efflux pump genes like *Erg11* and *Afr1* on Chr1 was shown to correlate with azole resistance [66]. Disomy on Chr4 has been associated with genes required for endoplasmic

reticulum integrity under azole stress [214]. However it is not known whether increasing uses azoles were responsible for the development of cryptococcal heteroresistance or whether resistant subpopulations always existed in the global cryptococcal population [213].

1.12.2. Genomic features associated with adaptation for survival and in-host virulence

In addition to chromosomal aneuploidy following exposure to antifungals, other forms of chromosomal variations that are associated with adaptation to environmental selection were also detected. For instance, close examination of the sub-telomeric regions of *C. neoformans* var. *grubii* strains has identified an enrichment of hexose transporters and tandem repeats of an arsenite resistance gene (Arr3) whose copy numbers were proportional to resistance to arsenite compounds[124]. Interestingly, this genomic variation was unique to MLST-ST5[124]. Since the sub-telomeric regions in *Saccharomyces cerevisae, Candida glabrata* and *Plasmodium falciparum* were known for extensive accumulation of gene families that are essential for niche adaptation, the *Arr3* repeats, though not important for in pathogenesis or antifungal resistance, may be essential for survival in environmental niches contaminated with high concentration of arsenite compounds [124]. The highly diverse sub-telomeric regions of cryptococcal strains from the VNI, VNIB and VNBII lineages all showed evidence of enrichment for transporters, which may have unknown functions related to niche adaptation

[215]. In addition, fungal transcription factors including FZC20, FZC41, SIP402, and FZC22, the last of which has been shown to affect virulence in mice when deleted [216], have been shown to be enriched in the 40kb sub-telomeric regions.

Functional enrichment analysis of genes under positive selection in VNI and the two VNIB lineages revealed sugar transporters from the MFS family (Major facilitator superfamily) were highly selected in all 3 lineages [215]. Of note, isolates from the VNI clades seem to harbor high number of inositol transporters and catabolism genes that are under selective pressure [215]. As inositol is present in high concentration in human brain as well as being involved in cryptococcal mating and virulence [96,217–219], selection for inositol transporters and utilization could potentially influence lineage-specific host range and pathogenicity in human hosts [215].

1.13. Transcriptomics and stress response pathways of *C. neoformans*

In addition to genomics studies, a wealth of information has recently been attained from transcriptional profiling of *C. neoformans* molecular responses to stress conditions mimicking conditions in the host. Most studies employed *in vitro* infection models and well-characterized laboratory strains of *C. neoformans* to study the transcriptional response to a range of stress conditions including high temperature [220–222], oxidative stress [223] and

capsule inducing conditions [224,225], to expression during infection of murine macrophages [226,227] and mammalian hosts [228–230]. These findings provided the basis of the current understanding of cryptococcal pathogenesis in the host.

1.13.1. Response to high temperature

The genes and pathways that are associated with cryptococcal temperature-dependent growth are among the most widely studied and characterized. These genes are often involved in key regulatory and metabolic pathways, which mean they are essential for multiple stress responses beside growth at high temperature, with direct or indirect impact on the expression of key virulence factors. For example, the gene VPH1, encoding a vesicular proton pump, is a universal regulator of capsule production, urease expression and laccase expression, as well as growth at 37^{o}C [231]. The transcriptional activator *MGA2*, was previously found to be associated with growth at high temperature and virulence, was also involved in fatty acid synthesis [222]. In addition, temperature-dependent growth tends to be linked to genes involved in oxidative stress response, due to the fact that *C. neoformans* cells produce more oxidative waste as ambient temperature increases [185]. An example here is the mitochondrial gene *SOD2* (manganese superoxide dismutase) which is responsible for detoxification of intracellular organelles but also has a role in regulating growth at high temperature [232]. Furthermore, temperature-regulated genes also tend to be a part of the

cryptococcal virulence composite. For instance, *AOX1, SOD1, SKN7 and MGA1* are previously identified virulence-associated genes whose transcription is regulated by temperature [93,185,233,234].

However, not all temperature regulated genes are clearly associated with virulence. One such example is CBP1 which has temperature regulated expression but is not clearly associated with virulence [235]. In contrast, genes can be essential for thermo-tolerance but their expression may not be temperature-regulated. An example of this is *CNA1* (calcineurin A subunit) [234,236,237].

Notably, there could be species/varietal-specific differences in transcriptional response to changes in temperature, as demonstrated for *COX1* [237]. High levels of expression of heat shock proteins (HSP60, HSP70 and HSP90) at 37^{o}C were detected in the serotype D strain B3501A but not in the serotype A H99 strain, suggesting that temperature as high as 37^{o}C is not necessary a stress condition for serotype A strains [230]. In fact, induction of HSP60, HSP70 and HSP80/90 at 37^{o}C does occur in low-iron environments, suggesting an interconnecting relation between iron concentrations in the host and regulation of heat shock proteins *in vivo* [230].

1.13.2. Response to oxidative stress

Phagocytic cells of the host innate immunity such as macrophages and neutrophils generate reactive oxygen (ROS) and nitrogen (RNS) species that are toxic to most invading pathogens, including *C. neoformans.* The oxidative stress defense mechanism of *C. neoformans* includes production of non-enzymatic antioxidants (melanin [238] and mannitol) and enzymatic antioxidants (peroxidases[239], catalases[240], superoxide dismutase[241], among others). The catalase family of *C. neoformans* consists of 4 members (*CAT1*-*CAT4*), whose deletion from the wild-type strain does not result in defects in oxidation resistance or mouse virulence[240], implying there is a degree of functional redundancy between this class and other components of the cryptococcal antioxidant defense system [240].

Another constituent of the antioxidant defense system in *C. neoformans* is the thiol-peroxidases (*TSA1* and *TSA2)*, which are essential for resistance to oxidation as well as virulence [223,242]. In addition, the disulfide reduction thioredoxins *TRX1* and *TRX2;* the thioredoxin reductase *TRR1*, are involved in the reduction and recycling of the oxidized, inactive form of peroxiredoxin as well as virulence and survival in macrophages[243]. Other enzymes that have antioxidative properties in *C. neoformans* include the glutathione peroxidases *GPX1* and *GPX2*[244], the cytosolic copper-zinc superoxide dismutase

(*SOD1*)[93], the mitochondrial manganese superoxide dismutase (*SOD2*)[232], the cytochrome c peroxidase (*CCP1*)[239] and the alternative oxidase (*AOX1*)[234].

1.13.3. Gene expression during phagocytosis by macrophages

It is the employment of stress response pathways that enable *C. neoformans* to survive and replicate following phagocytosis by host macrophages [245–249]. To elucidate the transcriptional profile under oxidative stress the fungal cell transcriptome is sequenced either after phagocytosis by macrophages or grown in nutrient rich YPD medium and treated with exogenous H_2O_2 [227,250]. The extent and pattern of the transcriptional response was found to be much weaker in the cells residing inside the macrophages compared to the robust transcriptional response observed in the cells treated with exogenous H_2O_2 in YPD medium, suggesting that the environment has a direct effect on the transcriptional response.

Gene expression profiling of *C. neoformans* upon phagocytosis by murine macrophages and *Acanthamoeba castellanii* have identified gene sets that are both up or down-regulated in both model systems, highlighting the similarities of the two intracellular niches[251]. Mitochondria-localized peroxidases, superoxide dismutases and catalases are among the most up-regulated genes upon phagocytosis of *C. neoformans* by murine macrophage[68]. A NADH-ubiquinone oxidoreductase, a zinc-binding oxidoreductase, a putative glutathione transferase and the flavohemoglobin denitrosylase gene *FHB1* are among the most highly-

upregulated [68]. *FHB1* has previously been associated with sensitivity to nitrosative stress and virulence in both murine macrophage and murine model of infection [252].

Phagocytosis also induced the up-regulation of a number of transmembrane transporters, believed to indicate increased metabolic activity in response to nutrient starvation in the phagosome [68,251]. Carbohydrates transporters are among the most induced, including the hexose transporter *ITR4* (homolog of JEC21 *ITR1*), and the glucose transporter *GTH1*, which is important for melanin production and virulence [68]. Other types of highly up-regulated transporters include those associated with nitrogen starvation (*AMT1* and *AMT2*), iron acquisition (*FET3* and *FTR1*) and peroxisomal protein transport/biogenesis (*PEX5* and *PEX7*).

Genes identified as essential for cryptococcal virulence were also induced during macrophage infection, including laccase (*LAC1* and *LAC2*), capsule production and modification genes (CAP10, *CAS1*, *CAS2*, *CAS31*, *CAS32*), the G protein α-subunit *GPA1*, the cAMP pathway (*PKA1*) and calcineurin (*CNA1*) [68]. Another interesting aspect of *C. neoformans* transcriptional response to phagocytosis in the murine macrophage *in vitro* is the repression of genes involved in the translation process (maintenance of the ribosome, processing of pre-rRNA, or translation initiation and elongation), which is presumably a result of nutrition starvation in the phagosome [69].

1.14. *C. neoformans* gene expression in humans at the site of infection

The bulk of our knowledge on the cryptococcal transcriptome is derived from carefully controlled *in vitro* experiments under specific test conditions, which enable sufficient biological and technical replication. While this produces reproducible and robust transcriptomics data, most experiments were conducted using a few well-characterized laboratory strains under specifically-defined *in vitro* conditions, and remains to be seen how these data would relate to complex *in vivo* conditions and human disease. Cryptococcal gene expression in the host is supposed to be both site and time specific [253]. For instance, it has been proposed that human cryptococcal meningitis involves at least six stages: (i) colonization and establishing infection in the lungs following the inhalation of infectious propagules; (ii) pulmonary yeasts survival and proliferation; (iii) dormancy of yeast cells in the host tissue; (iv) reactivation of latent infection with renewed yeast growth; (v) in-host dissemination of the yeasts; and finally (vi) growth of yeasts in brain tissue and the sub-arachnoid space. The transcriptional responses of *C. neoformans* would vary in response to the unique host tissue and stages of infection.

To date there is only one of study of *in vivo* cryptococcal gene expression in humans in the literature, reported by Chen and colleagues from Dr. John Perfect's research team at Duke University, North Carolina, USA [253]. This study involves comparative RNAseq profiling of

yeast pellets directly originated from human cerebral spinal fluid (CSF) samples and RNA from yeasts of the same isolates growth in either rich medium (Yeast Peptone Dextrose-YPD) or ex *vivo* human CSF. It was revealed that transcriptional profiles of yeasts in human CSF are highly similar to those cultured in YPD under *in vitro* conditions [253]. Gene ontology analysis of the differentially expressed genes in the patient's CSF and in YPD in comparison to cells grown in *ex vivo* human CSF indicated that the expression of genes in the cellular metabolism category increased, suggesting that yeast cells are actively growing in patient CSF. A number of up-regulated genes that were specific for the CSF condition were detected, including genes previously predicted to be essential for virulence. These included *SRX1*, which was involved in resistance to oxidative stress [254]; *ENA1* and *RIM101* which were important for cryptococcal virulence in animal models [255–257]. Further transcriptional profiling studies on a larger number of samples from human specimens at various stages of infection would be required to better understand cryptococcal gene networks and pathways involved in *in vivo* human pathogenesis.

1.15. Host immune response to cryptococcal infection

1.15.1. Role of cell-mediated immunity in response to cryptococcal infection

Understanding the host immune response to cryptococcal infection has the potential to improve disease management. Much of the current understanding of host immune response to cryptococcal infection came from various *in vitro* and animal studies. Cell mediated Immunity (CMI) contributes to fungal control and clearance through direct cytotoxic effects or immune regulatory effects of natural killer T cells (NKT) and T-lymphocytes. Various studies have demonstrated the essential roles of CD4+ and CD8+ T-cells in immune response against cryptococcal infection [258–265]. Secreted granulysin and perforin, which are expressed by both NKT cells, CD4+ and CD8+ T-cells, are involved in CMI-regulated killing of cryptococcal yeasts[258,262,266–268]. An IFN-γ/TNF-α–producing peripheral CD4+ T-cell stimulated by cryptocccal mannoprotein response was associated with increased concentrations of proinflammatory cytokines at the site of infection ,which was linked to better outcome [269].

The regulatory effect of CMI in cryptococcal infection is complicated and equally essential for fungal clearance since effective host immune response is essential for better outcome. Various studies in mice have linked the balance between Th1 (regulated by T helper cell type 1) and Th2 (regulated T helper cell type 2) cytokines and mortality [270–273]. While Th-1

cytokines such as TNF-α, IL-12 and Interferon γ (IFN- γ) confer better survival and fungal clearance in mice[274–278], Th2 cytokines such as IL-4, IL-5 and IL-10 were not protective[279–282]. M1-polarized macrophages associated with a Th1 response have been shown to be fungicidal while Th2-associated M2-polarized macrophages were not[283–285]. Interaction with host macrophages, which has been previously associated with cryptococcal persistence and dissemination in the host, is modulated by host cytokine response[272]. In addition, IL-17 and the Th-17 response has recently been associated with better fungal clearance in *C. neoformans* -infected mice[286,287].]

1.15.2. Role of B-cell immunity during cryptococcal infection

B-cell immunity was demonstrated to be involved in control of cryptococcal infection at different stages/site of infection. For example, studies of B-cell response in B-cell-deficient SCID mice suggest B-cell immunity also plays an important role in the brain when T-cell immunity is impaired [288]. The fact that B-cells are the most prevalent lymphocytes in the lungs of *C. neoformans* -infected A/JCr mice [289] and that B-cell-deficient C57BL/6J mice resulted in higher mortality and increased pulmonary pathology [290] suggest that B-cells play an active role in modulating immune response in the lung.

Another role of B-cells is to produce “natural occurring” IgM antibody that has an intrinsic ability to bind conserved fungal cell wall components such as α- and β-glucans [291]. It has

previously been shown that peripheral blood IgM memory B cell levels were lower in HIV-infected individuals who developed cryptococcal disease than in those who did not [292] and that HIV-infected patients had lower levels of serum GXM-binding IgM than did HIV-uninfected individuals [293].

1.15.3. Cytokine response in human infection

Data from humans are limited. The fact that individuals with underlying immunosuppressive conditions, especially HIV/AIDS, are most susceptible for cryptococcal infection suggests that cell-mediated immunity (CMI) plays a central role in host defense against cryptococcosis. Disease in HIV infected patients is associated with advanced disease and profound immunosuppression. The median CD4 count in HIV infected patients in Vietnam is less than 20 cells per mm^3 (normal range 500 – 1500 cells/mm^3 [294,295]. Patients with HIV-associated cryptococcal meningitis presenting with high fungal burdens in cerebrospinal fluid (CSF) and slow rates of yeast clearance had lower levels of proinflammatory TNF-α , IFN- γ and IL-6 in the CSF [296]. Diminished Th1 response in HIV-infected patients [297] and increased levels of Th2 cytokines in organ-transplant patients[298] imply that the Th1/Th2 balance plays a role in determining the risk of infection and disease outcome. However, while animal studies support the Th1/Th2 dichotomy, its association with disease outcome in late stage HIV-infected patients with cryptococcal meningitis is less apparent[269]. This likely reflects the

discrepancy between controlled conditions of experimental animal models and the complexity of human disease, especially with regards to late-stage HIV infection.

1.16. *C. neoformans* var. *grubii* infection in immunocompromised hosts

The vast majority of cryptococcal disease is due to infection with *C. neoformans* and is associated with immunosuppressive conditions including HIV/AIDS, malignancy, organ transplantation, chronic organ failure and immunosuppressive therapy. Globally, HIV/AIDS remains the primary risk factor for cryptococcal disease despite the available of antiretroviral therapy. Global cryptococcal disease burden is most severe where there is high number of people with HIV/AIDS infection, especially in Sub-Saharan Africa or Southeast Asia [1]. The first estimation of the global annual incidence of cryptococcosis was about 957,900 cases per year (range 371,700–1,544,000) resulting in 624,700 deaths by 3 months after infection [1]. However this estimation was conducted using data from before the widespread use of ARTs. The global introduction of effective antiretroviral therapy (ART) has helped reduce the number of newly acquired HIV infection but at the same time increase the number of people living with AIDS [9]. This, along with increasing number of solid organ transplantation and immunosuppression therapy in recent decades, mostly in developed countries, represent an

increasing human population with immunosuppression highly susceptible to cryptococcal disease.

A new study in 2017 that takes into account the vastly changed landscape of the global HIV epidemiology and involves more new data estimates that 278,000 people have cryptococcal antigenaemia every year, with 73% of meningitis cases occurring in sub-Saharan Africa [2]. Global incidence of cryptococcosis is summarized in **Figure 1.16-1**. Other known underlying immunosuppressive conditions include prolonged treatment with corticosteroids, organ transplantation, advanced malignancy, diabetes, sarcoidosis and idiopathic CD4 lymphocytopenia [5,16,78,299,300].

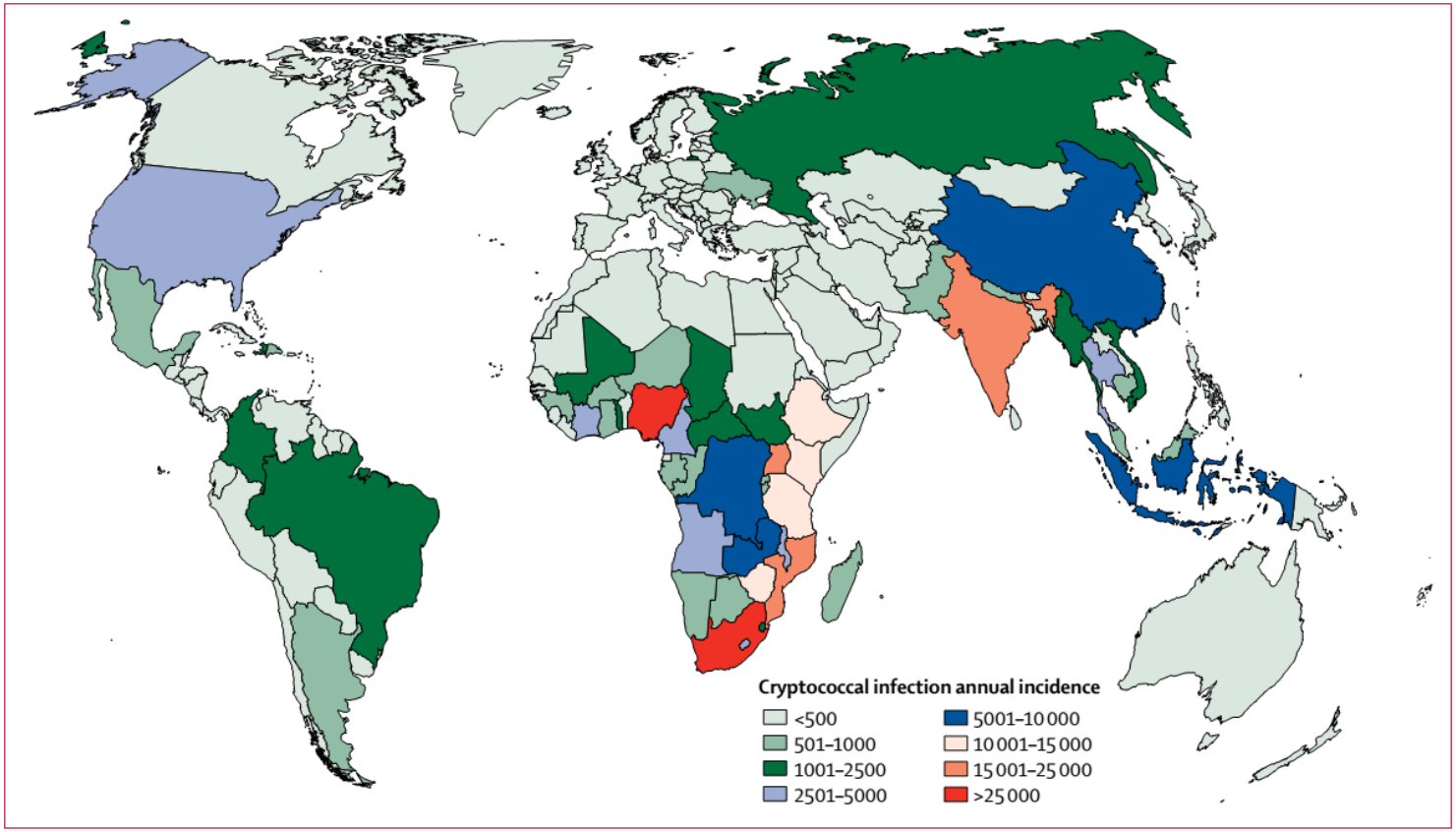

Figure 1.16-1. Global estimation of annual incidence of cryptococcosis (the number of people positive with antigenaemia) according to country in 2014 (adapted from Rajasingham *et al*. 2017) [2].

1.17. *C. neoformans var*. *grubii* infection in apparently immunocompetent hosts

1.17.1. Global epidemiology of *C. neoformans var*. *grubii* infection in apparently immunocompetent hosts

Cryptococcal disease in immunocompetent hosts is often attributed to *C. gattii*, which is now considered a primary human pathogen [301–305]. This species is well recognized in the tropics, has most usually been associated with immunocompetent patients, and is infrequently found in HIV infected patients even in highly HIV-endemic regions [301,302,306].

Less frequently, disease in apparently healthy individuals due to *C. neoformans is* reported. In particular, disease in HIV uninfected apparently immunocompetent patients has been reported form Vietnam, Australia, China and elsewhere in Asia. For instance, the incidence of cases in immunocompetent patients due to *C. neoformans* in Australia from 1994 to 1997 was higher than *C. gattii,* except for in the tropical Northern Territories [301]. In East/Southeast Asia, the majority of disease in HIV uninfected patients is due to *C. neoformans* var. *grubii*, even in tropical areas where *C. gattii* would be expected to be more common [107,109,111,307]. In contrast to Thailand in Southeast Asia where the majority of reported cases of cryptococcosis are associated with HIV infection [92,102]; most cases

reported from China and Japan were from HIV-uninfected patients [103,105–107,109,307–312]. Though some of these patients may have other underlying immunosuppressive diseases, a significant number are from patients with no apparent immune defects. For instance, a retrospective epidemiological analysis of cryptococcal meningitis in China from 1981 to 2013 reported that 40% of cases occurred in otherwise apparently healthy patients without any obvious immunosuppressive condition. 21% were HIV-associated and the remaining 39% occurred in HIV-uninfected patients with other underlying diseases [310]. This contrasts with the US, where cases in apparently immunocompetent hosts account for 17% to 22% of the reported total number of cases in patients without HIV infection or organ transplantation [313].

1.17.2. Proposed mechanisms of *C. neoformans* var. *grubii*-associated infection in apparently immunocompetent individuals

While mechanisms such as intracellular parasitism and atypical mitochondrial morphology have been linked to increased virulence in *C. gattii* infection in immunocompetent hosts [8,138,314–316], it is less clear how *C. neoformans* var. *grubii* causes disease in the immunocompetent. Several potential mechanisms have been proposed. For example, given that *C. neoformans* var. *grubii* co-exist in similar environments and can both cause mammalian infection, it is possible *C. neoformans* var. *grubii* has acquired features

associated with infecting immunocompetent hosts from *C. gattii,* possibly through mating. In fact, clinical hybrid isolates of *C. neoformans* (both serotype A and D) and *C. gattii* have been described and reported [317–319]. However these hybrids are rare - a large scale screening of over 350 international clinical isolates only identified 4 serotype A/B hybrid strains, suggesting that mating between species is extremely rare [320]. Furthermore, where hybridization with *C. gattii* has occurred it has not been associated with increased virulence of *C. neoformans* var. *grubii* [321].

Previously, regulation of the cAMP signaling system has been associated with changes in virulence phenotype of *C. neoformans* var. *grubii*. Mutants lacking the downstream repressor *pkr1* are hypervirulent in mice [200,321–323]. However, no association between *pkr1* and in the ability to cause disease in apparently healthy patients has been seen. Exactly how *C. neoformans* var. *grubii* strains can infect and cause disease in immunocompetent patients is still unknown.

The mechanisms of cryptococcal virulence is highly complex and diverse, as reflected by considerable genomic plasticity and phenotypic variations [113,148,324–330]. Variation in the expression of known virulent including the capsule, susceptibility to antifungal drugs, anti-phagocytosis mechanisms, and others are also well-documented [331–336]. High degree of phenotypic variation among closely related strains suggests that some of these strains may

also be inherently more virulent than others. The fact that ST5 strains (synonymous to the AFLP-defined cluster VNI-γ in Vietnam which is later characterized as ST5 in Chapter 2 of this thesis) from China and Vietnam infect both HIV-infected and HIV-uninfected patients as well as being the most prevalent genotype isolated from HIV-uninfected patients implies that the virulence composition of an infecting strain may play equally essential roles as the host's defenses. The genetic makeup of a strain i.e. a genotype or lineage may be associated with higher prevalence or mortality in a host group. For example, MLST typing of HIV-associated pediatric isolates *C. neoformans* var. *grubii* (VNI) from South Africa revealed that boys are more likely to be infected with ST8 than girls while other STs were equally distributed between both sexes [337]. MLST genotyping also suggested an association between ST93 and its closely related variants with higher mortality in Ugandan HIV-associated patients with cryptococcal meningitis, compared to ST4 or ST5 isolates [338]. However, genotype as a standalone factor cannot explain for the complexity of cryptococcal virulence. For instance, clinical *C. neoformans* var. *grubii* isolates were more virulent in mice than environmental isolates while having the same MLST genotypes [339]. On the other hand, it is important to keep in mind that disease in human hosts is more complicated and dynamic than in well-controlled animal models. While HIV-associated CM patients appear uniformly immunosuppressed, non HIV-associated CM patients represent a more immunologically heterogeneous population with or without subclinical innate or acquired immunodeficiency.

Therefore, phenotypic variation among strains with the same genotype, especially with regard to infection in apparently immunocompetent patients, may indicate a role for microevolution within the host. Alternatively, phenotypic variations among a single cryptococcal lineage could have been a result of adaptation to diverse selection forces in the environment.

1.17.3. Epidemiology of *C. neoformans* var. *grubii*-associated infection in apparently immunocompetent patients in Vietnam

In the tropical setting of Vietnam, *C. neoformans* var. *grubii* accounts for the vast majority of cases, regardless of HIV status [307]. Over 70% of cases in HIV-uninfected patients (total n=57), most of whom had no obvious underlying immunosuppressive conditions, were attributed to *C. neoformans* var. *grubii* while the remaining cases were caused by *C. gattii* [307]. Mortality rate among this patient group at discharge is 19% with 20% of survivors affected by blindness [307]. All *C. neoformans* var. *grubii* isolates from HIV-uninfected and HIV-infected patients in Vietnam were URA5 molecular type VNI [103]. Subsequent AFLP-genotyping of 144 representative isolates from both HIV-infected and HIV-uninfected defined two major clades of *C. neoformans* var. *grubii* (termed VNI-γ and VNI-δ) [103]. 84% of infections in HIV uninfected patients were due to VNI-γ strains; this compared with HIV infected patients, where only 38% of strains were from this cluster (odds ratio 8.30; 95%

confidence interval (CI): 3.04 to 26.6; $p<0.0001$) [103]. Moreover, in HIV-uninfected patients with VNI-γ infection, underlying disease was less common than in patients with VNI-δ infection, occurring in 23% versus 67% (odds ratio 6.43; 95% CI: 0.75 to 85.1; $p = 0.05$) [103]. No association was found between HIV risk group, age, gender or temporal/geographic distribution and AFLP cluster [103].

The fact that a clonal group of *C. neoformans* var. *grubii* isolates were found in apparently healthy hosts with no underlying immunosuppressive conditions suggests that these isolates derived from a lineage with increased pathogenicity. The fact that a smaller number of organisms were able to induce the same degree of mortality, as reflected by lower baseline VNI-γ fungal burden in CSF and similar patients survival rate [325], would also suggest higher pathogenicity of the VNI-γ organisms. The lower prevalence of VNI-γ isolates in HIV-infected patients could be explained by their potentially lower environmental prevalence due to their association with a rare and unique environmental niche, compared to VNI-δ. This hypothesis is highly plausible since cryptococcal virulence in mammals and human hosts has been considered an effect of survival adaptation to environmental stresses [94,112,340,341]. Alternatively, since higher number of CM cases in apparently healthy hosts due to *C. neoformans* var. *grubii* were reported in China, Japan, Korea and Vietnam than any other locations, it is possible that there are as yet unidentified host factors specific to

East/Southeast Asians that contribute to higher susceptibility to cryptococcal disease among these populations.

1.18. Aims of the thesis

Cryptococcosis has long been associated with HIV/AIDS and other immunosuppressive conditions. In Asia and Vietnam *C. neoformans* var. *grubii* is the main variety accounted for the majority of cryptococcosis cases. However in Vietnam we also observe high number of cases in apparently immunocompetent, HIV-uninfected patients caused by *C. neoformans* var. *grubii,* which is highly unusual. Given that the strains that cause disease in immunocompetent patients are largely derived from a single AFLP defined cluster, we hypothesize that strains of this cluster have increased virulence potential. The research questions resolved in this thesis was developed from this main hypothesis. The specific questions and aims of this study, with corresponding hypotheses when available, are as follow. (Data chapter 2 and data chapter 4 were purely exploratory thus no hypotheses were stated)

1. **What is the genetic structure of clinical *C. neoformans* var. *grubii* isolates in Vietnam and Laos? How do they relate to the global population?**

This is an exploratory chapter aiming to describe the population structure of clinical *C. neoformans* var. *grubii* isolates from HIV-infected and HIV-uninfected patients from Vietnam and the neighboring country Laos using Multilocus Sequence Typing (MLST). The emphasis would be to integrate the Vietnamese/Laos *C. neoformans* var. *grubii* population structure into the global context.

2. **What phenotypic differences distinguish the lineage that causes disease in immunocompetent hosts (VNI-γ) from other Vietnamese lineages?**

Hypothesis: VNI-γ strains are more virulent than VNI-δ strains

I aim to compare *in vitro* phenotypes previously associated with virulence between strains of the lineages that can and cannot cause disease in immunocompetent patients. I will use a mouse model of infection to compare strains of different lineage *in vivo* including tissue dissemination, host survival, immune responses, and pathological patterns.

3. **Does a macrophage model of infection distinguish lineages that can and cannot cause disease in immunocompetent patients?**

Hypothesis: *in vitro* macrophage parasitism could predict and indicate lineage-specific virulence potential.

While animal models are a useful tool to study pathogenesis and virulence, they are expensive, time-consuming, and ethically complex. This limits the number of strains that can be tested, and therefore effects that are significant at the population level can be missed if there is significant within lineage variability. Previous studies with outbreak *C. gattii* strains have shown that *in vitro* intracellular proliferation rate (IPR) in macrophages is associated with increased mortality in mice. Therefore, in the thesis I adapt the established *in vitro* macrophage model for higher throughput to compare IPR and yeast uptake of macrophages for *C. neoformans* var. *grubii* isolates from HIV-infected and HIV-uninfected patients in Vietnam.

4. **What are the differences in transcription that distinguish lineages that affect immunocompetent patients from those that only affect the immunosuppressed?**

C. neoformans var. *grubii* isolates from HIV-infected and HIV-uninfected patients in Vietnam are mostly identical i.e. strains from both groups possess all known cryptococcal virulence factors and are both pathogenic to human hosts. While comparative genomics has revealed a homology as well as unique genetic features between *C. neoformans* var. *grubii* isolates from HIV-infected and HIV-uninfected patients, little is known about how strains from each genotype regulate their genes. We aim to study genotype-specific patterns of gene expression at baseline by investigating gene expression profiles of representative strains

from each genotype during normal *in vitro* growth conditions. These results would help generate more hypotheses for further investigation of cryptococcal virulence.

Chapter 2

POPULATION STRUCTURE OF *CRYPTOCOCCUS NEOFORMANS* VAR. *GRUBII* FROM VIETNAM IN A REGIONAL AND GLOBAL CONTEXT

2.1. Chapter 2 Introduction

The clinical and environmental *Cryptococcus neoformans* var. *grubii* isolates from South, East and Southeast Asia exhibit a clonal population structure[101,103]. Multilocus Sequence Typing (MLST) epidemiological studies from East Asia have shown limited genetic diversity among the majority of environmental and clinical isolates [104,106,111]. Different geographical areas have distinct population structures, particularly in relation to the predominant sequence types [101]. Previous studies suggested that though in relatively close geographical proximity, the population structure of *Cryptococcus neoformans* var. *grubii* from Thailand and China are significantly different [92,342]. We recently reported the population structure of *Cryptococcus neoformans* var. *grubii* from Vietnam [325], but analyses were focused on associations between clinical features and population structure. My specific goals were (i) to describe the genetic structure of the Laotian *Cryptococcus neoformans* var. *grubii* population using MLST, and (ii) to set the Vietnamese and Laotian populations within the global context.

2.2. Chapter 2 Materials and Methods

2.2.1. Ethics statement

All studies from which samples were derived were approved by the relevant institutional review board: the Hospital for Tropical Diseases Ethical Review Board, Ho Chi Minh City, the National Ethics Committee for Health Research Viet Nam, the Ministry of Health, Lao PDR, and either the Oxford Tropical Ethics Committee, University of Oxford, or the Ethics Committee of the Liverpool School of Tropical Medicine. All patients were adults and gave written informed consent to enter the clinical studies. Where the patient lacked capacity to consent through illness, the written consent of the responsible next of kin was obtained. All clinical data and samples were anonymized.

2.2.2. Patients and isolates

The Vietnamese isolates (total n=136) included in this work were clinical isolates from the cerebrospinal fluid (CSF) of patients enrolled in a randomized controlled trial of antifungal therapy in HIV-infected patients (n=98) between 2004 and 2011, and a prospective, descriptive study of HIV-uninfected patients with central nervous system (CNS) infections (n=38) enrolled between 1998 and 2009 [103,307]. The Laotian isolates were from 81 patients with cryptococcal meningitis (67 HIV-infected, 8 HIV-uninfected and 6 with unknown

HIV status) consecutively admitted to Mahosot Hospital, Vientiane, between 2003 and 2015.

2.2.3. DNA extraction and Restriction Fragment Length (RFLP)

Total genomic DNA was extracted from all organisms using the Masterpure Yeast DNA kit (Epicentre Biotechnologies, Madison, WI, USA) according to the manufacturer's instructions. Restriction fragment length polymorphism analysis (RFLP) of the orotidine monophosphate pyrophosphorylase (URA5) gene was used to confirm species/varietal status of all *C. neoformans* var. *grubii* isolates [343]. PCR of the URA5 gene was conducted in a final volume of 50 µL. Each reaction contained 50 ng of DNA, 1X HotStart PCR buffer (NEB, USA), 0.2 mM each of dATP, dCTP, dGTP, and dTTP (Roche Diagnostics GmbH), 2 mM magnesium acetate, 0.5 U HotStart Taq DNA polymerase (NEB, USA), and 0.15 µM of each primer URA5 (5'- ATG TCC TCC CAA GCC CTC GAC TCC G - 3') and S01 (5'- TTA AGA CCT CTG AAC ACC GTA CTC - 3'). PCR was performed in an Nexus SX1 thermal cycler (Eppendorf, USA) at 95°C for 15-min, followed by 35 cycles of 20s denaturation at 94°C, 40s annealing at 61°C, and 1 min extension at 72°C, followed by a final extension cycle for 3 min at 72°C. 10 µL of PCR products were double digested with Sau96I (0.2 U/µL) and HhaI (0.8 U/µL) for 3 h at 37^{o}C, followed by a final 10min incubation at 60^{o}C. Restriction products are separated by 3% agarose gel electrophoresis at 100 V for 5 h. RFLP patterns were assigned visually by comparing them

with the patterns obtained from the control strains (VNI-VNIV and VGI-VGIV) kindly provided by Prof. Wieland Meyer, University of Sydney.

2.2.4. Multilocus Sequence Typing (MLST)

Seven MLST loci (CAP59, GPD1, IGS1, LAC1, PLB1, SOD1, and URA5) were amplified and sequenced following the procedures of the International Society for Human and Animal Mycology (ISHAM) MLST consensus typing scheme for *C. neoformans* (http://mlst.mycologylab.org) [30]. Sequencing was performed using BigDye v3.1 Chemistry (Applied Biosystems, CA, USA) on an ABI 3130 Genetic Analyzer (Applied Biosystems, CA, USA). Both forward and reverse amplicons of each locus were sequenced. Consensus sequences were manually edited using ContigExpress and aligned in AlignX , implemented in VectorNTI Suite 7.0 [344]. A single Allele Type (AT) number was assigned to each of the seven loci by comparing consensus DNA sequences with the ISHAM database, resulting in a seven-number allelic profile for each isolate. The allelic profiles defined the corresponding STs.

MLST profiles and DNA sequences at each MLST loci for isolates from regions other than Laos and Vietnam were obtained from NCBI. For the global analysis, we used data reported by Simwami *et al.* [92], Mihara *et al.* [107] and Cogliati *et al.* [152] included in Khayhan *et al.* [101], and from Chen *et al.* [82], Ferreira-Paim *et al.* [151], Beale *et al.* [345]and Dou *et al.* [105].

2.2.5. Phylogenetic analyses

For global comparison, information on MLST genotypes, patient HIV status, and source of isolation for 1047 isolates from other countries across Asia and Southern Africa were obtained from NCBI [82,92,101,107,152]. These consisted of clinical and environmental *C. neoformans* var. *grubii* isolates from Southeast Asia (Indonesia, Thailand, Vietnam); East Asia (Japan, China, South Korea); South Asia (India), Middle East (Qatar, Kuwait); North America (USA); South America (Brazil, Argentina); Europe (Germany, Italy, France, Belgium); Australasia (Australia) and Africa (Botswana, Malawi, Tanzania, Uganda, Zaire, South Africa). Further details of the isolates information are presented in **Appendix 1** .

First, we determined the best DNA substitution model for the concatenated dataset using MEGA v6.0.6 [346]. The Kimura 2-parameters model with gamma distribution was selected as the best fit model using the Bayesian information criteria (BIC) calculated with MEGA v6.0.6 [346]. To evaluate patterns of evolutionary descent among genotypes according to their source and geographic region, the allelic profile of the Vietnamese, Laos and global dataset were applied to the goeBURST algorithm in PHYLOVIZ 2.0 software available at http://www.phyloviz.net [347,348]. A group founder was defined as the sequence type with the most number of linked single locus variants (SLV). The concept of a clonal complex (CC) was adopted when a SLV linkage with the founder ST was observed.

2.2.6. Multidimensional (MDS) clustering

Genetic distance (Fst) and geographical distance were visualized by the non-metric multidimensional scaling method. Fst were calculated from concatenated sequences of the 7 MLST housekeeping genes using DnaSP v5 [349]. MDS calculation was performed using RStudio Version 0.98.1103 built with R-3.4.0 (https://www.rstudio.com and https://www.r-project.org). Network analysis and visualization was conducted using the R package *igraph* (version 1.1.2, http://igraph.org/r/).

2.3. Chapter 2 Results

2.3.1. MLST reveals dominance of ST4 and ST6 sequence types in Laos

All isolates from Vietnam were previously determined as molecular type VNI by RFLP, mating type α [350]. The 136 Vietnamese isolates consisted of 13 different sequence types (ST) of which ST5 (n=66; 48%) and ST4 (n=32; 23%) were the most prevalent, followed by ST6 (n=12; 9%), ST93 (n=8; 6%), ST32 (n=7; 5%), ST39 (n=3; 2%) and 7 less common STs with less than 3 isolates each. Of 13 STs detected in Vietnam, were previously undefined in the MLST database: ST306, ST338, ST339 and ST340. These 4 STs were singletons, each accounting for <1% of the total number of isolates. Isolates from the AFLP-defined VNI-γ cluster were ST5 while those from the VNI-δ were attributed to all other STs in the Vietnamese population.

All 81 Laotian isolates belonged to the RFLP-defined VNI group. Among them, ST4 and ST6 accounted for over 40% each of the total number of isolates, and were 4-fold more prevalent than ST5; (ST4, n=35 (43%); ST6, n=33 (41%); ST5, n=9 (11%), **Figure 2.3-1** and **Table 2.3-1**). Less than 3% of isolates from Laos (n=2) were ST93. This contrasted with its adjacent neighbor, Vietnam, where ST5 predominated (48%), followed by ST4 (24%), ST94 (9%) and ST6 (9%).

Table 2.3-1. Distribution of major Sequence Types (ST) in the Asia/Middle East regions

Country/ HIV status	Sequence Type (ST)*															
	4	**5**	**6**	**31**	**32**	**39**	**53**	**69**	**93**	**174**	**177**	**187**	**188**	**194**	**195**	**306**
China		**104**		**1**			**5**		**1**					**2**	**1**	
HIV(-)		80		1			4		1					1		
HIV(+)		24					1							1	1	
India	**1**		**2**	**7**					**28**	**3**	**1**	**1**				
HIV(-)	1			4					6	2	1	1				
HIV(+)			2	3					22	1						
Indonesia	**8**		**10**					**2**	**16**		**3**					
HIV(-)											1					
HIV(+)	8		10					2	16		2					
Japan		**20**														
HIV(-)		20														
HIV(+)																
Kuwait	**1**	**2**						**1**	**1**	**1**						
HIV(-)		2						1		1						
HIV(+)	1								1							
Laos	**32**	**8**	**32**						**1**			**1**				**1**
HIV(-)	3	2	2						1							
HIV(+)	29	6	30									1				1
Qatar	**1**	**2**		**2**												
HIV(-)		1		2												
HIV(+)	1	1														
Thailand	**64**	**20**	**57**						**3**							
HIV(-)	2								1							
HIV(+)	62	20	57						2							
Vietnam	**32**	**66**	**12**		**7**	**3**			**8**				**2**		**1**	**1**
HIV(-)	3	31	1		2											1
HIV(+)	29	35	11		5	3			8				2		1	
Total	**139**	**222**	**113**	**10**	**7**	**3**	**5**	**3**	**58**	**4**	**4**	**2**	**2**	**2**	**2**	**2**

(*): any minor sequence type with only one isolate was excluded from this

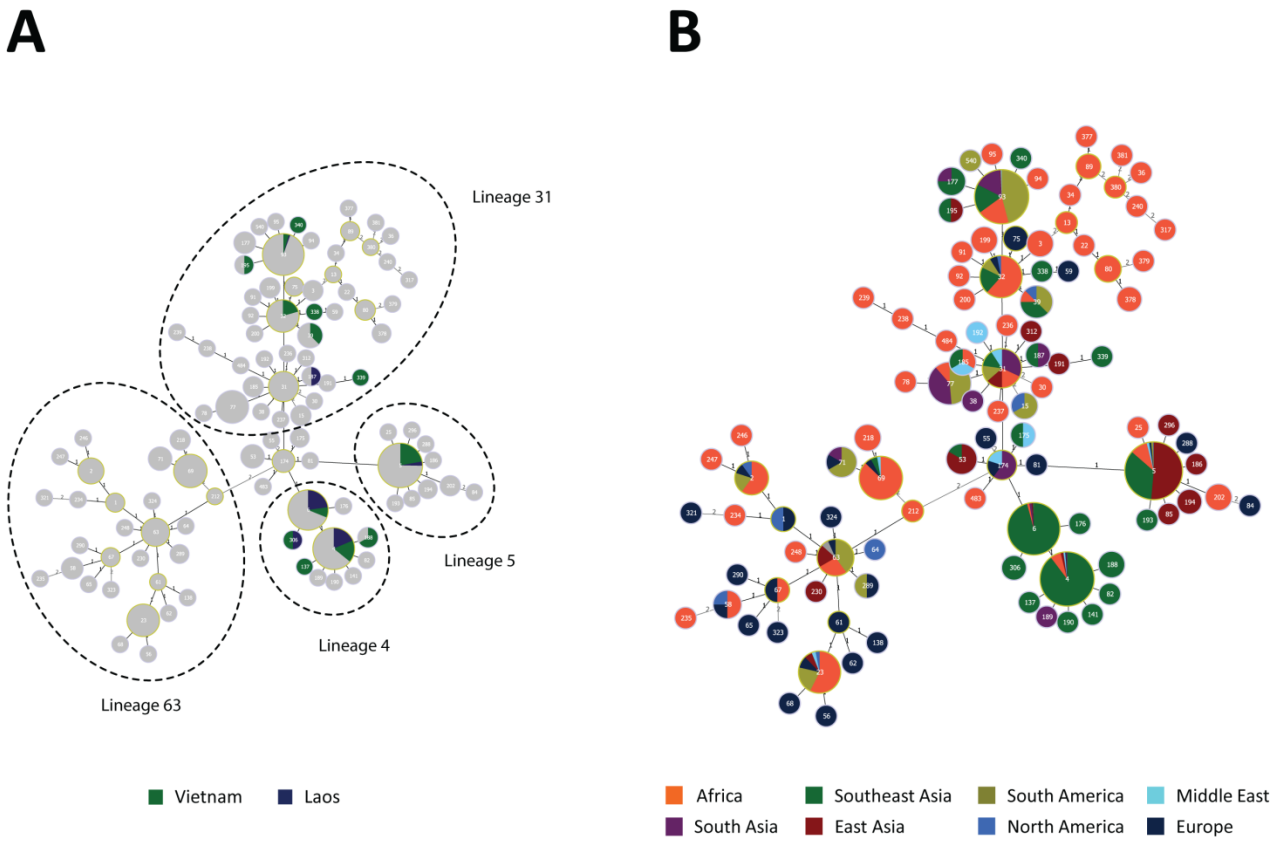

Figure 2.3-1. goeBURST analysis integrating the Laotian and Vietnamese *C. neoformans* var. *grubii* isolates into the major Asian clonal complex. Minimum spanning tree showing the major Asian clonal complex. (A): Laos and Vietnam as part of the global population. The main subgroups of the major clonal complex are indicated by circles. (B): the major clonal complex broken down into geographical regions: East Asia (China and Japan), Southeast Asia (Vietnam, Laos, Thailand and Indonesia), South Asia (India), plus the reference groups Middle East (Qatar and Kuwait), Europe, North/South America and Africa.

2.3.2. Correlation between infection with ST5 and HIV status

Isolates of ST5 have previously been reported to be associated with HIV uninfected patients in East Asia and Vietnam [103,106,107,307,312]. Most cases of cryptococcal meningitis in Laos were associated with HIV infection. The ST5 lineage accounted for just 9% (6 of 67) of infections in HIV infected patients, suggesting a relatively low prevalence in the environment. Of 8 cases of meningitis in Laos in HIV uninfected patients, 2 were due to ST5 isolates (Odds Ratio 3.39 [95%CI: 0.56 to 20.64], p=0.18, Fisher's exact test). HIV serostatus was not known for the remaining 6 patients.

To increase the power to test an association between ST5 isolates and HIV infection, I gathered previously described data from Asia, Europe, South America and Africa on lineage and patient HIV serostatus [82,101,325,345]. Clinical isolates with unknown HIV status were excluded from the analysis. Of 194 HIV uninfected patients, 136 (70%) were infected with ST5 isolates; of 791 HIV infected patients, 117 (15%) were infected with ST5 isolates (Odds Ratio 13.51 [95%CI: 9.38 to 19.45], p<0.0001, Fisher's exact test). There were 296 clinical or environmental ST5 isolates in the dataset; East and Southeast Asia accounted for the majority of these (n=153 (51%) and n=104 (35%), respectively). Here, the relative proportion of ST5 isolates from each country decreased along a clockwise arc from Northeast to Southwest: Japan (n=36; 86%, 95%CI: [72 - 94]), China (n=116; 86%, 95%CI: [80 - 92]), Vietnam (n=66; 48%, 95%CI: [40 - 57]), Thailand (n=29; 13%, 95%CI: [9 - 18]) and Laos (n=9; 11%, 95%CI: [5 - 20]). ST5 accounted for 20% (n=2) and 40% (n=2) of the total number of

isolates from Kuwait and Qatar in the Middle East, respectively. The majority of cases of disease in apparently immunocompetent, HIV-uninfected patients were from East and Southeast Asia. ST5 has been reported from elsewhere, including Brazil (n=3; 2%, 95%CI: [5 – 7]), South Africa (n=27; 15%, 95%CI: [10 - 22]), Uganda (n=1; 6%, 95%CI: [0 - 30]) and Botswana (n=1; 0.7%, 95%CI: [0.0 – 3.7]), but in these regions disease in HIV uninfected patients due to the type has rarely been reported [82,151,345].

2.3.3. goeBURST analysis and geographical distribution

I used the previously published data to elucidate how the Laotian and Vietnamese populations fit in the wider global context [82,101,104,151,345]. GoeBURST analysis placed *C. neoformans* var. *grubii* isolates from Vietnam and Laos, along with those from all other Asian, North/South American, Middle Eastern and African countries in a clonal complex (**Figure 3.2-1**). The main clonal complex included 3 main goeBURST sub-groups derived from ST174; sub-group 63 (ST63), sub-group 4 (ST4/ST6), sub-group 5 (ST5) and sub-group 31 (ST31/ST32/ST93) (Fig 1A). Sub-group 63 was a Double Locus Variant (DLV) from ST174 and was more distant to the other 3 sub-groups. While most South African and Ugandan isolates were included in the main clonal complex, the bulk of isolates from Botswana were separated from the major clonal complex by at least 5 SLVs. ST174 was placed at the center of the clonal complex and was identified as a potential group founder of the clonal complex when analyzed by both parsimony (**Figure 2.3-1**) and maximum likelihood analyses (**Figure 2.3-2**).

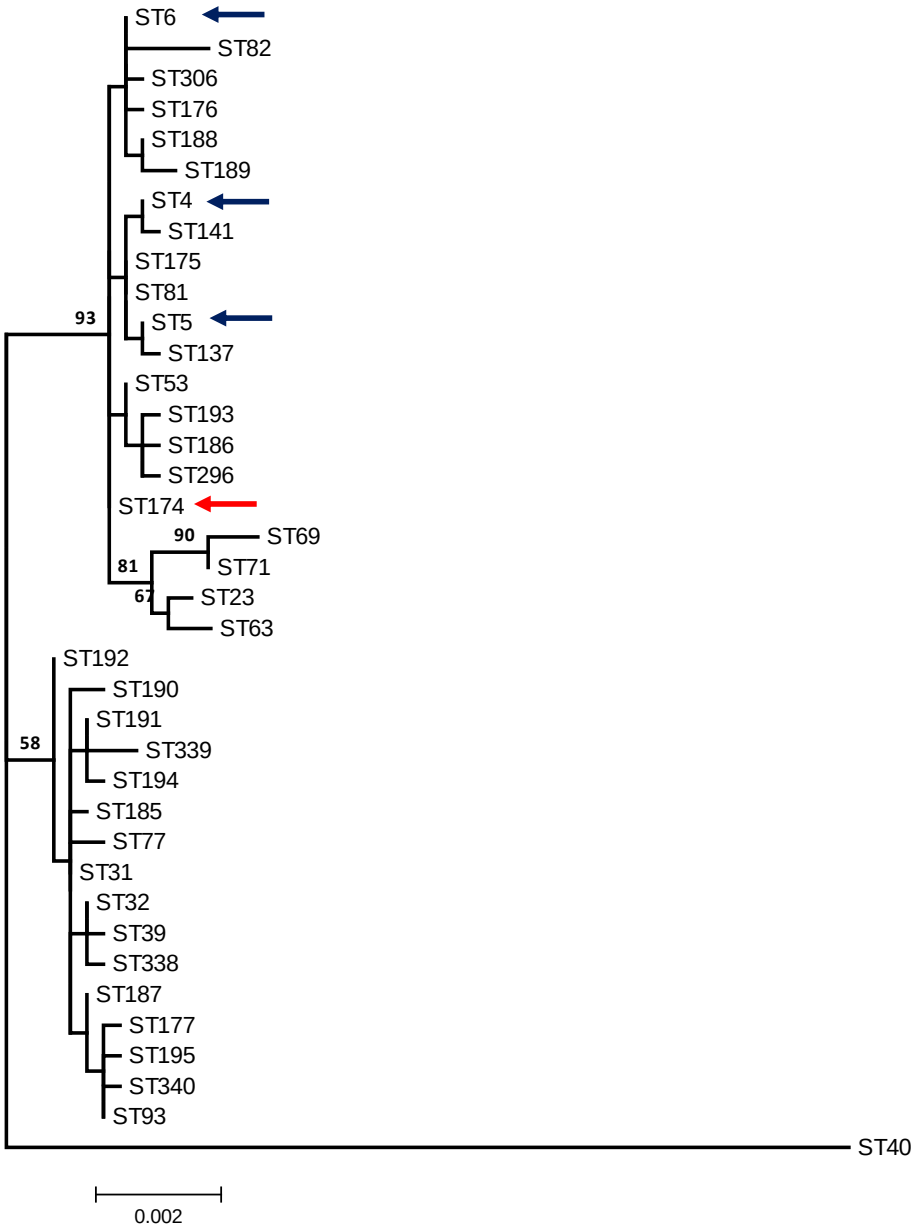

Figure 2.3-2. Molecular Phylogenetic analysis by Maximum Likelihood method.
The evolutionary history was inferred by using the Maximum Likelihood method based on the Kimura 2-parameter model. The tree with the highest log likelihood (-6364.7916) is shown. The percentage of trees in which the associated taxa clustered together is shown above the branches. Bootstrap values over 50% were shown. ST174 was indicated by red arrow and ST4/ST5/ST6 by dark blue arrow. ST174 is suggested to be the most recent ancestor observable for ST4, ST5 and ST6 lineages.

I observed an association between geographical location and STs (**Figure 2.3-1**). Most Asian isolates were included in sub-group 4 and sub-group 5 while isolates from other regions were widely distributed across the clonal complex. Sub-group 63 included European, North/South American, African, as well as a few East Asian isolates, but none from Southeast Asia. While sub-group 4 was reported from other continents, it was highly prevalent in Southeast Asia (n=317, 66% of all Southeast Asian isolates (total N=479)). Isolates from sub-group 5 had a wide distribution but in different proportions depending on the geographical regions: the Middle East (n=4; 33% (regional total N=15)), Africa (n=33; 10% (regional total N=346)), Europe (n=5; 13% (regional total N=39)), North America (n=1; 11% (regional total N=9)), South America (n=3; 2% (regional total N=133)), Southeast Asia (n=105; 22% (regional total N=479)) and most notably from East Asia (n=158; 88% (regional total N=180)). Similarly, sub-group 31 was also widely distributed but was most prevalent in South America (n=110; 83% (regional total N=133)) and South Asia (n=53; 85% (regional total N=62)). Other regions with sub-group 31 populations included Africa (n=86; 25% (regional total N=346)), the Middle East (n=4; 27% (regional total N=15)), North America (n=3; 33% (regional total N=9)), Europe (n=6; 15% (regional total N=39)). Sub-group 31 was much less common in East Asia (n=6; 3% (regional total N=180)) and Southeast Asia (n=52; 11% (regional total N=479)).

2.3.4. Genetic distance between *C. neoformans* populations from different geographical regions

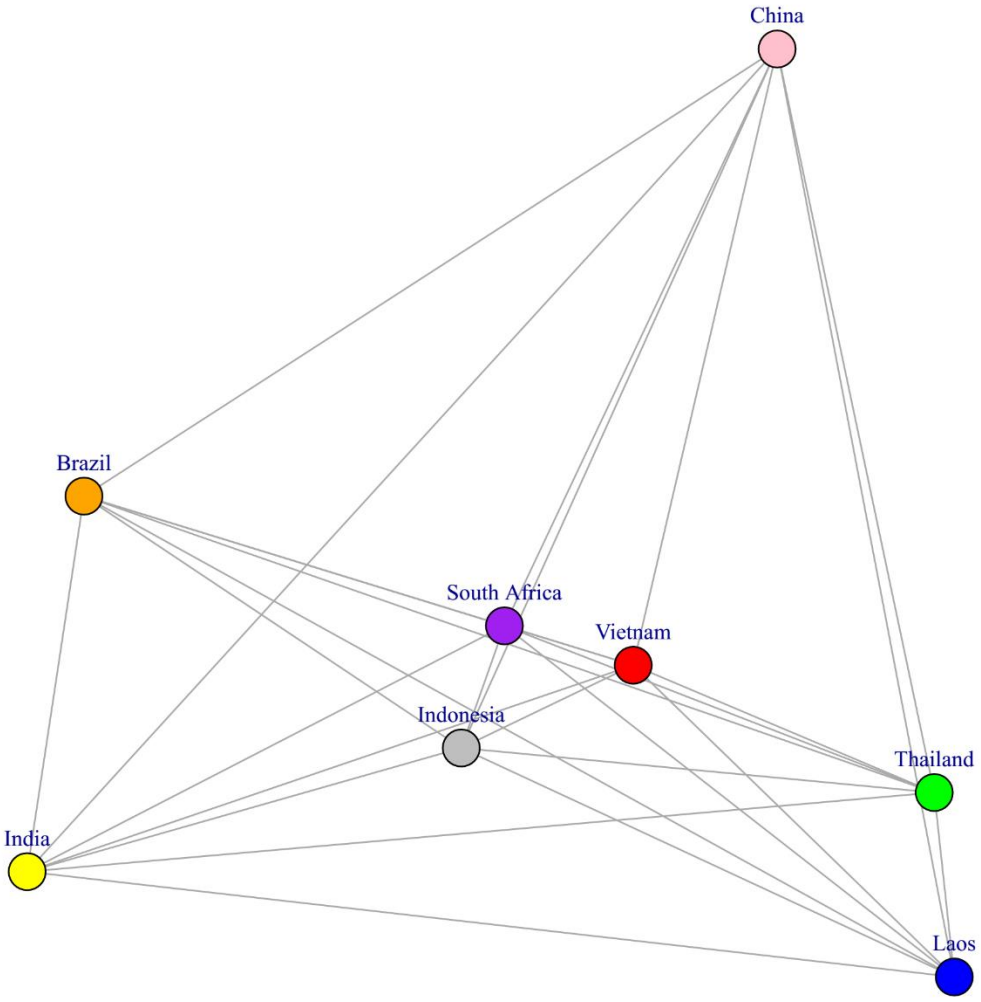

Figure 2.3-3. Mutidimensional scaling plot of genetic distances (Fst) of global *C. neoformans* var. *grubii* isolates from HIV-infected patients.
Vietnam appeared to represent an intermediate population between that from Laos/Thailand and that from China. Among Southeast Asian populations, that of Indonesia is most similar with the Indian population, possibly due to the uniquely high proportion of ST93, a feature also shared by *C. neoformans* var. *grubii* from India and Brazil.

Table 2.3-2– Genetic distance matrix (Fst) between different *C. neoformans* var. *grubii* populations

	Laos	Indonesia	Thailand	India	S. Africa	Vietnam	Brazil	China
Laos	0	0.263	0.002	0.676	0.158	0.09	0.62	0.424
Indonesia		0	0.245	0.155	0.029	0.077	0.146	0.285
Thailand			0	0.605	0.205	0.095	0.632	0.28
India				0	0.112	0.304	0.016	0.635
S. Africa					0	0.068	0.156	0.086
Vietnam						0	0.362	0.075
Brazil							0	0.495
China								0

I used the fixation index (*Fst*) to evaluate pairwise genetic differentiation between different geographical regions. Multidimensional scaling (MDS) was carried out to provide a 2-D visualization of the *Fst* distance matrix (**Figure 2.3-3** and **Table 2.3-2**). Botswana, being structurally highly diverse, is in stark contrast to other countries and therefore was removed from the analysis. On the other hand, due to the apparent propensity of ST5 towards HIV-uninfected patients, the *Fst* analysis only included isolates from HIV-infected patients from Laos, Thailand, Vietnam, Indonesia, China, India, South Africa and Brazil. Very few isolates from Japan, Korea, Kuwait or Qatar were known to be from HIV-infected patients and thus isolates from these countries were also excluded from the analysis. In addition, isolates from any countries with fewer than 20 isolates were also excluded on the grounds that it was difficult to be sure they were representative of the country's wider *C. neoformans* var. *grubii*

population.

The MDS plot revealed that the Indian *C. neoformans* var. *grubii* population was most closely related to the Brazilian population (*Fst*=0.016), followed by the Indonesian population (*Fst*=0.155), and was more distant to other Southeast Asian countries (Vietnam, Thailand and Laos, *Fst* ranging from 0.304 to 0.676). Of the Southeast Asian populations, those from Laos and Thailand were most genetically close (*Fst*=0.002); the Indonesian population was most closely related to the Vietnamese population (*Fst*=0.077). The population from Vietnam, while being placed closer to Indonesia in the MDS analysis, appeared to be intermediate between China in East Asia (*Fst*=0.075) and Laos/Thailand in Southeast Asia (*Fst*=0.090 and *Fst*=0.095, respectively). This is in spite of the fact that both Vietnam and Laos share northern borders with China (*Fst*=0.424 between Laos and China). In fact, the Thai and Chinese populations appeared genetically closer than the Laos-China populations (*Fst* = 0.280).

2.4. Chapter 2 Discussion

The population structure of *C. neoformans* var. *grubii* has been described for a number of Asian countries [101], including Vietnam[325], Thailand [92,102], India[100], China [308,312,351,352], Japan[107] and Korea[111]. However, data from Laos have been lacking, and Vietnamese data have not previously been placed into the global context. To address this, we typed 81 isolates from Laos and re-analyzed 136 previously published isolates from Vietnam using MLST. An advantage of our dataset is that it contains significant numbers of

strains from both HIV infected and uninfected patients. In contrast, reports from China and East Asian countries are dominated by clinical isolates from HIV-uninfected patients, while studies from Thailand and other Southeast Asian countries including Singapore[353], Malaysia[354] and Indonesia[355], present isolates predominantly from HIV-infected patients. The differences between the immune statuses of patients sampled in different countries complicate interpretation of the data, but also mean that Vietnam is in a unique position to demonstrate the association between *Cryptococcus neoformans* var. *grubii* ST5 and host immune phenotype.

In China, ST5 is the dominant sequence type, accounting for over 90% of infections [105,106,110]. While it is present in both immunocompetent and immunocompromised patients, relatively few cases of HIV-associated disease have been reported [105]. The reasons for this are unclear. While China has a relatively low prevalence of HIV (estimated at <0.1% of the adult population in 2015 [356]), given the size of its population the few cases of HIV-associated disease reported may represent bias in study design, HIV testing or research interests. However, a recent report of cryptococcosis cases from Jiangxi, China included 35 cases of cryptococcosis in HIV-infected patients, of which 33 were ST5. Overall, 73 out of 86 patients in this study infected with ST5 isolates (85% of all cases) [357].

In contrast to China, the *C. neoformans* var. *grubii* population from Thailand appears more diverse according to MLST, with 14 STs reported, among which ST4 and ST6 are most common, outnumbering ST5 infections 6 to 1 [92,101,102]. We found the population

structure of isolates from Laos to be similar to that in Thailand, with ST4 and ST6 (both belonging to sub-group 4) accounting for the majority of disease. This dominance of a single sub-group in both Thailand/Laos and China contrasts with Vietnam, where ST5, ST6 and ST4, belonging to two separate sub-groups, are similarly prevalent. The Thai data are notable for the lack of CM cases reported from HIV-uninfected patients. It seems unlikely that this represents under-reporting of non-HIV associated disease which is generally considered remarkable; rather, we hypothesize that this reflects a low prevalence of ST5 isolates in the environment, which is clearly associated with apparently immunocompetent patients elsewhere in Asia [103,105,106,110,325]. If the ST5 lineage was common in Thailand and Laos, we would expect to detect this from reporting of disease in HIV infected patients - in Vietnam it is responsible for >35% of cases of cryptococcal meningitis in HIV infected patients. Thus in Vietnam the *Cryptococcus* population seems to represents an intermediate population between Laos/Thailand to the West, and China to the Northeast, consistent with its geographical location.

Of note, Indonesia also appears to have two equally dominant burst groups among clinical isolates. ST4/6 isolates account for 44%, of human infections, with ST93, common in East Africa and also frequently reported from India, accounting for a further 44%[101].

The differences in population structure we see moving from west to east are likely driven by ecological and/or human factors. Ecological differences between the regions could select for enrichment of particular STs if there are differences in the relative fitness of the STs in those

niches. Southeast Asia is a geographically and ecologically diverse area known for its high species density [358,359]. The south of the region has a hot tropical climate with dry and wet seasons; the north is temperate with hot summers and cold winters. The Annamite mountain range, covered in dense rain forests, rises to over 3000 meters and runs the length of Vietnam, forming a barrier separating Thailand, Laos and Cambodia from Vietnam and southern China. There are also significant differences in elevation (for example, Chiang Mai, in Northern Thailand and the source of most published Thai data, and Vientiane in Northwestern Laos are at significantly higher elevation than Ho Chi Minh City and much of Southeastern China (170-300 meters versus 10-20 meters above sea level). Other than elevation and temperature, localized differences in soil biogeochemistry, environmental predators such as amoebae [115], and tree species may also be relevant. For example, Laos, Cambodia, Vietnam and China are among Asian countries where there is significant contamination of groundwater with high levels of arsenite [360,361]. Recently it has been shown that ST5 *C. neoformans* var. *grubii* isolates possess tandem repeats of the arsenite efflux transporter (Arr3) [124]. The greater the number of these repeat elements the higher the resistance to toxic arsenic containing compounds [124]. Differences in the distribution of this pollutant could correlate with the distribution of ST5. Other human activities that could influence ecology or human exposure to infection include irrigation, urbanization and mining, and human migration and international trade links could influence dispersal of *C. neoformans* var. *grubii* lineages in Asia and elsewhere.

In addition to ecological factors, the varying prevalence of lineages in particular human populations could be a result of differential host susceptibility to particular lineages. Such human genetic factors have previously been associated with susceptibility to tuberculosis [362]. However, the dominant ethnic group in Vietnam (Kinh, >80%) is genetically closer to ethnic groups in Northern Thailand than to the Han Chinese from Beijing or Southern China [363]. In fact, the differences between the Thai and Vietnamese *C. neoformans* populations we demonstrated here suggest that the diversity of the pathogen population is not driven by host susceptibility. Nevertheless, it remains possible that subtle human genetic polymorphisms exist that result in differential susceptibility to different cryptococcal species/lineages.

Our observations augment the findings of Ferreira-Paim and co-workers who suggest that the populations of *C. neoformans* var*. grubii* found in many geographical regions across Asia and the Middle East arose from ST174, [151]. The ST174 expansion model is supported by goeBURST and maximum likelihood phylogeny analyses which show it is the most parsimonious candidate as the group founder of sub-groups 4, 5 and 31, which account for over 90% of the Southeast Asian isolates. We did not observe ST174 in either Vietnam or Laos but it has been present in previously published datasets from South Asia and the Middle East, with 3 isolates from India and 1 isolate from Kuwait[101], and has also been from Germany in a patient of Asian origin[364]. The prevailing hypothesis with respect to the evolution of CN, suggests that the current circulating Asia population emerged “Out-of-

Africa"[81]. Our data neither confirms nor support this hypothesis but rather is showing that the extant population of CN associated with human disease in Asia has descended from a single common ancestor. Given the age of *C. neoformans* as a species, and the fact that it is not primarily a human pathogen, nor is it spread from person to person, it seems somewhat unlikely that its global distribution is driven by migration of (latently or actively) infected humans. However, as described earlier, other human factors may be relevant. The emergence of the preponderance in most countries of strains of a single burst group on a background of greater diversity, suggests different fitness of different STs to particular ecological types.

2.5. Chapter 2 Conclusion

This chapter addresses the lack of knowledge of the molecular epidemiology of *C. neoformans* var. *grubii* from Vietnam and Laos and places these populations into a broader context. I detected a change in predominant STs as one moves from western to eastern longitudes and that the Vietnamese *C. neoformans* var. *grubii* population appears intermediate between Thai/Laotian and Chinese populations. My data also suggest that ST174 is a putative most recent common ancestor for the majority of *Cryptococcus neoformans* var. *grubii* sequence types in Asia. The *C. neoformans* var. *grubii* population in Asia present in this study appeared mostly clonal, which is similar to previous reports. Most studies focusing on VNI, including mine, are weakened in that while cryptococcosis results from the inhalation of infectious propagules from the environment, few environmentally

sourced isolates have been characterized and thus the true diversity of the species in any country may be underestimated. More efficient environmental isolation techniques and systematic sampling would facilitate further understanding of the true species diversity by regions and could potentially reveal bottleneck events leading to the rise of pathogenic lineages.

CHAPTER 3

IN VITRO AND *IN VIVO* VIRULENCE OF CLINICAL *C. NEOFORMANS* VAR. *GRUBII* ISOLATES FROM HIV-INFECTED AND HIV-UNINFECTED PATIENTS IN VIETNAM

3.1. Chapter 3 Introduction

The burden of cryptococcal meningitis is highest in sub-Saharan Africa and South/Southeast Asia where there are more people living with HIV/AIDS. In these tropical and subtropical regions, *C. gattii* CM is relatively uncommon in HIV-infected patients, usually accounting for only 1-2% of cryptococcosis in HIV-infected individuals, although higher rates have been reported from Botswana and Malawi (up to 30% of all CM cases) [365,366]. It is widely acknowledged that *C. gattii* primarily causes disease in immunocompetent patients while *C. neoformans* is associated with disease in immunocompromised patients [80,304].

Where cryptococcal meningitis due to *C. neoformans* var. *grubii* occurs in HIV-uninfected individuals, reports most often describe patients with an increased disease susceptibility due to some other underlying immunosuppressive conditions [302,367,368]. However, in Australasia and the USA no clear underlying immune deficit is identified in approximately 20% of CM cases in HIV-uninfected individuals [369,370]. In Vietnam, disease in HIV-uninfected patients accounts for approximately 10% of all CM cases admitted to our referral hospital in Ho Chi Minh City (HCMC) [307]. We have previously reported that the majority of HIV-uninfected patients had no identified cause of immunosuppression, and that >80% of HIV-uninfected CM patients were infected by yeasts belonging to a single amplified fragment

length polymorphism (AFLP)-defined cluster of *C. neoformans*, which we had named VNI-γ [103]. Our clinical observation has been replicated in China where over 70% of CM cases from apparently immunocompetent individuals were infected with *C. neoformans* [109]. The yeasts isolated from immunocompetent patients in China were closely related to each other, and belonged to a single multi-locus sequence type (MLST), sequence type (ST)5 [106]. Similarly, this ST accounted for more than 80% of non-HIV-associated cases of CM in South Korea, although some patients from this group had other underlying, potentially immunosuppressive conditions [111]. The association between a particular ST/genotype and host immune phenotype could be explained by a lineage-specific increase in pathogenic potential or microbial fitness, a currently unidentified host immune deficit, or a combination of these factors.

This chapter aims to explore the hypothesis of whether VNIγ/ST5 isolates are more virulent than VNI-δ/non-ST5 isolates:

- Compare virulence-associated phenotypes in a range of *in vitro* experiments between ST5 and non-ST5 *C. neoformans* var. *grubii* strains from HIV-infected and HIV-uninfected patients from Vietnam.
- Compare the relative *in vivo* virulence and immune responses of ST5 and non-ST5 *C. neoformans* var. *grubii* strains using a mouse model of cryptococcosis.

3.2. Chapter 3 Material and Methods

3.2.1. *C. neoformans* isolates and culture conditions

This study included clinical isolates from the cerebrospinal fluid (CSF) of patients enrolled in a randomized controlled trial of antifungal therapy in HIV-infected patients, and a prospectively descriptive study of HIV-uninfected patients with central nervous system (CNS) infections [103,307]. All studies were approved by the Institutional Review Board of the Hospital for Tropical Diseases, Ho Chi Minh City, Vietnam and the Oxford Tropical Ethics Committee or Liverpool School of Tropical Medicine (UK). Bulk isolate from each patient was kept at -80^{o}C using Microbank beads (Pro-Lab Diagnostics, UK). Isolates were single-colony-purified for all subsequent experiments. I randomly selected 15 isolates from each HIV group (15 from HIV-infected patients and 15 from HIV-uninfected patients) for characterization. Mating type, AFLP fingerprints and 7-digits consensus MLST profiles (CAP59, GPD1, IGS1, LAC1, PLB1, SOD1, URA5) for all isolates were previously determined [30,325,371]. *C. neoformans* yeasts were propagated using Yeast Peptone Dextrose (YPD) broth and incubated overnight at 30^{o}C with agitation. Cells were harvested and washed 3 times in phosphate-buffered saline (PBS). Inoculum was quantified using the Cellometer X2 cell-counter (Nexelom Biosciences, USA). Isolates and clinical information from corresponding patients were summarized in **Table 3.2-1**.

3.2.2. Growth at high temperature/*ex vivo* human CSF and melanin production

Growth at high temperature and in *ex vivo* human CSF were tested as previously described [372] with modifications for quantitative assessment. Unless otherwise specified, all reagents and media for phenotyping were purchased from Sigma-Aldrich, USA (now Merck, USA). To assess fungal growth at different temperatures, inoculum was adjusted to 10^8 cells/ml, serially diluted, spot-inoculated in duplicate on YPD agar in 5µl and incubated at 30^{o}C or 37^{o}C for 48 hours. After 48 hours, colony forming units (CFU) were counted and recorded in CFU/ml. For the ex vivo CSF growth assay, baseline pre-antifungal treatment CSF supernatant from random de-identified HIV-infected patients enrolled into an antifungal therapy trial was pooled, filtered, and stored at -80^{o}C until use. 10µl of 10^8 cells/ml yeast suspension was inoculated into 90µl of pooled CSF and incubated at 37^{o}C with 5%CO_2. Inoculated CSF was serially diluted and spotted on YPD agar at days 1 and 3 post-inoculation. All experiments were repeated in triplicate. The H99-derived mutant *Δena1*, lacking a cation-ATPase-transporter which resulted in decreased viability in human CSF and within macrophages, was used as a negative control for the *ex vivo* CSF assay [373]. H99 was included as a reference in all experiments. Data were standardized by expressing the results as a ratio of the CFU/ml of the test isolate to the CFU/ml of H99. Melanin production was assessed by plating 5µl of 10^6cells/mL cell suspension on L-DOPA agar containing 1g/L L-asparagine, 1g/L glucose, 3g/L KH_2PO_4, 250mg/L $MgSO_4.7H_2O$, 1mg/L Thiamine HCl, 5µg/L Biotin, 100mg/L L-DOPA, 20g/L Bacto Agar (Becton Dickinson, USA) ([374,375]. Plates were incubated in the dark at 30^{o}C or

37^{o}C for 3 days. Difference in colony melanization was compared visually with reference to H99 and a mutant with diminished melanin pigmentation.

3.2.3. Extracellular urease and phospholipase activity

Time to complete pigmentation on Christensen's urea agar medium was used as a marker for extracellular urease activity. 10µl of 10^8 cells/ml yeast suspension was spotted on Christensen's urea agar and incubated at room temperature. Time to complete pigmentation was recorded using timelapse imaging in 1 minute interval using a Gopro Hero 6 camera (Gopro, USA). Extracellular phospholipase activity was screened on egg yolk medium as previously described, with minor modifications [376]. The egg yolk medium contained Sabouraud agar with 1M sodium chloride, 0.005M calcium chloride and 8% sterile egg yolk enrichment (Merck, USA). 5 µl of *C. neoformans* yeast suspension (10^8 cells/ml) was spotted on egg yolk agar and incubated at 30^{o}C for 72 hours. Diameter of the precipitation zone (D) formed around the colonies and diameter of the respective colonies (d) after 72 hours were recorded. A D/d ratio for each isolates was calculated. H99 was included in each experiment batch. Final data were expressed as a ratio between the test isolate's D/d ratio and that of H99. Each isolate was tested in 3 technical triplicates.

3.2.4. *In vitro* capsule enlargement and cell size measurement

To measure *in vitro* cryptococcal capsule thickness, all isolates were streaked onto capsule-inducing agar containing powdered Dulbecco Modified Eagle Medium (DMEM)

[supplemented with 4.5g/L glucose, L-glutamine, sodium pyruvate], $NaHCO_3$ 250mM, NaMOPS 1M, Neomycin 200mg/ml, Cefotaxime 100 mg/ml. Plates were incubated at 37^{o}C in 5% CO_2 until single colonies were visible [377]. Unless otherwise specified, all reagents were purchased from Sigma-Aldrich. India ink smears were prepared on a glass slide and visualized at 100X magnification using a CX41 microscope (Olympus, Japan). Images were captured using a DP71 Camera system with DP Controller software (Olympus, Japan) and processed using ImageJ (rsb.info.nih.gov/ij/). Capsular thickness was calculated by subtracting the cell body diameter (D_{CD}, no capsule) from whole cell diameter (D_{WC}, including capsule). At least 30 individual microscopic yeast cells were assessed for each isolate.

3.2.5. Mouse inhalation infection model of cryptococcosis

All mouse infection experiments were conducted as previously described according to Duke University's Institutional Animal Care and Use Committee guidelines and approvals [228]. 6-weeks old female A/J mice were sedated with isoflurane and inoculated intranasally with the selected *C. neoformans* var. *grubii* isolate by dropping 25µl of yeast suspension containing $5x10^4$ cells into the nares. Five ST5 strains (BK147, BK44, BMD700, BMD1338 and BMD1646) and three non-ST5 strains (BMD1415, BK80 (both ST4) and BMD1367 (ST306)) were chosen for animal experimenting. Animals were monitored daily and euthanized by CO_2 inhalation at indicated time points (fungal burden and *in vivo* responses) or until loss more than 15% body weight was observed (virulence assay).

3.2.6. Determining *in vivo* fungal burden

5 mice were infected with each isolate on two independent experiments for assessment of virulence at 7 and 14 days post-infection. All animals in each experiment set were euthanized by CO_2 inhalation either on day 7 or day 14 post-infection. Fungal burden at each time point was assessed by excising the left superior lobe of the lung and homogenizing the tissue by bead beating. Tissue homogenate was serially diluted and plated onto YPD agar supplemented with 100mg/ml ampicillin. The plates were incubated at 30^{o}C for 48 hours and the number of *C. neoformans* colony forming units (CFU) recorded. Fungal burdens were expressed as CFU per gram of tissue (CFU/g). At each time point, additional lung lobes were also collected for determining *in vivo* histopathology and cytokine response, as described below.

3.2.7. Determining *in vivo* histopathology

At specific time points (7 or 14 days post-infection), the right superior lung lobe from each mouse was excised and immersed in 10% formalin (replaced with 70% Ethanol after 24 hours) for fixation. Fixed, uninflated lung specimens were stored at 4^{o}C until further processing. After paraffin embedding, sliced sections were stained using the period acid-Schiff (PAS) or mucicarmine. Histopathological examination was performed by an independent pathologist blinded to the infecting strain. The resulting tissue damage was scored from 0 (no changes) to 10 (severe changes), corresponding to the severity of

pathology in 4 different categories: necrosis, hemorrhage, edema and inflammation as per the Duke Veterinary Diagnostic Laboratory (Division of Laboratory Animal Resources).

3.2.8. Determining *in vivo* cytokine response

To assess the severity of the inflammatory responses at specific time points (day 7 and day 14 post-infection), the middle lobe from the right lung of each infected mouse was excised and homogenized by bead beating in 1ml sterile PBS/Protease inhibitor. 500µl of lung homogenate was used for cytokine profiling. Cytokines representing T-helper type 1 (Th1) (IL-12p70, TNF-α, IFN-γ), T-helper type 17 (IL-17) and T-helper type 2 (Th2) (IL-4, IL-5, IL-10) responses were measured using a customized Bio-Plex Pro™ Mouse Cytokine Th1/Th2 Assay kit (Biorad, USA) with the BioPlex 200 platform according to the manufacturer's guidelines. Data were retrieved using BioPlex Manager Software. The upper and lower limits of quantification (ULOQ and LLOQ) were based on a standard curve. All values falling below the LLOQ were replaced with the midpoint between zero and the LLOQ. Data were standardized by lung weight and presented as picogram of cytokines per gram lung tissue (pg/g).

3.2.9. *In vivo* virulence assay

The virulence assay was conducted independently from the day 7/day 14 experiment. Each of the 8 selected isolates was intranasally inoculated in 10 A/J mice. Mice were monitored daily until loss of more than 15% body weight, which is a sign of distress, was observed. Mice

were then euthanized by CO_2 inhalation at point of impending death. *In vivo* fungal burden at the point of impending death was also recorded as previously described.

3.2.10. Statistical analysis

GraphPad Prism version 5.04 for Windows (GraphPad Software, San Diego California USA; www.graphpad.com) was used for data visualization and statistical analyses of fungal loads, cytokine profiling, capsular/cell size, and survival proportions. Mann-Whitney U-test was used for comparing fungal load and cytokine concentrations. Kaplan-Meier survival curves, and the log-rank test were used for survival analysis. Capsule/cell size was analyzed in GraphPad Prism 5.04 for Windows and compared using Welch's t-test. The Fligner-Killeen test of variance homogeneity for analyzing variation in capsule/cell size and Fisher's exact test were performed using R software, version 3.2.4 (http://www.r-project.org). One way ANOVA with a post hoc multiple comparison test (Dunnett or Bonferroni) integrated in Graphpad was used to compare cytokine concentrations between individual isolates.

Table 3.2-1. Typing and corresponding patients information for *C. neoformans* var. *grubii* isolates selected for phenotyping (n=30)

NO.	ISOLATE DATA			PATIENT DATA	
	Strain name	**AFLP**	**MLST**	**Underlying Disease**	**Sex**
1	BK14	VNI-δ	4	HIV	M
2	BK163	VNI-δ	4	HIV	M
4	BK225	VNI-δ	4	HIV	M
6	BK48	VNI-δ	4	HIV	M
7	BK59	VNI-δ	4	HIV	F
8	BK69	VNI-δ	4	HIV	M
9	BK74	VNI-δ	4	HIV	M
10	BK80*	VNI-δ	4	HIV	M
11	BK87	VNI-δ	4	HIV	M
12	BK88	VNI-δ	4	HIV	M
13	BK89	VNI-δ	4	HIV	M
15	BMD1415*	VNI-δ	4	Lupus	M
3	BK218	VNI-δ	6	HIV	M
5	BK234	VNI-δ	6	HIV	F
14	BMD1367*	VNI-δ	306	Gastric cancer	F
16	BK147*	VNI-γ	5	HIV	M
17	BK44*	VNI-γ	5	HIV	M
18	BMD101	VNI-γ	5	None known	M
19	BMD1228	VNI-γ	5	None known	F
20	BMD1291	VNI-γ	5	None known	F
21	BMD1338*	VNI-γ	5	None known	M
22	BMD1353	VNI-γ	5	None known	M
23	BMD1452	VNI-γ	5	None known	F
24	BMD1646*	VNI-γ	5	None known	M
25	BMD1716	VNI-γ	5	None known	F
26	BMD367	VNI-γ	5	None known	M
27	BMD673	VNI-γ	5	None known	F
28	BMD700*	VNI-γ	5	None known	M
29	BMD854	VNI-γ	5	None known	F
30	BMD899	VNI-γ	5	None known	F

AFLP = AMPLIFIED FRAGMENT LENGTH POLYMORPHISM
MLST = MULTI LOCUS SEQUENCE TYPING
M = MALE, F = FEMALE
** INDICATES ISOLATES SELECTED FOR MOUSE EXPERIMENT*

3.3. Chapter 3 results

3.3.1. ST5 *C. neoformans* isolates from Vietnam expressed higher *in vitro* capsular enlargement than non-ST5 isolates.

We assessed and compared common *in vitro* virulence-related phenotypes between selected ST5 and non-ST5 isolates from HIV-uninfected and HIV-infected patients, respectively. Phenotypes tested included extracellular urease and phospholipase production, melanin production, *in vitro* capsular enlargement, growth at high temperature and in pooled human CSF. Upon microscopic examination we observed that the ST5 *C. neoformans* yeast cells developed significantly thicker capsule during *in vitro* culture than non-ST5 isolates ($p<0.0001$, Welch's t-test; also see **Table 3.2-1**).

Table 3.3-1. Variability in *in vitro* capsule thickness and cell diameter between ST5 and non-ST5 *Cryptococcus neoformans* strains from Vietnam

	MLST Group	
Variable	**ST5**	**Non-ST5**
Capsule Thickness (µm)		
Mean*	2.64	2.01
Median	2.25	1.94
95% CI	2.49 - 2.79	1.94 - 2.07
Range	0.01 - 9.56	0.02 - 6.16
Coefficient of Variation[$] (%)	0.63	0.37
Cell diameter (µm)		
Mean*	11.38	9.69
Median	10.00	9.56
95% CI of Mean	10.96 - 11.79	9.52 - 9.87
Range	4.74 - 27.22	5.25 - 19.89
Coefficient of Variation[$] (%)	0.41	0.20

** P<0.0001, t-test with Welch's correction.*

[$] *P< 0.0001, Fligner-Killeen test of homogeneity of variance.*

Individual ST5 *C. neoformans* cells were also significantly larger in size than cells from the non-ST5 strains (p<0.0001, Welch's t-test; also see **Table 3.3-1**). A high degree of variation in both capsule size and cell diameter was detected between individual ST5 isolates (**Figure 3.3-1** and **Table 3.3-1**). A Fligner-Killeen test for homogeneity of variance confirmed this variation to be significantly greater for ST5 than non-ST5 isolates (p<0.0001) for both capsule size and cell diameter. BMD1646, a ST5 strain, appeared markedly bigger and highly encapsulated than any other isolates. The differences in capsule thickness and cell diameter, as well as intra-genotype variation among ST5 isolates was significant and was not an effect driven by the outlier BMD1646.

In contrast, there were no genotype-specific differences in all other *in vitro* phenotypes tested: growth at 30^{o}C (p=0.10, Welch's t-test) and 37^{o}C (p=0.23, Welch's t-test); *ex vivo* survival in CSF after 1-day exposure (p=0.72, Welch's t-test) and 3-days exposure (p=0.77, Welch's t-test) (see **Figure 3.3-2** and **Figure 3.3-3**), extracellular urease activity and phospholipase activity (**Figure 3.3-4** and **Figure 3.3-5**).

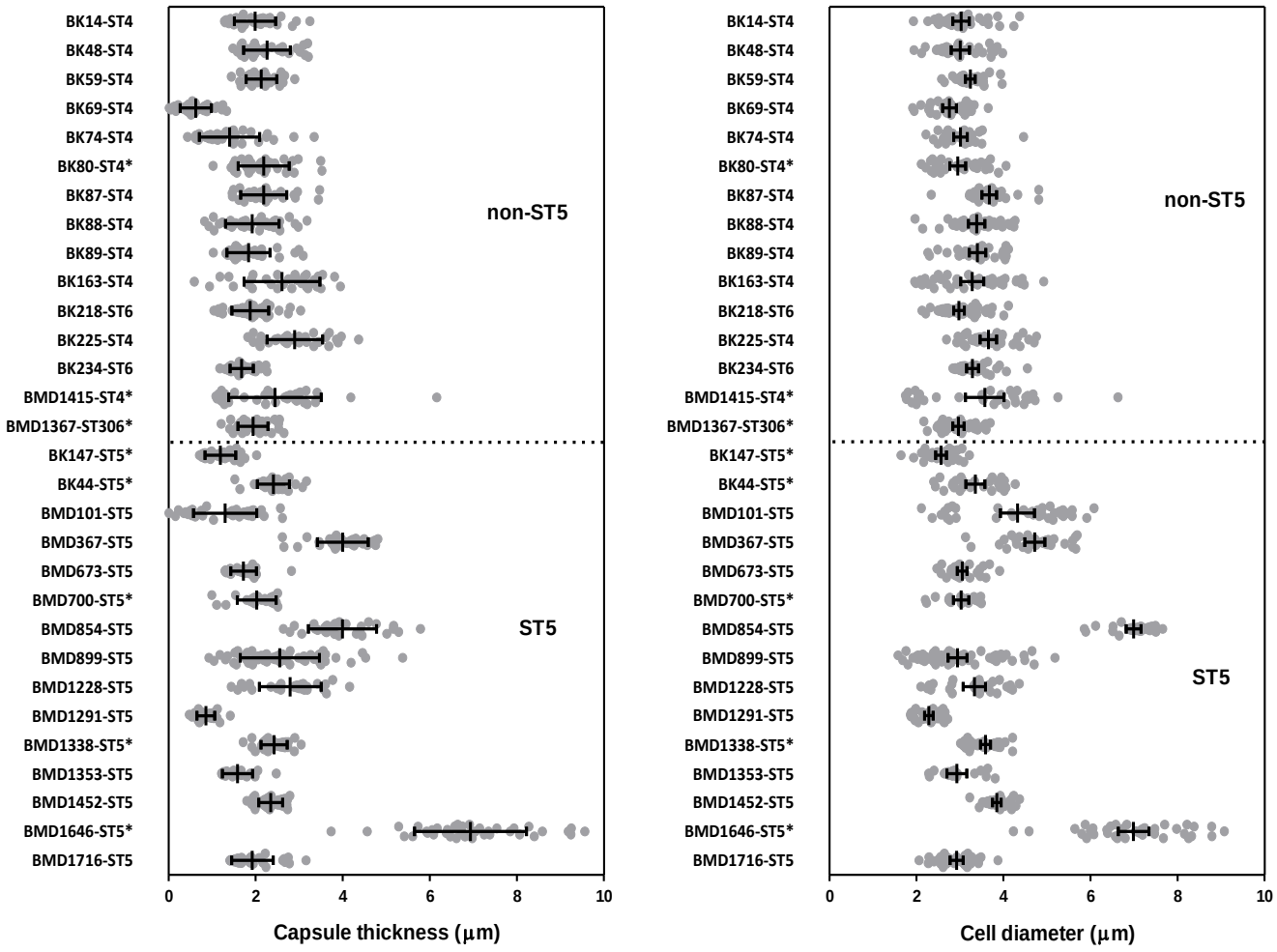

Figure 3.3-1. *In vitro* induced capsule thickness and cell diameter of individual *Cryptococcus neoformans* strains from Vietnam.

AFLP-VNI-γ/MLST-ST5 strains expressed higher degree of variation in both capsule size and cell diameter *in vitro*, which remains significant even when the outlier BMD1646 was removed from the analysis (p<0.0001 for both capsule and cell size, Fligner-Killeen test). Scattered plot represents single cells from an individual strain. Data for individual strains are presented as mean with error bars denoting standard deviation. Strains selected for experiment in mice were indicated by asterisks.

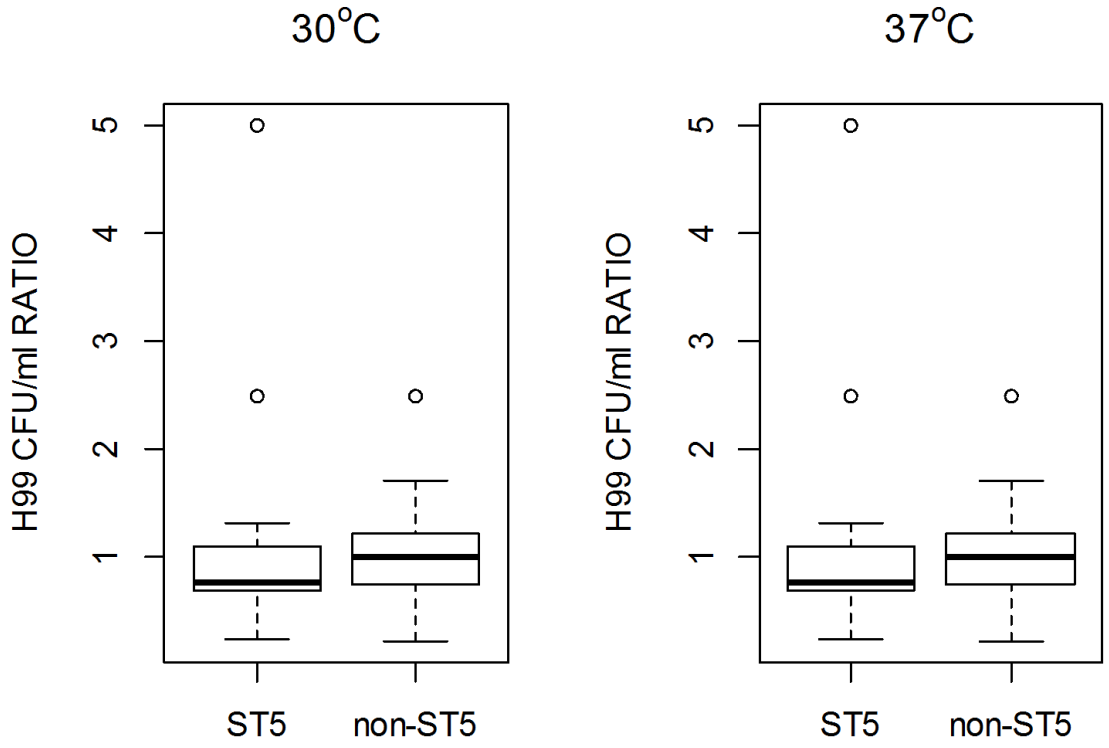

Figure 3.3-2. Growth of ST5 (n=15) and non-ST5 (n=15) *C. neoformans* var. grubii isolates from Vietnam at 30°C and 37°C.

Data were obtained from 30 isolates (15 ST5 and 15 non-ST5) in 3 different experiment batches. Identical cell inoculum for each isolates was serial diluted on YPD agar and grown at 30°C or 37°C until visible colonies could be seen and counted. H99 was included in each experiment batch as internal control. Data were expressed as Colony Forming Unit (CFU) per ml ratio between a test isolate and that of H99 in the same experiment batch. Boxplots (Tukey method) describe the median and interquartile range with whiskers indicating the lower and upper quartiles. Values lower or higher than 1.5 times the lower or upper quartile, respectively, are indicated by clear circles. No statistically significant differences could be detected in growth at both 30°C (p=0.10) and 37°C (p=0.23) (Mann-Whitney test).

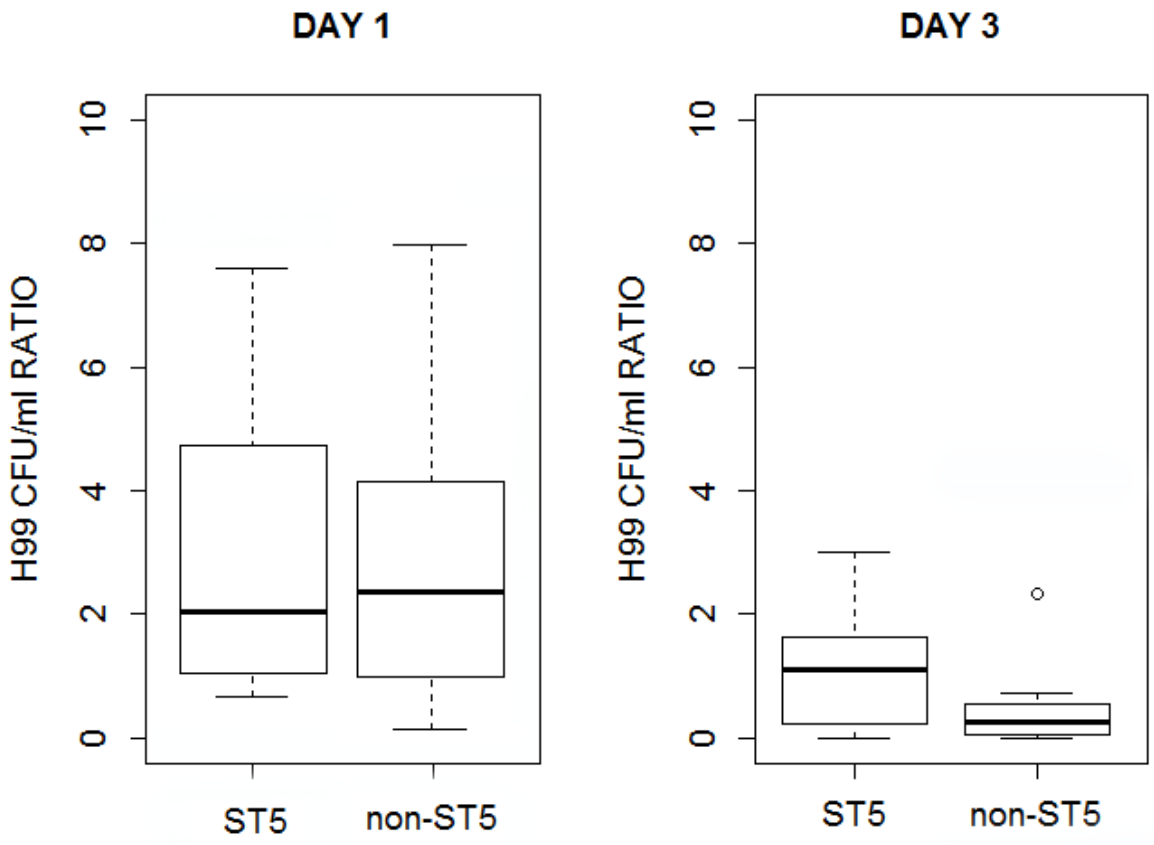

Figure 3.3-3. *Ex vivo* growth in human CSF of ST5 (n=15) and non-ST5 (n=15) *C. neoformans* isolates from Vietnam.

Data were obtained from 30 isolates (15 ST5 and 15 non-ST5) in 3 different experiment batches. 10^7 cells from each isolates was inoculated in pooled human CSF and incubated at 37°C/5% CO_2. At day 1 and day 3 post-inoculation, cell suspension is serial diluted on YPD agar and grown at 30°C until visible colonies could be seen and counted. H99 was included in each experiment batch as internal control. Data are expressed as Colony Forming Unit (CFU) per ml ratio between a test isolate and that of H99 in the same experiment batch. Boxplots describe the median and interquartile range with whiskers indicating the lower and upper quartiles. Values lower or higher than 1.5 times the lower or upper quartile, respectively, are indicated by open dots. No statistically significant differences could be detected in *ex vivo* CSF growth at both day 1 and day 3 post-inoculation (p=0.72 and p=0.77, Mann-Whitney test).

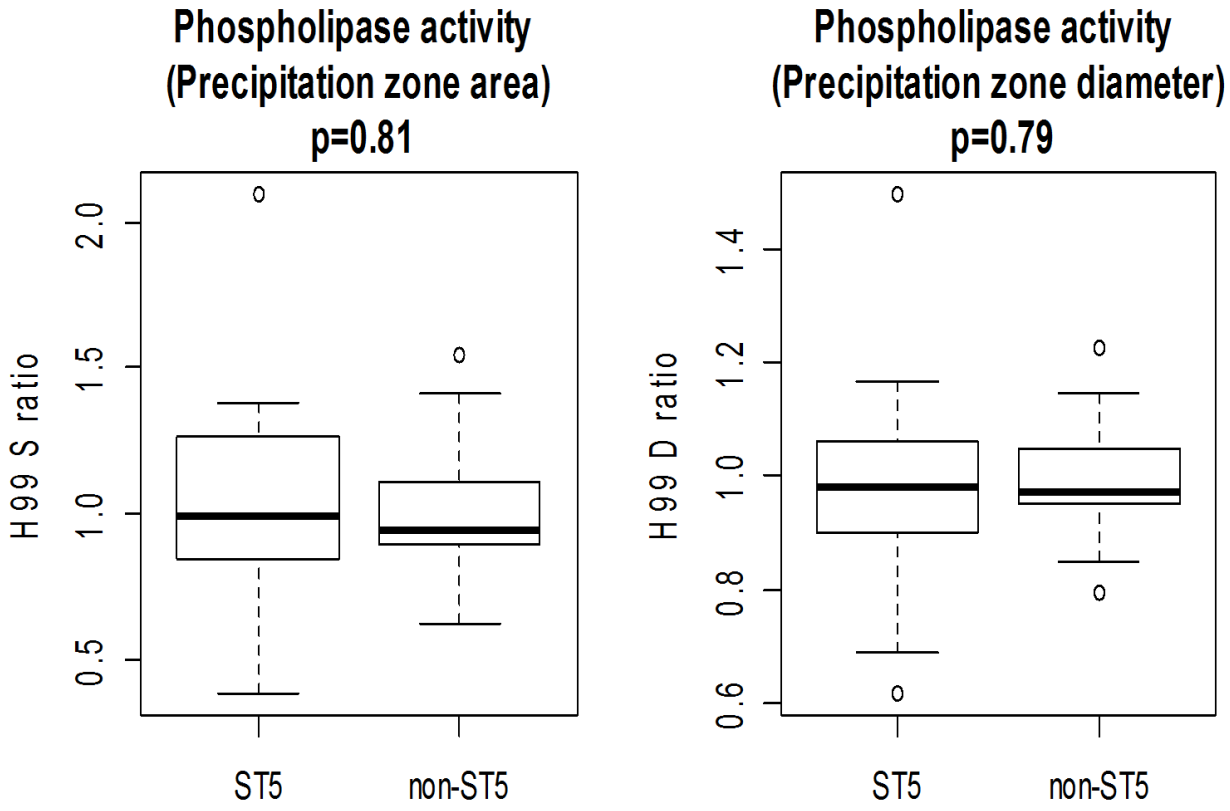

Figure 3.3-4. Extracellular phospholipase activity of *C. neoformans* var. *grubii* isolates from Vietnam (ST5: n=15 and non-ST5: n=15).

10 µl of 10^8 cells/ml yeast suspension were spotted on Sabouraud agar with egg yolk supplement for assessment of phospholipase activity after 72 hours as previously described. Data are expressed as a ratio between measurements of the test isolates and that of H99. Boxplots (Tukey method) describe the median and interquartile range with whiskers indicating the lower and upper quartiles. Values lower or higher than 1.5 times the lower or upper quartile, respectively, are indicated by open dots. No statistically significant differences in phospholipase activity between the two test groups were observed.

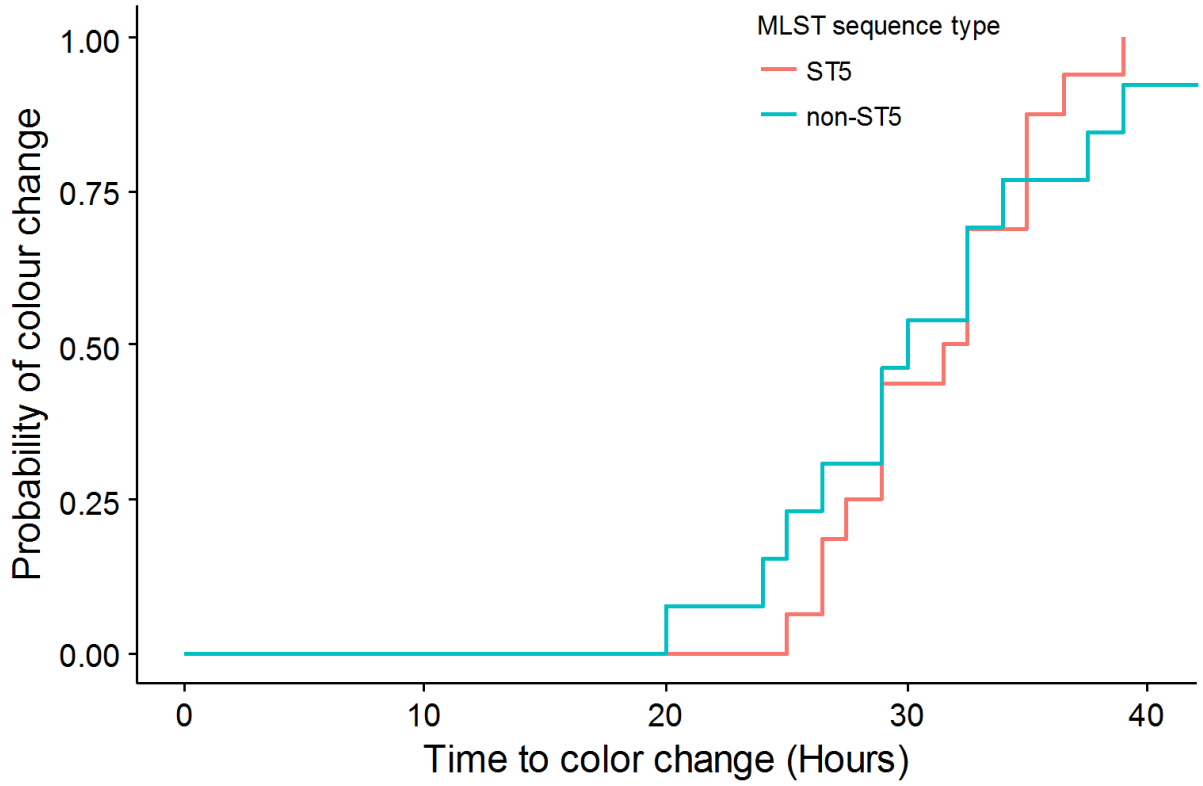

Figure 3.3-5. Extracellular urease activity of *C. neoformans* var. *grubii* isolates from Vietnam (ST5: n=15 and non-ST5: n=15), according to time to complete color change on Christensen agar.

10µl of 10^8cells/ml yeast suspension was spotted on individual Christensen's urea agar. Medium color would change from yellow to pink due to pH changes when urea in the medium was broken down by extracellular urease. Since all *C. neoformans* var. *grubii* isolates tested positive for urease activity, time to complete color change on Christensen agar was used as an indirect measure of extracellular urease activity. Each isolates were tested in triplicates. No significant difference in urease activity was observed (p=0.77, log-rank test).

Phenotyping data for the 8 isolates selected for mice experiment are shown in the following **Figure 3.3-6**, **Figure 3.3-7** and **Figure 3.3-8**. The reference *C. neoformans* var. *grubii* H99 strain and H99-derived mutants as controls were also included in each respective experiment (see below).

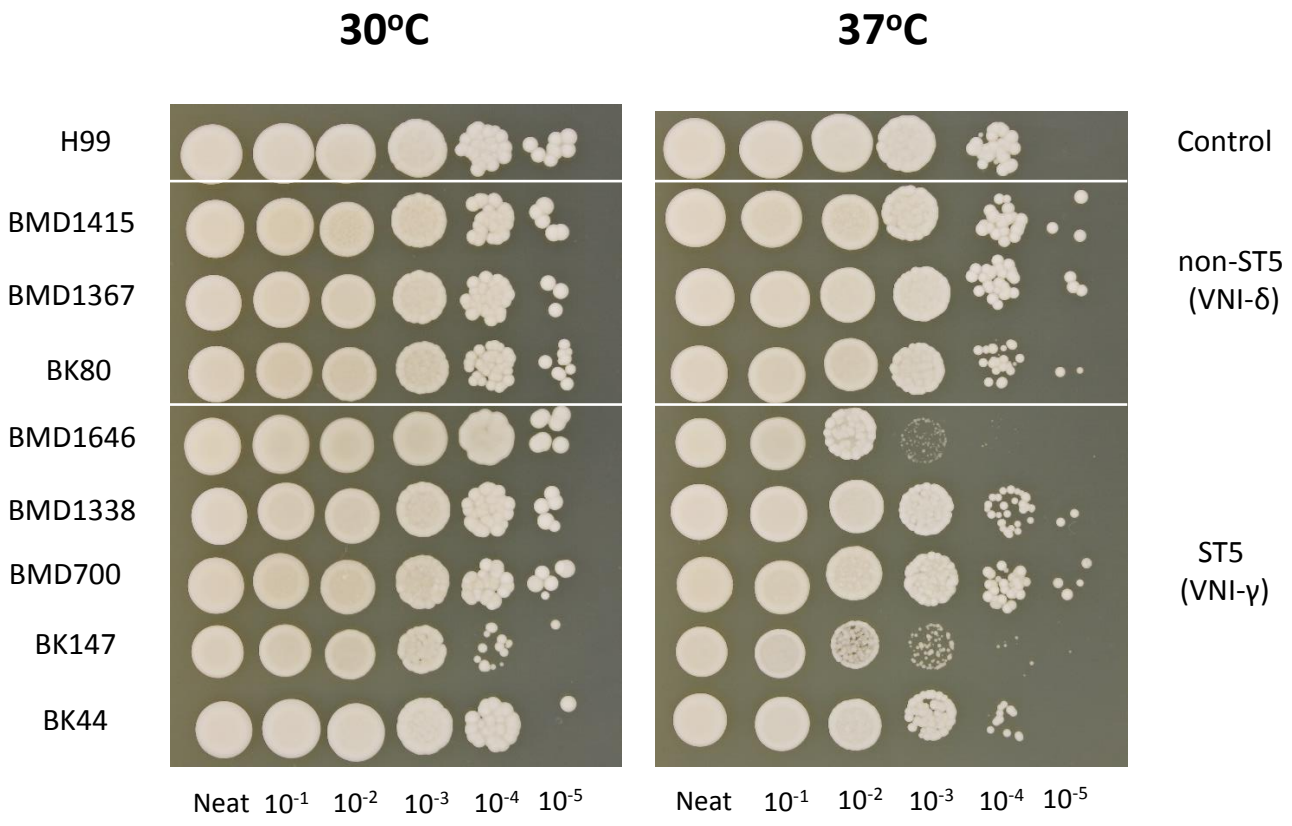

Figure 3.3-6. Growth at different temperature of 8 *C. neoformans* isolates from Vietnamese patients that were tested for virulence in mice, representing both ST5 (n = 5) and non-ST5 (n = 3).

A similar inoculum of yeasts from each isolates were spotted onto YPD agar and incubated at either 30°C or 37°C. All strains expressed similar growth at 30°C. Two ST5 strains (BMD1646 and BK147) appeared less viable than other strains at 37°C. H99 was included as a reference.

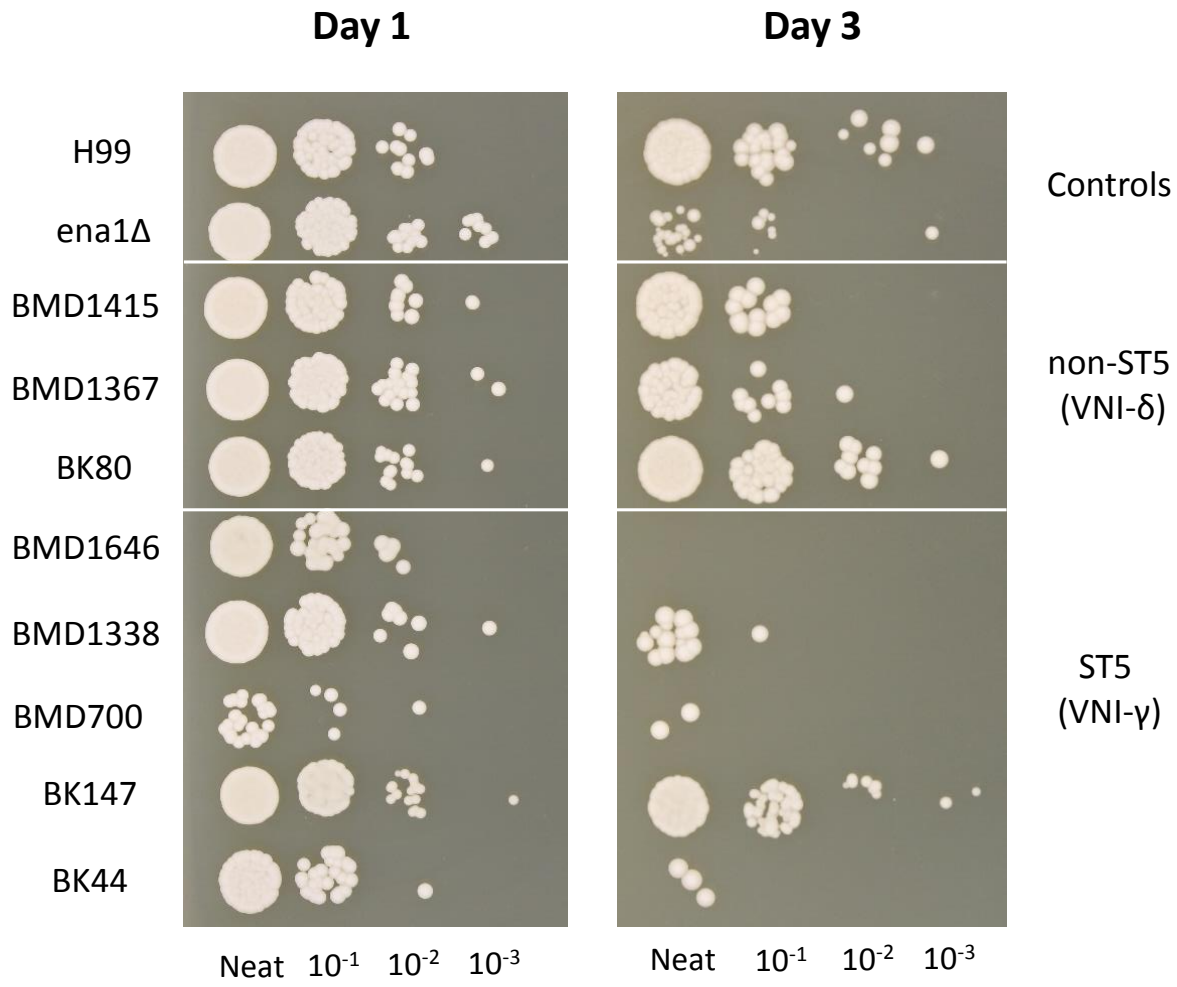

Figure 3.3-7. ***Ex vivo*** **growth in human cerebrospinal fluid (CSF) of 8 clinical** ***C. neoformans*** **isolates from Vietnamese patients that were tested for virulence in mice, representing both ST5 (n = 5) and non-ST5 (n = 3) genotypes.**

The same inoculum of yeasts were inoculated in pooled human CSF and incubated at 37^{o}C. Inoculum was diluted and plated on YPD agar at day 1 and day 3 post-inoculation. One ST5 strains (BMD700) appeared less viable than all other strains at day 1. At day 3 post-inoculation four out of the 5 ST5 strains displayed markedly reduced viability than the 3 non-ST5 strains. The H99-derived mutant *Δena1*, lacking a cation ATPase transporter which resulted in decreased viability in human CSF and within macrophages, was used as a negative control for the *ex vivo* CSF assay.

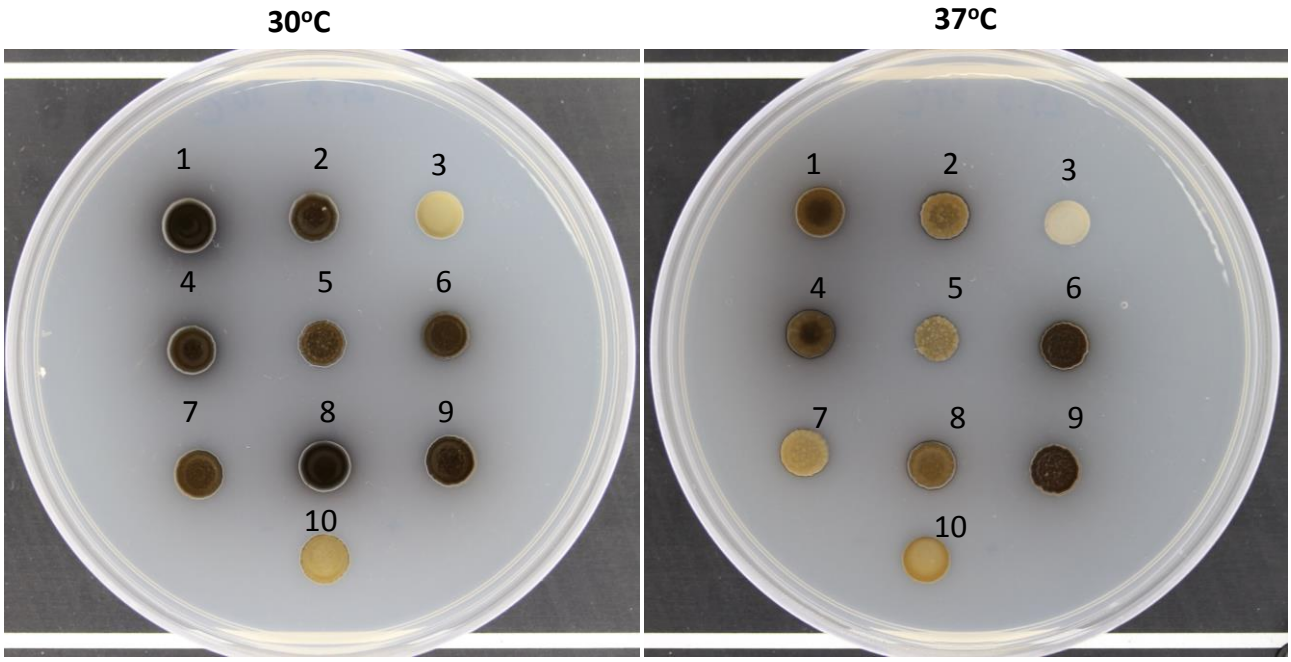

Figure 3.3-8. Melanin production on L-DOPA medium of eight clinical *C. neoformans* isolates from Vietnamese patients representing both S5 (n =5) and non-ST5 (n = 3) genotypes that were tested for virulence in mice.

For each isolates, 10 µl of 10^6 cell suspension was inoculated on L-DOPA agar and incubated in the dark at 30°C and 37°C. No clear genotype-specific patterns of melanization were observed at either 30°C or 37°C. The five ST5 strains displayed marked variation in the degree of pigment production, from mildly melanized (BK147) to highly melanized (BK44 and BMD1646). Strain order: 1:BK44 (ST5); 2:BK80 (ST4); 3:BK147 (ST5); 4:BMD700 (ST5); 5:BMD1338 (ST5); 6:BMD1367 (ST306); 7:BMD1415 (ST4); 8:BMD1646 (ST5); 9:H99; 10: an insertion mutant with diminished melanin production used as negative control.

3.3.2. ST5 isolates from were less virulent than non-ST5 isolates in experimental mice infection

We tested the hypothesis of whether higher prevalence of ST5 infection in apparently healthy hosts was associated with higher virulence potentials of these strains using a murine model of infection. Infections with the ST5 strains were associated with significantly longer survival time than infection with the non-ST5 strains (p<0.0001, log-rank test, also see **Figure 3.3-9**).

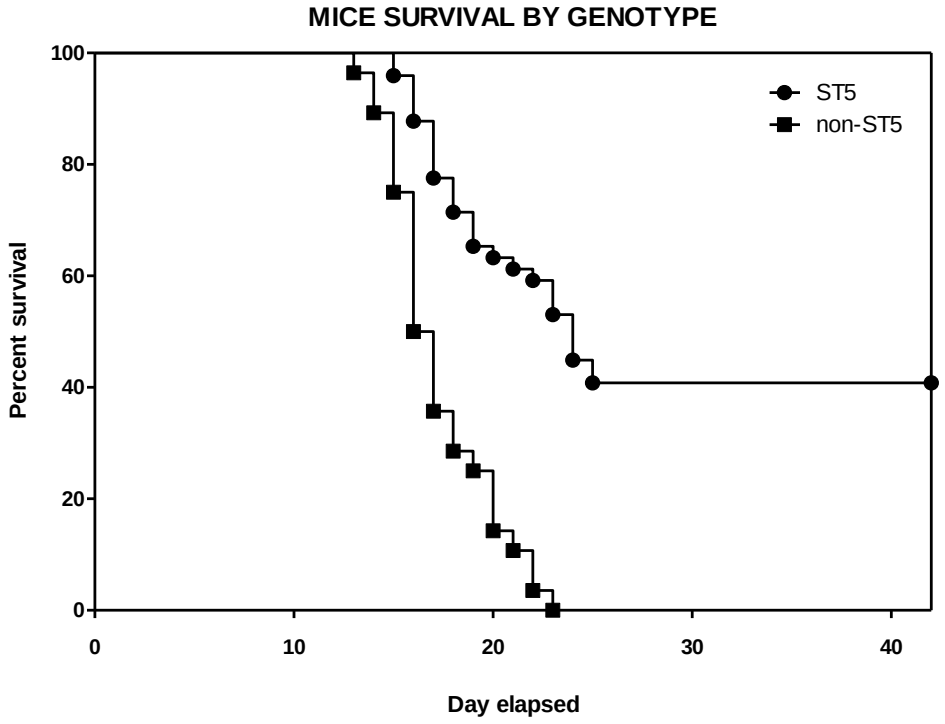

Figure 3.3-9. Kaplan-Meier survival curves for mice infected with either VNI-γ or VNI-δ *Cryptococcus neoformans* strains. 10 mice were infected per strain (ST5: n=5, non-ST5: n=3).

Mice were monitored daily until the point of more than 15% weight loss or visible suffering and were then sacrificed by CO_2 inhalation. Mice infected with ST5 strains had statistically significantly longer survival times than those infected with non-ST5 strains (P<0.0001, Mantel-Cox log rank test).

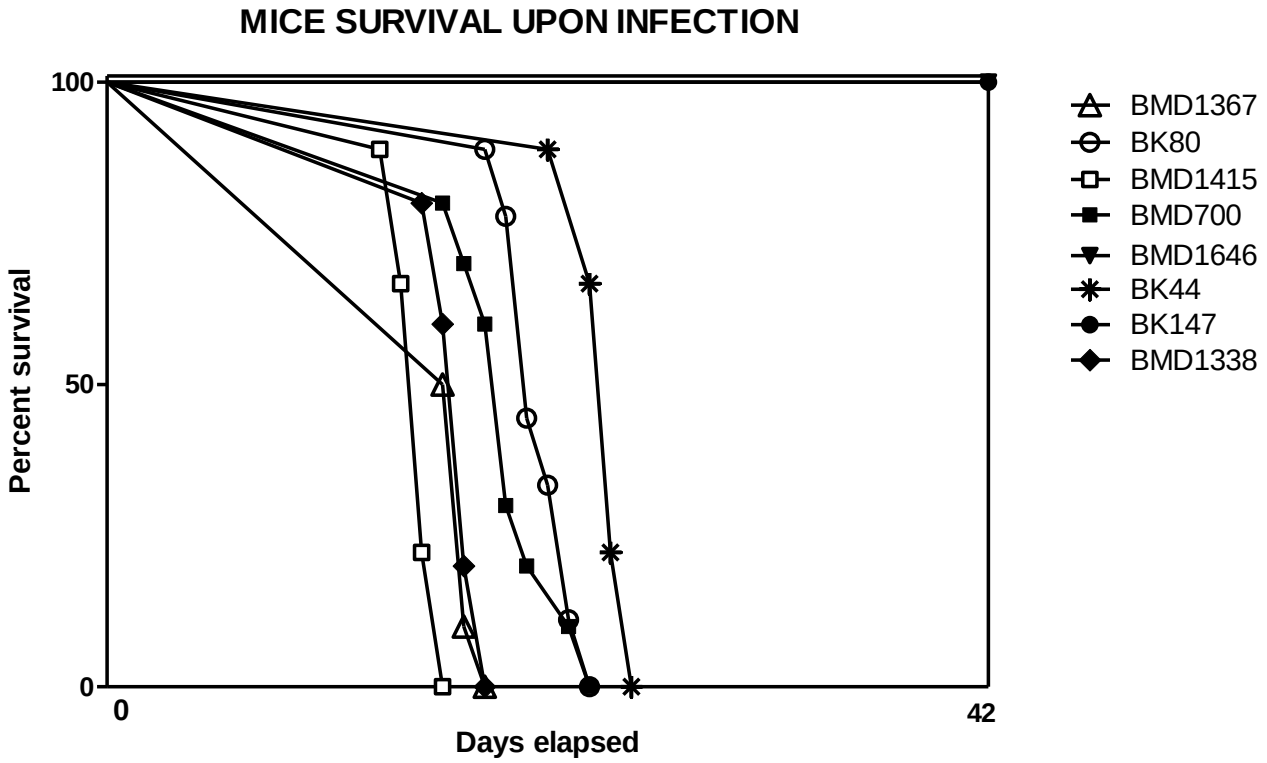

Figure 3.3-10. Survival proportions for mice infected with 8 individual *Cryptococcus neoformans* strains representing 2 main cryptococcal genotypes in Vietnam.

A/J mice were infected with 8 representative *Cryptococcus neoformans* strains (5 VNI-γ/ST5 strains, denoted by black symbols, and 3 VNI-δ/non-ST5 strains, denoted by open symbols). 10 mice were included for each strain from each genotype. Mice were monitored daily until over 15% weight loss and were sacrificed by CO_2 inhalation.BMD1415 and BMD1338 represent the most virulent VNI-δ and VNI-γ strain, respectively. Mice infected with BK147 and BMD1646 (indicated by straight Kaplan-Meier lines at 100% survival rate) survived for as long as 42 days post-infection, at which point the experiment was terminated and all infected mice euthanized.

There was significant variability in the effect of individual yeast strains of the same lineage on survival time (**Figure 3.3-10**). Notably, two ST5 strains (BK147 and BMD1646) appeared to be substantially attenuated in comparison to the other ST5 strains with mice infected with these strains surviving up to day 40 post infection. Due to the time constraint all mice infected with these two attenuated strains were euthanized at day 40 post-infection. The differences in survival times between mice infected with ST5 and non-ST5 strains remained significant when data from these two isolates were removed from the comparative analysis (p=0.003, log-rank test, data not shown). Of the eight strains selected for infecting mice, the two most virulent were BMD1415 (ST4), and BMD1338 (ST5); infection with these isolates resulted in 100% mortality by days 17 and 18, respectively (median survival 15 and 17 days, respectively). BMD1338 was significantly less virulent than BMD1415 (p=0.0015, log-rank test). No significant difference in virulence was detected between BMD1338 and BMD1367, the second most virulent non-ST5 strain.

All strains successfully established lung infection and disseminated to the brain of the mice as early as day 7. Consistent with the survival data, the non-ST5 strains established a higher fungal burden in the lung than the ST5 organisms at all time-points (p=0.0002, p<0.0001, and p<0.0001 at day 7, day 14, and at the point of 15% weight loss, respectively, Mann-Whitney U-test) (**Figure 3.3-11** and **Table 3.3-2**). Moreover, these data were not driven by the two severely attenuated isolates (BK147 and BMD1646) as the fungal loads associated with ST5 infections remained low even when these two isolates were excluded from the analysis. Lung

fungal burdens from mice infected with BMD1646 (ST5) and BK147 (ST5) were mostly low for as long as day 14 (**Figure 3.3-12**). On the other hand, despite these differences in fungal burden in the lung, there were no genotype-specific differences in fungal burden in the brain up to day 14. However, brain fungal burdens in non-ST5 infections were significantly higher than the brain fungal burdens in ST5 infections at the point of 15% weight loss (mean $\log CFU.g^{-1}$ (95%CI); 4.5 (3.9-4.7) and 2.9 (2.2-3.6) for non-ST5 and ST5 respectively, p=0.01, Mann-Whitney U-test).

Table 3.3-2. Tissue fungal burden in mice at days 7, 14 and death by infecting MLST Sequence Type

Tissue	Fungal burden (Mean $\log_{10}$ colony forming units per gram tissue) [95%CI] ST5	Non-ST5	P-value
Lung (Day 7)	4.96 [3.86 - 6.05]	7.07 [6.85 - 7.29]*	<0.01
Brain (Day 7)	0.81 [0.38 - 1.24]	1.59 [0.87 - 2.30]	0.05
Lung (Day 14)	5.48 [4.34 - 6.62]	8.00 [7.77 - 8.23]*	<0.0001
Brain (Day 14)	1.56 [0.81 - 2.31]	1.91 [1.12 - 2.69]	0.36
Lung (Death)	3.81 [3.05 - 4.57]	6.53 [6.30 - 6.76]*	<0.0001
Brain (Death)	2.90 [2.23 - 3.56]	4.29 [3.90 - 4.68]*	0.01

**Statistical significance by Mann-Whitney test.*

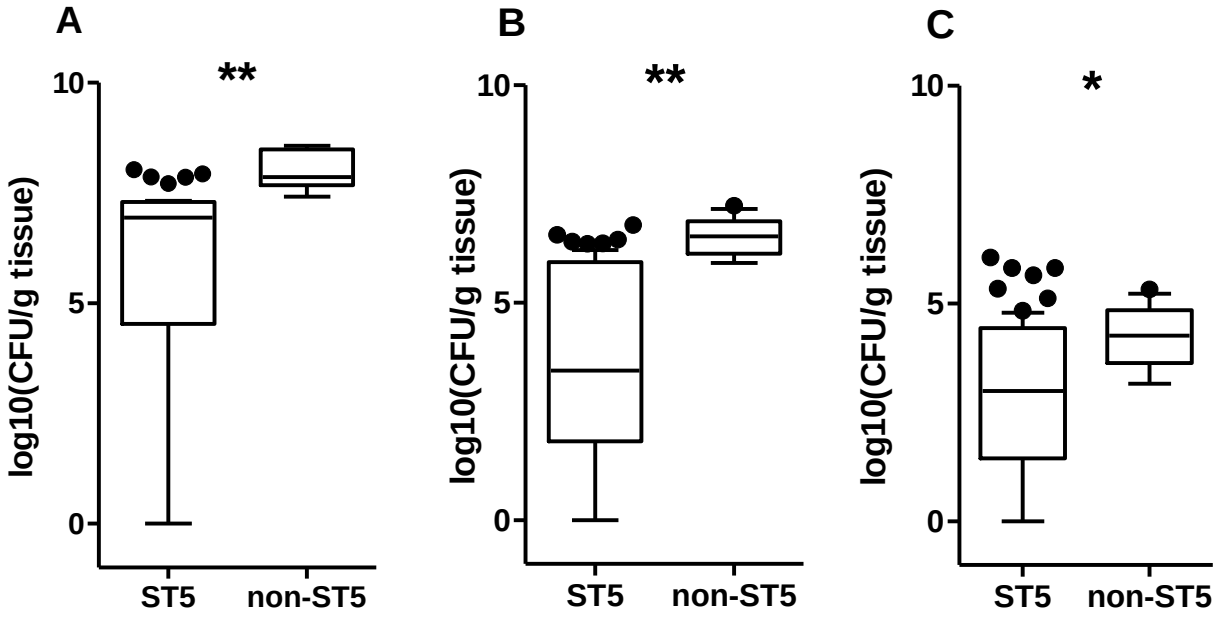

Figure 3.3-11. Fungal burden in lung tissue at day 14 (A), lung fungal burden at point of impending death (B) and brain fungal burden at point of impending death (C) according to infecting genotype. 5 mice were infected per strain (ST5 N = 5, non-ST5 N = 3).

Mice were monitored daily until there was > 15% weight loss or visible suffering and were then sacrificed by CO_2 inhalation. Non-ST5 fungal burden appeared higher than that of ST5 in both lung and brain tissue at all time-points (Mann-Whitney test, **: P<0.0001, *: P<0.05). The horizontal line within the box indicates the median; boundaries of the box indicate the 25th and 75th percentile and the whiskers indicate the highest and lowest values of the results; outliers are denoted as black dots.

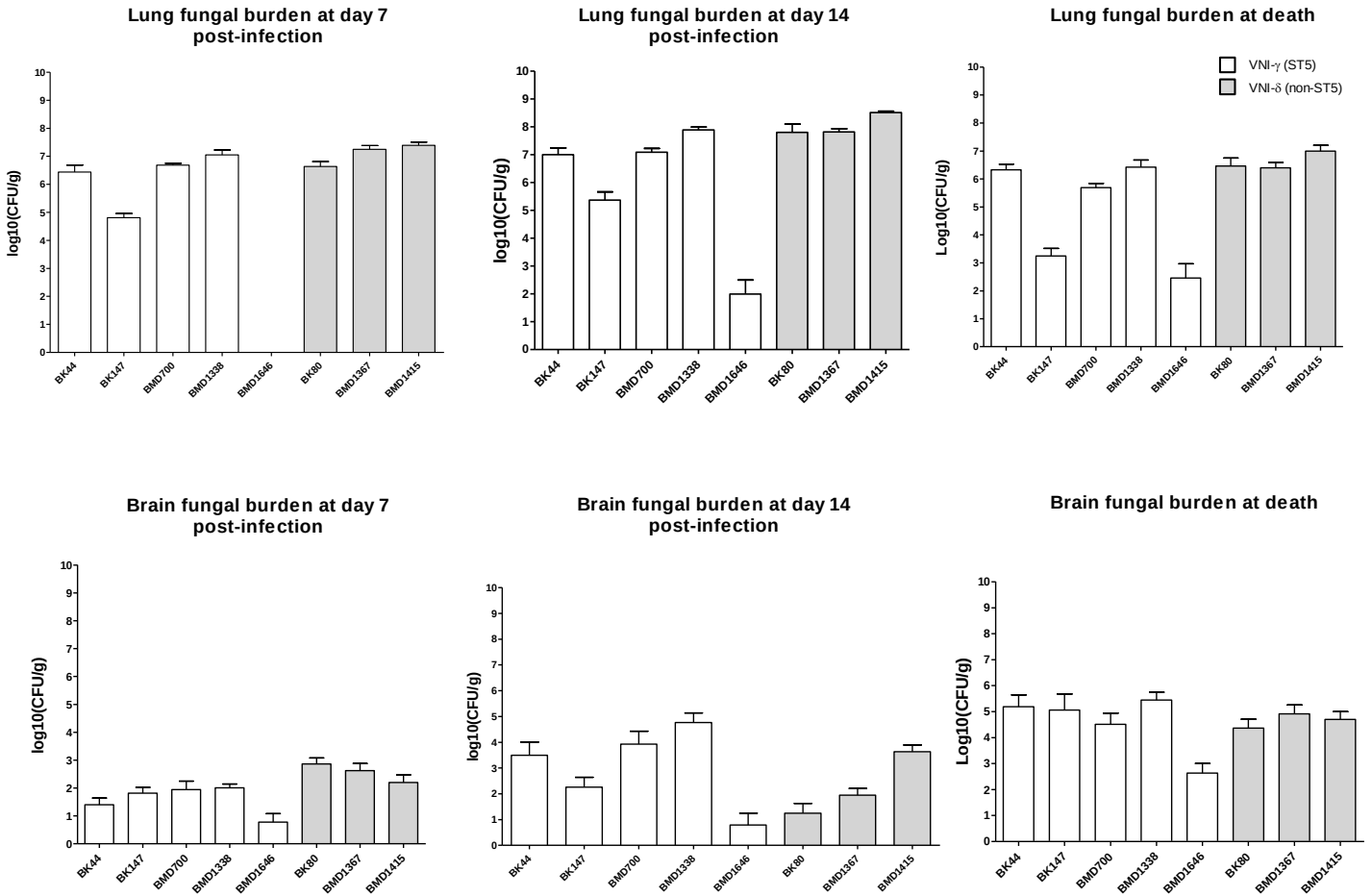

Figure 3.3-12. Fungal burden in mice tissue at specific time points during the course of experimental mice infection (day 7 and day 14 post-infection, point of impending death).

Chosen ST5 (n=5) and non-ST5 (n=3) isolates were inoculated into five A/J mice on different experimental batches to assess *in vivo* virulence. Fungal load were standardized into CFU per gram tissue (CFU/g). Data for each isolates were presented as averaged CFU/g from five mice in the same group with error bars denoting standard deviation.

1

3.3.3. *C. neoformans* isolates from HIV-uninfected patients induced higher levels of pro-inflammatory TNF-α production in the lungs of infected mice

We next measured the concentration of cytokines from lung homogenates of A/J mice infected with the various strains at days 7 and day 14 post-infection. Cytokine concentrations at these time points are shown in

Figure 3.3-13, according to the genotype of the infecting organism. At day 7, ST5 infections were associated with significantly higher concentrations of TNF-α in the lung than non-ST5 strain infections (p=0.01, Mann-Whitney U-test; also see **Table 3.3-3**). Furthermore, among ST5 strain infections at day 7, TNF-α concentrations were highest for the two specific strains that appeared to be most attenuated in the mouse survival model (BK147 and BMD1646), and lowest in BMD1338, the most virulent ST5 isolate in the mouse model. By day 14, mean TNF-α concentration associated with the ST5 strains had declined from 3933.71 pg/g to 2802.36 pg/g. Other Th-1 cytokines including IL-12, IL-17 and IFN-γ also decreased in ST5-infected mice between day 7 and day 14 (p<0.001, p<0.01 and p=0.02, Mann-Whitney U-test, respectively).

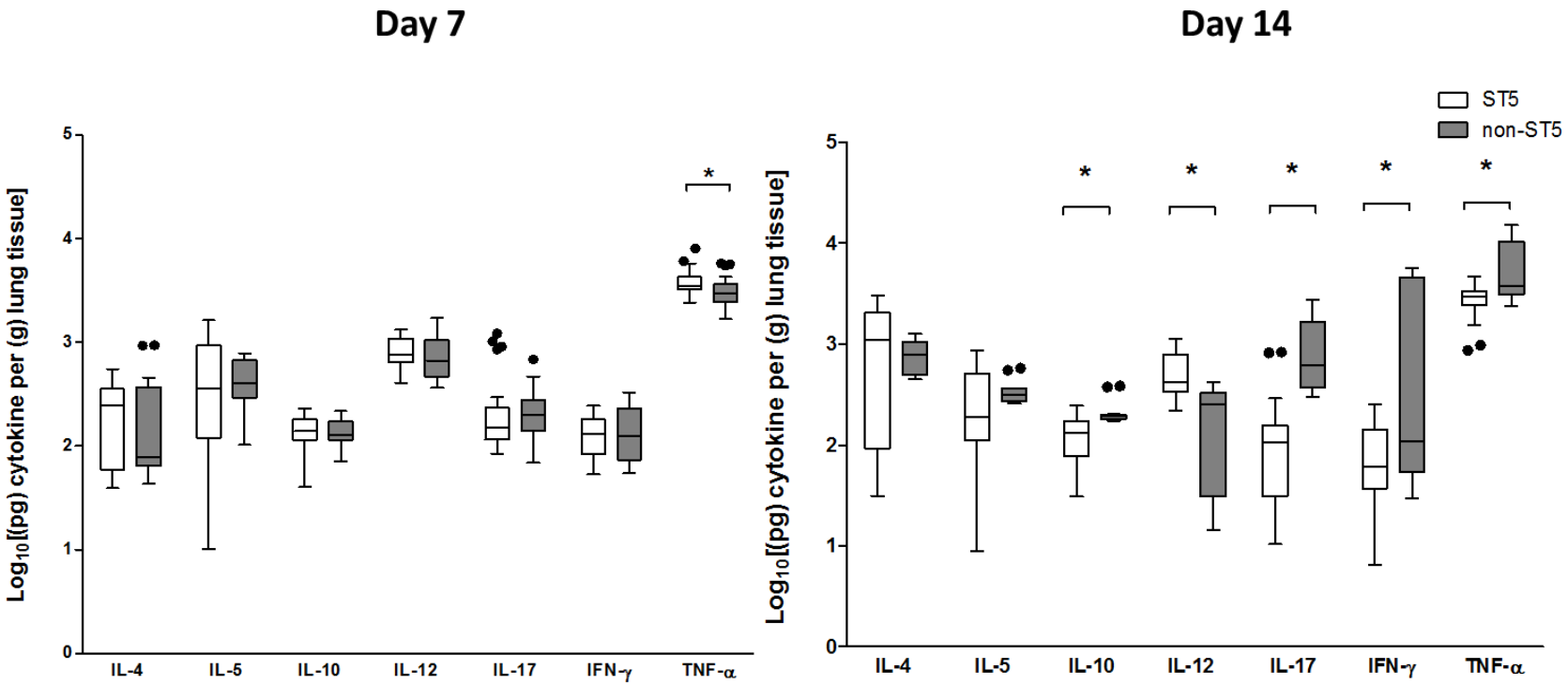

Figure 3.3-13. Genotype-specific cytokines concentrations from lung homogenate of A/J mice at 7 and 14 days post infection with 5x10^4 *C. neoformans* cells/mouse.

Five mice were infected with each strain from each genotype at each time points. Box and whisker plots comparing levels of each cytokine between each genotype at day 7 and day 14 post-infection. ST5 strains induced significantly higher level of TNF-α at day 7 but by day 14 mice infected with non-ST5 strains appeared to have much higher proinflammatory cytokines. The horizontal line within the box indicates the median; boundaries of the box indicate the 25th and 75th percentile and the whiskers indicate the highest and lowest values of the results; outliers are denoted as black dots. Data are standardized as picogram of cytokine per gram lung tissue. Asterisks show statistical significance by Mann-Whitney test.

Table 3.3-3. Cytokine concentrations from lung homogenate of infected mice at day 7 and day 14 post-infection according to infecting *Cryptococcus neoformans* AFLP group

Cytokine		Mean cytokine concentration (pg per gram of lung tissue) [95%CI] ST5	Mean cytokine concentration (pg per gram of lung tissue) [95%CI] Non-ST5	*P Value (ST5 vs non-ST5)
Day 7				
Th-1	IL-12	853.12 [750.50 - 955.80]	822.87 [608.90 - 1037.00]	0.30
	IFN-γ	136.02 [115.00 - 157.00]	150.59 [105.80 - 195.30]	0.97
	TNF-α	3933.71 [3486.00 - 4381.00]	3256.25 [2630.00 – 3882.00]	**0.01**
Th-2	IL-4	230.79 [162.80 - 298.80]	253.24 [11.60 - 349.90]	0.92
	IL-5	561.05 [369.00 - 753.10]	459.85 [344.40 - 575.40]	0.91
	IL-10	145.01 [128.20 - 161.80]	139.99 [119.30 - 160.70]	0.68
Th-17	IL-17	268.48 [155.90 – 381.00]	243.41 [165.60 - 321.20]	0.24
TNF-α/IL-10 ratio		27.13	23.26	N/A
Day 14				
Th-1	IL-12	547.84 [412.40 - 683.30]	213.72 [120.50 - 306.90]	**<0.01**
	IFN-γ	91.2 [57.25 - 125.20]	1760.67 [166.50 - 3355.00]	0.09
	TNF-α	2802.36 [2385.00 - 3220.00]	6378.76 [3374.00 - 9384.00]	**<0.01**
Th-2	IL-4	1154.72 [673.50 – 636.00]	800.35 [604.70 – 996.00]	0.60
	IL-5	294.6 [170.40 - 418.80]	347.55 [279.20 - 415.90]	0.15
	IL-10	132.76 [102.10 - 163.40]	220.15 [172.40 - 267.90]	**0.01**
Th-17	IL-17	175.75 [65.54 – 286.00]	1012.49 [459.20 – 1566.00]	**0.01**
TNF-α/IL-10 ratio		21.11	28.97	N/A

** Mann-Whitney test.*

In contrast, non-ST5 strain infections resulted in increased mean TNF-α levels from 3256.25 pg/g to 6378.76 pg/g (p=0.0003 and p=0.0235, Mann-Whitney U-test, respectively; also see **Table 3.3-3**) between days 7 and 14. However, the high concentration of TNF-α seen in non-ST5 strain infections at day 14 was driven by a single isolate - BMD1415; TNF-α concentrations in the lung in mice infected with this isolate were significantly higher than for infections with any other ST5 or non-ST5 isolate (p<0.05, Mann-Whitney U-test). There were no statistically significant differences in TNF-α concentration at day 14 when data from infections due to this isolate were excluded from the analysis. The same BMD1415-driven pattern also occurred when comparing IFN-γ and IL-17 concentrations at day 14. The concentrations of these two cytokines in BMD1415-infected mice appeared significantly higher than in mice infected with any other isolates (p<0.05, Mann-Whitney U-test; see **Figure 3.3-14**). However, IL-12 concentrations fell in non-ST5 strain infected mice, including BMD1415, between day 7 and 14 (4 fold decrease, p<0.0001, Mann-Whitney U-test) **(Figure 3.3-15**).

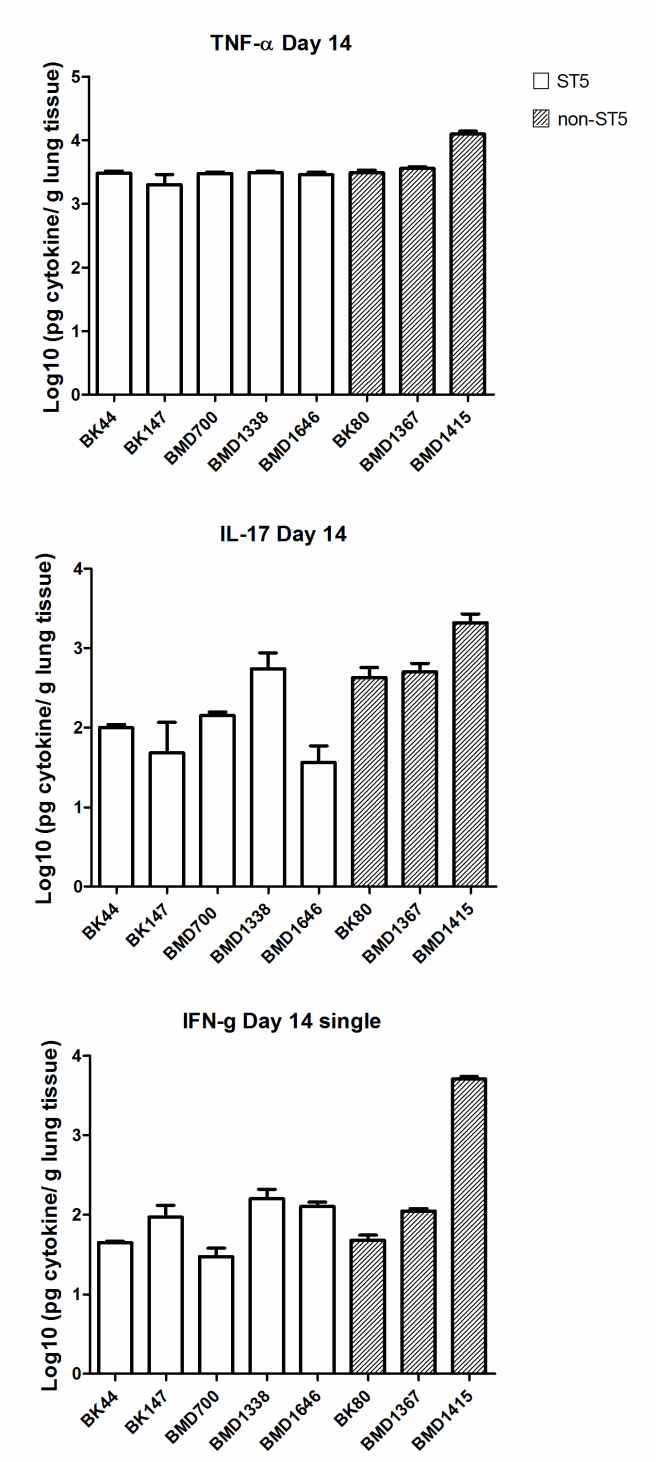

Figure 3.3-14. TNF-α, IFN-γ and IL-17 levels associated with individual isolates at day 14.
TNF-α, IFN-γ and IL-17 at day 14 were significantly higher in mice infected with non-ST5 strains. BMD1415 induced significantly higher levels TNF-α, IFN-γ and IL-17 than any other isolates (p<0.05, ANOVA with Dunnett's multiple comparison test). Bar plot presents picogram of cytokine per gram lung tissue. Error bars denote standard deviations.

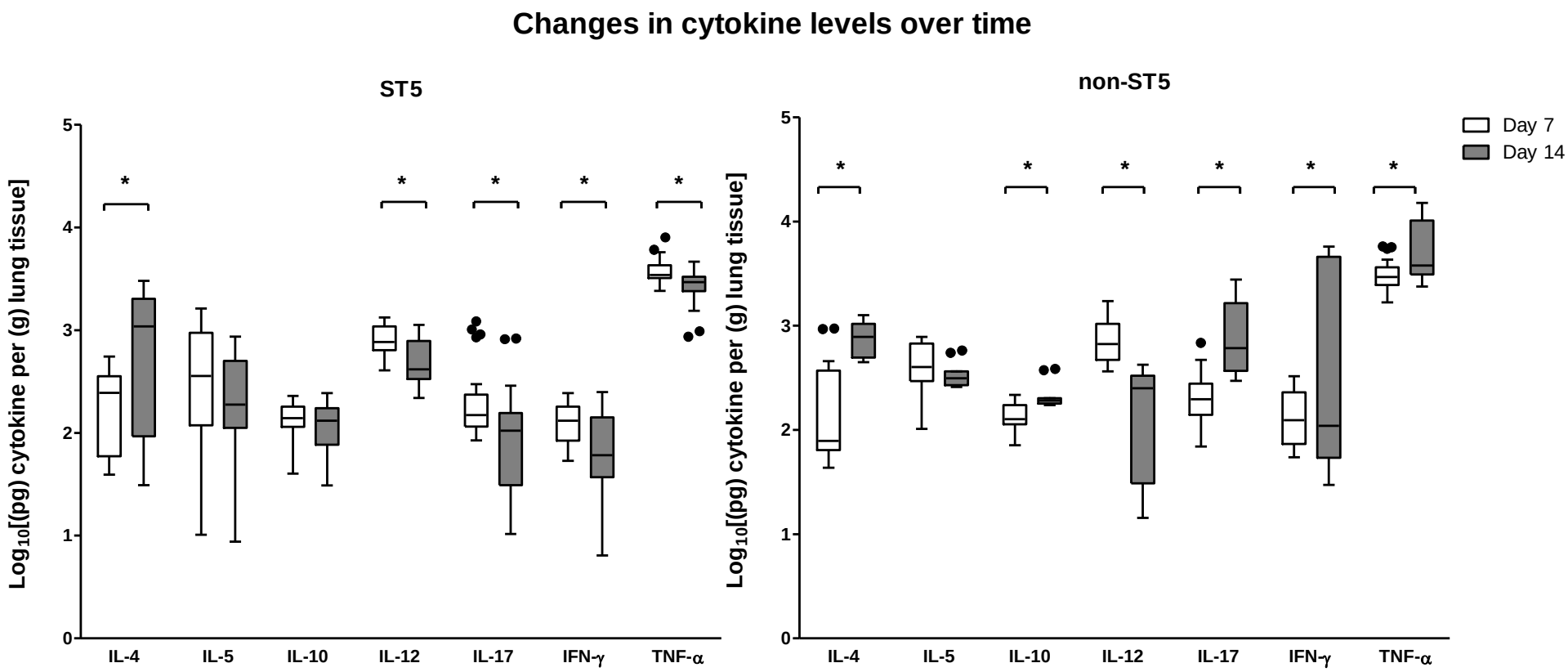

Figure 3.3-15. Genotype-specific changes of cytokine concentration from lung homogenate of A/J mice infected with 5x10^4 *C. neoformans* cells/mouse between day 7 and day 14 post-infection.

Box and whisker plots compare levels of each cytokine between day 7 and day 14 for each genotype. The horizontal line within the box indicates the median, boundaries of the box indicate the 25th and 75th percentile and the whiskers indicate the highest and lowest values of the results; outliers are denoted as black dots. Data are standardized as picogram of cytokine per gram lung tissue. Asterisks show statistical significance by Mann-Whitney test.

1

I also measured the TNF-α/IL-10 ratio as a proxy marker of the relationship between a Th-1 and a Th-2 response [378]. From day 7 to day 14 post-infection, the TNF-α: IL-10 ratio decreased almost 1.28 fold in mice infected with ST5 isolates while those infected with non-ST5 strains exhibited a TNF-α: IL-10 ratio increase of 1.25 fold. However, when BMD1415 (ST4) was excluded from the analysis the TNF-α/IL-10 ratio in mice infected with non-ST5 strains decreased by a factor of 0.67. By day 14 we detected elevated concentrations of IL-17 and IFN-γ in non-ST5 infected mice (5-fold and 17-fold increments, respectively (**Table 3.3-3**), but not in ST5 infected mice. Again, this effect was largely associated with BMD1415, since the concentrations of IL-17 and IFN-γ induced by this isolate at day 14 were significantly higher than for all others (p<0.05, one way ANOVA test; also see

Figure 3.3-14**).**

3.3.4. Histopathological examination

Histological examination of infected lung tissue revealed evidence of inflammation, hemorrhage, edema and necrosis in most cases. These changes were generally greater by day 14 in comparison to day 7. There were no clear differences in histological scores between

sequence types, other than strain BMB1646 (ST5) which had only mild inflammation with no necrosis or hemorrhage seen (**Figure 3.3-16**). PAS staining revealed extensive perivascular infiltration of leukocytes in mice tissue associated with both infecting genotypes (BMD1338-ST5 and BMD1415-ST4, **Figure 3.3-17**). The extrapulmonary space of BMD1338-infected mice was markedly packed with localized infiltrating leukocytes (**Figure 3.3-17**). Though we could not quantitatively assess and compare genotype-specific capsule size *in vivo,* ST5 yeasts appeared extensively encapsulated in the lung sections, especially at day 14 (**Figure 3.3-17**). Diffuse capsular localization could be observed in the mucicarmine staining images (**Figure 3.3-18**).

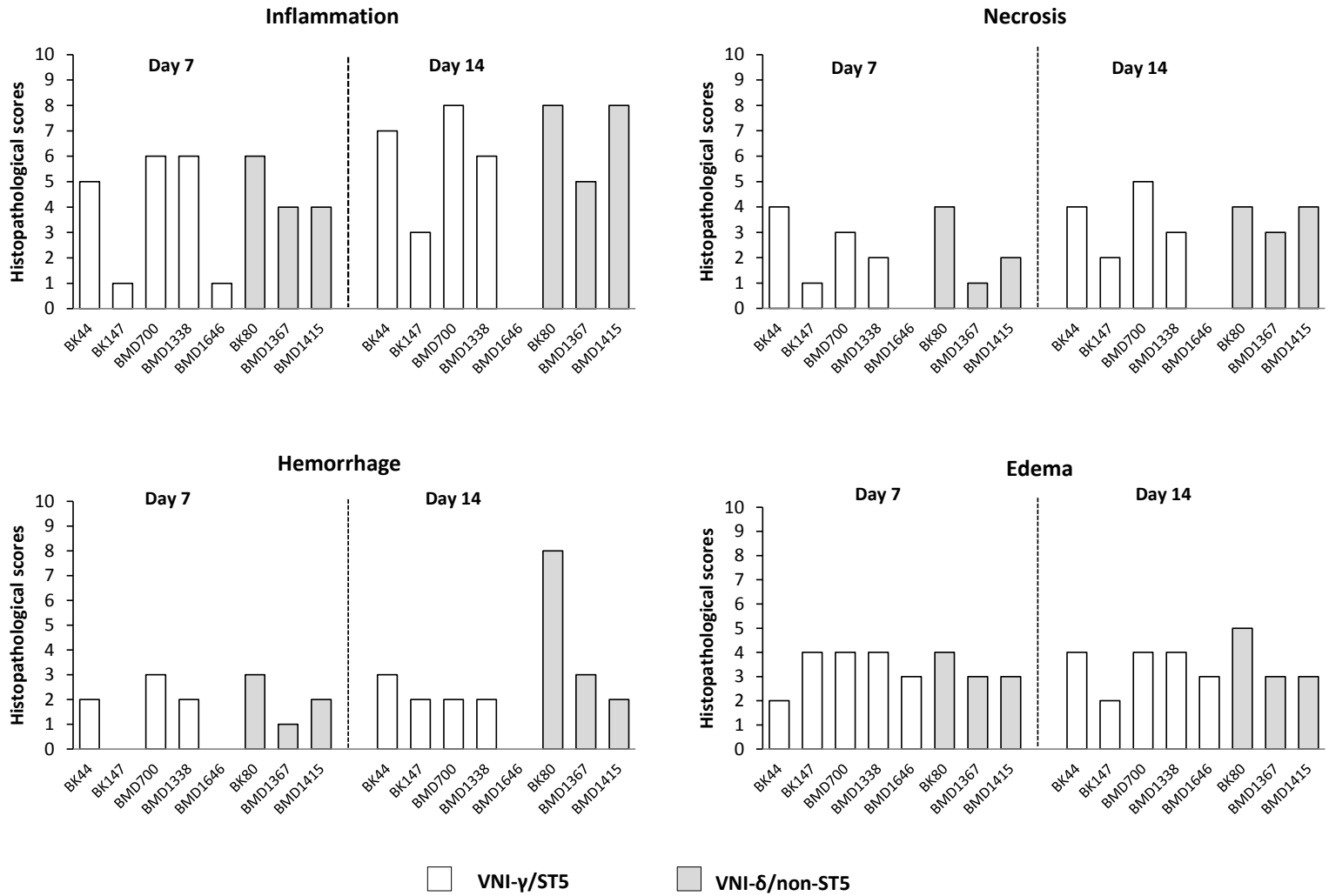

Figure 3.3-16. Histopathological scores in 4 categories of tissue damage (Inflammation, necrosis, hemorrhage and edema).
Thin sections of parafin-embedded lung specimens from infected mice were stained using the Periodic Acid Schiff (PAS) method. Specimens were randomized, blinded and assessed by an independent pathologist. Histopathological scores ranged from 0 (no changes) to 10 (severe changes), corresponding to the severity of pathology in 4 different categories: necrosis, hemorrhage, edema and inflammation as per the Duke Veterinary Diagnostic Laboratory protocol (Division of Laboratory Animal Resources).

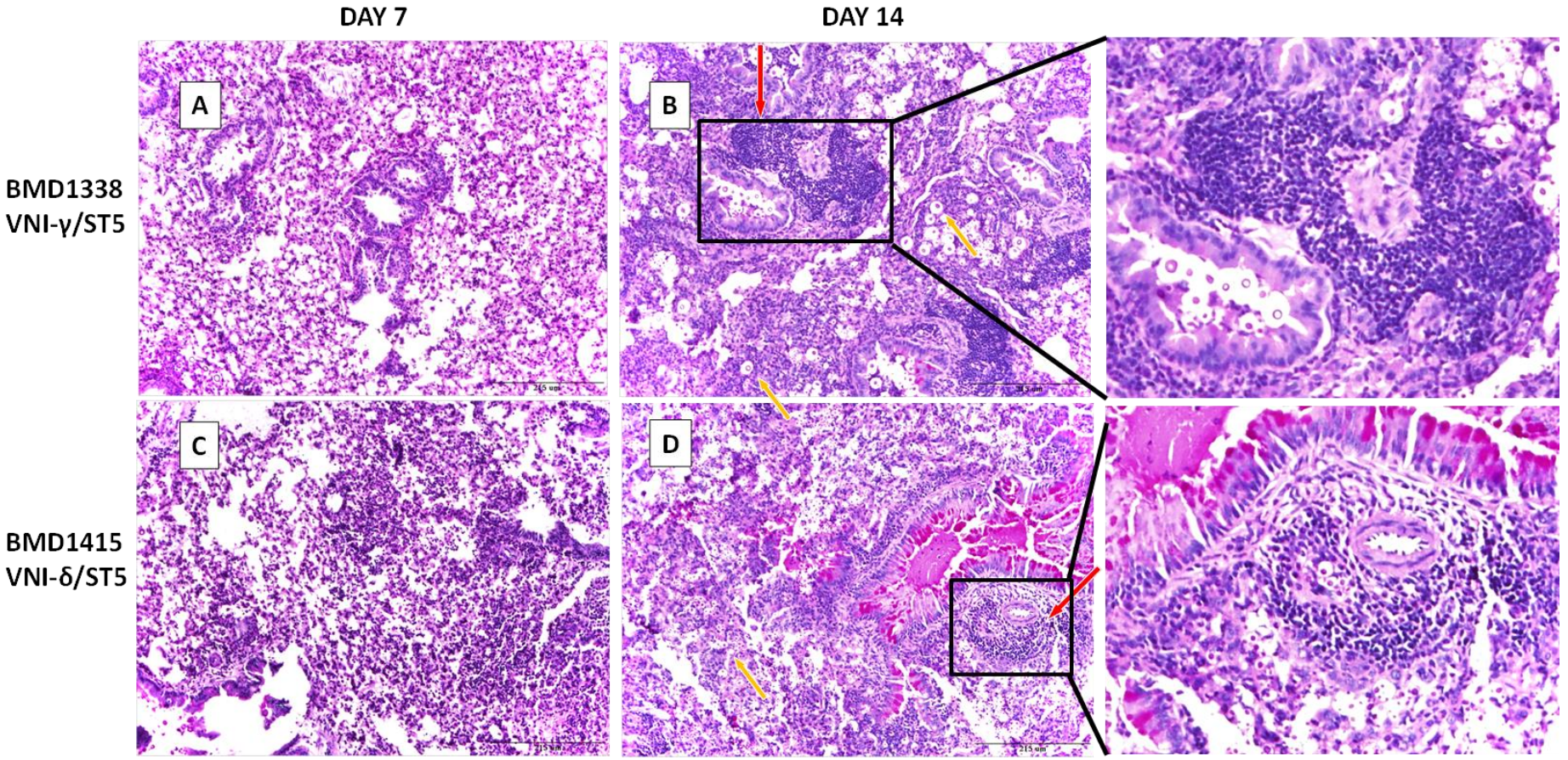

Figure 3.3-17. Periodic acid Schiff (PAS) staining of pulmonary tissue from mice infected with BMD1338 and BMD1415 on days 7 ad 14.
The two strains represent ST5 and non-ST5, respectively. A/J mice were inoculated intranasally with $5x10^4$ yeast cells. Lung specimens were harvested at days 7 and 14 for histopathological examination. Photomicrographs were obtained at 200X magnification; the scale bar represents 215 µm). (A-B): lung sections from mice infected with BMD1338 (VNI-γ/ST5) at day 7 and day 14, respectively. (C-D): lung sections from mice infected with BMD1415 (VNI-δ/ST4) at day 7 and day 14, respectively. Perivascular infiltration (red arrows) and necrosis are more marked by day 14 for both strains. Encapsulated yeasts (yellow arrows), notable for the larger cell size and capsule thickness of BMD 1338 compared with BMD1415. Sections with leukocytes localization are enlarged on the outer right panels.

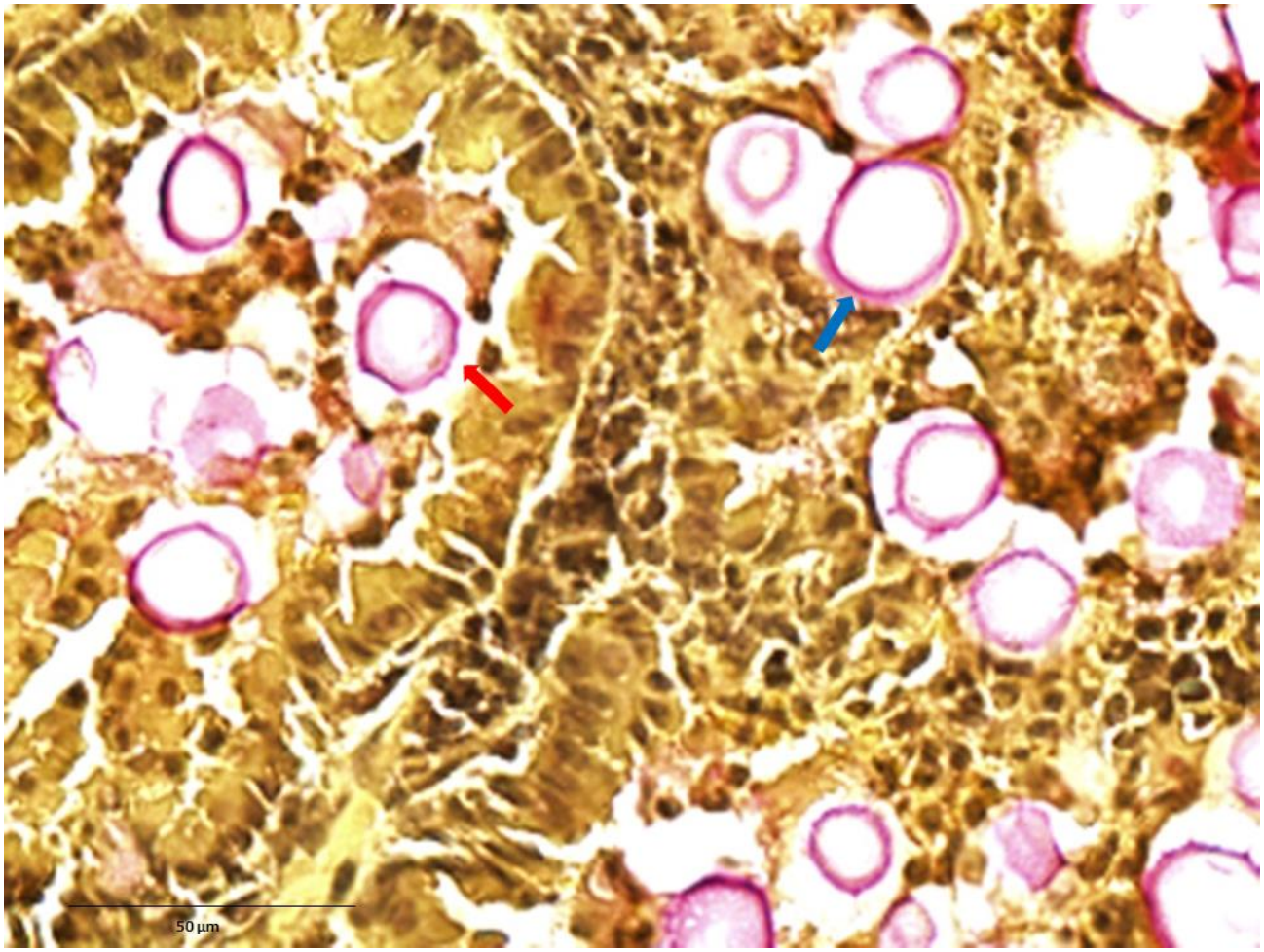

Figure 3.3-18. Mucicarmine staining from paraffin-embedded mice pulmonary tissue.
Polysaccharide components from the capsule of *Cryptococcus neoformans* yeasts are visualized in pink stain. Photomicrographs were obtained at 400X magnification. The scale bar indicates 50 µm. Red and blue arrows indicate where the inner and outer layers of the capsule are stained, respectively. These indicate the white spaces in and around the alveolar tissue are evident of the capsules presence.

3.4. Chapter 3 Discussion

Previous work from my group described two distinct AFLP-defined clusters of *C. neoformans* var. *grubii* in Vietnam: VNI-γ, which accounted for the majority of cases in HIV-uninfected patients and were all MLST-ST5, and VNI-δ which mostly consisted of isolates from HIV-infected patients and included all other MLST sequence types in the population [103,325]. The high prevalence of ST5 infection in HIV-uninfected patients could be explained either by these strains being intrinsically more virulent or due to unidentified lineage–specific host immune defects or exposures. In this study we investigated the first hypothesis by comparing previously identified virulence-associated phenotypes and *in vivo* virulence and immune responses in the mouse model by lineage. The strains were grouped on the basis of their genetic relatedness using AFLP and MLST genotyping. There could have been genomic variations within and between the lineages that MLST did not have enough resolution to distinguish. However since all ST5 strains fitted well within the AFLP-defined cluster of VNI-γ in our study, we believe our random sampling was well-justified in that it well-represented the two major clades of the *C. neoformans* var. *grubii* population from Vietnam.

Strains from all STs were able to grow in *ex vivo* human CSF and at 37^{o}C as well as having extracellular urease and phospholipase activity - essential characteristics for establishing human infection. However, we could not identify any apparent ST-specific difference of growth under these conditions, suggesting that the ability to establish disease in HIV-uninfected/immunocompetent patients is not driven by simple adaptations to high

temperature or growth in human CSF. However, we found ST5 cells to be both significantly larger than non-ST5 cells and to have thicker capsules *in vitro*. The capsule of *C. neoformans* plays important roles in pathogenesis, from interfering with phagocytosis by host macrophages to modulating the host immune response [164,379–381]. Previously, it has been shown that variation in capsule size correlates with pathogenic potential of *C. neoformans* [382]. *Ex vivo* capsule size has also been associated with higher intracranial pressure, slower clearance of yeasts and paucity of inflammation in humans [164]. Our study demonstrates that while ST5 isolates have significantly higher capacity for *in vitro* capsule enlargement, this phenotype did not translate into increased virulence in the mouse model. Mice infected with ST5 isolates not only had better survival but also lower tissue fungal burdens than those infected with non-ST5 strains, contrary to recent human data which supports morphological changes being associated with more severe pathology in the human host (e.g *ex vivo* capsule size and capsular shedding has been associated with increased intracranial pressure in CM patients with HIV[164]).

There are several possible explanations for the lower virulence of ST5 in mice we observed. First, virulence in mice is variable depending on mouse breed and may not accurately reflect the immunological heterogeneity of the human population [383]. Second, yeasts with different pathogenic potentials, associated with their isolation from different sources (i.e. clinical versus environmental, immunocompromised vs immunocompetent patients) may have the same or paradoxical pathogenic potential in experimental animal models. For

instance, *C. gattii* is often associated with infection in immunocompetent patients and therefore is considered more virulent (or fit) in the human host than *C. neoformans*. However, it has been shown that the hypervirulent *C. gattii* strain R265, responsible for the on-going Vancouver outbreak, has similar virulence in both C57BL/6 and A/J mice to the *C. neoformans* H99 strain, which is derived from a patient on chemotherapy with Hodgkin's disease [384]. Similarly, R272, a Vancouver outbreak *C. gattii* VGIIb strain also displayed identical degree of virulence as WM276, an environmental isolate from Australia, in murine models [384]. Third, the A/J mouse strain is not immunologically intact and thus may be an imperfect model of infection for immunocompetent hosts [385]. Rather, A/J mice may be a better model of disease in immunosuppressed patients, as they are highly susceptible to cryptococcal disease, and the patterns of cytokine expression in mice with disseminated cryptococcosis are similar to those seen in HIV-infected patients with CM [386]. Our results suggest that additional models that better mimic infection in apparently immunocompetent hosts may be needed to explain the complex interaction between *C. neoformans* and the human host.

In cryptococcal infection in mice, a Th1 type immune response, defined by the TNF-α/IL-10 ratio, is considered to be protective, while a Th2 response is associated with poor outcomes [271,282]. We did not detect genotypic-driven changes in TNF-α/IL-10 ratios over time, although higher TNF-α concentrations were induced by ST5 strains at day 7 suggesting this genotype elicited a more intense initial inflammatory response. This finding could be

explained by the increased capsular size of ST5 organisms - previous studies have suggested that capsule components, or cryptococcal cells themselves, have a dose-dependent ability to stimulate TNF-α production by various immune effector cells [387,388]. ST5 organisms, though present in mice in fewer number than non-ST5, induced stronger inflammatory response in mice 7 days post-infection, suggesting that TNF-α production may be driven by capsular components rather than cell number. Previously, it has been suggested that *C. gattii* is able to cause disease in apparently immunocompetent patients because it induces a less severe inflammatory response than other cryptococci [384]. However data generated from our murine infection experiments do not support a less severe inflammatory response being the mechanism underlying the ability of ST5 *C. neoformans* var. *grubii* organisms to cause disease in the immunocompetent.

In vivo controlled infection studies in mice commonly define pathogenicity as the microbe's capability to cause disease in a susceptible host, whereas virulence corresponds to the severity of the ensuing pathology [68]. Using the same infective dose for all strains we failed to demonstrate that ST5 strains had greater virulence than non-ST5 organisms. The difference we observe in prevalence of different lineages in immunocompetent and immunosuppressed human patients may alternatively represent a specific difference in the ability of the organisms to colonize the host and establish infection, which we were unable to assess with our experimental system.

Spores are presumed to be the main infectious propagule for *Cryptococcus* spp [69]. Capsule biosynthesis genes are required for both efficient sexual development and spore formation and dispersal [70]. Given the higher rate of capsular enlargement and higher variation in capsule size in ST5 strains, it is possible that capsule biosynthesis genes are more active in ST5 yeasts, resulting in qualitative differences in their spores that confer higher infectivity when interacting with immunocompetent hosts. Moreover, the higher rates of variability that we see in this and other virulence phenotypes (for example, growth at 37^{o}C) within ST5 strains in this study hint that higher phenotypic variability in ST5 may be an adopted strategy that facilitates the exploitation of novel niches. This strategy could have resulted in a phenotype which allowed the successful colonization of one or more novel environmental nich(es), and as a bystander-effect, allowed the exploitation of infrequent specific human immune deficits. This hypothesis should be investigated further to better understand any links between *in vitro* capsular enlargement and cryptococcal disease in apparently healthy hosts.

Thus, our cohort of ST5 yeast isolates displayed two notable phenotypes. First, in general they appeared to be less virulent in a murine model than the other sequence types, as demonstrated by reduced fungal burdens in tissue, induction of greater early immunological responses and prolonged mouse survival. Second, ST5 strains induced larger in vitro capsule and cell sizes than the other genotypes, and notably greater variability between individual strains for this phenotype. Our data lead us to three main conclusions. First, clinical isolates,

which have by their nature already undergone selection within the human host, can possess wide variability in the expression of virulence phenotypes within a single lineage. Secondly, the use of host risk factors and immune phenotype to derive an understanding of the factors that drive the pathogenicity of *Cryptococcus neoformans* may be more complex than anticipated. Associations may be difficult to make due to the relevance of the particular *in vitro* phenotypes, animal models used, within strain heterogeneity, and population substructure. Moreover, there may be significant heterogeneity in the immune response of apparently immunocompetent patients which selects particular sub-cohorts of isolates of the same lineage. Thirdly, the categorization of strains into specific clades with limited genetic information such as MLST may lack precision to understand the relative fitness of specific strains in the human host. It is likely that whole genome sequencing will provide better mapping of the relationships between strains and virulence. Lastly, we tested a relatively small number of strains, and may have lacked power to detect relevant differences that are present at the wider population level.

3.5. Chapter 3 Conclusion

In this study, I demonstrated genotype-specific differences in *in vitro* and *in vivo* virulence phenotypes between *C. neoformans* var. *grubii* strains isolated from hosts with different immune status. There was also significant variation among strains isolated from apparently immunocompetent patients in specific *in vitro* and *in vivo* phenotypes tested. This higher rate of phenotypic variation may represent an evolutionary strategy for *C. neoformans* var. *grubii*

to take advantage of novel niches and contribute to their ability to infect apparently immunocompetent hosts, despite generally being less virulent in a mammalian animal model. Furthering the understanding of the pathogenesis of cryptococcal meningitis will require investigation of large numbers of strains with associated robust clinical information, and the development of high throughput laboratory phenotypic studies that have clinical relevance in humans.

Chapter 4

ASSESSING INTRACELLULAR PARASITISM OF *C. NEOFORMANS* VAR. *GRUBII* ISOLATES FROM VIETNAM USING A HIGH-THROUGHPUT *IN VITRO* MACROPHAGE MODEL OF INFECTION

4.1. Chapter 4 Introduction

Phagocytic cells of the innate immune system (e.g. dendritic cells, macrophages and polymorphonuclear leukocytes) are the first line of host defense against cryptococcal infection [389–391]. These phagocytic cells are also important in modulating the nature and outcome of adaptive immune responses. However, cryptococcal yeasts have also acquired the ability to avoid intracellular killing, proliferate inside host macrophages, transfer laterally between adjacent macrophages and escape from macrophages using lytic or non-lytic (vomocytosis) mechanisms [131,392,393]. This intracellular parasitism capacity is thought to have evolved through interactions with predating amoebas in the environment, which in turn delivers a survival advantage in the mammalian host [94]. Intracellular parasitism of macrophages has important implications. First, it directly affects fungal burden in the host, which has been shown to be correlated with outcome in human disease [135]. In fact, it has been shown that intracellular *C. neoformans* yeasts proliferate faster inside human macrophages than extracellular yeasts [394]. Second, an intracellular niche potentially provides an alternative mode of dissemination within the host and facilitates immune evasion [392]. Hijacking host monocytes in a 'Trojan-horse' mode of action has been

identified as one of the many routes employed by *C. neoformans* to cross the Blood-Brain Barrier[132].

Macrophage parasitism may also be important in both the establishment and maintenance of latent infection, active disease being believed to be the result of reactivation from latency [395]. Repeated lateral transfer of intracellular yeasts between adjacent macrophages has been suggested as a frequent event occurring during latent infection, aiding both immune avoidance and dissemination [393].

Generally, previous *in vitro* studies of cryptococcal pathogenesis employed a few well-characterized strains (e.g. *C. neoformans* var. *grubii* H99, *C. gattii* R265 etc.). It is unclear how results from the use of these repeatedly passaged single examples of particular varieties generalize to the wider clinical context. For example, isolates from the same molecular genotypes or isolation source (both clinical and environmental) may possess different *in vitro*/*in vivo* phenotypes and virulence potential [333,396]. Further understanding of cryptococcal pathogenesis may depend upon studying large numbers of strains with detailed associated clinical information. There is a need to develop high throughput *in vitro* models to test phenotypes with clinical relevance to humans.

Using an *in vitro* murine macrophage model of infection, Ma Hansong and colleagues demonstrated that high intracellular proliferation capacity, both in murine macrophages and human peripheral blood mononuclear cells, was predictive of experimental murine virulence and presumably contributed to virulence in humans [130]. This correlation is independent of

cryptococcal species (*C. neoformans* or *C. gattii*) or mouse breed used [130]. Alanio *et al.* [136] demonstrated that disease outcome in humans involved a complex interplay between host response and specific cryptococcal virulence properties by employing a high-throughput flow-cytometry based macrophage model that allowed simultaneous and rapid quantification of *C. neoformans* intracellular proliferation and yeast uptake by macrophages. In this study, patients infected with isolates that with high yeasts uptake rate and high intracellular proliferation rate (26%; n=14) had a 5-fold-increased risk of death [136]. On the other hand, patients infected with isolates exhibiting both a low yeasts uptake rate and low intracellular proliferation rate (19%; n=10) had a 15-fold-increased risk of having positive CSF cultures after 2 weeks of antifungal therapy [136]. Therefore, intracellular proliferation and macrophage yeast uptake could potentially be used as a parameter to indicate cryptococcal virulence.

In this chapter I employ and develop the *in vitro* macrophage models of infection developed by Ma Hansong *et al.,* [130]and Alanio *et al.,*[136] in order to determine how it relates to the clinical virulence of *C. neoformans* var. *grubii* isolates defined by their ability to infect HIV-uninfected and HIV-infected patients in Vietnam.

Specific Chapter aims are:

1. Develop and refine a high throughput *in vitro* macrophage model of infection to compare the pathogenicity of Vietnamese *C. neoformans* var. *grubii* isolates at the lineage level.

2. Compare and identify possible differences in macrophage parasitism capacity between the VNI-γ/ST5 lineage and the VNI-δ/non-ST5 lineage of *C. neoformans* var. *grubii* in Vietnam. I hypothesize that the VNI-γ/ST5 lineage would have higher virulence potential than other lineages, consistent with its ability to exclusively infect immunocompetent patients.
3. Identify any association between macrophage parasitism characteristics and patient outcomes.

4.2. Chapter 4 Materials and Methods

4.2.1. Clinical *C. neoformans* var. *grubii* isolates and culture conditions

The *C. neoformans* var. *grubii* isolates used in this study were clinical isolates from the cerebrospinal fluid (CSF) of patients enrolled in a randomized controlled trial of antifungal therapy in HIV-infected patients between 2004 and 2011, and a prospective, descriptive study of HIV-uninfected patients with central nervous system (CNS) infections enrolled between 1998 and 2009 [294,307]. All studies were approved by the Institutional Review Board of the Hospital for Tropical Diseases, Ho Chi Minh City, and the Oxford Tropical Ethics Committee or Liverpool School of Tropical Medicine UK.

On positive growth from CSF, a sweep was taken through colonies for archiving. Yeasts were archived at -80^{o}C in Microbank beads (Pro-Lab Diagnostics, UK). Unless otherwise specified, all isolates were single-colony purified prior to experiments and were propagated in Yeast Peptone Dextrose (YPD) broth at 30^{o}C overnight with agitation. Data for mating type and

Amplified Fragment Length Polymorphism (AFLP) genotyping were previously determined and published [103]. MLST genotyping was done and presented in Chapter 2 of this thesis.

A total of 47 *C. neoformans* var. *grubii* isolates were randomly chosen from a list of 136 clinical isolates and included in the screening experiment using method 1. These included 24 AFLP/VNI-γ isolates and 23 AFLP/VNI-δ isolates, randomly chosen from each respective AFLP group. Among the 24 AFLP/VNI-γ isolates, 14 were isolated from HIV-infected patients while the remaining 10 were isolated from HIV-uninfected patients. All 23 AFLP/VNI-δ isolates were isolated from HIV-infected patients. As reported in Chapter 1, while AFLP/VNI-γ isolates infect both HIV-uninfected and HIV-infected patients, all AFLP/VNI-γ isolates isolated from HIV-uninfected patients were MLST-ST5. Isolates other than ST5 were collectively called "non-ST5".

4.2.2. Cell line and cell culture techniques

The J774.A2 cell line (hereafter J774) was purchased from the American Type Culture Collection (ATCC) to study the interaction of *C. neoformans* clinical isolates with macrophages. J774 is a murine macrophage-like cell line derived from a reticulum sarcoma. Cells were maintained at 37°C in the presence of 5% CO2 in Dulbecco's modified Eagle's medium (DMEM) supplemented with 10% heat-inactivated fetal bovine serum (FBS) and 1% penicillin–streptomycin (fresh medium) (all from Invitrogen). The cell monolayer was inspected for viability and density daily and passaged when cells reached 70-80% confluence. Cells were used between 10 and 35 passages.

4.2.3. Phagocytosis assay

J774 cells ($2.5x10^5$ cells/ml) were seeded in 24-well plates one day before the assay. On the day of experiment, cells were incubated for one hour in Serum Free Medium (SFM) containing 100 ng/ml phorbol myristate acetate (PMA). Meanwhile, overnight YPD-grown cryptococcal cells were washed three times with PBS and inoculum quantified using a Cellometer cell counter (Nexcelcom, USA). For experiments with opsonized cryptococci, yeast cells were incubated with 20% pooled human sera (healthy volunteer derived in accordance with OUCRU policy) at 37°C for one hour. Non-opsonised yeasts were used as negative control by replacing opsonins with PBS. To commence the assay, SFM medium containing PMA was removed from the 24-well plates and the cells washed once with PBS; then 1ml SFM medium containing 2.5 $x10^6$ yeast cells were added (Infection Ratio 10 Yeast to 1

Macrophage). The phagocytosis assay was allowed to proceed for two hours in a humidified incubator at 37°C with 5% CO_2. Non-internalized yeasts were then removed by successive washes with pre-warmed SFM or PBS, at which point the experiment is stopped for Phagocytic index scoring or extended for determining intracellular proliferation rate. The experiment design is summarized in **Figure 4.2-1.**

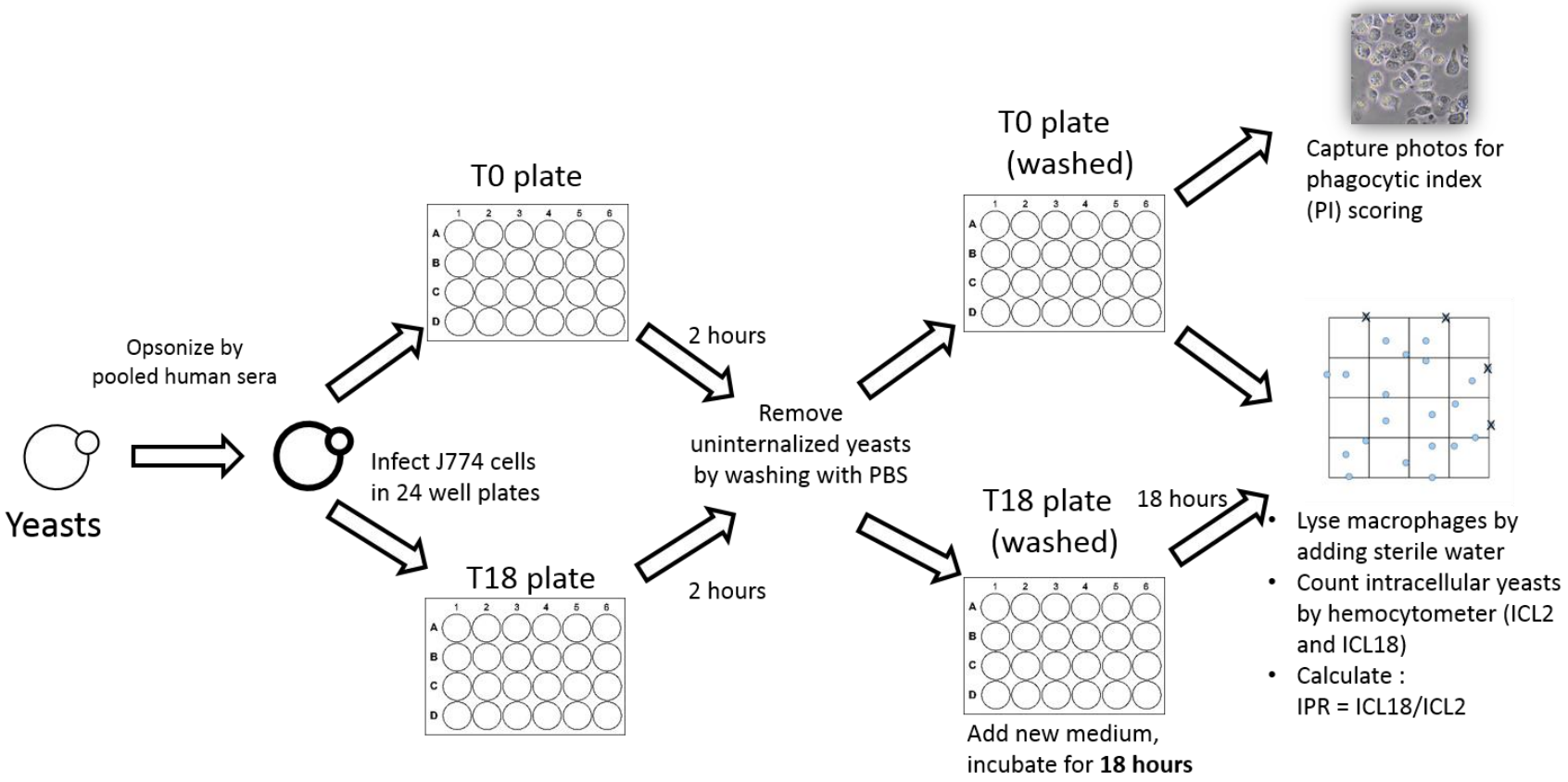

Figure 4.2-1. *In vitro* Intracellular proliferation experiment design (adapted from Ma Hansong's method) [130]**.**

1

4.2.4. Assessing macrophage parasitism parameters using an in vitro macrophage model of infection

Four main parameters are assessed in the current model:

Phagocytic Index (PI) is the proportion of macrophages that have ingested any cryptococcal cell, i.e. the number of macrophages with internalized yeasts divided by the total number of macrophages assessed at 2-hours post-infection. PI is an indicator of phagocytosis efficacy. It is influenced by phagocytosis routes (opsonin-dependent or opsonin-independent) and any intrinsic anti-phagocytic capabilities of the C. neoformans isolate. The PI does not take into account the actual number of yeasts phagocytosed by each individual macrophage.

PI = No. Macrophages with internalized yeasts/ No. Total Macrophages assessed

Intracellular Cryptococcus Load at 2-hours (ICL2 in cells/ml) measures how readily and in what quantity yeast cells are phagocytosed by macrophages and is directly related to IPR. ICL2 is positively correlated with PI. ICL2 is determined by counting the number of internalized yeasts after lysing macrophages, assuming clean removal of uninternalized, extracellular yeasts, using a hemocytometer.

Intracellular Cryptococci Load at 18-hours (ICL18 in cells/ml): similar to ICL2, ICL18 is the number of intracellular yeasts after 18 hours. A high intracellular cryptococci load post-internalization by macrophages at later time points indicates either a high rate of intracellular replication (if initial yeast uptake was low) or high initial yeast uptake. ICL18 is

determined by counting the number of intracellular yeasts after lysing macrophages 18 hours post-infection using a hemocytometer.

Intracellular Proliferation Rate (IPR) is an index of how rapidly ingested yeasts replicate inside macrophages. IPR is the ratio between ICL18 and ICL2, thus having no quantification unit. IPR>1 indicates active intracellular replication, IPR<1 suggest that intracellular replication is exceeded by intracellular killing.

$$IPR = ICL18 / ICL2$$

Each isolate was assessed using the same inoculum repeated in 3 wells (technical replicates) in each experiment batch and the experiment was repeated on 3 different occasions (biological replicates) to account for intra and inter-experimental variations, respectively. A final value for each variable (IPR, PI, ICL2 and ICL18) was calculated as a mean of 3 biological replicates.

4.2.5. Determining Intracellular proliferation rate (IPR) and Phagocytic Index (PI) (Ma's method)

The phagocytosis assay was left to progress for 2 hours ($37^{o}C$, 5%CO_2) in 2 separate 24-well plates in order to determine the PI at T = 0 (2 hours post inoculation and T = 18 (18 hours after the initial phagocytosis assay). At each time point (T = 0 and T = 18) un-internalized yeast cells in each plate were removed by repeated gentle washing with PBS. 1ml of SFM

medium was added to each well of the T18 plate, which was then incubated at 37^{o}C with 5% CO_2 for another 18 hours.

Initial yeast uptake in the T0 plate was determined by adding 200µl of sterile water in each well to lyse macrophages. After 15-30 minutes, macrophages lysate containing released yeast cells were aspirated and transferred to a clean tube. Another 200 µl of sterile water was added to collect remaining yeast cells at the bottom of the plates. Yeast cells were stained and diluted 1:3 in Trypan Blue and count under the 20X objective of a CX41 upright microscope (Olympus) using disposable glasstic hemocytometers (KOVA, Fisher Scientific, USA).

Intracellular proliferation rate (IPR) was calculated by dividing total internalized yeast cell at T18 by the initial yeast uptake at T0. Intracellular cryptococci load (ICL) at 2 hours and 18 hours post-infection were total yeast count at T0 and T18, respectively. The T18 time point was chosen because maximum IPRs are reached maximum between 16 hours and 24 hours post-infection[130].

Each strain was tested in triplicate (technical replicates) and in 3 different batches of macrophage culture (biological replicates). Cell images in 24-well plates at 2 hours post-phagocytosis were observed and captured using a Nikon Eclipse TS100F inverted bright-field microscope with phase-contrast capability and a Nikon D5200 digital camera for subsequent phagocytic index scoring. Captured images were manually scored for phagocytic index using ImageJ software (rsb.info.nih.gov/ij/). Phagocytic index (PI) was defined as the percentage of

macrophages with internalized yeast cells divided by the total number of macrophages counted (at least 400 cells).

4.2.6. Data analysis

Analyses were performed using mean values from 3 biological replicates obtained for all strains. Additional analyses were done following removal of outliers for each isolate. Outlier values among 3 biological replicates were detected and removed using the Median Absolute Deviation (MAD) method. As a measure of dispersal, the MAD uses the median for the deviation scores and is less susceptible to the influence of outliers compared to the standard deviation [397]. The absolute deviation from the median is the difference of the value and median after the positive or negative sign is removed: |X-Median|. The median absolute deviation is calculated by taking the median of the absolute deviations from the median:

$$MAD = median\ (|X1 - Median|, |X2-Median|, \ldots , |Xn-Median|)$$

Data values (x_i) are selected such that:

$$Median - MAD*2.5 \leq x_i \leq Median + MAD*2.5$$

The final value of each variable (IPR, PI, ICL2 and ICL18) for each isolate was the mean from the 3 biological replicates with outliers removed. The Mann-Whitney test was used for between-groups statistical comparisons. All analyses were performed using R version 3.4.0 (https://www.r-project.org).

4.2.7. Assessing yeast-macrophage interaction using flow cytometry (method 2)

4.2.7.1. Reagents and *C. neoformans* labeling

Solophenyl flavine 7GFE 500 specifically stains chitin contained in the cell wall of fungi and was used to label *C. neoformans*. Solophenyl flavine exhibits maximum emission at a wavelength of 490 nm when excited at 365 nm; this is similar to Pacific Blue stain (maximum emission at 452nm when excited at 401nm) and is detectable using the Pacific Blue channel on the FACSCanto II flow cytometer (BD, USA). Yeast cells were collected from standard YPD culture, washed twice, and re-suspended in phosphate-buffered saline (PBS). The cells were then incubated with Solophenyl flavine at 10 μg/ml in PBS for 10 min in the dark at room temperature, followed by washing twice in PBS. Following monoclonal antibody opsonization-based J774 phagocytosis assay (**Figure 4.2-3** and **Section 4.2.7.2,** described below), AF546-conjugated anti-mouse IgG monoclonal antibodies from goat were used to differentiate selectively stain extracellular yeasts population (Alexa Fluor-546 with Ex-max 562nm/Em-max 570). After cell lysis, AF647-conjugated anti-mouse IgG monoclonal antibodies from goat were then used to differentiate cell debris and all yeasts (Alexa Fluor-647 with Ex-max 650nm/Em-max 668nm). Since fluorescence spectrum of Alexa Fluor-546 and Alexa Fluor-647 were almost identical to R-phycoerythrin (PE) and Allophycocyanin (APC) in the respective yellow and red channel of FACSCanto II, we used the PE and APC channels for flow-cytometry experiments involving Alexa Fluor-546 and Alexa Fluor-647, respectively (**Figure 4.2-2**). The overall experiment design is summarized in **Figure 4.2-3**.

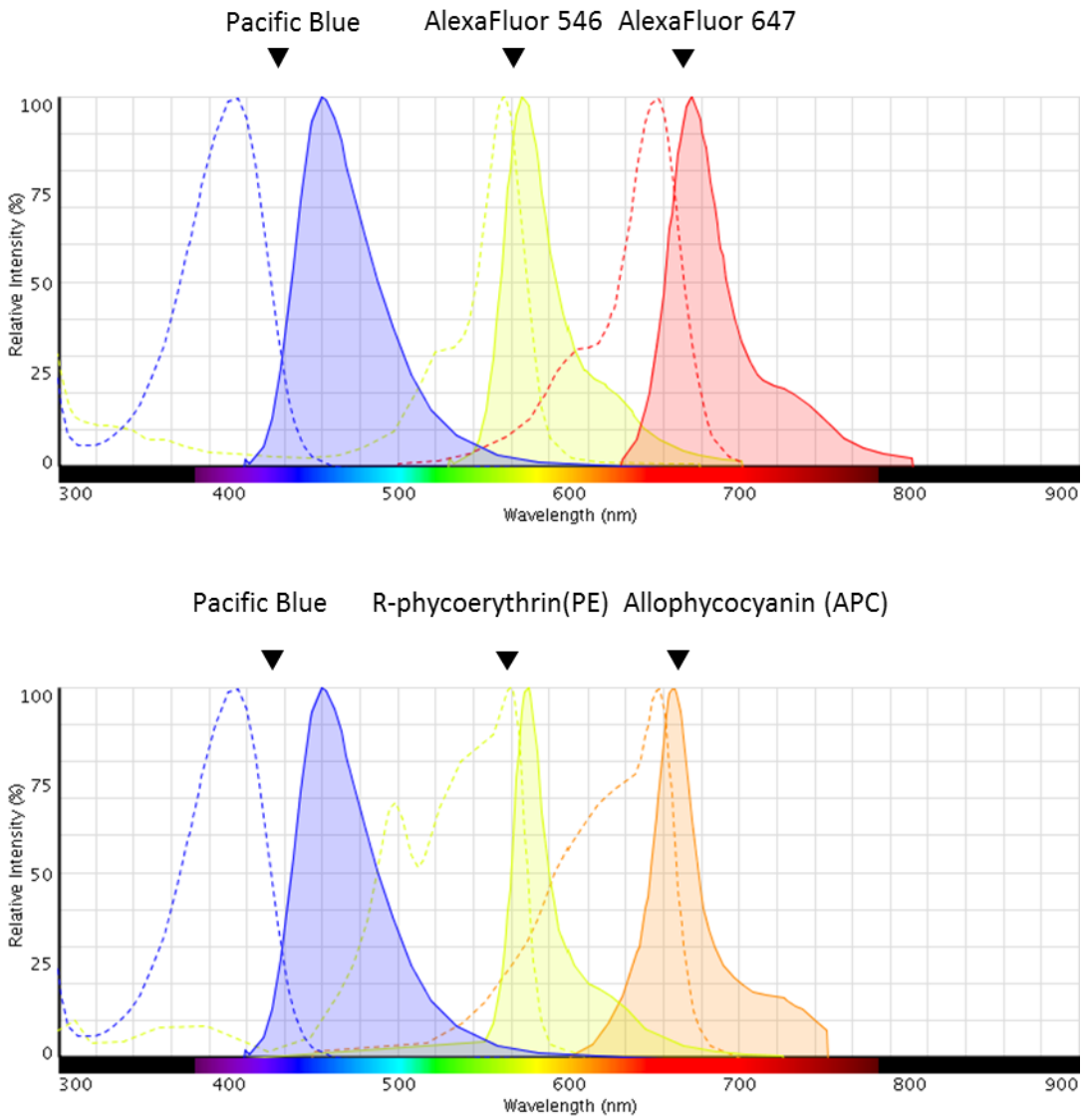

Figure 4.2-2. Fluorescence excitation and emission spectra of fluorophores used in the flow cytometry modification of Ma's method.

Solophenyl flavine (SF; Max Ex: 410nm/Max Em: 455nm), Alexa Fluor-546(AF546; Max Ex: 556nm/Max Em: 573nm) and Alexa Fluor-647 (F647; Max Ex: 650nm/Max Em: 665nm), which have similar excitation and emission spectra to Pacfic Blue, R-phycoerythrin (PE) and Allophycocyanin (APC) were used to stain yeast cell wall, extracellular yeasts and all yeast cells after macrophage lysis, respectively. Flow cytometry analyses were performed using the FACSCanto II cell sorter and FACS Diva software (BD).

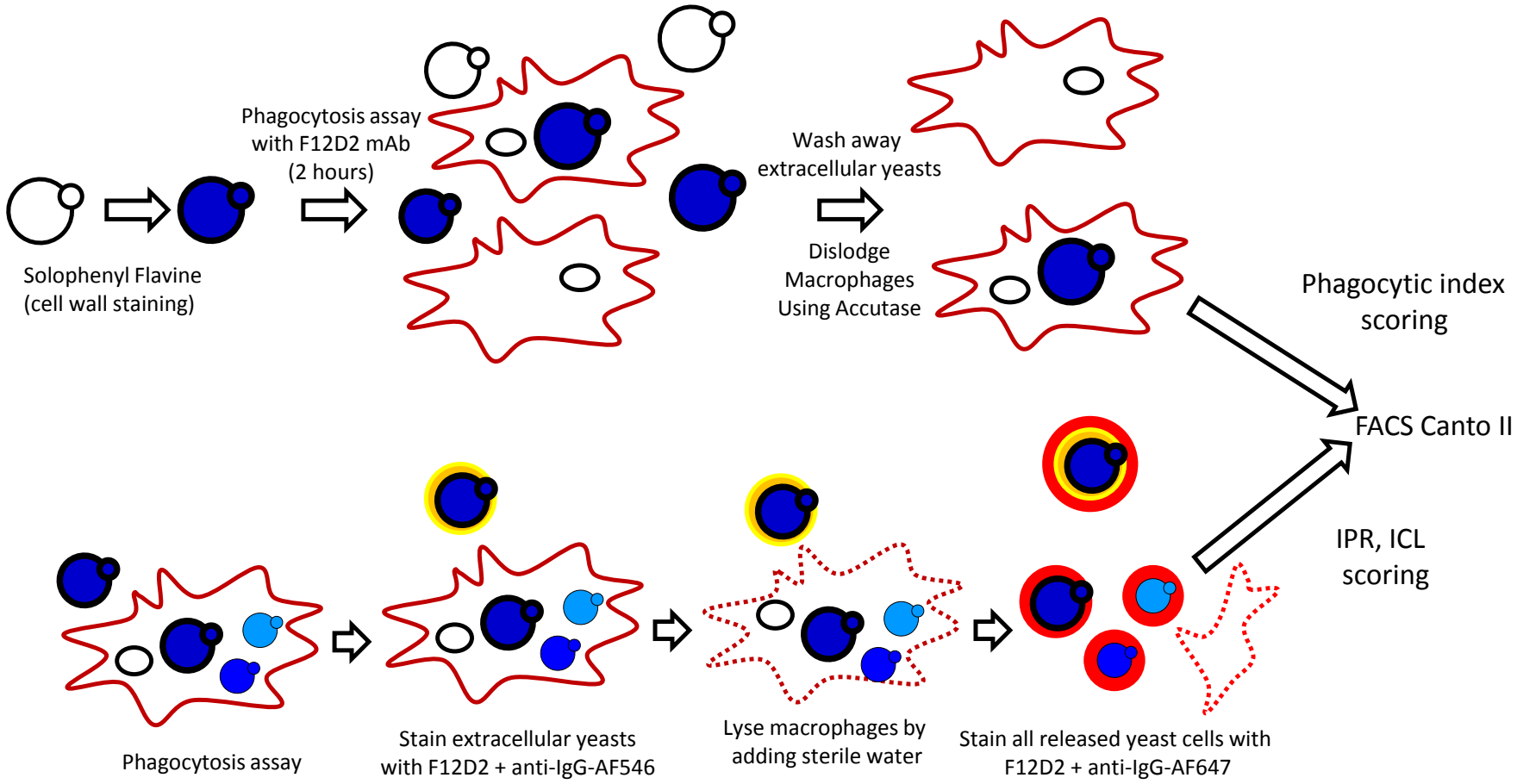

Figure 4.2-3. Flow cytometry experiment design for in vitro intracellular parasitism screening

1

4.2.7.2. Phagocytosis assay for flow cytometry

J774 macrophages were cultured and seeded in 3 separate 24-well plates at $2.5x10^5$ cells per well as previously described. The first plate was used for phagocytic index measurement; intracellular proliferation rates were assessed using the remaining 2 plates. H99 is included in every batch as a control for inter-experiment variation. On the day of the experiment, 250µl of 10 µg/ml working stock of F12D2 anti-cryptococcal capsular polysaccharide IgG1 monoclonal antibody from mouse (a kind gift from Prof. Thomas Kozel, University of Nevada, Reno, USA) and 250µl of SF- stained *C. neoformans* cell suspension were added to the J774 cell-monolayer and incubated at 37°C in 5% CO_2 for 2 hours (*C. neoformans*/J774 ratio, 2.5:1). Non-adherent extracellular yeast cells were then removed by PBS washing, and incubation was stopped to assess phagocytosis or extended to determine intracellular proliferation. Phagocytic Index (PI) was determined after dislodging adherent macrophages from the bottom of plate 1 by adding 400µl of Accutase enzyme solution (Invitrogen).

To determine the intracellular cryptococci load at 2 hours (ICL2) and 18 hours (ICL18), residual extracellular yeast cells were stained by addition of F12D2 monoclonal antibodies (0.5 µg/ml) and antimouse IgG1 pre-conjugated with Alexa Fluor-546 for 30 minutes and washed in PBS, after which J774 cells were lysed by adding 400µl sterile water. In order to differentiate potentially unstained *C. neoformans* cells from cell debris, an additional step was performed using F12D2 and antimouse IgG1 pre-conjugated with Alexa Fluor-647. All

yeast cells were APC(+), while only extracellular yeast cells were APC(+) PE(+). Intracellular yeasts would be those gated with APC(+)/PE(-)/Pacific Blue(+). Intracellular proliferation was determined for each clinical *C. neoformans* var. *grubii* isolate at 18 hours post-infection (IPR). Phagocytosis and proliferation were analyzed in two independent experiments. Refer to **Figure 4.2-3** for experiment design.

4.2.7.3. Flow cytometry data analysis

Flow cytometry analyses were performed using FACSCanto II and FACSDiva software 2.0 (Miltenyi BioTeC, USA) to provide absolute quantification. Samples were analyzed using FlowJo 10.0 software (Tree Star, Inc.). Aggregates were excluded by gating relevant events in the forward scatter/side scatter (FSC/SSC) contour plot. Four parameters were calculated:

(i) The phagocytic index (PI) as the number of gated macrophage events in the Pacific Blue(+) gate (plate 1)

(ii) Intracellular proliferation (IPR) as the ratio between daughter cells (Pacific Blue+) at 18 hours post-infection and mother cells (Pacific Blue+) at 2 hours post-infection.

(iii) Intracellular cryptococci load at 2 hours post-infection (ICL2) as the number of events at the APC(+)/PE(-)/Pacific Blue(+) at the relevant time point.

(iv) Intracellular cryptococci load at 18 hours post-infection (ICL18) and as the number of events at the APC(+)/PE(-)/Pacific Blue(+)at the relevant time point.

Results were expressed as the ratio of the given parameter for the test strains compared to the H99 parameter determined in the same run. Details of fluorescence staining and flow-cytometry gating are summarized in **Table 4.2-1**.

Table 4.2-1. Flow cytometry staining strategy for selection of different yeast populations

Inoculum		Intracellular yeasts		Extracellular yeasts	
	Unstained		$PB^{pos}APC^{pos}$		$PB^{pos}PE^{pos}$ (before lysis)
	PB^{pos}	 			$PB^{pos}PE^{pos}APC^{pos}$ (after lysis)

4.3. Chapter 4 Results

4.3.1. Macrophage parasitism parameters using Ma's method

4.3.1.1. General assessment of macrophage parasitism parameters among the Vietnamese *C. neoformans* var. *grubii* isolates

All isolates information and macrophage data are presented in **Table 4.3-1**. Scoring of Phagocytic Index of infected and non-infected macrophages is illustrated in **Figure 4.3-1**. Using pooled human serum for opsonization, most isolates had PIs in the range of 30% to 50% (median [IQR]: 35.7% [29.6-47.4]). Only 23% of the test isolates (11 out of 47) had PIs ≥ 50%. The majority of isolates underwent active replication within macrophages, i.e. had IPR values being greater than 1 **Table 4.3-1**. There was a moderate positive correlation between IPR and PI (r=0.44, p=0.002, Spearman test), as well as PI and ICL18 (r=0.40, p=0.006, Spearman test) across the whole population (**Figure 4.3-2**). An association between ICL2 and ICL18 (r=0.25) was observed, though this just failed to reach conventional levels of statistical significance (p=0.08, Spearman test, see **Figure 4.3-3**).

Table 4.3-1. Isolates information and result summary for method 1

No.	ID	AFLP	MLST	goeBURST cluster	HIV	ICL2 (log10 cells/ml)	ICL18 (log10 cells/ml)	IPR	PI
1	BMD700	VNI-γ	5	5	Negative	6.19	6.39	1.15	0.12
2	BMD1646	VNI-γ	5	5	Negative	6.68	6.45	1.06	0.16
3	BMD1338	VNI-γ	5	5	Negative	6.15	6.43	1.99	0.41
4	BMD1232	VNI-γ	5	5	Negative	6.39	6.23	1.65	0.31
5	BMD1353	VNI-γ	5	5	Negative	5.99	6.13	1.16	0.49
6	BMD1452	VNI-γ	5	5	Negative	6.12	6.29	1.48	0.54
7	BMD1198	VNI-γ	5	5	Negative	6.06	6.16	1.10	0.24
8	BMD1228	VNI-γ	5	5	Negative	6.23	6.12	2.17	0.36
9	BMD1291	VNI-γ	5	5	Negative	5.96	6.60	1.72	0.70
10	BMD1465	VNI-γ	5	5	Negative	5.58	6.33	1.69	0.62
11	BMD101	VNI-γ	5	5	Negative	6.33	6.52	1.86	0.68
12	BK48	VNI-δ	4	4	Positive	6.60	6.39	0.77	0.30
13	BK23	VNI-δ	4	4	Positive	6.49	6.69	1.07	0.35
14	BK73	VNI-δ	4	4	Positive	5.94	6.19	0.84	0.31
15	BMD1415	VNI-δ	4	4	Positive	6.56	6.42	1.06	0.24
16	BK61	VNI-δ	4	4	Positive	6.03	6.46	2.48	0.39
17	BK80	VNI-δ	4	4	Positive	5.94	6.09	1.46	0.25
18	BK111	VNI-δ	4	4	Positive	5.96	6.52	1.43	0.55
19	BK69	VNI-δ	4	4	Positive	6.18	6.48	1.18	0.54
20	BMD394	VNI-δ	4	4	Positive	6.23	6.42	1.30	0.56
21	BK139	VNI-γ	4	4	Positive	5.98	6.37	1.30	0.46
22	BK76	VNI-γ	5	5	Positive	6.18	5.92	0.71	0.12
23	BK169	VNI-γ	5	5	Positive	6.43	6.66	1.04	0.59
24	BK190	VNI-γ	5	5	Positive	6.27	6.44	1.28	0.31
25	BK47	VNI-γ	5	5	Positive	6.58	6.72	1.18	0.35
26	BK78	VNI-γ	5	5	Positive	6.40	6.57	1.22	0.37
27	BK39	VNI-δ	5	5	Positive	6.24	6.56	1.47	0.64
28	BK60	VNI-γ	5	5	Positive	6.19	6.37	1.04	0.50
29	BK147	VNI-γ	5	5	Positive	6.38	6.37	1.63	0.41
30	BK38	VNI-γ	5	5	Positive	6.37	6.38	1.37	0.38
31	BK4	VNI-γ	5	5	Positive	5.96	6.18	1.05	0.37
32	BK116	VNI-γ	5	5	Positive	6.07	6.24	1.05	0.36
33	BK175	VNI-γ	5	5	Positive	5.85	5.98	0.75	0.15
34	BK182	VNI-δ	5	5	Positive	5.64	6.66	1.39	0.66
35	BK45	VNI-γ	5	5	Positive	6.33	6.13	1.18	0.29

No.	*ID*	*AFLP*	*MLST*	*goeBURST cluster*	*HIV*	*ICL2 (log10 cells/ml)*	*ICL18 (log10 cells/ml)*	*IPR*	*PI*
36	BK33	VNI-δ	5	5	Positive	6.06	6.00	1.08	0.04
37	BK189	VNI-δ	6	4	Positive	6.32	5.90	0.89	0.19
38	BK46	VNI-δ	32	93	Positive	5.97	6.41	1.37	0.30
39	BK167	VNI-δ	39	93	Positive	5.53	6.19	1.00	0.41
40	BK24	VNI-δ	93	93	Positive	6.11	6.55	1.34	0.24
41	BK157	VNI-δ	93	93	Positive	6.48	6.48	0.83	0.32
42	BK213	VNI-δ	93	93	Positive	5.94	6.25	1.31	0.32
43	BK12	VNI-δ	93	93	Positive	6.15	6.09	1.33	0.43
44	BK85	VNI-δ	93	93	Positive	6.04	5.96	0.89	0.26
45	BK241	VNI-γ	93	93	Positive	6.38	6.12	1.08	0.38
46	BMD1367	VNI-δ	306	4	Positive	6.51	6.61	0.86	0.33
47	BK150	VNI-δ	338	93	Positive	6.50	6.39	0.71	0.41

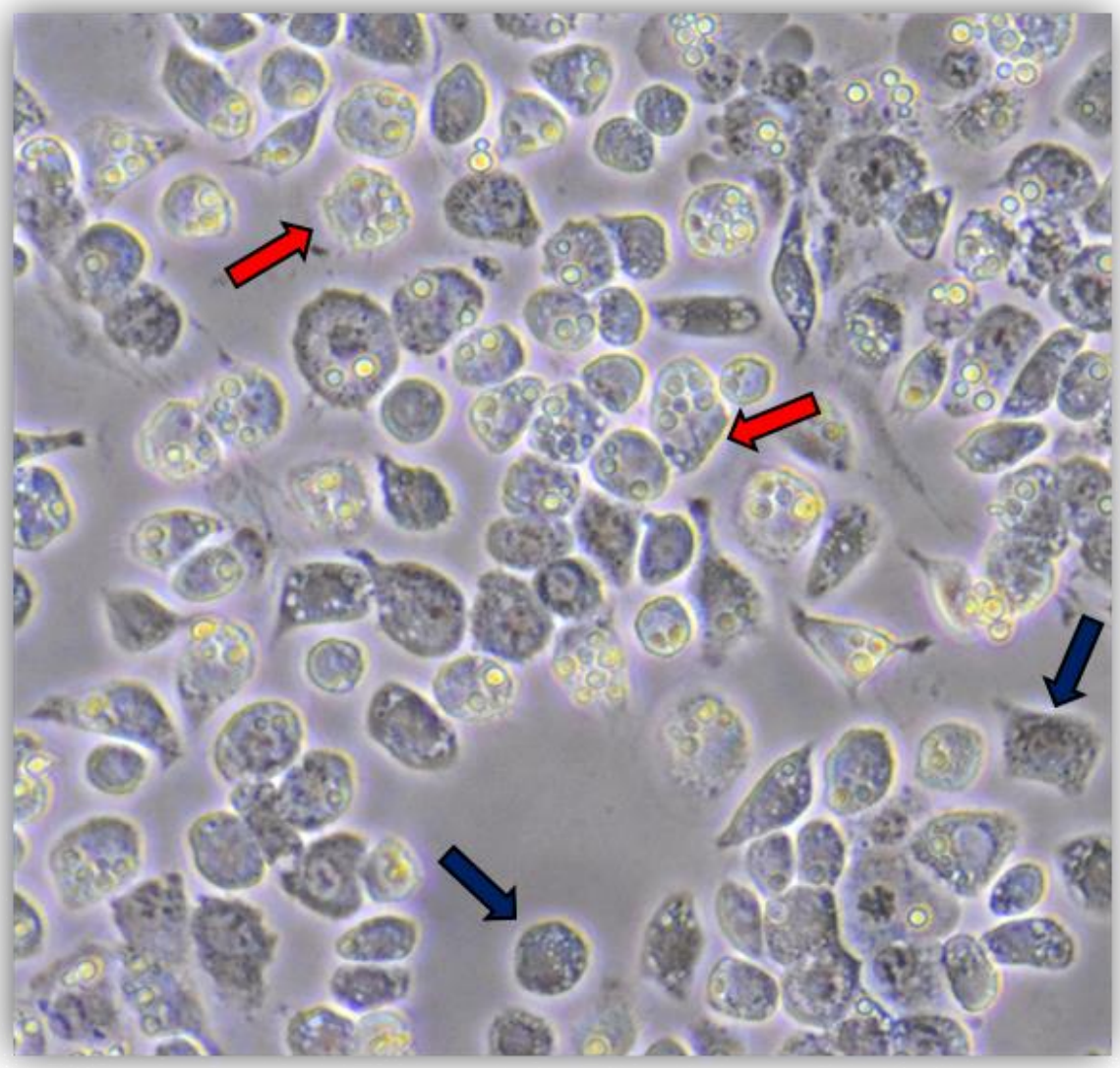

Figure 4.3-1. *In silico* Phagocytic Index (PI) scoring using ImageJ software.
Cell images were captured at 200X magnification after 2 hour of phagocytosis assay and PBS washing to remove residual non-internalized extracellular yeasts. Red arrows indicate macrophages with internalized yeasts (N1). Blue arrows indicate uninfected macrophages (N2). PI was calculated using the formula: PI = N1/(N1+N2)

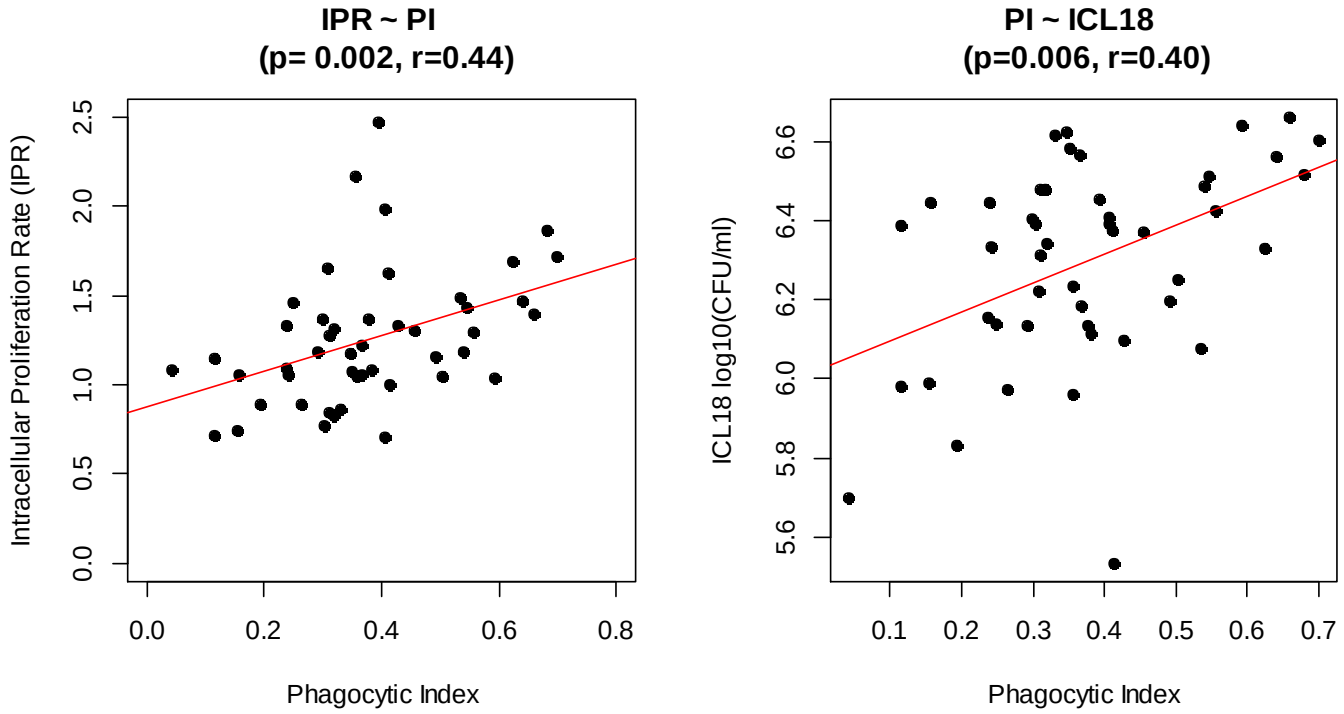

Figure 4.3-2. Correlation between IPR, ICL18 and Phagocytic Index.

Test of correlation was performed using the Spearman rank test. Resulting P-value and Rho value from the Spearman test of correlation are shown on the graphs. Red lines indicate the linear regression model (R^2=0.15, p=0.001 and R^2=0.19, p=0.001 for IPR vs PI and PI vs ICL18, respectively)

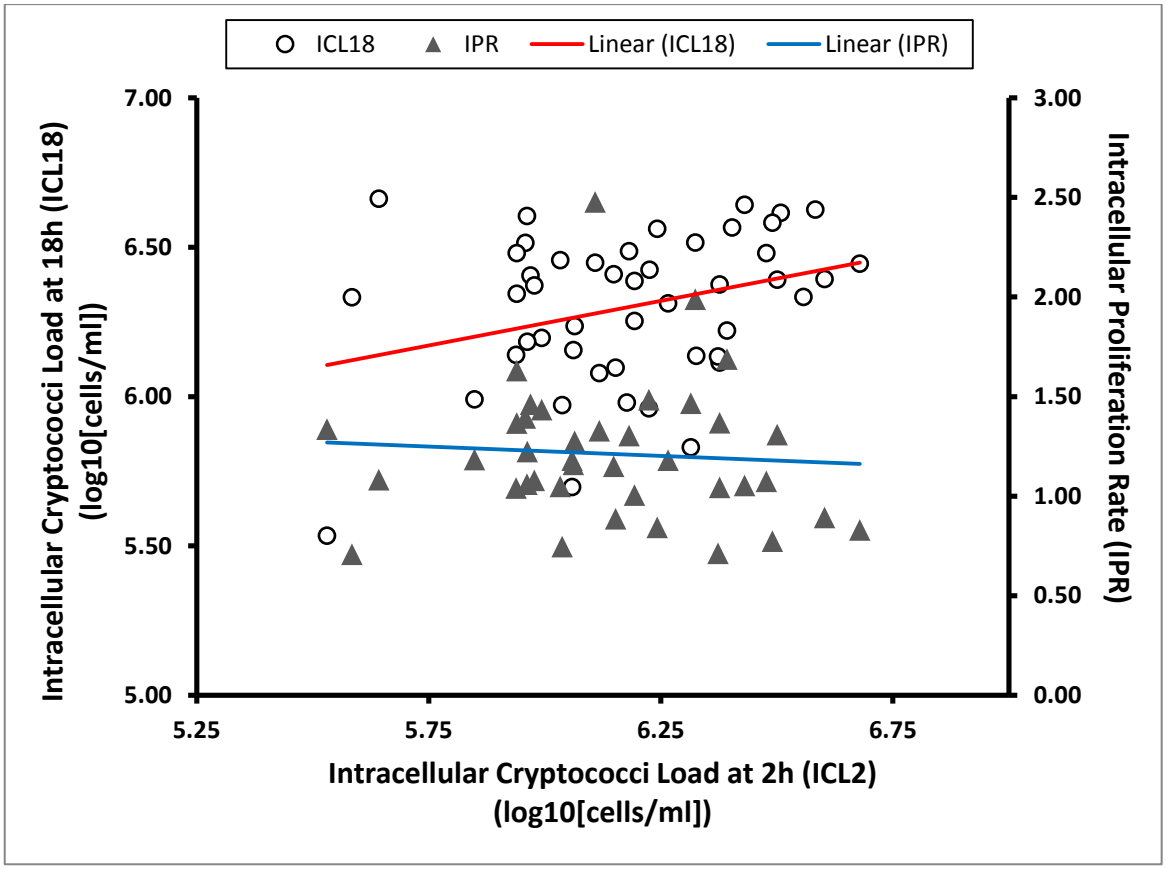

Figure 4.3-3. Correlation between ICL2 /ICL18 and IPR
Spearman test of correlation between population-wise ICL2, ICL18 and IPR was performed. Though all correlation failed to reach statistical significance at α=0.05, there seemed to be a positive correlation between ICL2 and IPR (r=0.25, p=0.08), as well as an inverse correlation between ICL19 and IPR (r=-0.24, p=0.11).

4.3.1.2. No difference in any macrophage parasitism parameters was observed based on AFLP and MLST clustering

Macrophage interaction parameters according to AFLP genotypes are summarized in **Table 4.3-2**. No statistically significant differences based on AFLP grouping (VNI-γ, n=25 and VNI-δ, n=22) were observed. Next, *in vitro* macrophage parasitism parameters were tested for any correlation with goeBURST clusters. As previously described in Chapter 1, the clinical *C. neoformans* var. *grubii* population in Vietnam consists of 3 main goeBURST subgroups formed by ST5 (subgroup 5, n=26), ST4 (subgroup 4, n=12) and ST93 (subgroup 93, n=9), respectively. Data for each MLST sub-group according to goeBURST are summarized in **Table 4.3-3**. There were no correlations between any goeBURST lineages and macrophage parasitism parameters. Isolates from lineage 93 seemed to be less efficient at intracellular proliferation than lineage 4 or lineage 5, though this observation again did not quite reach statistical significance (p=0.07, Kruskal-Wallis rank test).

Table 4.3-2. Macrophage parasitism parameters according to AFLP genotype

Parameter	Original (Mean ± SD)			Outliers removed by MAD (Mean ± SD)		
	VNI-γ (n=25)	VNI-δ (n=22)	*p-values	VNI-γ (n=25)	VNI-δ (n=22)	*p-values
IPR	1.366 ± 0.35	1.223 ± 0.356	0.12	1.316 ± 0.369	1.185 ± 0.379	0.24
PI%	38.6 ± 16.3	36.5 ± 15.1	0.62	ND$^{\$}$	ND$^{\$}$	ND$^{\$}$
ICL2 log10(cells/ml)	6.20 ± 0.21	6.27 ± 0.23	0.22	6.20 ± 0.24	6.16 ± 0.29	0.49
ICL18 log10(cells/ml)	6.35 ± 0.20	6.35 ± 0.23	0.46	6.29 ± 0.20	6.31 ± 0.30	0.28

IPR: Intracellular Proliferation Rate
PI: Phagocytic Index
ICL2, ICL18: Intracellular Cryptococci Load at 2 hours or 18 hours post-infection.
ND$^{\$}$*: PI data from 1 or more biological replicates were missing for the respective isolates due to technical errors, therefore MAD adjustment could not be done.*
**Data are presented as mean ± standard deviation. Pairwise statistical comparison was performed using Mann-Whitney test.*

Table 4.3-3. Macrophage parasitism parameters according to MLST goeBURST sub-groups

Parameter	Original (Mean ± SD)				Outliers removed by MAD (Mean ± SD)			
	Sub-group 4 (n=12)	Sub-group 5 (n=26)	Sub-group 93 (n=9)	p-values*	Sub-group 4 (n=12)	Sub-group 5 (n=26)	Sub-group 93 (n=9)	p-values*
IPR	1.320 ± 0.434	1.370 ± 0.345	1.067 ± 0.157	0.06	1.228 ± 0.462	1.322 ± 0.363	1.095 ± 0.250	0.28
PI%	39.0 ±15.0	39.6 ±16.7	30.3 ± 11.9	0.41	ND$^{\$}$	ND$^{\$}$	ND$^{\$}$	ND$^{\$}$
ICL2 log10(cells/ml)	6.31 ± 0.24	6.20 ± 0.21	6.20 ± 0.21	0.37	6.20 ± 0.30	6.20 ± 0.24	6.09 ± 0.29	0.49
ICL18 log10(cells/ml)	6.40 ± 0.23	6.33 ± 0.20	6.26 ± 0.21	0.26	6.41 ± 0.23	6.30 ± 0.21	6.15 ± 0.35	0.08

IPR: Intracellular Proliferation Rate
PI: Phagocytic Index
ICL2, ICL18: Intracellular Cryptococci Load at 2 hours or 18 hours post-infection.
ND$^{\$}$*: PI data from 1 or more biological replicates were missing for the respective isolates due to technical errors, therefore MAD adjustment could not be done.*
**Data are presented as mean ± standard deviation. Groupwise statistical comparison was performed using Kruskal-Wallis test.*

4.3.1.3. Isolates from HIV-uninfected patients, especially ST5s, tend to have higher IPR

I performed an exploratory analysis of clustering by the HIV infection status of the isolate source, in order to determine whether there was any association between this and the *in vitro* macrophage variables. As previously described, VNI-γ isolates are found in both HIV infected and HIV uninfected patients, but account for almost all disease in HIV-uninfected patients, particularly when there is no other underlying disease. VNI-δ isolates, on the other hand, are mostly associated with disease in HIV-infected patients. Among 25 AFLP-defined VNI-γ isolates included in the current study population (n = 47) there were 14 isolates from HIV-uninfected patients. The remaining 33 isolates from HIV-infected patients included 11 VNI-γ and 22 VNI-δ isolates. Isolates from HIV-uninfected patients tended to have higher IPRs than isolates from HIV-infected patients (quote a ratio of the difference in the IPRs plus the confidence intervals), although this did not reach conventional levels of statistical significance (p=0.08, Mann-Whitney test). There were no differences in PI, ICL2 or ICL18. However, on removal of outlier results defined by the MAD method, the difference in IPR reached statistical significance (p=0.03, Mann-Whitney t-test, also see **Table 4.3-4** and **Figure 4.3-4)**.

Table 4.3-4. Macrophages parasitism parameters according to HIV group

	Original (Mean ± SD)			Outliers removed by MAD (Mean ± SD)		
	HIV-uninfected (n=14)	**HIV-infected (n=33)**	**p-values***	**HIV-uninfected (n=14)**	**HIV-infected (n=33)**	**p-values***
IPR	1.475 ± 0.416	1.224 ± 0.306	0.08	1.446 ± 0.404	1.174 ± 0.338	0.03
PI (%)	41.0 ± 19.1	36.2 ± 13.9	0.55	ND$^{\$}$	ND$^{\$}$	ND$^{\$}$
ICL2 log10(cells/ml)	6.22 ± 0.21	6.23 ± 0.22	0.79	6.21 ± 0.28	6.17 ± 0.26	0.44
ICL18 log10(cells/ml)	6.36 ± 0.16	6.33 ± 0.23	0.63	6.33 ± 0.19	6.28 ± 0.28	0.90

IPR: Intracellular Proliferation Rate
PI: Phagocytic Index
ICL2, ICL18: Intracellular Cryptococci Load at 2 hours or 18 hours post-infection.
ND$^{\$}$: PI data from 1 or more biological replicates were missing for the respective isolates due to technical errors, therefore MAD adjustment could not be done..
**: Data are presented as mean ± standard deviation. Pairwise statistical comparison was performed using Mann-Whitney test.*

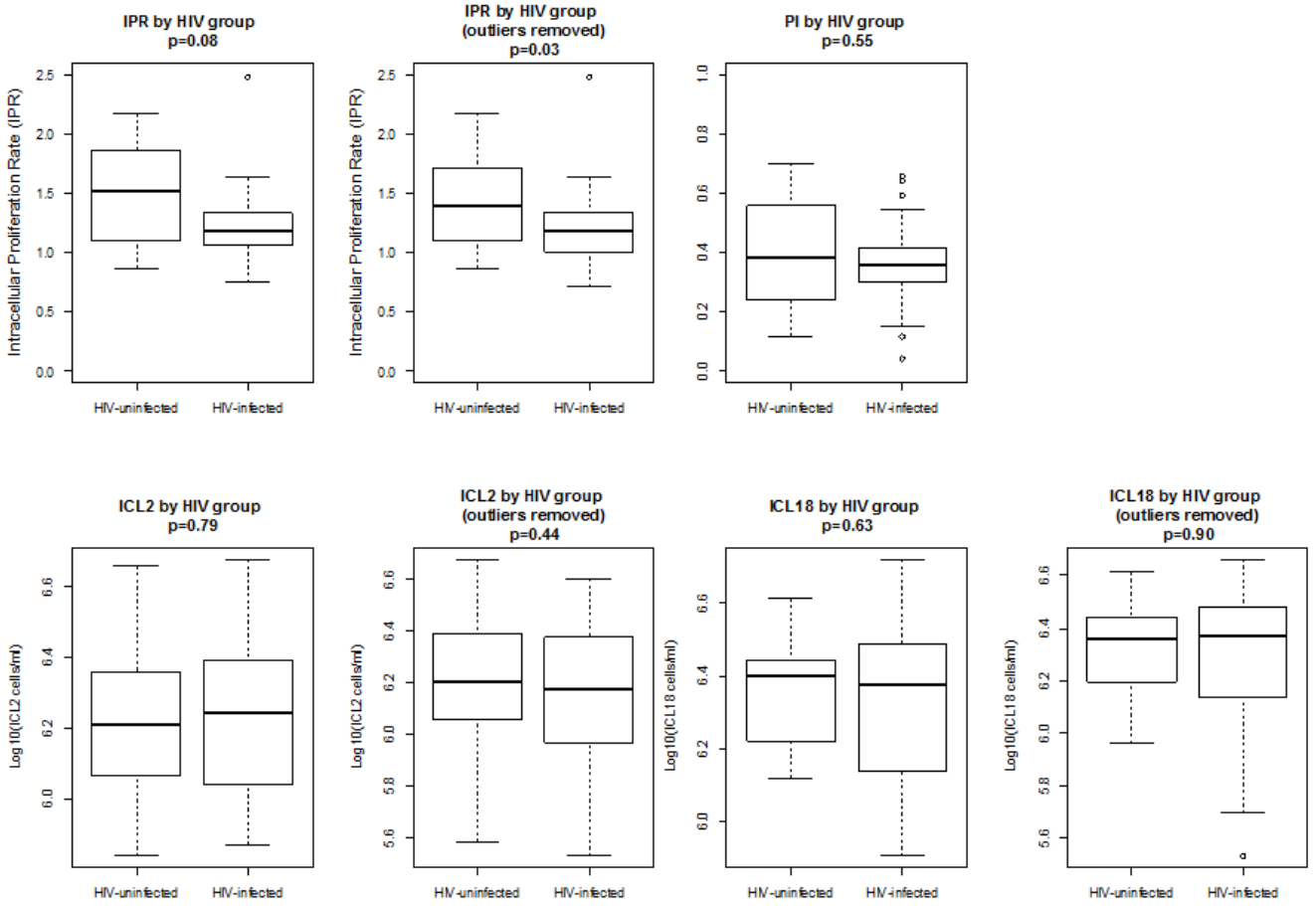

Figure 4.3-4. Pairwise comparison between isolates from HIV-uninfected (n=14) and HIV-infected patients (n=33).

Boxplot showing the median and interquartile range with whiskers indicating the lower and upper quartiles. Values lower or higher than 1.5 times the lower or upper quartiles were indicated as clear dots. A borderline difference in IPR according to HIV groups was previously observed (Mann-Whitney test). Only MAD-adjusted IPR values between HIV groups showed statistical significance.

While ST5 *C. neoformans* var. *grubii* isolates are found in both HIV-uninfected and HIV-infected patients, they are more highly associated with infection in HIV-uninfected patients with no apparent immunodeficiency. In fact, where non-ST5 infection occurs in HIV-uninfected patients it is usually accompanied by other serious underlying disease [103]. I next investigated if the observed difference in IPR between isolates from HIV-uninfected and HIV-infected patients could be attributed to ST5 isolates. This subset of ST5 isolates involved 11 ST5 isolates from HIV-uninfected and 15 ST5 isolates from HIV-infected. Data are summarized in **Table 4.3-5** and **Figure 4.3-5**. ST5 isolates from HIV-uninfected patients had statistically significantly higher IPRs compared with ST5 isolates from HIV-infected patients (p=0.05, Mann-Whitney test). Correcting for outliers again strengthened this finding (p=0.01, Mann-Whitney test).

Figure 4.3-5 and **Figure 4.3-6** suggest that there was a greater degree of variation in IPR among isolates from HIV-uninfected patients compared to that from HIV-infected patients. This observation was assessed using the Fligner-Killeen test which showed statistical significance for both group comparisons (p=0.04 for HIV-uninfected vs HIV-infected and p=0.05 for the ST5 subset of HIV-uninfected vs HIV-infected). MAD-adjusted IPR values for individual isolates are presented in **Figure 4.3-7**.

Table 4.3-5. Macrophage parasitism parameters of ST5 isolates according to HIV serostatus of isolate source (uninfected and infected)

	Original (Mean ± SD)			Outliers removed by MAD (Mean ± SD)		
	ST5 HIV-uninfected (n=11)	**ST5 HIV-infected (n=15)**	***p-values**	**ST5 HIV-uninfected (n=11)**	**ST5 HIV-infected (n=15)**	***p-values**
IPR	1.574 ± 0.399	1.220 ± 0.206	0.05	1.548 ± 0.387	1.157 ± 0.243	0.01
PI (%)	41.9 ± 20.4	37.8 ± 13.9	0.66	ND$^{\$}$	ND$^{\$}$	ND$^{\$}$
ICL2 log10(cells/ml)	6.15 ± 0.17	6.24 ± 0.24	0.57	6.15 ± 0.28	6.24 ± 0.20	0.29
ICL18 log10(cells/ml)	6.33 ± 0.16	6.34 ± 0.24	0.99	6.30 ± 0.20	6.30 ± 0.22	0.92

IPR: Intracellular Proliferation Rate

PI: Phagocytic Index

ICL2, ICL18: Intracellular Cryptococci Load at 2 hours or 18 hours post-infection.

ND$^{\$}$: PI data from 1 or more biological replicates were missing for the respective isolates due to technical errors, therefore MAD adjustment could not be done.

**: Data are presented as mean ± standard deviation. Pairwise statistical comparison was performed using Mann-Whitney test*

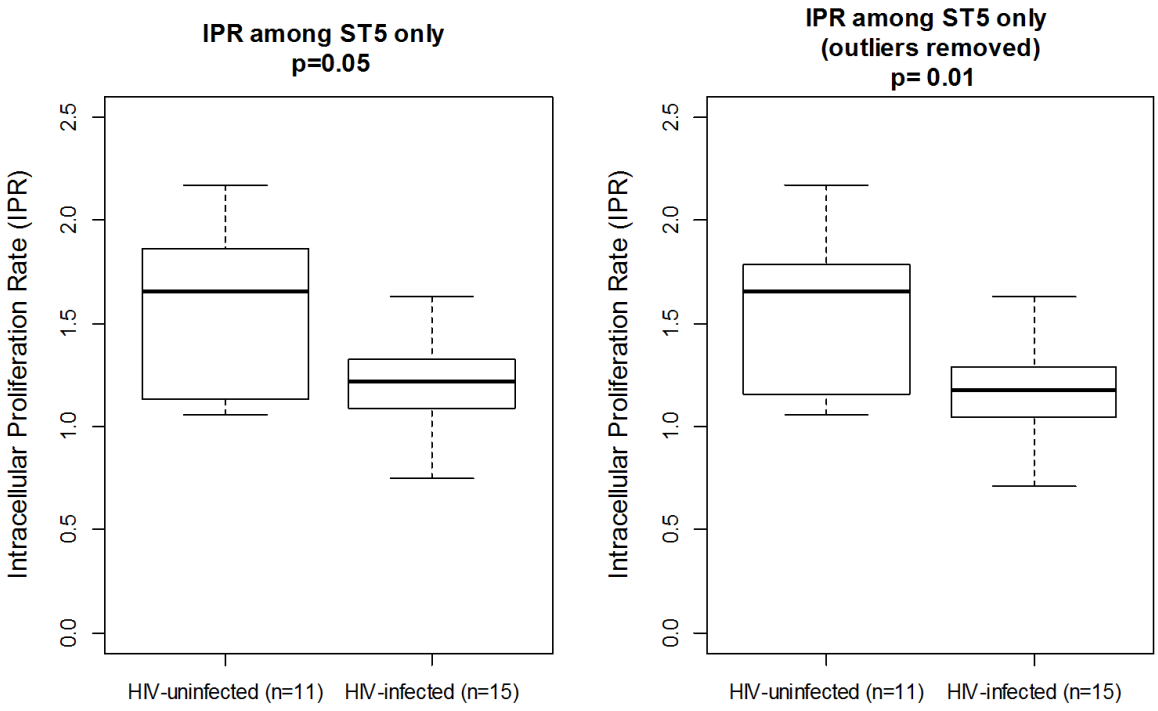

Figure 4.3-5. Intracellular Proliferation Rate (IPR) comparison between only ST5 isolates. Boxplot showing the median the interquartile range with whiskers indicating the lower and upper. Values lower or higher than 1.5 times the lower or upper quartiles are indicated as open dots. Among ST5 isolates, those isolated from HIV-uninfected patients replicated 34% faster than those from HIV-infected patients (p=0.01, Mann-Whitney test).

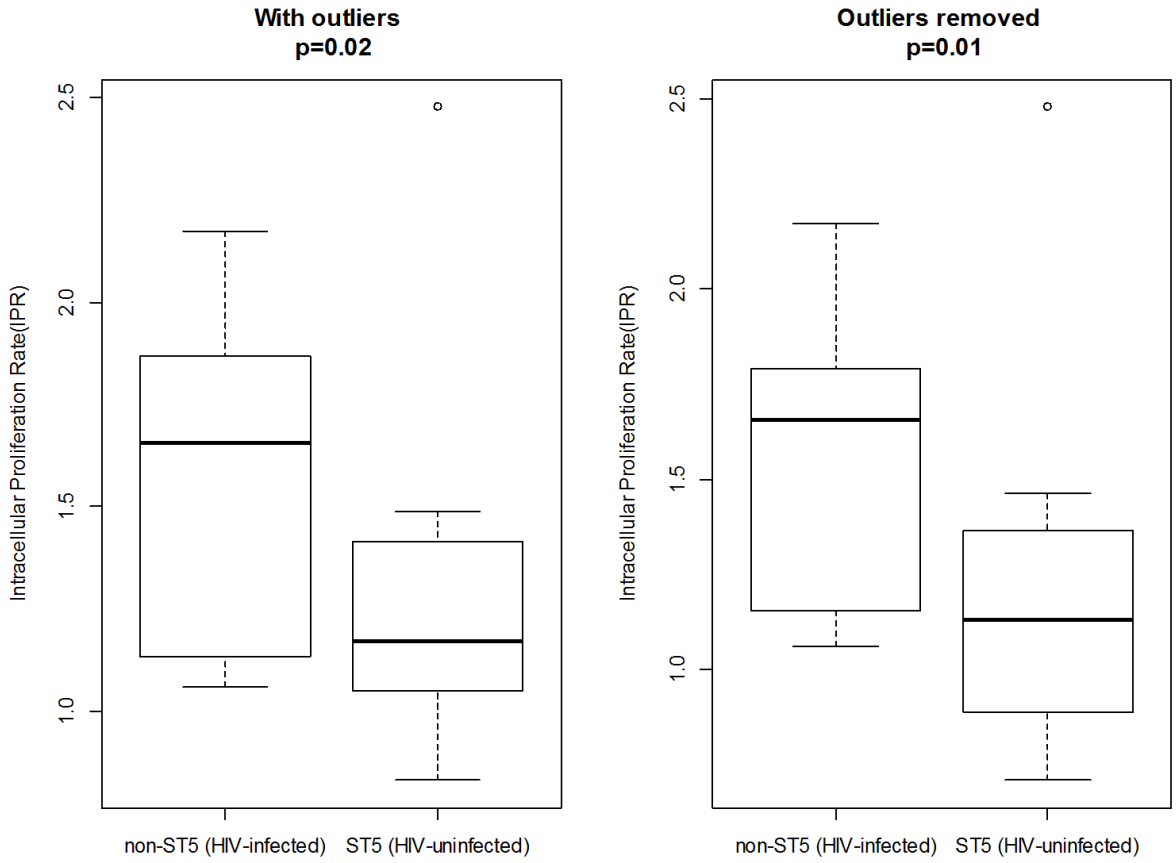

Figure 4.3-6. Intracellular Proliferation Rate (IPR) comparison between ST5 isolates from HIV-uninfected and non-ST5 isolates from HIV-infected patients.

Boxplot showing the median the interquartile range with whiskers indicating the lower and upper quartiles. Values lower or higher than 1.5 times the lower or upper quartiles are indicated as open dots. ST5 isolates from HIV-uninfected patients have significantly higher IPR than non-ST5 isolates from HIV-infected patients (p=0.01, Mann-Whitney test).

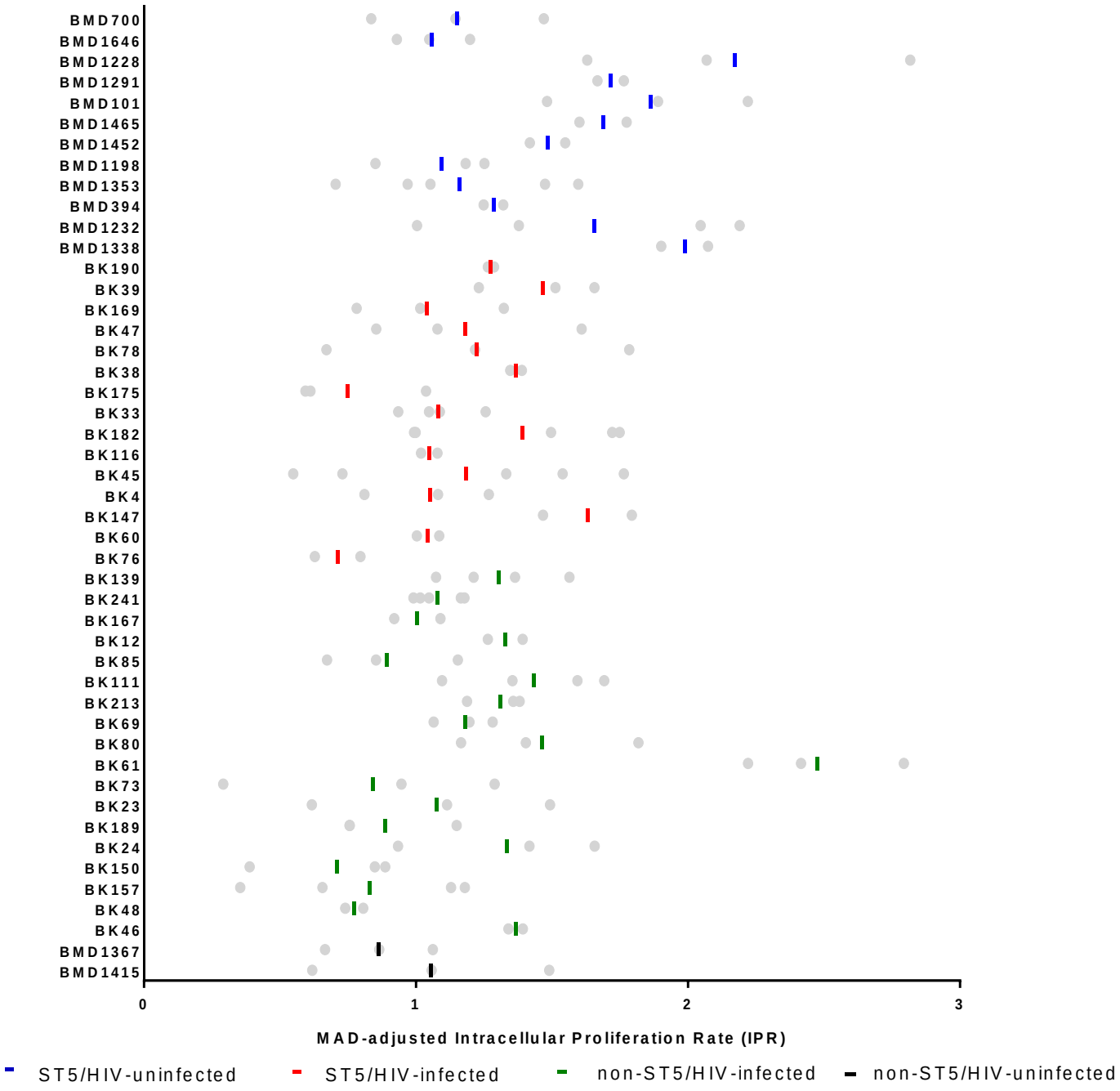

Figure 4.3-7. MAD-adjusted IPR for individual isolates.

Isolates are grouped according to MLST genotypes (ST5 and non-ST5) and host HIV immune types (HIV-infected and HIV-uninfected). Current data suggest that ST5 isolates from HIV-uninfected patients had significantly higher IPRs than either ST5 or non-ST5 isolates from HIV-infected patients. Scatter plot represents mean of all available biological replicates after removing outliers.

4.3.1.4. Association between *in vitro* macrophage interaction parameters and clinical outcomes

I examined to see whether intrinsic macrophage parasitism characteristics of isolates were associated with clinical outcome. From the test population (n=47), patients with known mortality-at-10-weeks (n=38; 25 survived and 13 died) and baseline fungal load in CSF (n=38) were selected for exploratory analysis of correlation between clinical outcomes and macrophage parasitism parameters **(Table 4.3-6)**. No significant association between patient's baseline fungal burden in CSF and any macrophages parasitism parameters could be found (p=0.07, p=0.67, p=0.82 and p=0.24 for IPR, PI, ICL2 and ICL18, respectively, Spearman test of correlation **Figure 4.3-8**. There seemed to be an inverse correlation between IPR and CSF fungal burden, though this correlation was insignificant, possibly due to a lack of power (p=0.07, Spearman r=0.29, **Figure 4.3-8)**. Likewise, there were no apparent differences between 10-weeks mortality (Alive/Dead) and any macrophage parasitism parameters tested (p=0.74, p=0.51, p=0.17 and p=0.70 for IPR, PI, ICL2 and ICL18, respectively (**Figure 4.3-9**).

Table 4.3-6. Mortality at 10-weeks of antifungal treatment and patients' fungal burden in CSF before treatment

No.	ID	AFLP cluster	MLST Sequence Type	HIV serostatus	*Log.Base.CSF	10-weeks mortality
1	BMD700	VNI-γ	5	Negative	*NA*	Alive
2	BMD394	VNI-δ	4	Negative	*NA*	Alive
3	BMD1228	VNI-γ	5	Negative	*NA*	Alive
4	BK4	VNI-γ	5	Positive	2.176	Alive
5	BK23	VNI-δ	4	Positive	2.550	Alive
6	BK39	VNI-δ	5	Positive	3.000	Alive
7	BK24	VNI-δ	93	Positive	3.244	Alive
8	BK78	VNI-γ	5	Positive	3.415	Alive
9	BK241	VNI-γ	5	Positive	3.477	Alive
10	BK80	VNI-δ	4	Positive	4.011	Alive
11	BK76	VNI-γ	5	Positive	4.439	Alive
12	BK150	VNI-δ	338	Positive	4.703	Alive
13	BK12	VNI-δ	93	Positive	4.947	Alive
14	BK33	VNI-δ	93	Positive	5.121	Alive
15	BK111	VNI-δ	4	Positive	5.130	Alive
16	BK147	VNI-γ	5	Positive	5.505	Alive
17	BK48	VNI-δ	4	Positive	5.708	Alive
18	BK69	VNI-δ	4	Positive	5.756	Alive
19	BK169	VNI-γ	5	Positive	5.851	Alive
20	BK190	VNI-γ	5	Positive	5.903	Alive
21	BK213	VNI-δ	93	Positive	5.908	Alive
22	BK46	VNI-δ	32	Positive	6.002	Alive
23	BK157	VNI-δ	93	Positive	6.057	Alive
24	BK116	VNI-γ	5	Positive	6.099	Alive
25	BK45	VNI-γ	5	Positive	6.190	Alive
26	BK47	VNI-γ	5	Positive	*NA*	Dead
27	BMD1232	VNI-γ	5	Negative	*NA*	Dead
28	BMD101	VNI-γ	5	Negative	*NA*	Dead
29	BK61	VNI-δ	4	Positive	2.823	Dead
30	BK73	VNI-δ	4	Positive	3.023	Dead
31	BK38	VNI-γ	5	Positive	4.477	Dead
32	BK175	VNI-γ	5	Positive	5.017	Dead
33	BK167	VNI-δ	39	Positive	5.484	Dead
34	BK60	VNI-γ	5	Positive	6.127	Dead
35	BK189	VNI-δ	6	Positive	6.732	Dead
36	BMD1338	VNI-γ	5	Negative	6.908	Dead
37	BK182	VNI-δ	4	Positive	7.149	Dead
38	BK85	VNI-δ	93	Positive	7.265	Dead
39	BK139	VNI-γ	5	Positive	7.302	Dead

No.	*ID*	*AFLP cluster*	*MLST Sequence Type*	*HIV serostatus*	**Log.Base.CSF*	*10-weeks mortality*
40	BMD1367	VNI-δ	306	Negative	*NA*	*NA*
41	BMD1353	VNI-γ	5	Negative	*NA*	*NA*
42	BMD1465	VNI-γ	5	Negative	*NA*	*NA*
43	BMD1415	VNI-δ	4	Negative	3.505	*NA*
44	BMD1291	VNI-γ	5	Negative	3.906	*NA*
45	BMD1452	VNI-γ	5	Negative	4.243	*NA*
46	BMD1646	VNI-γ	5	Negative	4.455	*NA*
47	BMD1198	VNI-γ	5	Negative	6.267	*NA*

CSF fungal burden for patients at diagnosis (log10 cells/ml CSF). Clinical information was mostly fully available for "BK" patients who enrolled in an intervention RCT for treatment of HIV-associated cryptococcal meningitis.

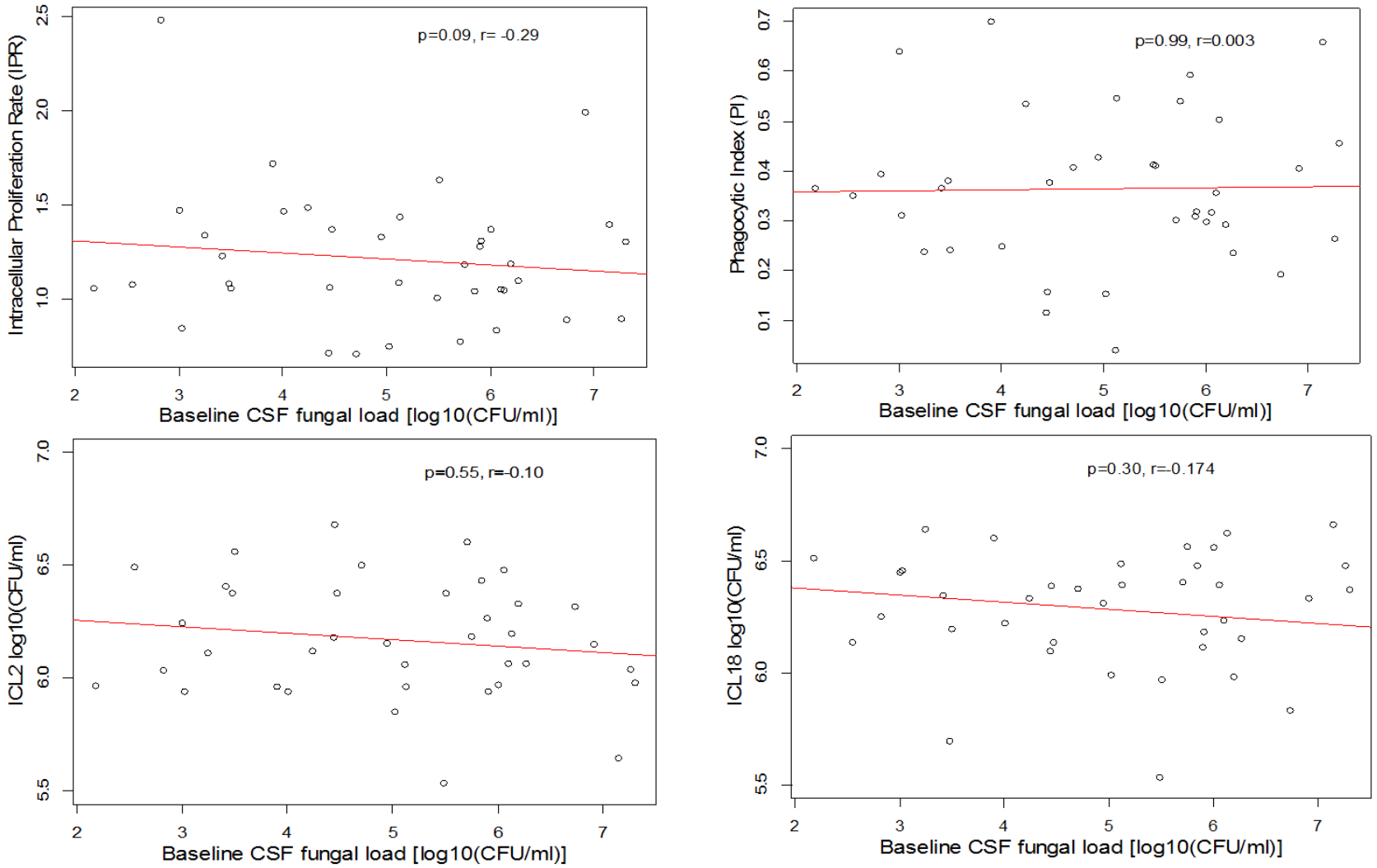

Figure 4.3-8. Correlation between IPR, PI, ICL2, ICL18 and corresponding patients' fungal load in the CSF at diagnosis.
Data represent mean of MAD-adjusted values for each parameter of each isolate. P-value and Rho coefficient of correlation were obtained from the Spearman test of correlation. Red lines indicate most probable fitted linear correlation.

1

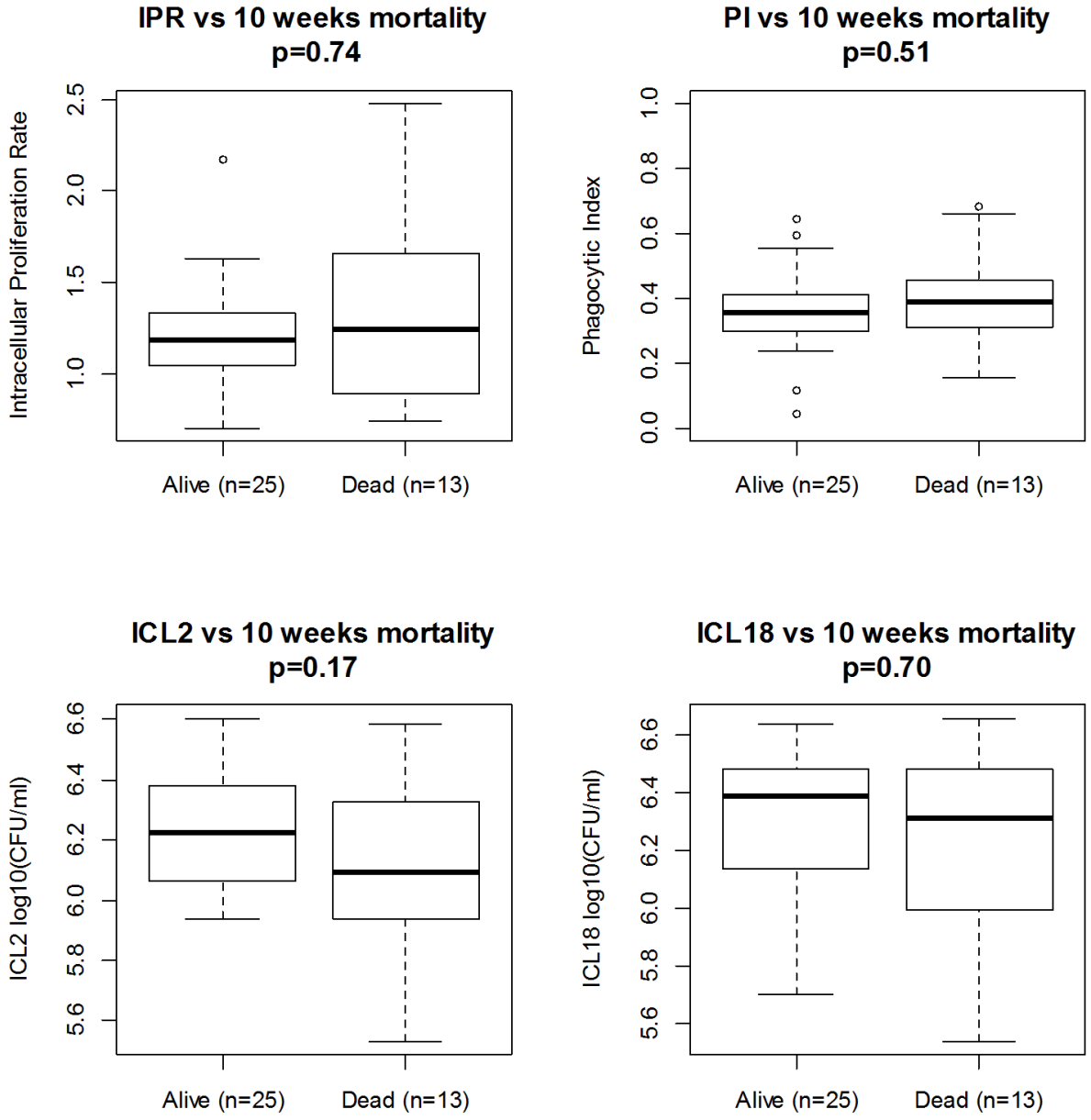

Figure 4.3-9. Association between macrophage parameters and patient mortality after 10-weeks of antifungal therapy.

Mortality information at 10 weeks was availble for 38/47 patients (25 survived and 13 died). P-values were obtained from pairwise comparison using the Mann-Whitney test.

4.3.2. Assessing macrophage parasitism using flow cytometry

Unwashed extracellular yeasts and time-consuming hemocytometer counting were among the major technical difficulties of Ma's original method that limited the model's throughput. Further modification of the original model was needed to improve accuracy and robustness. Here I report the optimization and adaptation of a flow-cytometry based modification of Ma's original model according to protocols reported by Voelz *et al.* (May lab, University of Birmingham, UK) [398] and Alanio *et al.* (Dromer lab, Institute Pasteur, France) [136].

4.3.2.1. Effects of Solophenyl flavine staining on yeast growth

Fluorescent fungal cell wall stain such as Calcofluor and 7GFF are known to be cell-wall stress inducers. In order to determine whether Solophenyl flavine (7GFF) staining affects growth of *C. neoformans* var. *grubii*, serial-diluted yeast cells were stained with different concentration of Solophenyl flavine and grown on YPD agar. There was no apparent growth defect detected even when cells from both test strains were exposed to the highest test concentration of Solophenyl flavine (1 mg/ml) (**Figure 4.3-10**). For subsequent FACS experiments yeast cells were stained with Solophenyl flavine at the lowest working concentration (10 µg/ml) for 10 minutes at room temperature in PBS buffer.

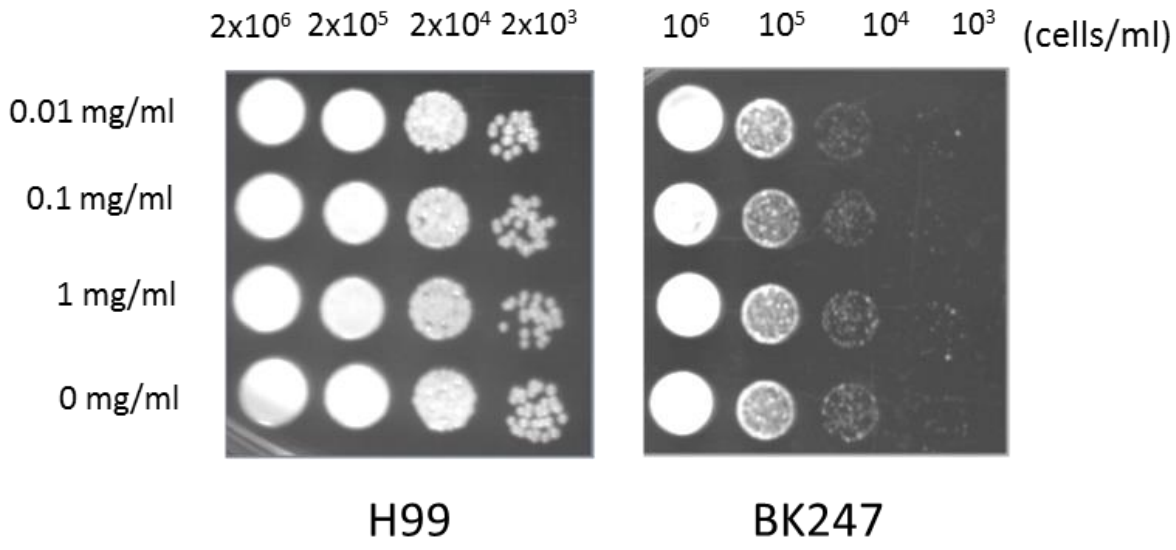

Figure 4.3-10. Effects of Solophenyl Flavine staining at various concentrations to growth of *C. neoformans* yeasts.

The reference strain H99 and one test isolate from Vietnam, BK247, were serially diluted and stained by incubating with various concentrations of Solophenyl Flavine in PBS buffer for 10 minutes at room temperature. Yeast suspension in 10 fold dilution were inoculated on Sabouraud agar and incubated at 30^{o}C for 2 days. Solophenyl Flavine has no obvious effect on growth of *C. neoformans* yeasts.

4.3.2.2. Optimizing the concentration of opsonizing antibody for phagocytosis assay and assessment of the Phagocytic Index using flow cytometry

After dislodging adherent J774 macrophages from 24-well culture plates (with or without ingested yeasts) using enzymatic Accutase treatment, the macrophage population were separated from extracellular, uningested yeasts (pre-stained with 7GFF) by size selection via FSC-SSC gating. The subset macrophage population was further separated into “Unaffected macrophages” and “Yeasts-associated macrophages” by gating at the Pacific Blue channel (corresponding to the excitation/emission spectrum of 7GFF, also see **Figure 4.2-2**). The

"Yeasts-associated macrophages" population would include both macrophages with ingested intracellular yeasts and membrane-bound extracellular yeasts. Phagocytic Index could then be determined by calculating the percentage of infected macrophages from the macrophage subset (**Figure 4.3-11**). A 10-fold increase in opsonizing F12D2 concentration (1µg/500µ/well to 10 µg/500µl/well) resulted in only a 10% increase of phagocytosis efficacy (**Figure 4.3-12**). As expected, antibody-opsonization resulted in more efficient phagocytosis. Specifically, antibody-mediated phagocytosis was 50% more efficient compared to complement-mediated phagocytosis in the previous experiment using Ma's method. Therefore for subsequent experiments I used 1µg/500µl/well as the standard F12D2 concentration for opsonization.

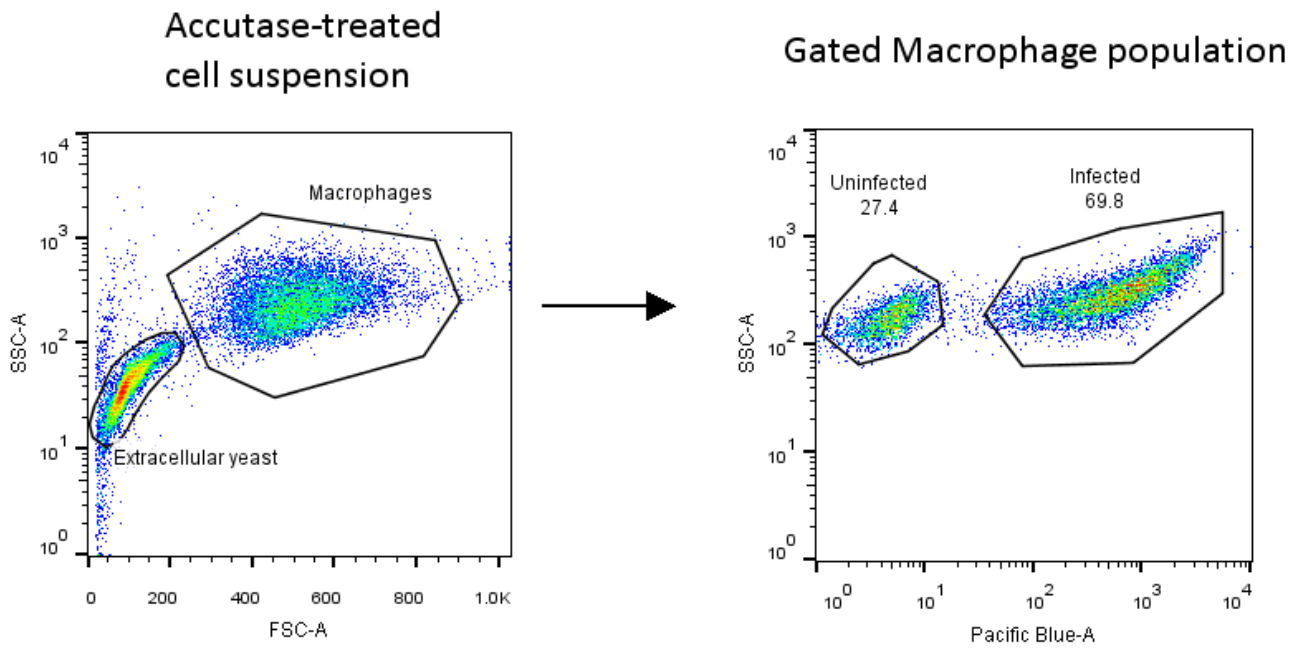

Figure 4.3-11. Gating strategy to determine Phagocytic index by flow cytometry.

The phagocytosis assay was carried out using J774 macrophages and F12D2-opsonized, Solophenyl Flavine-stained yeasts as described in the Methods section. After washing off extracellular non-internalized yeasts adherent J774 cells at the bottom were detached enzymatically using Accutase. Macrophages and extracellular yeasts populations are selected using SSC vs FSC scattering. Gated macrophages would subsequently be separated by plotting SSC and Pacific Blue. CN-infected macrophages would emit purple fluorescence and are gated accordingly.

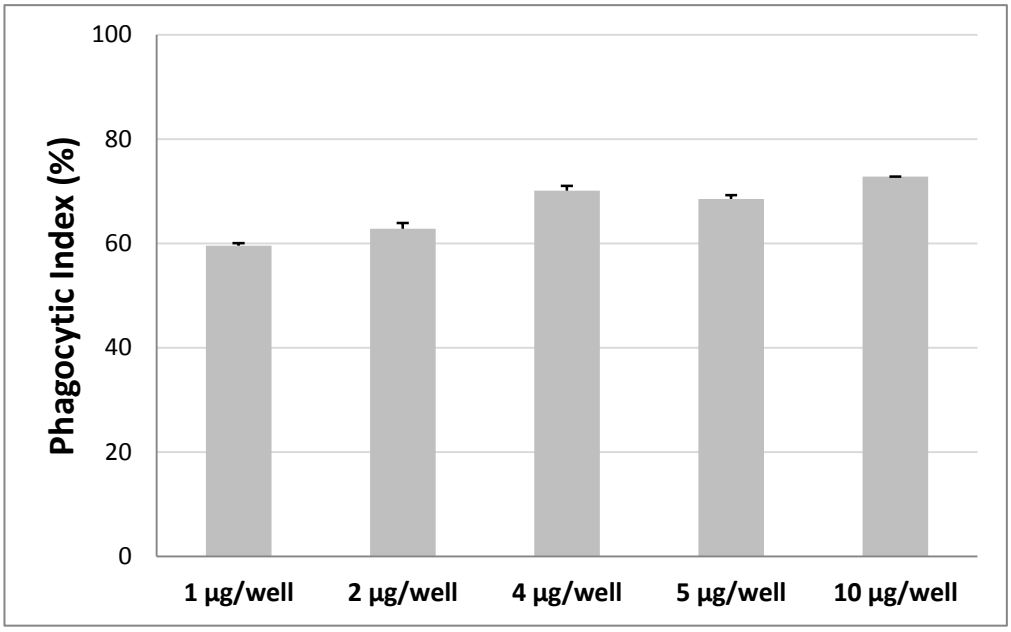

Figure 4.3-12. Optimizing F12D2 mouse IgG1 monoclonal antibody concentration for opsonizing of H99 yeasts.
Phagocytic Index corresponding to different concentrations of opsonizing monoclonal antibody was assessed. Barplot represents mean of 3 technical replicates at each concentration with error bars indicating standard deviations.

4.3.2.3. Optimizing multiple conjugated antibody staining

As seen in **Figure 4.3-13**, increasing primary antibody F12D2 concentrations did not result in any notable increase in fluorescence intensity. Any combination of concentrations of primary F12D2 and secondary AF647-conjugated anti-mouse IgG1 resulted in a clear separation from the unstained yeast population, indicating effective sandwiched antibody staining for flow cytometry. Since the differences in fluorescence intensity at different AF647-conjugated anti-mouse IgG1 concentrations were not significant, the F12D2 (1µg/ml)-AF647 antimouse IgG1 (1µg/ml) combination was chosen for subsequent experiments. Subsequent staining of

AF546-conjugated antibody was performed similarly using the same concentration combination.

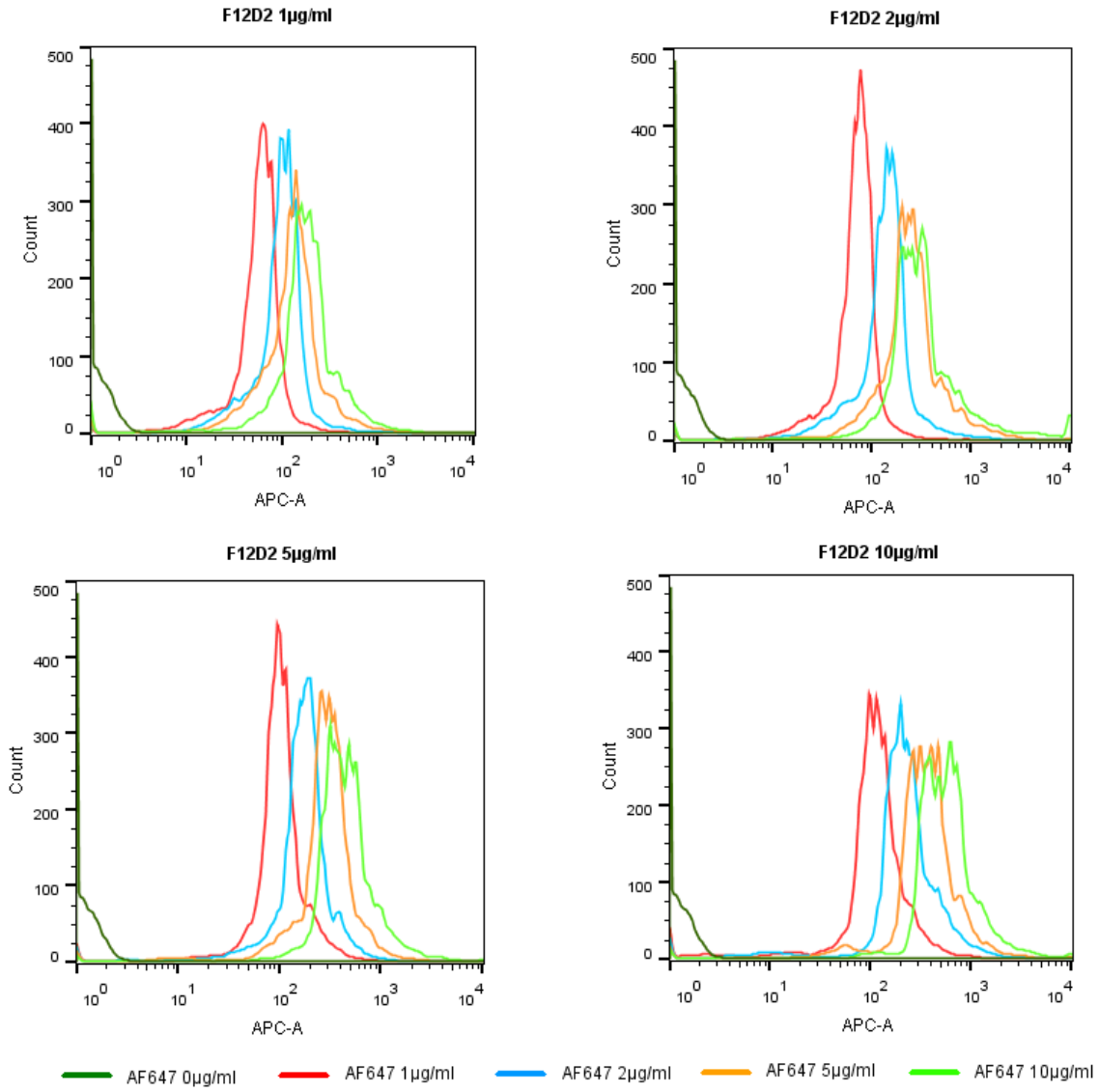

Figure 4.3-13. Optimizing antibody concentration combinations for staining yeast cells.
F12D2, a mouse monoclonal IgG1 specific for cryptococcal capsular polysaccharide was used as primary stain antibody for cryptococci. Antimouse IgG1 from mice pre-conjugated with Alexa Fluor 647 (AF746, having the same fluorescence spectrum as Allophycocyanin (APC)) was used as a secondary stain to detect and separate all cryptococci from macrophage cell debris after hypotonic lysis. Graphs display histograms of counted events for different F12D2 and AF647 combinations at the APC+ channel.

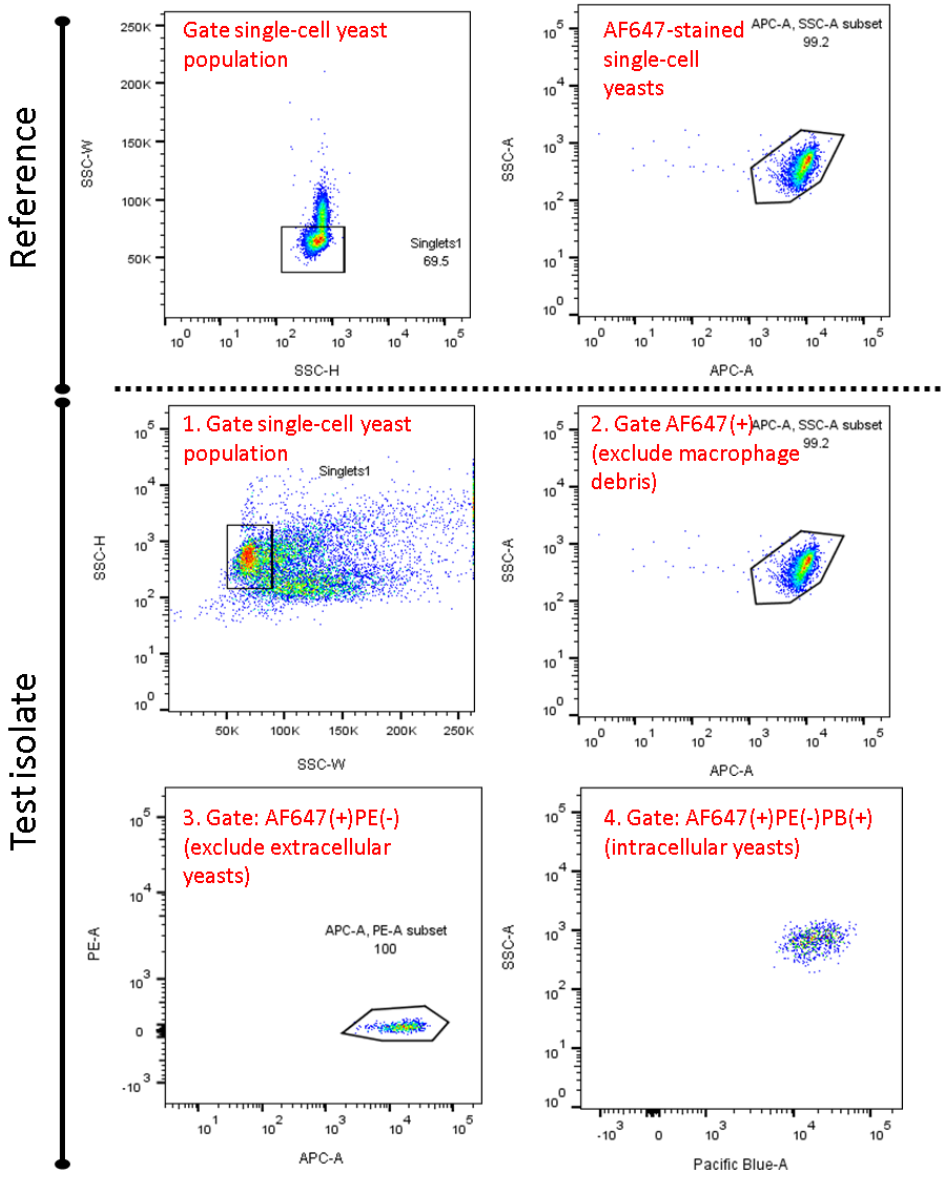

Figure 4.3-14. Optimizing gating strategy.

Relevant single-cell yeast populations for the test isolate were gated according to a reference sample containing only AF647-stained, freshly-grown H99 yeasts. Duplets were excluded by gating at SSC-H/SSC-W. AF647(+) cryptococci (both intra- and extra- cellular) were further subseted at the APC(+) channel. Intracellular yeasts were selected from the total cryptococci subset at the AF647(+)PE(-) gate. All 7GFF-stained intracellular yeasts were subsequent selected at the corresponding Pacific Blue channel.

4.3.2.4. Pilot application of flow cytometry for assessing macrophage parasitism

I screened randomly selected ST4 (n=21) and ST5 (n=18) isolates from each of the HIV groups for testing using the flow cytometry method (total n=39). Phagocytic Index data were available for all 39 isolates **(Table 4.3-7**). Due to technical problems and time constraints, the intracellular cryptococci load (ICL2 and ICL18) and intracellular proliferation rate (IPR) could only be obtained for 31 isolates (including 13 ST4 and 18 ST5 isolates) (**Table 4.3-7**). Again, outliers were removed using the MAD method as previously described, resulting in 13 ST4 isolates and 17 ST5 isolates.

The results are summarized in **Table 4.3-8** and **Figure 4.3-15**. Flow-cytometry and the use of H99 as an internal control provided remarkable precision for calculation of Phagocytic Index as no outliers were detected by MAD (n=38). Excluding 9 isolates without ICL and IPR data (8 ST4 and 1 ST5) and subsequent outlier filtering by MAD, 20 isolates (9 ST4 and 11 ST5) were suitable for further IPR analysis. Across the whole study population, I observed 2-fold, 7-fold, 23-fold and 21-fold variation in PI, ICL2, ICL18 and IPR, respectively. There were no differences in macrophage parasitism parameters, as assessed by flow-cytometry, according to MLST clustering (ST4 vs ST5) (**Figure 4.3-16** and **Figure 4.3-17**).

Table 4.3-7. Summary of results and isolates information for method 2

No.	ID	HIV	ST	PI	ICL2	ICL18	IPR	Log.base.CSF*	10-weeks mortality*
1	BK151	pos	4	1.04	0.39	1.28	3.27	5.61	Alive
2	BK156	pos	4	1.17	1.35	1.10	0.81	6.82	Alive
3	BK163	pos	4	0.90	0.49	1.35	2.77	5.54	Dead
4	BK188	pos	4	1.01	0.62	2.54	4.12	7.15	Alive
5	BK189	pos	4	1.25	0.60	2.04	3.40	5.90	Dead
6	BK205	pos	4	1.15	0.73	2.50	3.44	4.30	Dead
7	BK48	pos	4	1.42	2.07	6.31	3.04	5.71	Alive
8	BK87	pos	4	1.30	2.35	0.33	0.14	5.24	Alive
9	BK14	pos	4	1.42	NA	NA	NA	6.23	Alive
10	BK59	pos	4	1.29	NA	NA	NA	7.00	Dead
11	BK88	pos	4	1.32	NA	NA	NA	3.78	Alive
12	BK89	pos	4	1.46	NA	NA	NA	6.26	Alive
13	BK91	pos	4	1.17	NA	NA	NA	5.24	Alive
14	BK126	pos	4	1.17	NA	NA	NA	5.01	Alive
15	BK225	pos	4	1.26	NA	NA	NA	0.70	NA
16	BK74	pos	4	1.51	NA	NA	NA	6.38	Dead
17	BK11	pos	4	1.06	1.43	2.99	2.09	5.98	Dead
18	BK46	pos	4	1.31	1.41	13.86	9.82	6.00	Alive
19	BK68	pos	4	1.07	0.43	10.63	24.47	6.07	Alive
20	BK149	pos	4	1.06	0.59	9.05	15.44	0.00	Alive
21	BK150	pos	4	1.33	1.08	2.45	2.27	4.70	Alive
22	BMD101	neg	5	1.21	0.56	3.67	6.54	NA	Dead
23	BMD367	neg	5	1.07	0.38	1.61	4.25	NA	NA
24	BMD700	neg	5	1.17	0.36	1.44	4.00	NA	Alive
25	BMD1228	neg	5	0.86	0.54	1.32	2.45	NA	Alive
26	BMD1646	neg	5	1.06	0.64	1.41	2.22	4.46	NA
27	BMD367	neg	5	1.23	2.68	2.82	1.05	NA	NA
28	BMD854	neg	5	1.23	2.11	0.60	0.28	NA	NA
29	BMD973	neg	5	1.20	1.30	0.88	0.68	NA	NA
30	BMD1228	neg	5	1.22	1.37	5.78	4.22	NA	Alive
31	BMD1338	neg	5	1.11	1.22	8.62	7.08	6.91	Dead
32	BMD1353	neg	5	1.17	1.19	0.84	0.71	NA	NA
33	BMD1452	neg	5	1.39	NA	NA	NA	4.24	NA
34	BMD1198	neg	5	1.22	1.15	1.19	1.04	6.27	NA
35	BMD1232	neg	5	1.26	0.98	6.95	7.07	NA	Dead
36	BMD1465	neg	5	1.39	1.61	3.91	2.42	NA	NA

37	BMD1534	neg	5	1.39	5.40	1.10	0.20	NA	NA
38	BMD1592	neg	5	1.23	1.97	4.46	2.27	NA	NA
39	BMD1713	neg	5	1.44	1.52	7.36	4.83	NA	NA

**CSF fungal burden for patients at diagnosis (log10 cells/ml CSF). Clinical information was mostly fully available for "BK" patients who enrolled in an intervention RCT for treatment of HIV-associated cryptococcal meningitis. NA: ICL2, ICL18 and IPR data were unavailable for these isolates due to technical errors. These isolates were excluded in the subsequent analyses where ICL2, ICL18 or IPR were involved.*

Table 4.3-8. Summary of macrophage parasitism using flow-cytometry

	Original (Mean ± SD)			Outliers removed by MAD (Mean ± SD)		
H99 ratio	**ST4**	**ST5**	**p-values**	**ST4**	**ST5**	**p-values**
PI	1.22 ± 0.16	1.21 ± 0.14	0.89	1.22 ± 0.16	1.21 ± 0.14	0.89
ICL2	1.04 ± 2.64	1.47 ± 1.20	0.40	1.04 ± 0.64	1.21 ± 0.68	0.61
ICL18	4.34 ± 4.27	3.17 ± 2.60	0.53	4.67 ± 4.28	3.01 ± 2.60	0.24
IPR	9.39 ± 22.22	2.84 ± 2.77	0.92	1.43 ± 0.77	1.45 ± 0.78	0.98

IPR: Intracellular Proliferation Rate
PI: Phagocytic Index
ICL2, ICL18: Intracellular Cryptococci Load at 2 hours or 18 hours post-infection.
Data are presented as ratio between measured values of test isolate and that of H99 in the same experiment batch. Values presented in table as mean from 2 biological replicates with standard deviation. Pairwise statistical comparison was performed using Mann-Whitney test.

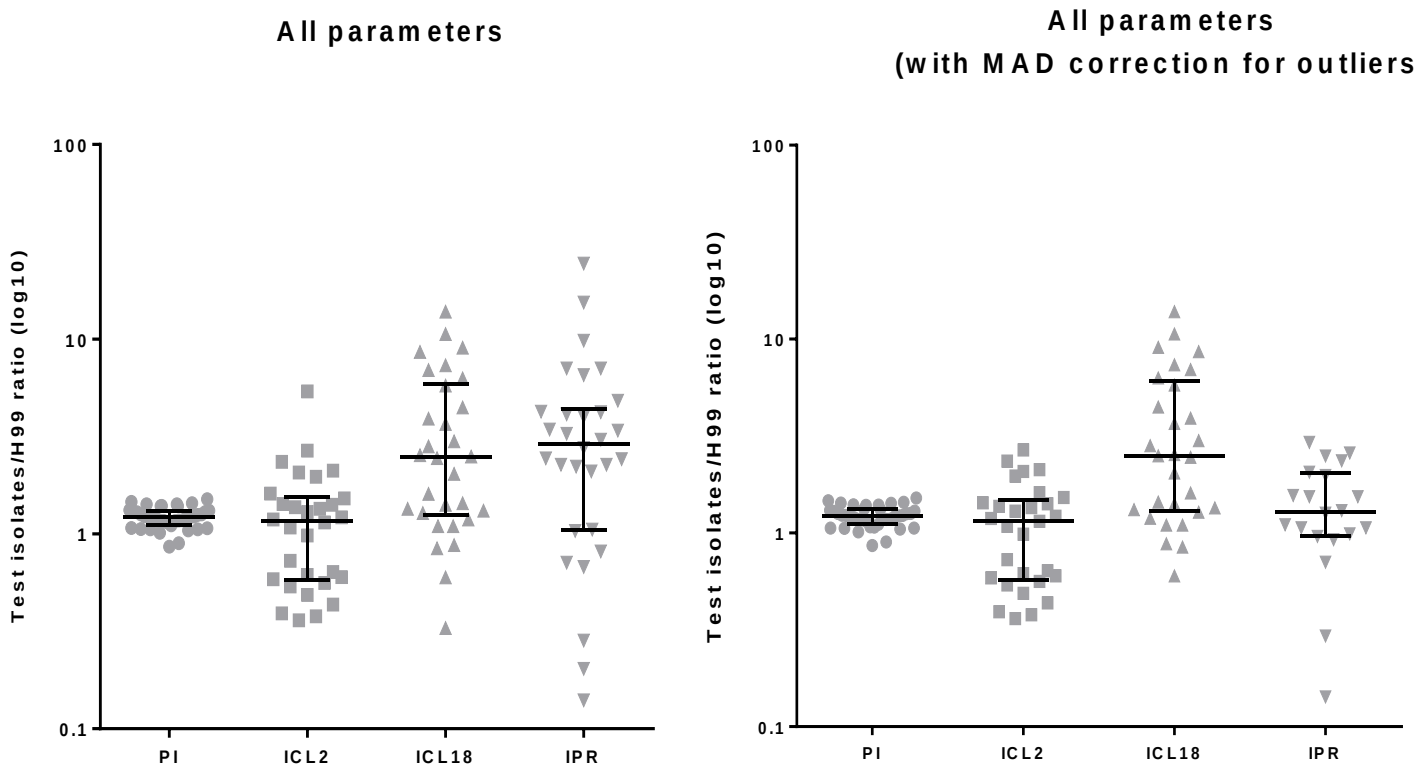

Figure 4.3-15. Variation of cytometry-based macrophage parasitism parameters in the test dataset.

Data are presented in scatterplots with standard deviations. Data for each category were pooled from all isolates in the dataset irrespective of AFLP/MLST genotypes or HIV status.

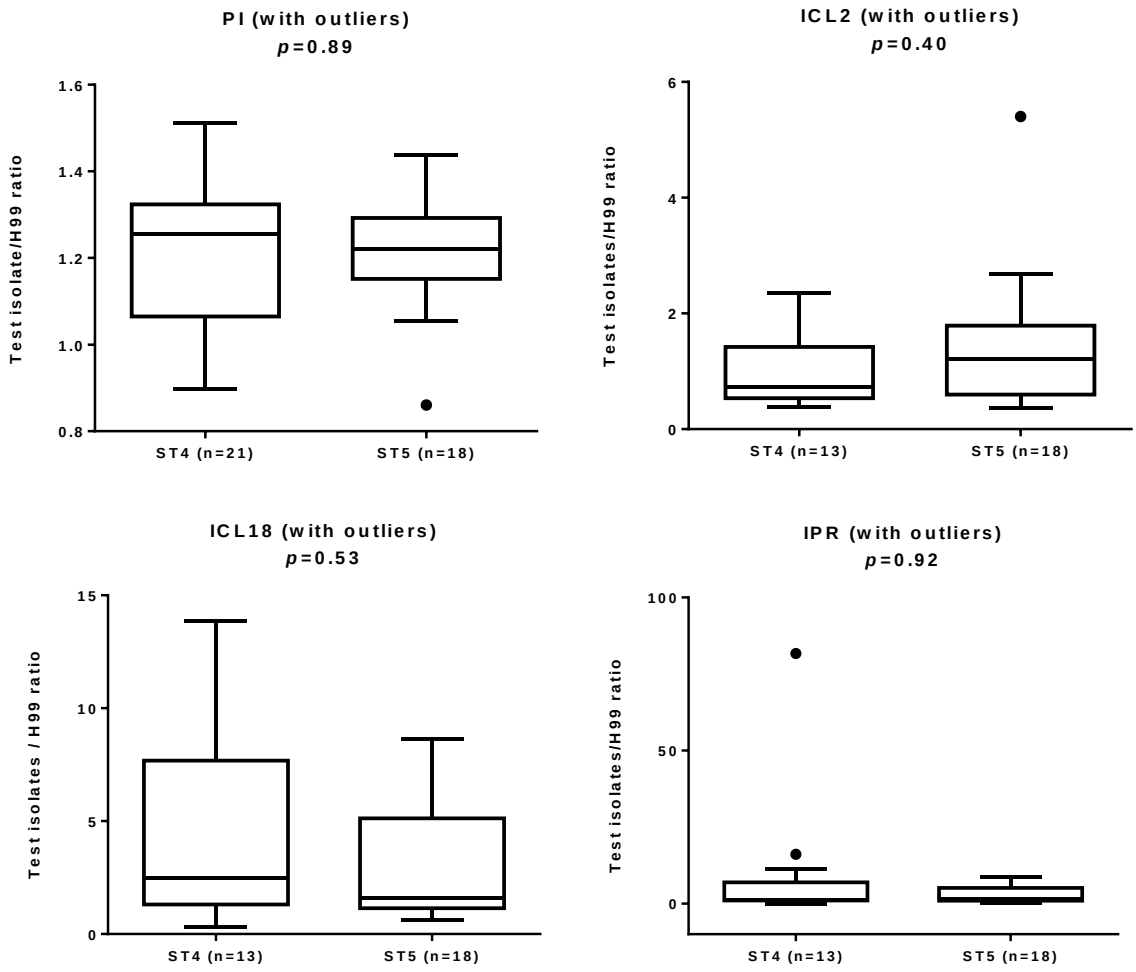

Figure 4.3-16. Comparison of macrophage parasitism parameters between ST4 from HIV-infected patients and ST5 from HIV-uninfected patients using flow-cytometry (uncorrected for outliers). Statistical comparison of groups was performed using the Mann-Whitney test. Boxplot presents the median with interquartile range. Data points outside the interquartile range are presented as clear dots.

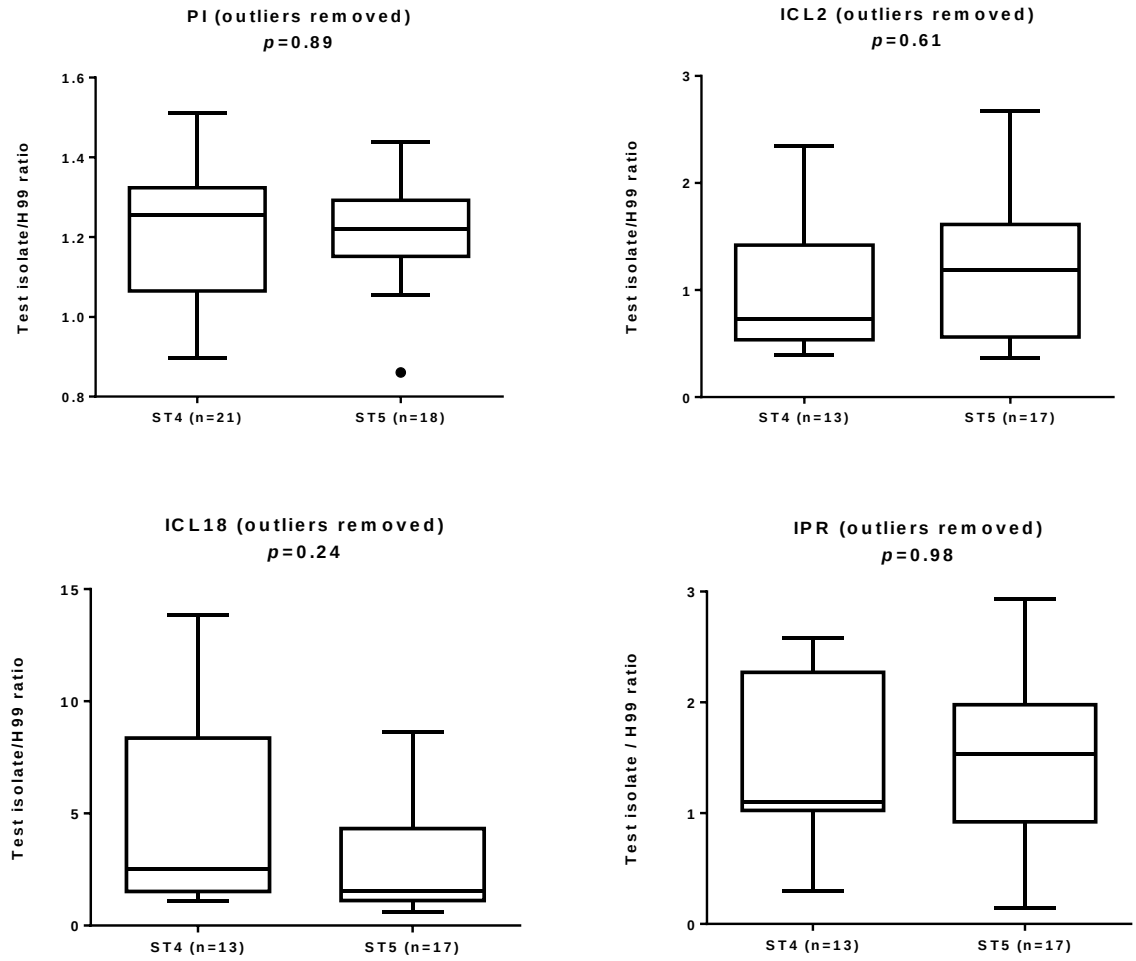

Figure 4.3-17. Comparison of macrophage parasitism parameters between ST4 from HIV-infected patients and ST5 from HIV-uninfected patients using flow-cytometry (corrected for outliers).
Statistical comparison of groups was performed using the Mann-Whitney test. Boxplot presents the median with interquartile range. Data points outside the interquartile range are presented as clear dots.

4.3.2.5. Associating FACS-based macrophage parasitism parameters and clinical outcomes

Comparison of flow cytometry-based Phagocytic Index (PI), Intracellular Cryptococci Load at 2 hours and 18 hours (ICL2 and ICL18) and Intracellular Proliferation Rate were conducted according to patient's available treatment outcome at 10 weeks (Alive, n=17 or Dead, n=9). Results are summarized in Figure 4.3-18. Overall there were no significant associations between any macrophage parasitism parameters and either patient mortality after 10 weeks of antifungal treatment or CSF fungal burden at baseline (**Figure 4.3-18** and **Figure 4.3-19**).

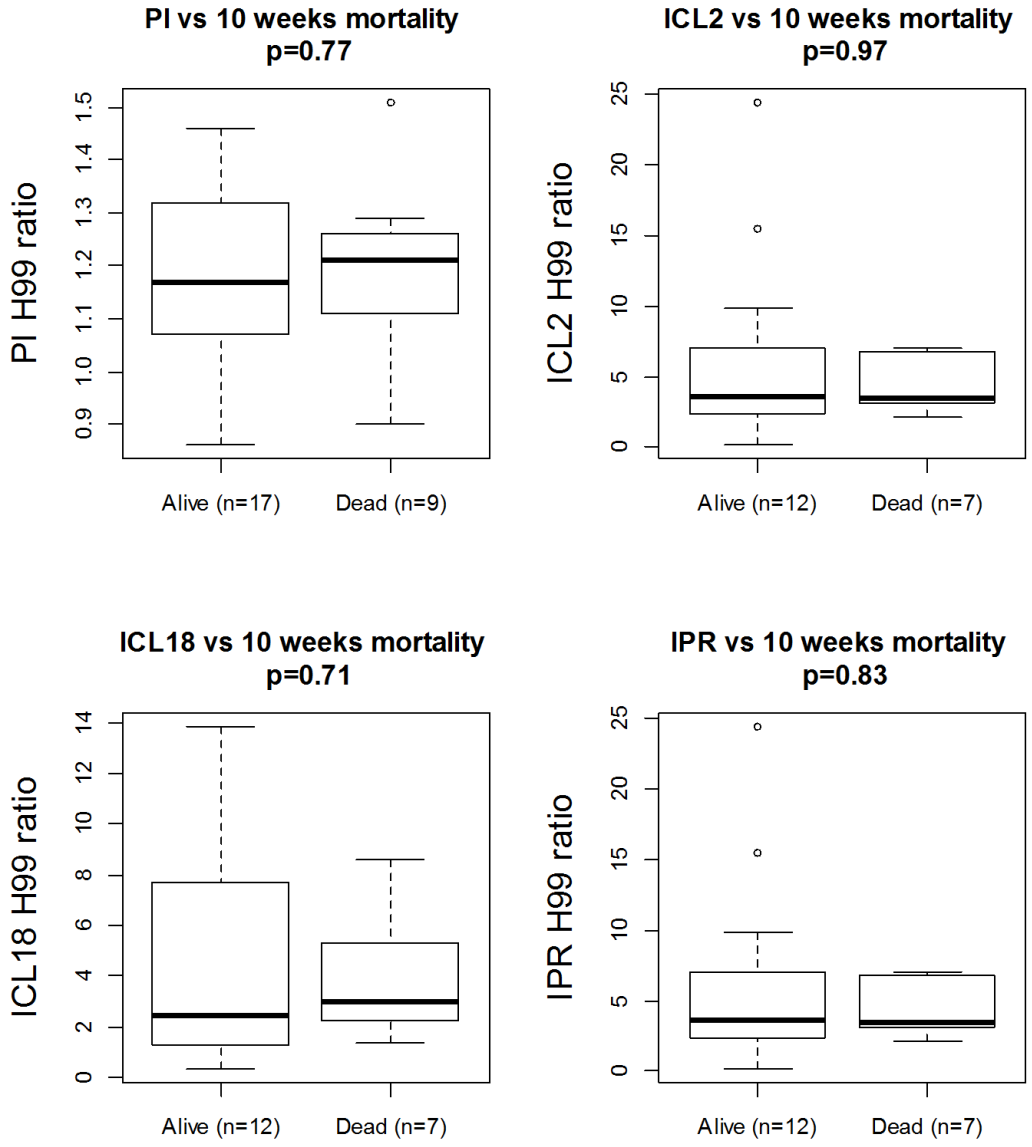

Figure 4.3-18. Associating FACS-based macrophage parasitism parameters and patient mortality after 10 weeks of antifungal treatment.

Statistical comparison of groups was performed using the Mann-Whitney test. Macrophage parasitism parameters were corrected for outliers by the MAD method. Boxplot presents the median with interquartile range. Data points outside the interquartile range are presented as clear dots.

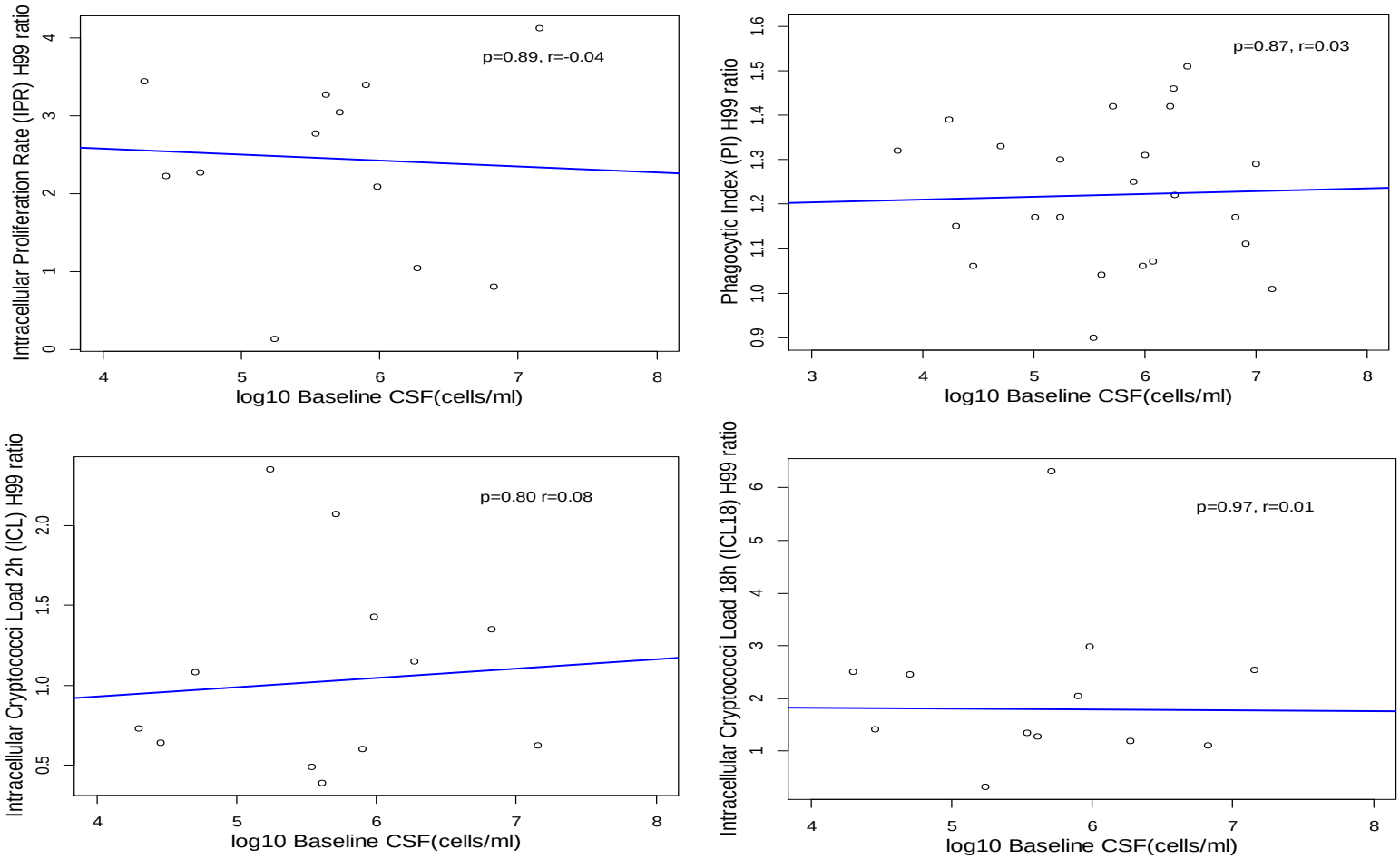

Figure 4.3-19. Correlation between PI, IPR, ICL2, ICL18 and patients' fungal load in the CSF at diagnosis.

Data were presented as ratios of the respective isolate's measurements against those of H99 in the same batch. Mean values were obtained from 2 biological replicates. P values and Rho (r) coefficients were from the Spearman test of correlation. Blue lines indicate most probable fitted linear correlation. No significant correlations were observed.

4.4. Chapter 4 Discussion

Here I employed *in vitro* macrophage models previously developed by Ma Hansong [130] and Alexandre Alanio [136] with slight modifications to see whether I could detect differences in the pathogenic potential of *C. neoformans* var. *grubii* isolates from Vietnamese patients with different host immune-type associations. I expected that ST5 strains, given that they can infect apparently immunocompetent patients, would have greater macrophage parasitism capacity. Using Ma's method, I found that there was considerable variability in these measures throughout the whole isolate population and no detectable differences driven by major AFLP or MLST-defined lineages. However, subsequent subgroup analyses revealed statistically significant differences in IPR according to host immune phenotype. For instance, isolates from HIV-uninfected patients seemed to have significantly higher intracellular growth rate than did isolates from HIV-infected patients. Specifically, the intracellular growth of ST5 isolates from HIV-uninfected patients was 30% higher than all other isolates (ST5 or non-ST5) from either HIV groups. Findings from the flow-cytometry method, however, did not reveal any significant differences.

The higher rate of intracellular proliferation detected in ST5 isolates from HIV-uninfected patients has a number of implications:

First, ST5 isolates from HIV-uninfected patients have higher virulence potential than other ST5 or non-ST5 isolates from HIV-infected patients. It is possible that such isolates from immunocompetent patients also have greater virulence potential than isolates from patients with other forms of immunosuppression. This is difficult to test, because other forms of immunosuppression are currently rare in Vietnam. This is likely to change as medical treatment advances.

Second, as there is variability in the virulence potential of strains within the same ST5 lineage, there may also be heterogeneity in virulence potential of other lineages. However any heterogeneity in virulence potential of lineages other than ST5 does not appear to be sufficient to result in disease in immunocompetent patients - we do not observe this in nature.

Third, it is not clear how this increased virulence potential of ST5 strains develops. There are broadly 2 possibilities – the quality exists prior to human infection, driven by some environmental stress or adaptation, and disease occurs through selection by the human host, or the quality is induced during human infection by in-host factors present only within immunocompetent hosts.

Fourthly, it is not clear from my work whether all, or only a subset, of ST5 isolates have the potential to cause disease in immunocompetent patients. While there is currently a trend for challenge studies in humans with other organisms, for example *Salmonella*

enterica serovar Typhi, and *Plasmodium* species, treatment for cryptococcal disease is currently too inefficient for this to be contemplated in humans, and as seen in chapter 3, the mouse model certainly seems to be inadequate for delineating differences between Vietnamese lineages that clearly correlate with host immune phenotype. The ST5 lineage appears to have diverged many millions of years ago from other lineages but are still highly clonal [325]; it therefore seems likely that all strains should have similar virulence potential. This could reflect a similar evolutionary history since most cryptococcal virulence factors play important roles in survival/adaptation to environment stresses. Understanding how the virulence potential is regulated may enable the identification of novel drug targets.

Another possibility is that this result was an artifact associated with the complex experimental design. In fact, the model's applicability is based on several assumptions:

(i) **Test isolates must have similar baseline growth rate**. This means that any differences in intracellular growth would be attributed to the isolates' intrinsic ability to survive in an intracellular niche rather than an effect of differential generation time. Since there was no underlying genotype-specific difference in growth in YPD at either 30^{o}C or 37^{o}C (described in Chapter 4), a different underlying growth rate could be ruled out as a confounding factor to any differences in IPR.

(ii) **Extracellular yeasts must be effectively washed off since residual extracellular yeasts would severely affect downstream IPR calculation**. However since the protocol was standardized and performed similarly for every isolates, it would be expected that any systematic artifacts due to unwashed extracellular yeasts would be similar for every isolates.

(iii) **Macrophage uptake must be high enough to assess intracellular proliferation**. The model is less appropriate for screening of low-uptake isolates [130]. Low phagocytic uptake could be due to the isolate's intrinsic anti-phagocytic capabilities (with or without opsonization). Phagocytosis of cryptococci occurs through 2 main routes: opsonin-dependent (complement and antibody-mediated) and opsonin-independent (recognition of fungal cell wall components by pattern recognition receptors (PRR) on immune cells) [392]. Both routes are dependent upon a balance between the ability of the capsule to inhibit phagocytosis and the ability of the capsule to bind to opsonins at the capsular surface [24]. Since encapsulated *C. neoformans* yeasts are highly resistant to phagocytosis in the absence of opsonins, the yeasts in this study (Ma's method) were opsonized in 20% pooled human serum from immunocompetent volunteers because we did not have enough anti-capsular monoclonal antibodies at this time. I did not determine the exact opsonic compositions of the pooled human serum used since IPR was reportedly independent of uptake routes (complements/antibody-mediated or via recognition of

specific fungal cell wall components by immune cells)[130]. Given the points made above, I do not think the differences I detected are technical artifacts.

I have previously demonstrated that *in vitro* capsular enlargement was more profound in ST5 yeasts under stimulating conditions compared to non-ST5s (data Chapter 2). It would not have been surprising to find that the ST5 yeasts were more resistant to phagocytosis, given the capsule's anti-phagocytic properties [179,399]. However, I found no evidence supporting any differences in either phagocytic index or yeast uptake according to AFLP/MLST genotypes or HIV immune groups. It is possible that such differences were obfuscated within the model due to the fact that all test isolates were uniformly opsonized (either by serum or capsular-specific monoclonal antibody) in the phagocytosis assays. In other words, any potential intrinsic differences in anti-phagocytic capability between isolates from different lineages/HIV groups may have been neutralized by the use of opsonins.

Alanio *et al.* previously reported that isolates with smooth colonies had higher PI and lower binding by capsular-specific monoclonal antibody, in contrast to mucoid colonies which had lower PI and high monoclonal antibody binding [136], indicating that capsular composition and structural configuration may affect opsonin binding and phagocytosis efficacy. Zaragora *et al*. reported that complement-mediated phagocytosis efficacy was inversely correlated with capsule volume, in contrast to IgG1-opsonized yeasts which

showed no correlation between phagocytic index and capsule volume [400]. Therefore the models I used could be inherently incapable of demonstrating differences in phagocytosis efficacy, even though ST5 isolates responded more rapidly to capsule-inducing *in vitro* conditions (reported in Chapter 2) that would otherwise confer increased resistance to phagocytosis.

While I found that serum-opsonized ST5 isolates from HIV-uninfected patients were actively replicating inside murine macrophages at a significantly higher rate than either ST5 or other non-ST5 isolates from HIV-infected patients (34% and 22% more rapidly, respectively), I demonstrated this only using Ma's method. I could not replicate this difference using flow-cytometry experiment (Alanio's method). This discrepancy could be due to the technical flaws while performing the flow-cytometry model, in which case more calibrations is needed. Alternatively, it could be due to the differences in opsonization method used in the two experiments i.e. the use of (highly specific) monoclonal antibodies versus human serum. Compared to complement, monoclonal antibody opsonization would result in a higher initial yeast uptake rate, which in turn could lead to increased competition for nutrients between intracellular cryptococci and subsequent stagnation of intracellular proliferation. In fact Sabiiti *et al.,* (2014) observed that increased burden of 18B7 antibody-opsonized *C. neoformans* yeasts in macrophages was more a result of high initial uptake rather than subsequent intracellular proliferation [135].

While previously IPR has been associated with the virulence of Vancouver outbreak *C. gattii* strains, this is in contrast with *C. neoformans* var. *grubii*, where initial yeast uptake by macrophages, not IPR, has been associated with higher fungal burdens and worse mortality [135]. This latter result, reported by Sabiiti and colleagues, contrasts with my findings. However, an important difference with Sabiiti's study is that my study involves apparently immunocompetent patients, whereas his work focused on strains from patients with HIV-associated cryptococcal meningitis. *C. gattii*, especially the Vancouver outbreak strains, predominantly infect immunocompetent patients. It is perhaps not surprising that my findings, focused on strains from immunocompetent hosts, are consistent with the *C. gattii* data, and hint at a mechanism whereby *Cryptococcus* adapts to a more aggressive immune environment. The ST5 isolates' increased intracellular replication in immortalized murine macrophages *in vitro* is consistent with the lineage having a higher virulence potential. However, I did not see increased mouse mortality in my previous murine survival experiment. Rather, the pattern of disease in mice was similar to that which we have reported in HIV patients [325]. This paradox could either be a consequence of lack of power in the murine model (I tested only 8 clinical strains), or be a consequence of the mouse model in fact being a poor model of disease in the immunocompetent human. Of note, murine inflammatory response in cryptococcal disease has been shown to be similar to that in HIV-infected patients [386].

The molecular mechanism explaining the increased IPR of ST5 *C. neoformans* var. *grubii* isolates from HIV-uninfected patients and its exact role in human disease is unknown. It is biologically plausible that an (30%) increase in IPR confers a pathogenic advantage. Intuitively, an increased replication rate within host macrophages suggests better adaptation to an intracellular lifestyle and the mammalian immune system. An increased IPR implies one or more efficient mechanisms of nutrient scavenging, higher resistance to reactive oxygen species in the lysosome, more effective immune avoidance and a potential advantage for in-host dissemination. Alanio and colleagues demonstrated worse outcomes for HIV patients infected with high-uptake/high-intracellular *C. neoformans* isolates – there was an increased risk of death by month 3 post diagnosis [136]. I was unable to detect any such significant clinical correlations using either method (Ma's or Alanio). This might represent a lack of power on our part, given the relatively small number of isolates tested. Furthermore, work parallel to this PhD has reported that mortality at 10 weeks or 6 months in HIV-associated cryptococcal meningitis is similar for patients infected with ST5 or non-ST5 *C. neoformans* var. *grubii*, although CSF fungal burden at baseline was lower for those infected with ST5 strains [325]. However, my works here suggests that HIV ST5 strains may assume a 'just good enough', less virulent phenotype in less aggressive immune environments.

Given the fact that disease outcome could be a result of the complex interactions between host macrophages and invading cryptococci, it could be the case that the higher

rate of intracellular growth, possibly at an early stage of cryptococcal colonization and dissemination in the human host, would result in increased CSF fungal burden and slower rate of clearance upon antifungal treatment among apparently immunocompetent patients infected with ST5 yeasts. Prospective screening of a larger number of isolates from both HIV-groups with more complete clinical data would potentially reveal any possible connections between macrophage parasitism and disease in humans.

Lastly, the model did not take into account other important macrophage parasitism phenotypes such as vomocytosis (non-lytic expulsion of ingested yeasts) and lateral transfer (direct transfer of yeasts between adjacent host cells) which may play important roles in disease progression (i.e. non-lytic dissemination in the host without triggering immune retaliation or crossing the Blood-Brain-Barrier[130,131,393]). Vomocytosis occurs independent of uptake routes (antibody/serum opsonized and non-opsonized) in both J774 and primary human macrophages, though the vomocytosis rate in J774 (~10%) was lower than in human primary macrophages (~27%) [131]. Lateral transfer, in conjunction with vomocytosis, represent one of the mechanisms for dissemination and latency of cryptococci by hijacking host phagocytes [130]. Future studies should investigate this aspect of macrophage parasitism since colonization, dissemination, crossing the Blood-Brain-Barrier and latency could be among the underlying factors contributing to ST5-associated disease in apparently immunocompetent patients.

4.5. Chapter 4 Conclusion

In this Chapter I employed and further refined an *in vitro* macrophage model of infection to compare virulence potential of *C. neoformans* var. *grubii* isolates associated with different host HIV immune types in Vietnam. I was able to demonstrate that ST5 isolates from HIV-uninfected patients could replicate more rapidly within macrophages, suggesting higher virulence potential. Whether this difference has any relevance from a clinical perspective could not be determined due to the small number of isolates tested and missing clinical information from the HIV-uninfected group. Based on these findings, it is possible that isolates from the ST5 lineage may be better suited to an intracellular lifestyle which facilitates host immune evasion and dissemination/latency. These properties may promote initial host infection and colonization, particularly within the immunocompetent patients. In the next chapter, I will use RNAseq to investigate genotype-specific genes and pathways that are differentially expressed which may contribute to differential metabolism and virulence potential.

Chapter 5

COMPARATIVE TRANSCRIPTOMICS OF *C. NEOFORMANS* VAR. *GRUBII* FROM HIV-INFECTED AND HIV-UNINFECTED PATIENTS IN VIETNAM

5.1. Chapter 5 Introduction

Previously the AFLP-defined cluster of *C. neoformans* var. *grubii* VNI-γ that was associated with infection in the apparently immunocompetent [103] was revealed to be all sequence type (ST) 5 by Multi Locus Sequence Typing (MLST); the VNI-δ cluster included all other non-ST5 MLST sequence types in the Vietnamese *C. neoformans* var. *grubii* population [325] (also presented in Chapter 2). Comparative genomics further confirmed that ST5 and non-ST5 isolates were phylogenetically distinguishable and both were distantly related to the reference strain H99 [325]. The findings that there are in total over 165kbp of sequence (in >500bp segments) specific for either the H99 reference or the VN strains, along with the absence of the unique H99 chromosomal rearrangement at chromosome 3 and chromosome 11 among the Vietnamese strains suggested that they shared a more recent common ancestor than H99. Despite having significantly different capability to cause disease in apparently immunocompetent individuals, ST5 and non-ST5 strains shared common genomic architecture features such as comparable number of retro-transposons and repeat elements which were enriched proximal to telomeres and centromeres. Closer inspection of non-redundant lineage-specific coding sequences

identified a number of pleiotropic genes and proteins from known key metabolic processes that are also associated with virulence. Functional analysis has the potential to greatly enhance the understanding of lineage-specific genomic structures by providing information on differentially expressed genes.

Therefore in this chapter I aimed to compare gene expression between ST4 and ST5 lineages during log-phase growth in rich medium (YPD). The rationale for doing RNAseq in YPD but not in any stress conditions was that: (i) despite known genetic differences between ST4 and ST5, it is unclear how these genes/pathways are regulated and expressed, (ii) many cryptococcal virulence factors are also involved in basic metabolic processes/growth. Data from our group also suggest that *C. neoformans* cells express virulence-inducing genes during normal growth in YPD.

5.2. Materials and Methods

5.2.1. *C. neoformans* var. *grubii* isolates

Two ST4 isolates: BK80, BK224 and two ST5 isolates: BMD854, BMD973 were selected from the same isolate collection described in previous chapters [103,307] for RNAseq profiling. All studies were approved by the Institutional Review Board of the Hospital for Tropical Diseases, Ho Chi Minh City, and the Oxford Tropical Ethics Committee or Liverpool School of Tropical Medicine UK. Bulk isolate archives from patient CSF were stored at -80^{o}C using Microbank beads (Pro-Lab Diagnostics, UK). Mating type and

Amplified Fragment Length Polymorphism (AFLP) genotyping for each strain had been determined and published previously [10]. MLST genotyping was performed and presented in Chapter 2 of this thesis.

5.2.2. Total RNA extraction and RNA sequencing

All isolates were single-colony purified prior to experiments. From previous growth kinetics experiments, *C. neoformans* isolates from my collection reached mid log-phase growth in YPD broth at approximately 18 hours post-inoculation. Yeasts growing at mid-log phase were propagated by incubating 10^6 yeast cells in YPD broth at 30^{o}C with agitation for 18 hours. Six biological replicates were performed for each isolate [401]. Yeast pellets were collected by centrifugation and total RNA extracted using the Ribopure Yeast DNA Purification Kit (Ambion, USA) according to the manufacturer's instructions. Extracted total RNA was stored in isopropanol and sent to Macrogen (Seoul, Republic of Korea) for RNA sequencing. Paired-end RNAseq library construction was performed using a TruSeq stranded mRNA preparation kit (Illumina, San Diego, CA). The cDNA libraries were sequenced on the Illumina HiSeq 2000 (Illumina, San Diego, CA) instrument. Assuming a transcriptome of 12 Mbp, I aimed for 20 million reads per experiment which would result in at least 150-fold coverage.

5.2.3. RNA sequencing and quantitative analysis

The latest *C. neoformans* var. *grubii* H99 reference genome with annotations were downloaded from Fungidb database (www.fungidb.org). After initial quality check of sequencing using fastQC (https://www.bioinformatics.babraham.ac.uk/projects/fastqc/), adapters and low quality regions were removed using Scythe (https://github.com/vsbuffalo/scythe) and Trimmomatic (http://www.usadellab.org/cms/?page=trimmomatic), respectively. Short reads were mapped to the H99 reference genome using HISAT2 (Hierarchical Indexing for Spliced Alignment of Transcripts) [402]. Output SAM (Sequences Alignment Map) files were converted to BAM (Binary Alignment Map) files using SAMtools [403]. Reads counting and assignment of mapped reads to genomic features on the reference genome were done using featureCounts [404]. In the subsequent quantitative analysis, 12 replicates were assigned for each of the two genotypes under comparison (ST4 and ST5), corresponding to 2 isolates x 6 biological replicates/ genotype. The R package Deseq2 was employed for differential gene expression analysis[405]. Un-normalized count matrices from featureCounts were used as input because Deseq2 internally corrects for library size. False Discovery Rate (FDR) was simulated using the R package *qvalue* and a critical value was selected as threshold [406]. Analysis process is summarized in **Figure 5.2-1.**

5.2.4. Gene Ontology (GO) enrichment analysis

Gene Ontology (GO) is a collective set of universal vocabularies to facilitate the process of describing genes and gene products across all species [407]. The GO Consortium consists of three main umbrella categories: Biological Processes, Molecular functions and Cellular Components [407]. Biological processes describe specific biological objectives that genes/gene products contribute via their respective molecular functions (hydrolase, transport, DNA binding etc.) at specific cellular localizations (cellular components). Differential gene expression analysis identified sets of over-expressed or under-expressed genes, which can be further characterized and categorized into groups of biological relevance using GO enrichment. GO enrichment analysis, done using the R package topGO, detects which GO terms appear more frequently than would be expected by random chance when assessing the set of GO terms assigned to the input genes. A statistical test (e.g. Fisher's Exact test), is performed to test whether a certain GO term is statistically enriched for the given set of genes. Correction for multiple testing is not needed as topGO takes into account GO term hierarchy which is considered in the resulting Fisher test. GO term hierarchy interrogation was done using QuickGO (https://www.ebi.ac.uk/QuickGO).

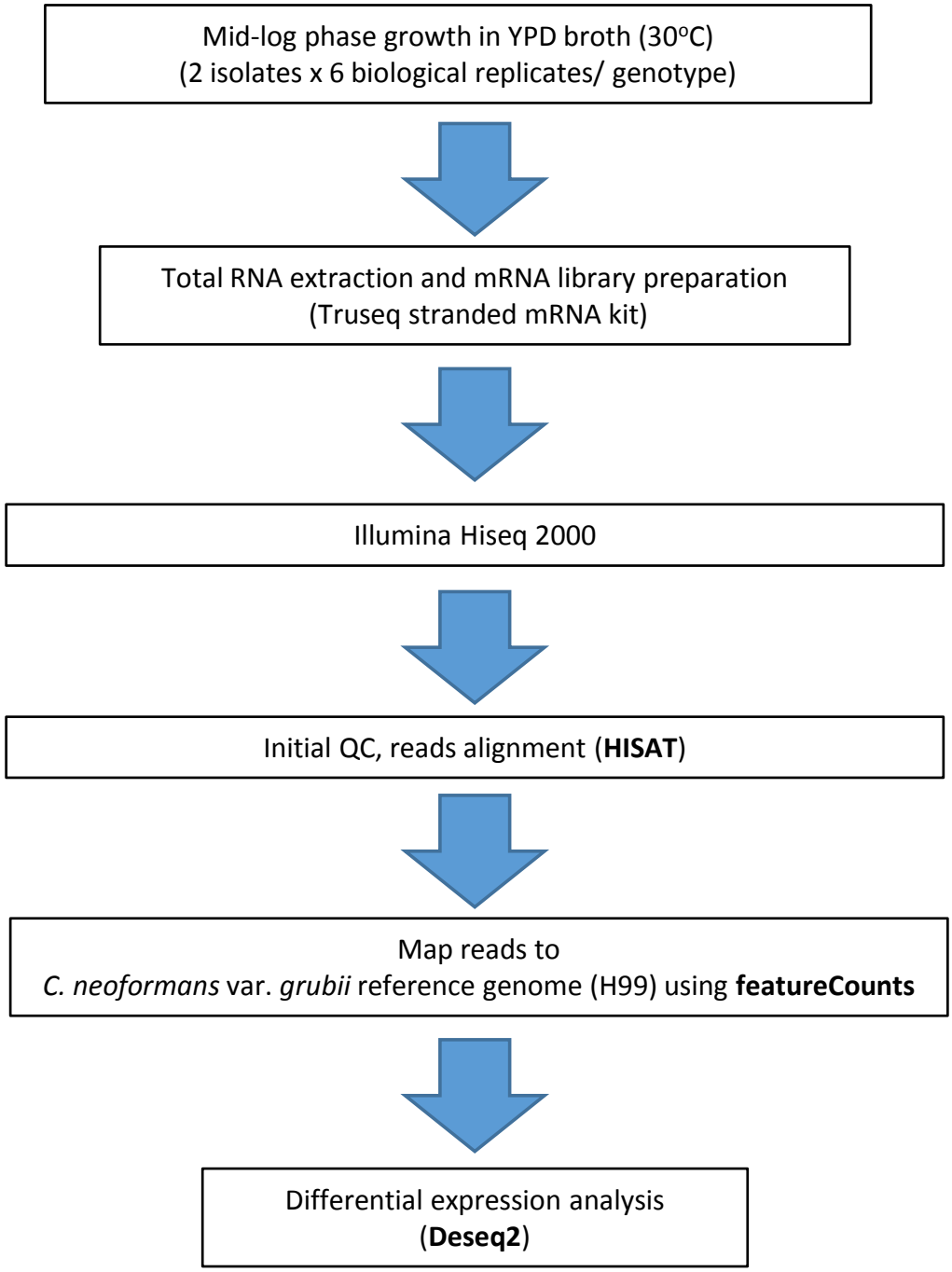

Figure 5.2-1. Overview of RNA sequencing and analysis workflow

5.3. Chapter 5 results

5.3.1. RNA Sequencing results

For each of the two genotypes, 12 cDNA libraries (2 x 12 = 24) were constructed for high-throughput Illumina mRNA sequencing. In total, more than 200 million reads were generated, representing on average more than 100X coverage of the *C. neoformans* var. *grubii* genome length for each sample. For most samples, more than 95% of sequencing reads were mapped to the *C. neoformans* var. *grubii* H99 reference genome (**Table 5.3-1**). Library sizes varied from 8 million to over 14 million reads across different samples. During the subsequent differential gene expression analysis, Deseq2 adjusted for differences in library size by automatically calculating a size factor for each library under investigation that would then be used for normalization and transformation of read counts.

Table 5.3-1. Number of RNA-seq reads for each sample and mapping results

Sample	MLST genotype	Total reads	Mapped reads	% Mapped
BK224-1	ST4	8,948,745	8,318,023	93%
BK224-2	ST4	8,544,613	8,228,891	96%
BK224-3	ST4	9,183,908	8,743,073	95%
BK224-4	ST4	7,995,350	7,488,070	94%
BK224-5	ST4	8,838,418	8,287,181	94%
BK224-6	ST4	9,013,005	8,540,765	95%
BK80-1	ST4	9,694,924	9,283,488	96%
BK80-2	ST4	9,345,272	9,041,266	97%
BK80-3	ST4	7,828,385	7,567,792	97%
BK80-4	ST4	7,906,881	7,537,289	95%
BK80-5	ST4	8,895,059	8,630,835	97%
BK80-6	ST4	8,288,584	7,883,358	95%
BMD854_1	ST5	10,904,916	10,554,533	97%
BMD854_2	ST5	11,088,729	10,769,941	97%
BMD854_3	ST5	10,649,622	10,346,549	97%
BMD854_4	ST5	13,552,139	13,170,531	97%
BMD854_5	ST5	14,489,682	14,050,898	97%
BMD854_6	ST5	15,252,684	14,793,015	97%
BMD973_1	ST5	12,802,306	12,400,641	97%
BMD973_2	ST5	8,497,101	8,229,088	97%
BMD973_3	ST5	12,523,132	12,142,748	97%
BMD973_4	ST5	13,193,453	12,779,229	97%
BMD973_5	ST5	6,513,845	6,313,054	97%
BMD973_6	ST5	6,663,738	6,462,363	97%
Total		**240,614,491**	**231,562,621**	**96%**

Figure 5.3-1 describes the distribution of counts per gene, which revealed a number of genes with zero counts. A pseudo-count of 1 was included prior to the log transformation to avoid minus infinite values resulting from these genes with no counts (null genes). **Figure 5.3-2** shows the proportions of genes-with-zero-counts per samples. Such genes would be filtered out in the next quantitative steps.

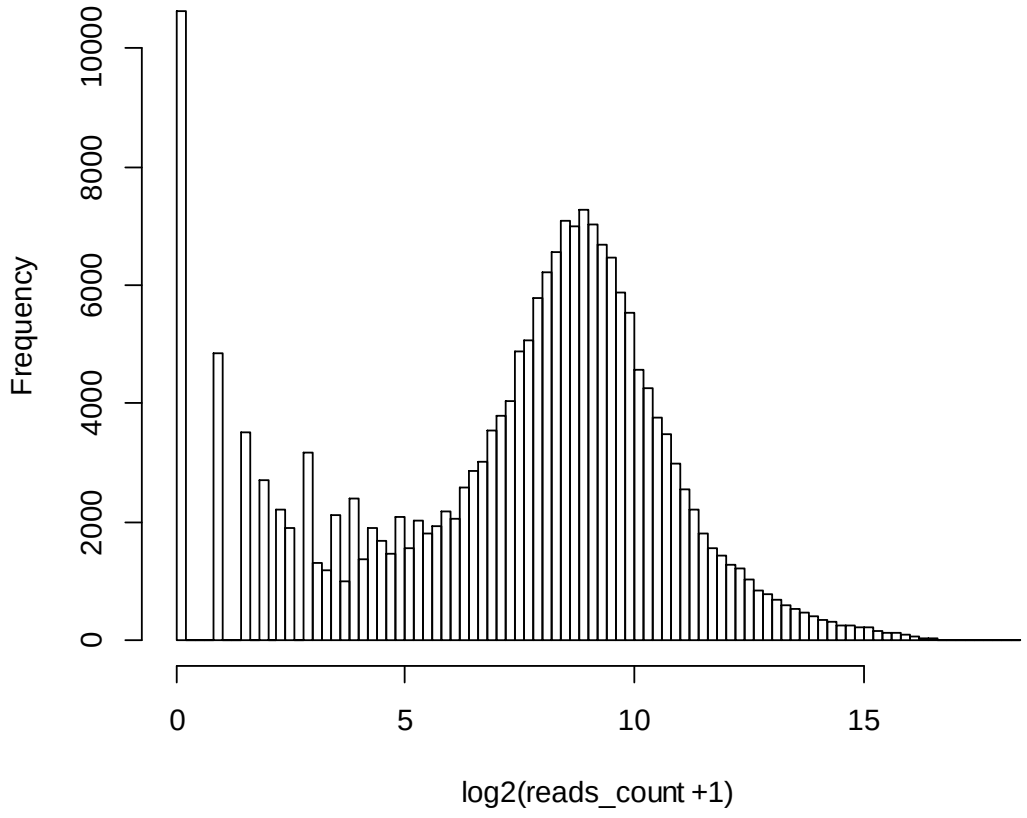

Figure 5.3-1. Distribution of transformed read counts per expressed genes across all samples.

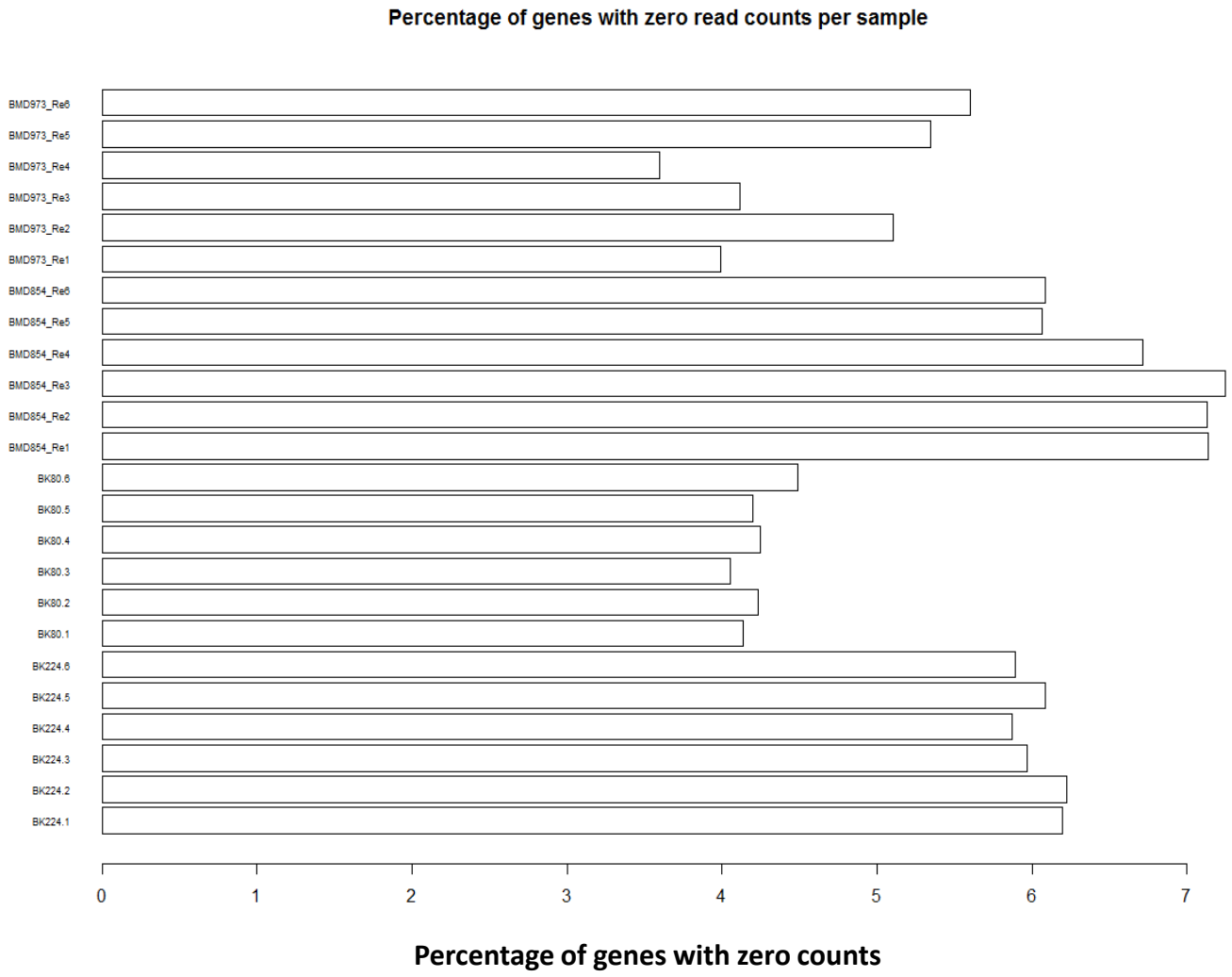

Figure 5.3-2. Proportions of genes with zero counts (null genes) per sample

5.3.2. Differential Gene Expression Analysis using Deseq2

5.3.2.1. Samples clustering analysis

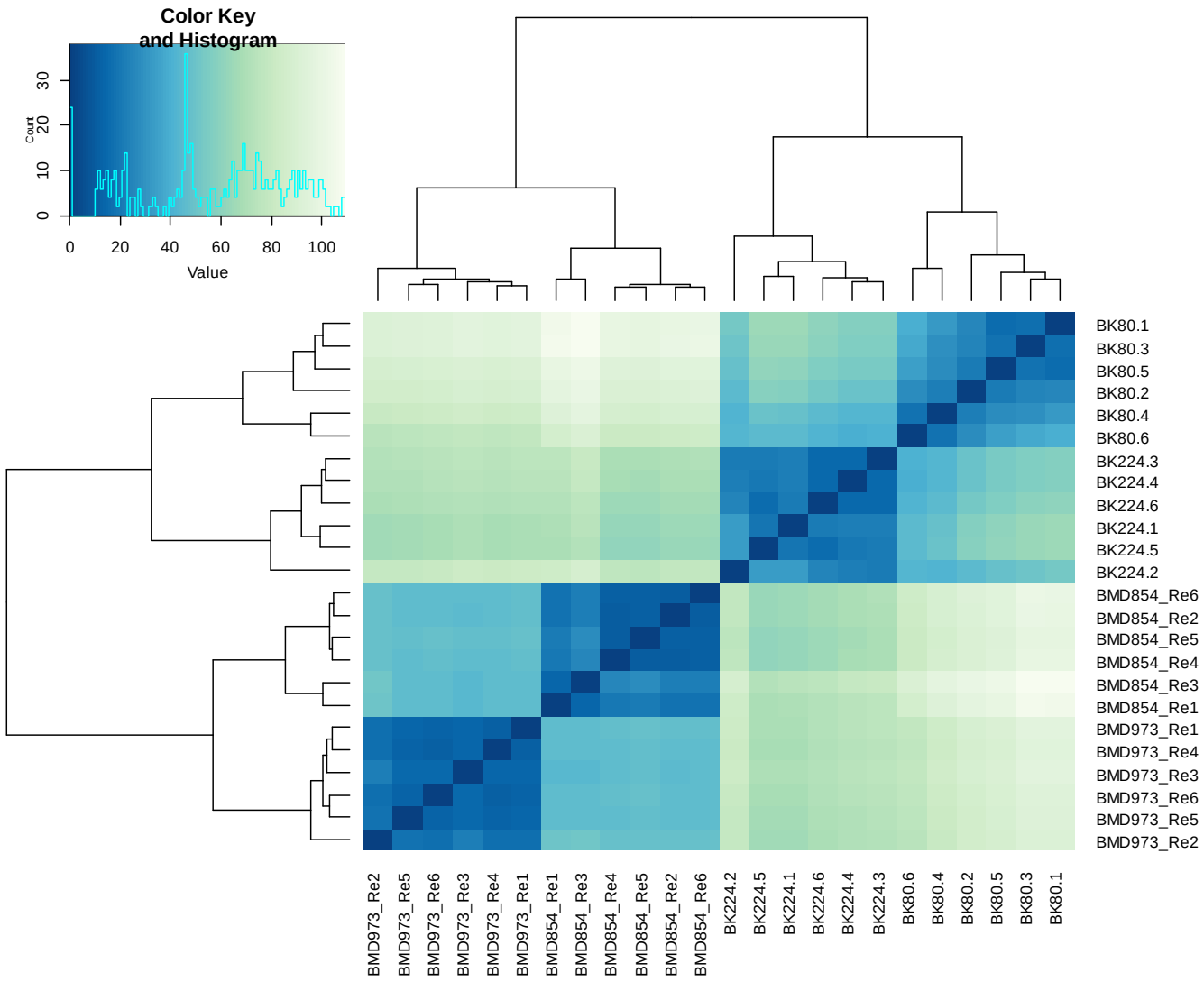

Figure 5.3-3. Sample-to-sample distance matrix from regularized-logarithm transformation (rld) of read counts.

Distance matrix-based dendrogram of all samples in the according to genotypes (ST4 (BK80 and BK224) and ST5 (BMD854, BMD973) indicates good technical reproducibility across all biological replicates. Color intensity (from blue to light green) indicates increasing number of read counts. No outliers were detected.

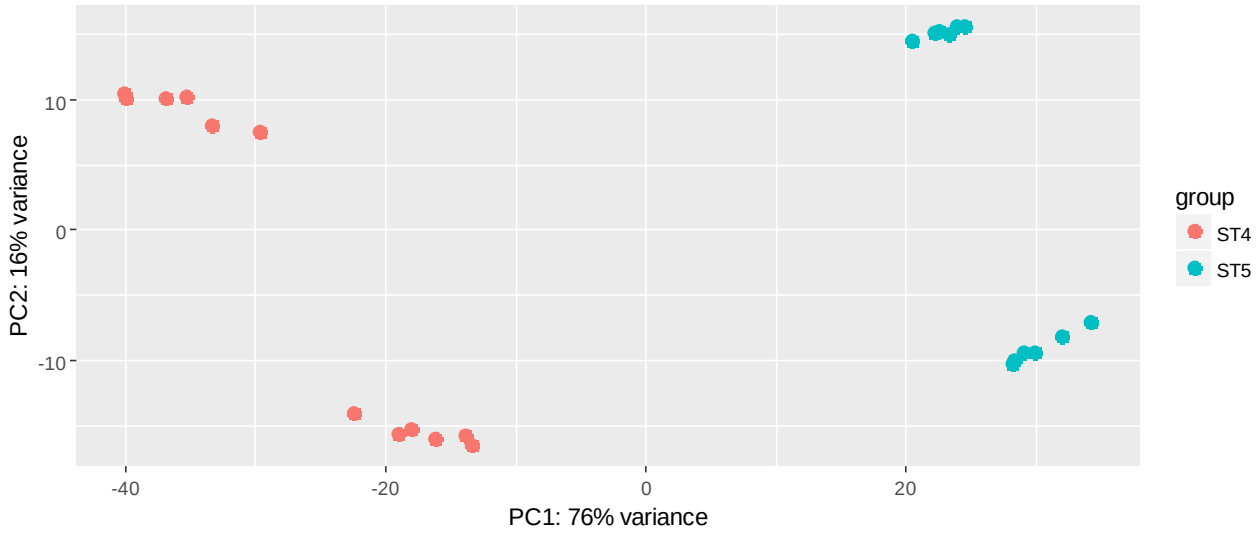

Figure 5.3-4. Samples clustering using Principle Component Analysis (PCA).

PCA analysis using regularized-logarithm transformation (rld) of read counts suggests that high degree of variation in the dataset was primarily attributed to difference in genotypes, not technical variation in sequencing or intra-genotype variation.

Euclidean distances between samples were calculated from regularized-logarithm transformation of counts per genes to avoid noises caused by a few highly variable genes, as well as providing a roughly equal contribution from all genes (**Figure 5.3-3**) [408]. Clustering of samples and respective replicates, as in **Figure 5.3-3**, agreed with the experimental design (ST4 vs ST5) since all samples were clustered with respect to their sequence type (ST5: BMD854, BMD973; ST4: BK80, BK224). Principle Component Analysis (PCA) revealed that most observed variation in the dataset was due to the difference in genotypes, indicated by PC1 (76% variance). Intra-group variation only accounted for 16% of all variance in the dataset. All biological replicates for each strain also closely clustered,

indicating good and robust sequencing efficiency. No outliers were detected in the dataset using either distance matrix or PCA clustering.

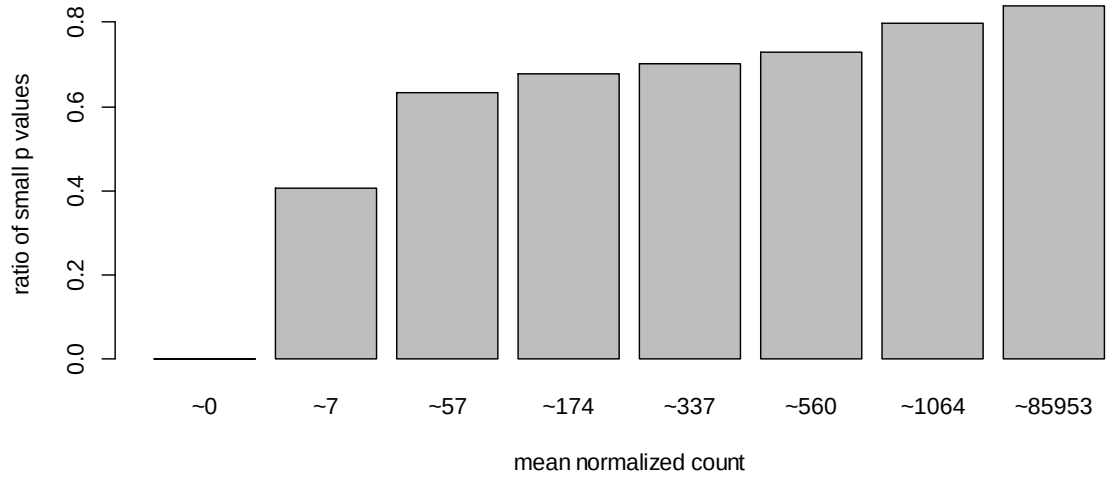

Figure 5.3-5. The ratio of small p values (p<0.01) for genes binned by mean normalized count.

Figure 5.3-5 demonstrates that genes with very low mean count have little or no power, and should be excluded from further testing. However it is also shown that a number of genes with ~7 normalized counts (i.e. weakly expressed) accounted for a considerable number of unadjusted small values. While these genes would be tested insignificant, they would potentially affect multiple testing robustness.

5.3.2.2. Determining False Discovery Rate (FDR) cutoff

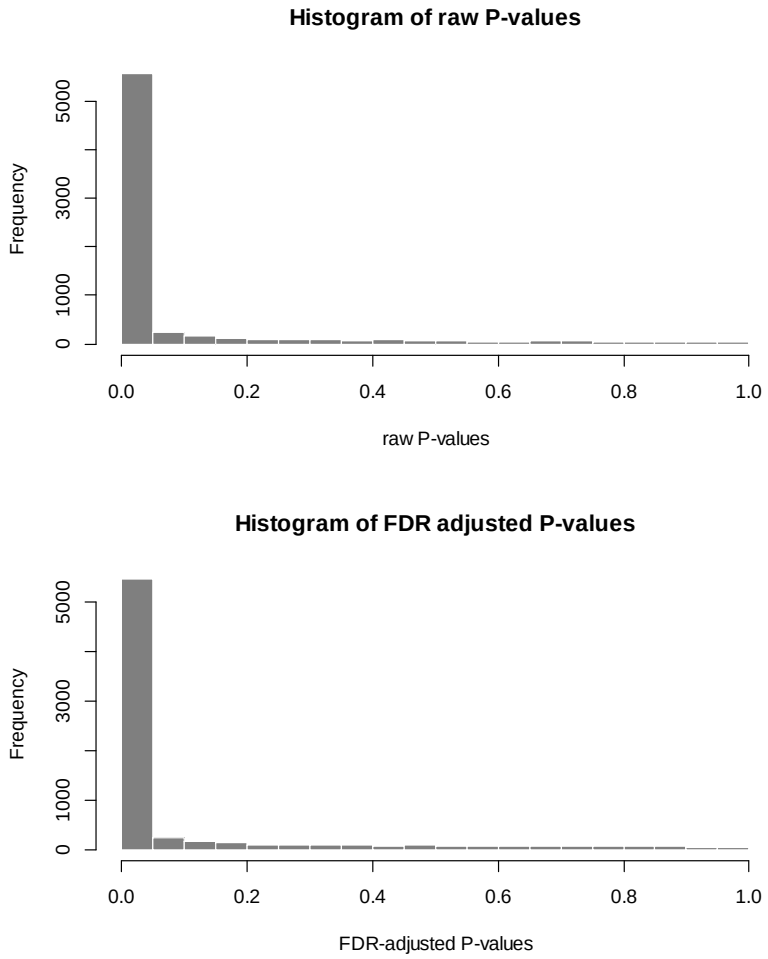

Figure 5.3-6.Histogram of p-values and q-values at FDR=0.1 for all expressed genes (Deseq2 mean normalized counts ≥1).

Highly left-skewed histograms of p-values indicate extremely high power for detecting differentially expressed genes at the expense of increasing false discovery rates.

At the default FDR of 10%, more than 6000 differentially expressed genes (DEGs) were detected out of 8001 genes with at least 10 normalized counts assigned. As seen in **Figure 5.3-6**, the histograms of raw p-values, including FDR-adjusted p-values, are highly left-skewed, which possibly indicates a high rate of false positive discovery. We had a high number of biological replicates for each condition (i.e. 12 replicates per genotype), resulting in very high power to detect differentially expressed genes; however, this also increases the potential false discovery rate. Therefore, I needed to use a more stringent FDR cutoff to minimize the risk of false positive discoveries. I used an empirical method for the determination of p-value and FDR threshold with the *qvalue* package implemented in R.

Using unadjusted p-values from a Wald test in Deseq2 as input, an estimation of the proportion of true null hypotheses (π_0) in the current dataset was calculated (π_0=0.135). The estimated proportion of true alternatives in this case would be 1- π_0 (~ 0.865). A corresponding q-value for each p-value would then be calculated such that the q-value reflects the minimum FDR incurred when calling a test significant. For example, when calling all p-values ≤0.01 significant, a corresponding false discovery rate of 0.002 could be calculated. This false discovery rate is the equivalent of the maximum estimated q-value among all p-values ≤0.01.

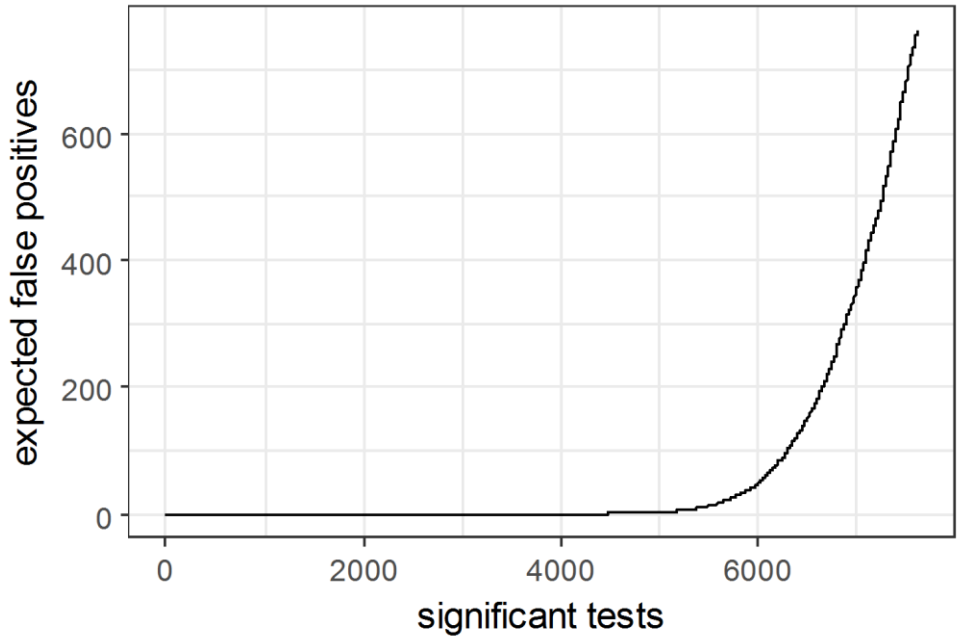

Figure 5.3-7. Simulation of false discovery rates using the qvalue package.

Figure 5.3-7 demonstrates the relationship between the numbers of DEGs meeting statistical significance and the corresponding estimated false discovery rates. It can be observed that the number of false discoveries starts to rise as the number of DEGs exceeds 5000. The number of resulting DEGs and corresponding p-values, q-values and local FDR at various significant cutoffs are summarized in **Table 5.3-2**. In order to minimize the number of false positive discoveries, I chose a local FDR cut off of 0.01. At local FDR<0.01 (i.e. less than 10 false positives per 1000 DEGs), 5036 genes were identified as significant DEGs. I chose an arbitrary level of biological significance of

difference in gene expression of log2FC±1 (i.e 2 fold up or regulation in gene expression). In other words, a gene would only be considered differentially expressed under a test condition when it was up or down-regulated at least two fold. Using these criteria, I identified 704 up-regulated (ST5 vs ST4) DEGs and 1362 down-regulated DEGs (ST5 vs ST4). I considered the remaining statistically significant DEGs to have little to no biological relevance due to the small degree of fold change in expression.

Table 5.3-2. Cumulative number of DEGs at different significant threshold of p-value, q-value and local FDR (generated from qvalue package)

	<0	**<10^{-8}**	**<0.00001**	**<0.0001**	**<0.001**	**<0.01**	**<0.025**	**<0.05**	**<0.1**	**<1**
For p-value	0	3193	4034	4401	4852	**5466**	5758	6046	6330	8001
For q-value	0	3322	4253	4670	5251	**6087**	6548	6994	7661	8001
For lcFDR	0	0	3799	4095	4492	**5036**	5341	5605	5901	8001

$\pi_{0=}$ 0.135 (proportion of true null p-values)
lcFDR is a Bayesian derived quantity measuring the probability that a significant test is a true null hypothesis (similar to adjusted p-values)

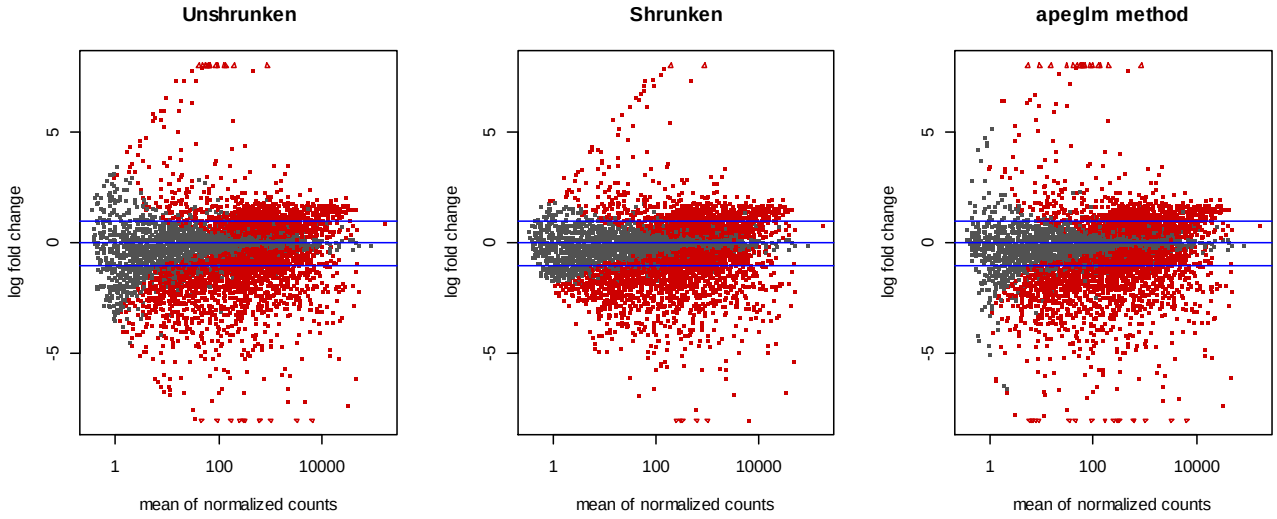

Figure 5.3-8. MA plots showing the log2 fold changes attributable to a given variable over the mean of normalized counts for all the samples in the Deseq2 dataset in 2 different log2 Fold Change (log2FC) shrinkage methods (normal prior and apeglm).

Points will be colored red if the adjusted p value is less than 0.01. Points which fall out of the window (i.e. off the scale) are plotted as triangles. Blue lines indicate log2 fold changes at -1 or 1.

Figure 5.3-8 illustrates the process of log2FoldChange shrinkage implemented in Deseq2. The shrinkage method identifies the largest fold changes that are not due to low counts and uses these to inform a prior distribution. This way the large fold changes from genes with lots of statistical information are not shrunk, while the imprecise fold changes are shrunk. This allows comparison of all estimated fold changes across experiments, for example, which is not really feasible without the use of a prior. Since genotype-specific genes would be expected to be highly expressed, the default *normal prior* method would potentially over-shrink these. Therefore I elected to use the *apeglm* method, which takes into account the proportion of highly/over-expressed genes for log2FoldChange

shrinkage. **Figure 5.3-9** demonstrates clustering of significant DEGs from individual samples and genotypes using transformed Z-scores.

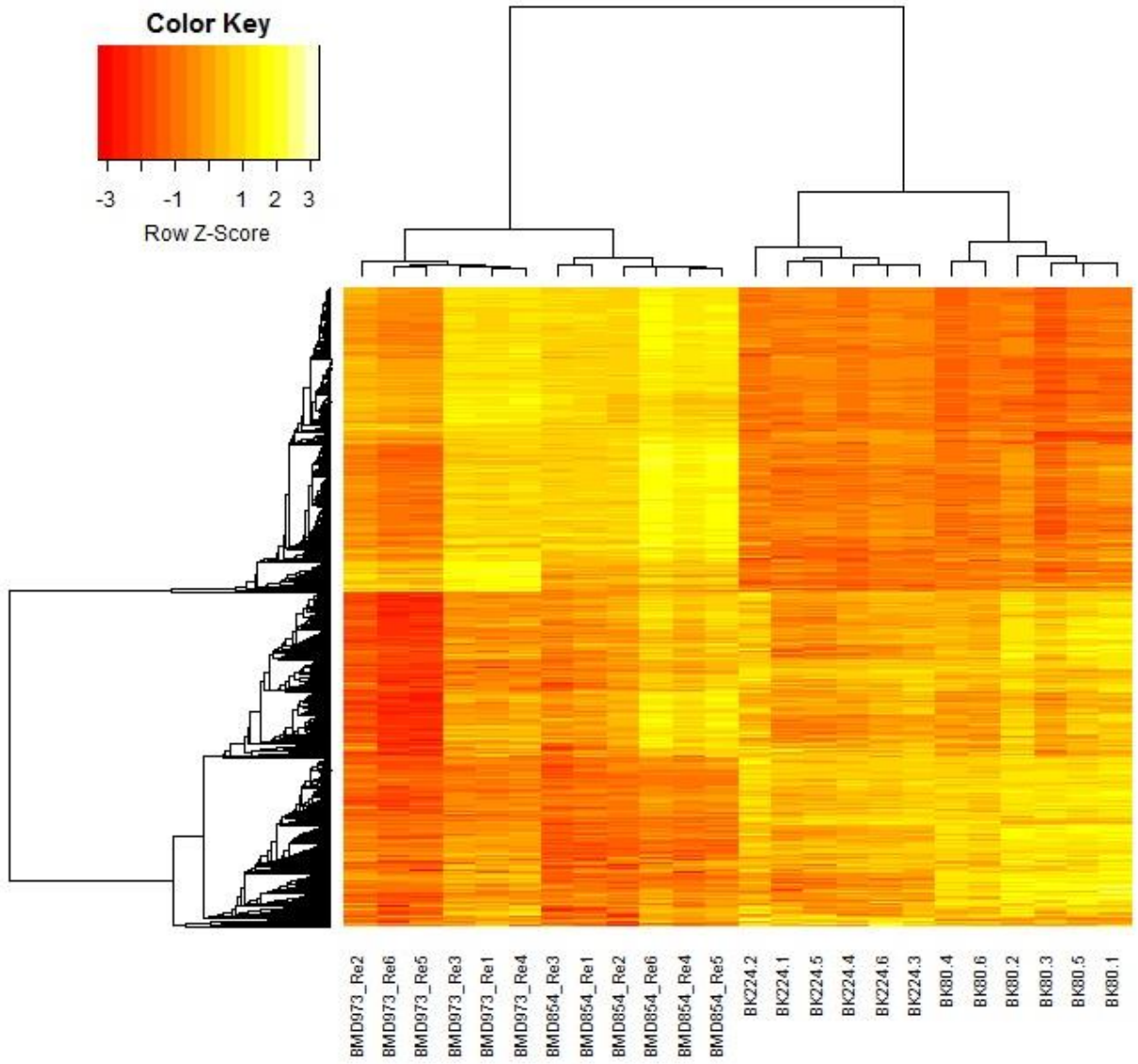

Figure 5.3-9. Heatmap of the genes declared significant with DESeq2.

Rows correspond to clusters of genes; columns correspond to individual samples. Heatmap intensity color corresponds to transformed Z-score (standard deviations away from the mean of expression of the reference). Higher Z-scores indicate higher expression of genes.

Table 5.3-3 summarizes the detailed components of detected DEGs. Overall 41% (n=2066) of the total number of detected DEGs (N=5036) were relevant DEGs (being at least 2 folds up or down regulated, n= 2066). Among the 2066 relevant DEGs, only 851 (41%) were annotated genes with known functions, the rest were either hypothetical proteins (n=787; 38%) or hypothetical RNAs with no coding capacity (n=428; 21%). More than 50% (n=2970) of the total number of detected DEGs (N=5036) were genes that were less than 2 fold up or down-regulated. While a small difference in fold expression of genes implies less biological relevance, these genes may have other unknown pleiotropic functions contributing to ST5-associated metabolism and virulence. Within the scope of this study, I have focused on the more relevant DEGs that are at least 2 fold differentially expressed.

Table 5.3-3. Summary of DEGs composition

	log2FC ≥ 1	**log2FC ≤ -1**	**0 < log2FC < 1 or -1 < log2FC <0**	**Total**
Annotated genes	474	377	1857	**2708**
Hypothetical proteins	169	618	1038	**1825**
Hypothetical RNAs	61	367	75	**503**
Total	**704**	**1362**	**2970**	**5036**

All DEGs were either up or down regulated in all ST5 strains tested compared to ST4 strains

5.3.2.3. GO terms enrichment analysis of annotated genes up-regulated in ST5

474 annotated DEGs that were up-regulated in ST5 were used as input for GO enrichment analysis over the total set of 8001 annotated genes in the H99 reference. All 3 main categories of Gene Ontology (Biological Processes, Molecular Functions and Cellular Components) were included in the analysis. The top 5 enriched biological processes associated with up-regulated genes in ST5 are presented in **Figure 5.3-10 .**

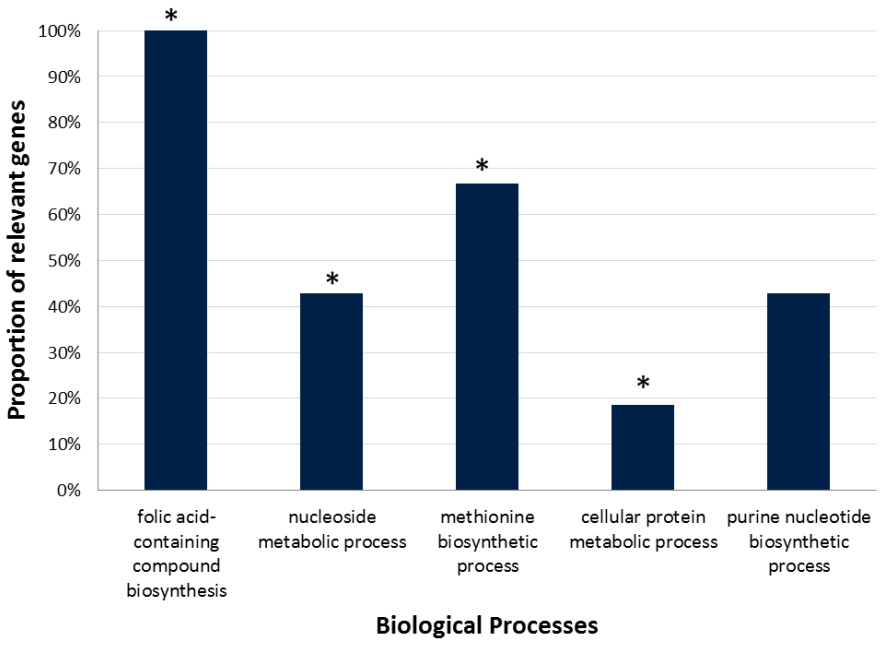

Figure 5.3-10. Top 5 highest ranked GO-Biological Processes associated with up-regulated DEGs in ST5.

The barplot describes the respective proportions of genes with relevant GO terms enriched in the input dataset. Asterisks indicate statistical significance by Fisher's Exact test in topGO (significance level α=0.05). Biological processes were ranked by Fisher's test significance (p-values in the order of most to least significant from left to right).

Table 5.3-4. Up-regulated genes associated with enriched Biological Processes

Biological process	Gene ID	Product	Basemean ST4*	Basemean ST5*	Log2FC
Folic acid-containing compound biosynthesis (GO:0009396)	CNAG_06645	Methylenetetrahydrofolate dehydrogenase [NAD(+)]	460	1255	8.847
	CNAG_07746	methylenetetrahydrofolate dehydrogenase (NADP)	1521	4425	10.571
Nucleoside metabolic process (GO:0009116)	CNAG_02285	nucleoside diphosphate kinase	3181	10434	11.636
	CNAG_01390	adenine phosphoribosyltransferase	471	2277	8.883
	CNAG_02546	transferase	550	1447	9.107
	CNAG_02794	dihydroorotate dehydrogenase (fumarate)	1565	2026	10.613
	CNAG_02853	amidophosphoribosyltransferase	1390	2345	10.442
	CNAG_04577	nucleoside-diphosphate kinase	2203	2713	11.106
	CNAG_04961	orotidine-5'-phosphate decarboxylase	827	1151	9.694
Methionine biosynthetic process (GO:0009086)	CNAG_00256	aspartate-semialdehyde dehydrogenase	1177	2378	10.202
	CNAG_02686	cystathionine beta-lyase	1503	1716	10.555
	CNAG_03898	phosphoadenosine phosphosulfate reductase	229	697	7.847
Cellular protein metabolic process (GO:0044267)	CNAG_01148	peptidyl-prolyl cis-trans isomerase	1382	6270	10.434
	CNAG_00058	T-complex protein 1 subunit epsilon	1717	3396	10.746
	CNAG_00252	transcription elongation factor B	119	83	6.912
	CNAG_00829	E3 ubiquitin ligase complex SCF subunit sconC	1435	1666	10.488
	CNAG_01209	1-phosphatidylinositol-3-phosphate 5-kinase	615	419	9.267
	CNAG_01522	phenylalanine-tRNA ligase	580	1090	9.181
	CNAG_02471	hypothetical protein	212	338	7.734
	CNAG_02710	T-complex protein 1 subunit gamma	2141	4195	11.065
	CNAG_00447	T-complex protein 1 subunit beta	1909	4212	10.899
	CNAG_02736	T-complex protein 1 subunit theta	1835	3893	10.842
	CNAG_03459	T-complex protein 1 subunit delta	1673	3620	10.709
	CNAG_04304	T-complex protein 1 subunit zeta	2714	7049	11.407
	CNAG_03188	histone-lysine N-methyltransferase, H3 lysine-36 specific	411	652	8.685
	CNAG_03891	hsp60-like protein	8664	17468	13.081
	CNAG_04822	deoxyhypusine synthase	183	306	7.523
	CNAG_04958	ubiquitin fusion degradation protein 1	926	766	9.857
	CNAG_04997	cytoplasmic protein	259	375	8.023
	CNAG_05195	ubiquitin-conjugation factor E4 B	1473	1111	10.525
	CNAG_06174	PEK/GCN2 protein kinase	545	786	9.092
	CNAG_06782	putative alpha-1,2-mannosyltransferase	850	591	9.733
	CNAG_07346	T-complex protein 1 subunit eta	2159	3896	11.077
	CNAG_00873	hypothetical protein	1205	441	10.236

(*) Basemean is the mean of normalized counts of all samples, normalizing for sequencing depth

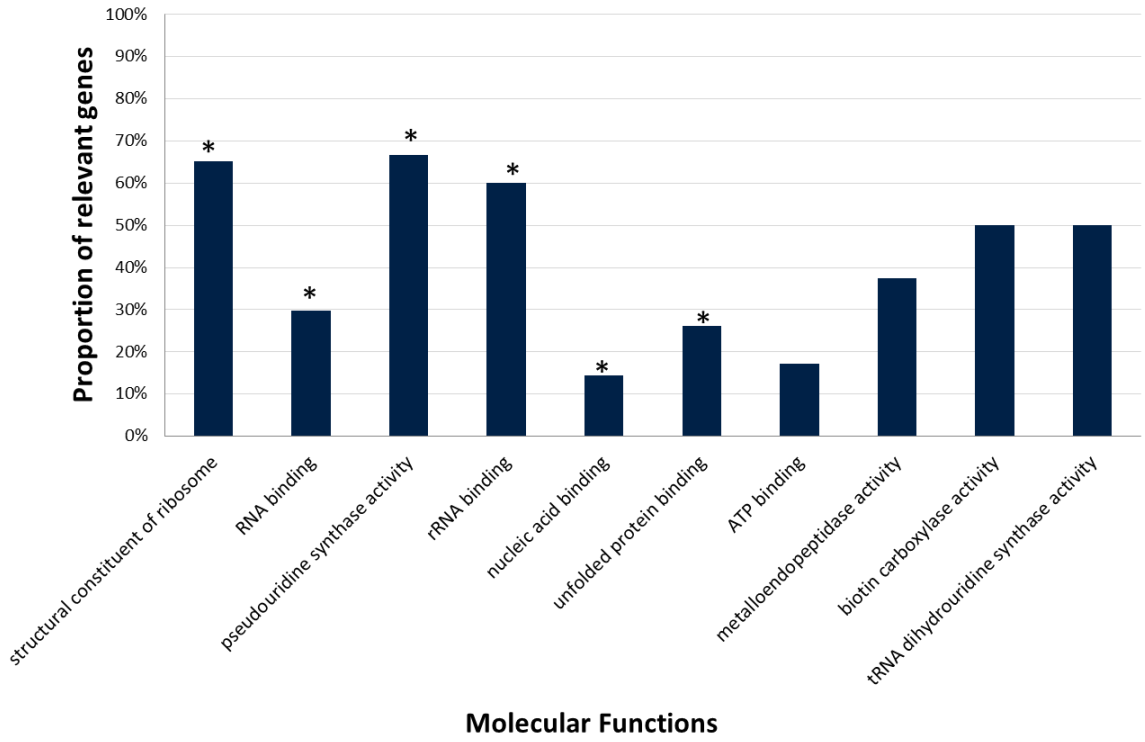

Figure 5.3-11. Top 10 highest ranked GO-Molecular Functions associated with up-regulated DEGs in ST5.

Barplot describes the respective proportions of genes with relevant GO terms enriched in the input dataset. GO terms were ranked by Fisher's test significance. P-values were in the order of most to least significant from left to right. Asterisks indicate statistical significance by Fisher's Exact test.

The four most significantly enriched GO Biological Processes included biosynthesis of folic acid-containing compound (GO:0009396, *p*=0.007), nucleoside metabolism (GO:0009116, *p*=0.02), methionine biosynthesis (GO:0009086, *p*=0.02) and general cellular protein metabolism (GO:0044267, *p*=0.03). Purine nucleotide biosynthesis process was not significantly enriched (*p*=0.08). Over-represented GO terms related to molecular functions among up-regulated ST5 DEGs were summarized in **Figure 5.3-11**. These

included: structural constituent of ribosome (GO:0003735 p<0.0001), RNA binding (GO:0003723, *p*=0.0007), pseudouridine synthase activity (GO:0009982 *p*=0.002), rRNA binding (GO:0019843, *p*=0.01), nucleic acid binding (GO:0003676, *p*=0.03) and unfolded protein binding (GO:0051082, *p*=0.05). The remaining 4 functions were not significantly enriched (*p*>0.05).

5.3.2.4. Virulence-associated DEGs in ST5

Two main groups of DEGs of particular interest were transcription factors and kinases which form complex regulatory networks and signaling cascades that govern many essential aspects of cryptococcal growth and virulence. Here I detected 29 proteins with known transcription regulation activities that were differentially expressed (**Table 5.3-5)**. These included 8 up-regulated and 20 down-regulated transcription factors in ST5. These factors and their targets have previously been identified as being able to positively/negatively regulate various virulence-associated phenotypes of *C. neoformans* [216].

Table 5.3-6 summarizes 27 detected kinases that were differentially expressed in ST5 and ST4 strains. For ST5 these include 14 up-regulated and 13 down-regulated kinases.

Table 5.3-5. DEGs that were identified as Transcription factors

No	Gene ID	Transcription Factor name	Basemean ST4*	Basemean ST5*	log2FC
1	CNAG_06871	FZC41	4	931	7.762
2	CNAG_04837	MLN1	22	102	2.012
3	CNAG_01626	ADA2	276	783	1.503
4	CNAG_05436	putative transcription factor	27	70	1.358
5	CNAG_05311	putative transcription factor	1352	2966	1.130
6	CNAG_03018	ASG101	201	432	1.098
7	CNAG_01438	MBS2	386	803	1.053
8	CNAG_04345	ARO8001	296	617	1.040
9	CNAG_05861	FKH101	175	78	-1.165
10	CNAG_02516	HLH5	99	43	-1.198
11	CNAG_00505	FZC28	219	90	-1.263
12	CNAG_05186	GRF1	325	133	-1.265
13	CNAG_04036	HSF3	98	39	-1.292
14	CNAG_01551	GAT201	417	157	-1.396
15	CNAG_04630	YAP2	4438	1521	-1.516
16	CNAG_04807	FZC8	1058	343	-1.579
17	CNAG_04804	SRE1	1670	547	-1.606
18	CNAG_06762	GAT204	571	183	-1.641
19	CNAG_03132	FZC5	31	9	-1.767
20	CNAG_01883	GAT8	23	7	-1.794
22	CNAG_01841	GLN3	74	20	-1.874
23	CNAG_06097	putative transcription factor	1021	241	-2.005
24	CNAG_00883	putative transcription factor	1033	251	-2.028
25	CNAG_00332	SIP4	390	93	-2.036
26	CNAG_00039	ZFC6	931	220	-2.058
27	CNAG_04457	FZC30	120	17	-2.426
28	CNAG_00871	CLR3	127	17	-2.870
29	CNAG_00791	HLH1	570	65	-3.061

(*) Basemean is the mean of normalized counts of all samples, normalizing for sequencing depth

Table 5.3-6. Annotated kinases that were differentially expressed

No.	Gene ID	Product	Gene Name	Basemean ST4*	Basemean ST5*	Log2FC
1	CNAG_04007	septin ring protein	N/A	1	32	4.613
2	CNAG_04927	hypothetical protein	YFH701	3	23	2.969
3	CNAG_04217	phosphoenolpyruvate carboxykinase (ATP)	N/A	400	3442	3.075
4	CNAG_02285	nucleoside diphosphate kinase	N/A	3181	10434	1.700
5	CNAG_04230	hydroxyethylthiazole kinase	THI6	471	1532	1.662
6	CNAG_04347	aspartate kinase	N/A	1077	3429	1.617
7	CNAG_03592	phosphomethylpyrimidine kinase	THI20	691	2042	1.555
8	CNAG_01364	guanylate kinase	N/A	622	1806	1.525
9	CNAG_06489	adenosine kinase	N/A	2147	5394	1.321
10	CNAG_01907	PLK/PLK1 protein kinase	N/A	258	676	1.302
11	CNAG_03167	CAMK/CAMKL/Chk1 protein kinase	CHK1	225	523	1.207
12	CNAG_01165	D-erythro-sphingosine kinase	LCB5	176	395	1.171
13	CNAG_05125	diphosphomevalonate decarboxylase	N/A	636	1406	1.137
14	CNAG_02847	thymidylate kinase	N/A	121	247	1.032
15	CNAG_05220	phosphatidylinositol 3-kinase	TLK1	108	49	-1.115
16	CNAG_00130	CAMK/CAMK1/CAMK1-RCK protein kinase	HRK1	8803	3812	-1.199
17	CNAG_02531	CMGC/MAPK protein kinase	CPK2	95	40	-1.259
18	CNAG_04755	STE/STE11/BCK1 protein kinase	BCK1	1993	797	-1.317
19	CNAG_02542	fructosamine kinase	IRK2	11179	4366	-1.330
20	CNAG_06432	acetate kinase	N/A	11377	4453	-1.338
21	CNAG_03355	hypothetical protein	TCO4	3881	1526	-1.342
22	CNAG_06632	Atypical/ABC1 protein kinase	ABC1	1459	558	-1.375
23	CNAG_06051	galactokinase	GAL1	826	291	-1.475
24	CNAG_06310	CAMK/CAMKL protein kinase	IRK7	226	71	-1.643
25	CNAG_02551	dihydroxyacetone kinase 1	DAK102	217	66	-1.690
26	CNAG_05104	CAMK protein kinase	FRK101	24	7	-1.778
27	CNAG_00454	hypothetical protein	N/A	316	43	-2.887

(*) Basemean is the mean of normalized counts of all samples, normalizing for sequencing depth

Transporters are among the most expressed genes in metabolically active yeasts. 16 transporters involved in trafficking and metabolism of different were up-regulated in ST5 **(Table 5.3-7).** At least five sugars transporters were detected (CNAG_05387, CNAG_04784, CNAG_01683, CNAG_05662 and CNAG_06963) and were likely involved in carbon utilization. Of note, CNAG_04217 (PCK1, phosphoenolpyruvate carboxykinase), one of the genes involved in regulation of gluconeogenesis, was highly up-regulated in ST5. PCK1 has previously been associated with fungal survival in the host lung due to the limited availability of glucose at that site [228].

Table 5.3-7. Annotated transporters up-regulated in ST5

No.	Gene ID	Product	Basemean ST4*	Basemean ST5*	log2FC
1	CNAG_07799	ABC transporter	333	871	1.349
2	CNAG_05387	galactose transporter	3139	8765	1.404
3	CNAG_06140	long-chain fatty acid transporter	1549	3891	1.324
4	CNAG_02361	MFS transporter, ACS family, pantothenate transporter	490	1193	1.262
5	CNAG_04784	monosaccharide transporter	31	637	4.058
6	CNAG_03910	myo-inositol transporter	342	2277	2.706
7	CNAG_06545	pim1 protein RNA transporter 2	741	1723	1.209
8	CNAG_01683	putative monosaccharide transporter	1894	9884	2.254
9	CNAG_01461	sodium/bile acid cotransporter 7-B/bile acid cotransporter 7-B	65	277	2.104
10	CNAG_01752	solute carrier family 25 (mitochondrial 2-oxodicarboxylate transporter), member 21	1356	3437	1.329
11	CNAG_01769	solute carrier family 25 (mitochondrial aspartate/glutamate transporter), member 12/13	681	1677	1.296
12	CNAG_02522	solute carrier family 25 (mitochondrial iron transporter), member 28/37	430	870	1.013
13	CNAG_02561	spermine transporter	190	440	1.160
14	CNAG_05662	polyol transporter protein 1 (ptp1)	197	2160	3.354
15	CNAG_06963	sugar transporter	994	2408	1.264
16	CNAG_04142	tartrate transporter	78	735	3.144

(*) Basemean is the mean of normalized counts of all samples, normalizing for sequencing depth

Table 5.3-8. DEGs involved in capsular polysaccharide and cell wall biosynthesis

No.	Gene ID	Product	Gene name	Basemean ST4*	Basemean ST5*	Log2FC
1	CNAG_07736	glucan endo-1,3-alpha-glucosidase agn1	Agn1	13	164	3.52
2	CNAG_00697	UDP-glucose 4-epimerase	Uge1	1119	3049	1.426
3	CNAG_04320	polysaccharide synthase Cps1p	Cps1	2604	1247	-1.046
4	CNAG_06016	alpha-1,3-mannosyltransferase	Cap6	980	454	-1.097
5	CNAG_01654	putative capsule structure designer protein	Cas34	494	195	-1.324
6	CNAG_00596	hypothetical protein	Utr2	115	39	-1.544
7	CNAG_02797	hypothetical protein	Cpl1	687	215	-1.642
8	CNAG_03644	capsule related protein	Cas3	52	10	-2.321
9	CNAG_04245	Chitinase CHI22	Chi22	4555	11590	1.282
10	CNAG_05818	CHS5 chitin synthase	Chs5	2452	898	-1.433
11	CNAG_01239	CDA3 chitin deacetylase	Cda3	3697	1273	-1.529
12	CNAG_05799	CDA1 chitin deacetylase	Cda1	15853	4655	-1.764
13	CNAG_00546	Chitin synthase 6	Chs4	1694	457	-1.877
14	CNAG_00897	SKN1 β-(1,6)-glucan synthase protein	Skn1	3069	485	-2.656
15	CNAG_06835	KRE61 β-(1,6)-glucan synthesis protein	Kre61	1425	110	-3.670

(*) Basemean is the mean of normalized counts of all samples, normalizing for sequencing depth

Differentially expressed genes previously known to be involved in biosynthesis of the polysaccharide capsule and cell wall of *C. neoformans* are showed in **Table 5.3-8.**

5.3.2.5. ST5-specific gene expression

Our group has identified genotype-specific genes were previously described from ST5 and non-ST5 *C. neoformans* var. *grubii* from Vietnam [325]. Their expression in ST5 is confirmed by this RNAseq experiment. They included 13 annotated genes, 22 hypothetical proteins and 4 hypothetical RNAs. (**Table 5.3-9** and **Table 5.3-10**).

Table 5.3-9. Expression of ST5-specific genes with annotated homologs in H99

No.	H99 Gene ID	Chr	Product	Basemean ST4	Basemean ST5
1	CNAG_00003	1	drug transporter	1	1742
2	CNAG_00005	1	TPR repeat-containing protein: carboxylic ester hydrolases	1	35
3	CNAG_03084	8	endoribonuclease L-PSP	1	32
4	CNAG_04007	2	septin ring protein	0	83
5	CNAG_04931	10	putative hexose transporter	0	113
6	CNAG_05991	12	glycosyl hydrolase family 88 variant	2	931
7	CNAG_06871	5	FZC41 transcription factor	0	122
8	CNAG_06872	5	5-oxoprolinase	0	135
9	CNAG_06873	5	5-oxoprolinase	0	190
10	CNAG_06874	5	HpcH/HpaI aldolase/citrate lyase family protein	1	71
11	CNAG_06875	5	allantoate permease	0	132
12	CNAG_06876	5	alpha-ketoglutarate-dependent taurine dioxygenase	0	394
13	CNAG_07651	6	DEAD-box ATP-dependent RNA helicase 26, variant	0	125

(*) Basemean is the mean of normalized counts of all samples, normalizing for sequencing depth

The identified ST5-specific genes included a DEAD- box ATP-dependent RNA helicase variant, a number of secreted enzymes, and several membrane transport proteins. Notably, 6 consecutive genes in the sub-telomeric region on chromosome 5 (>10kb) were detected (CNAG_06871 to CNAG_06876), including the transcription factor FZC41 (CNAG_06871) and adjacent genes encoding several proteases, dioxygenases and hydrolases.

Table 5.3-10. Expression of ST5-specific genes coding proteins with unknown functions

No.	H99 Gene ID	Chr	Product	Basemean ST4[$]	Basemean ST5[$]
1	CNAG_00001	1	hypothetical protein	3	35
2	CNAG_00002	1	hypothetical protein	0	18
3	CNAG_00004*	1	hypothetical protein: DNA binding, transcription regulator	0	276
4	CNAG_01349	5	hypothetical protein	3	70
5	CNAG_01901	11	hypothetical protein	1	16
6	CNAG_04932	4	hypothetical protein	0	61
7	CNAG_05331	4	hypothetical protein	0	38
8	CNAG_05911*	7	hypothetical protein: transmembrane, signal peptide, non-cytoplasmic	1	252
9	CNAG_05990*	12	hypothetical protein: transcription, DNA binding	0	176
10	CNAG_06307	13	hypothetical protein	2	36
11	CNAG_06521*	13	hypothetical protein: transmembrane transport	0	15
12	CNAG_06802	2	hypothetical protein	0	10
13	CNAG_06953	9	hypothetical protein	0	19
14	CNAG_07043	13	hypothetical protein	0	113
15	CNAG_07305	1	hypothetical protein	0	16
16	CNAG_07459	2	hypothetical protein	0	93
17	CNAG_07918	12	hypothetical protein	1	59
18	CNAG_07931*	13	hypothetical protein: transmembrane both cytoplasmic-non cytoplasmic	2	18
19	CNAG_07945*	13	hypothetical protein: disordered	0	12
20	CNAG_07946*	13	hypothetical protein: transmembrane both cytoplasmic + non cytoplasmic	2	22
21	CNAG_07990*	7	hypothetical protein: transmembrane, both cytoplasmic + non-cytoplasmic	8	373
22	CNAG_08001*	11	hypothetical protein: disordered, transmembrane	0	11
23	CNAG_12000	1	hypothetical RNA	0	30
24	CNAG_12212	3	hypothetical RNA	0	43
25	CNAG_12408	5	hypothetical RNA	0	15
26	CNAG_13142	13	hypothetical RNA	0	98

** indicates hypothetical proteins with manually curated molecular functions/cellular location using InterPro Scan (https://www.ebi.ac.uk/interpro/search/sequence-search).*

[$] *Basemean is the mean of normalized counts of all samples, normalizing for sequencing depth*

5.4. Chapter 5 discussion

VNI-γ/ST5 and VNI-δ/non-ST5 are genetically distinct clusters of *C. neoformans* var. *grubii* from Vietnam with markedly different host immune type disposition [103,325]. A number of chromosomal rearrangements and genes insertions/disruptions previously associated with virulence and fungal adaptation were detected in both lineages (VNI-γ/ST5 and VNI-δ/non-ST5), suggesting different evolutionary histories and virulence potential [325]. Differences in gene expression are implicated as one of the mechanisms regulating cryptococcal virulence [198,409]. In this chapter I characterized and described differences in key metabolic processes between ST4 and ST5 by comparing their transcriptomes at log-phase growth in rich medium. The majority of cryptococcal virulence-associated genes and pathways are pleiotropic, which means they are involved in key aspects of cryptococcal growth/survival that ultimately contributed to virulence in a facultative host [324,409–411]. Therefore, understanding the underlying gene expression differences between *C. neoformans* var. *grubii* lineages with different abilities to infect hosts with different immune phenotypes can potentially reveal insights into the development of lineage-specific virulence potential, selection for survival in adverse environmental niches and ultimately colonization/infection of mammalian hosts.

5.4.1. Up-regulated DEGs in ST5 are involved in nitrogen metabolism and amino acid biosynthesis

A search into GO term hierarchy revealed that biosynthesis of folic acid-containing compounds is associated with downstream nitrogen metabolism, biosynthesis of cellular cyclic/heterocyclic compounds and other important cellular cofactors/coenzymes. Nitrogen metabolism has been identified as an important factor governing cryptococcal virulence and survival in the environment [412]. Eight amino acid permeases were previously characterized in *C. neoformans* var. *grubii*, the regulatory mechanisms of which are similar to pathways that govern nitrogen and carbon source quality, amino acid availability in the extracellular environment and other nutritional starvation conditions in other fungi [413]. Amino acid permeases that were significantly up-regulated in Vietnamese ST5 *C. neoformans* var. *grubii* strains included: CNAG_01946 (allantoate permease, FC=3), CNAG_04276 (cytosine-purine permease), CNAG_04982 (putative cytosine-purine permease), CNAG_06875 (allantoate permease). Interestingly, contrary to *S. cerevisiae* which depended on amino acid scavenging from the environment, *C. neoformans* appeared to be more dependent upon amino acid biosynthesis than uptake [413]. As aforementioned, methionine biosynthesis was among the most significantly up-regulated amino acid biosynthesis process in ST5 strains. Whilst the methionine biosynthesis pathway is not particularly essential for normal growth of *C. neoformans*, mutants lacking methionine genes appeared attenuated in mice [414].

5.4.2. Roles of differentially expressed transcription factors

The signaling cascades governing the general biology and pathogenicity of *C. neoformans* have been subjects of extensive investigation over the past decades [198,409,415,416]. Repertoires of transcription factors are often the most divergent sets of signaling components in *C. neoformans* var. *grubii* [417]. A number of differentially expressed transcription factors were detected in ST5, likely involved in positive/negative regulation of gene expression.

The transcription factor FZC41, which was ST5-specific and was highly expressed, belongs to the family of Zn_2Cys_6 transcription factors specific for fungi [418,419]. Zn_2Cys_6 transcription factors are involved in regulation of growth, asexual development, conidia germination and pathogenicity in the rice blast fungus *Magnaporthe oryzae* [420]. Interestingly*, C. neoformans* var. *grubii* mutants lacking the FZC41 transcription factor were more susceptible to fludioxonil, a new fungicide that acts by inhibiting phosphorylation of glucose, which reduces mycelial growth rate in other filamentous fungi [418,421]. This suggests sugars assimilation and carbon metabolism as one of the regulation targets of FZC41. The facts that ST4 strains lack this whole >10 kb sub-telomeric DNA fragment on chromosome 5 could have been a result of chromosomal rearrangement during divergence of ST5 and ST4 from a most recent common ancestor. This is further supported by the finding that sub-telomeric regions in *C. neoformans*

encode numerous targets of selection across different lineages [422]. Previously cryptococcal sub-telomeric regions have been found to be heavily enriched with hexose transporters [124] as well as fungal transcription factors such as FZC20, FZC41, SIP402, and FZC22, the last of which has been shown to result in virulence attenuation in mice when deleted [418,422].

Another transcription factor highly up-regulated in ST5 is ADA2 (CNAG_01626). Increased expression of CNAG_01626 in H99 has been previously correlated with increased capsule size [224], consistent with the *in vitro* phenotype of capsular enlargement previously observed in ST5 isolates. ADA2Δ mutants displayed marked defects in sexual development, capsule formation, stress response, and virulence [216,224].

GAT201 (CNAG_01551) is a GATA family transcription factor reported to act as a positive regulator of capsule. Interestingly, there was significant overlap in the genes that are directly activated by ADA2 and those that are direct targets of GAT201, including the antiphagocytic genes BLP1 and GAT204 [418]. Since the SAGA complex typically works in concert with other transcription factors, this suggests that ADA2 may work with GAT201 to activate transcription. A proposed regulatory model for capsule size involving ADA2, GAT201 and other transcription factor is summarized in **Figure 5.4-1** (adapted from Ding et al., (2016) [423]. My current data, though incomplete, indicate different lineages of *C. neoformans* var. *grubii* from Vietnam (ST4 and ST5) utilize different set of regulatory

transcription factors/networks. Extensive characterization of these networks with regards to lineage-specific biological aspects and virulence would be required for a more complete picture of gene expression and regulation of transcription.

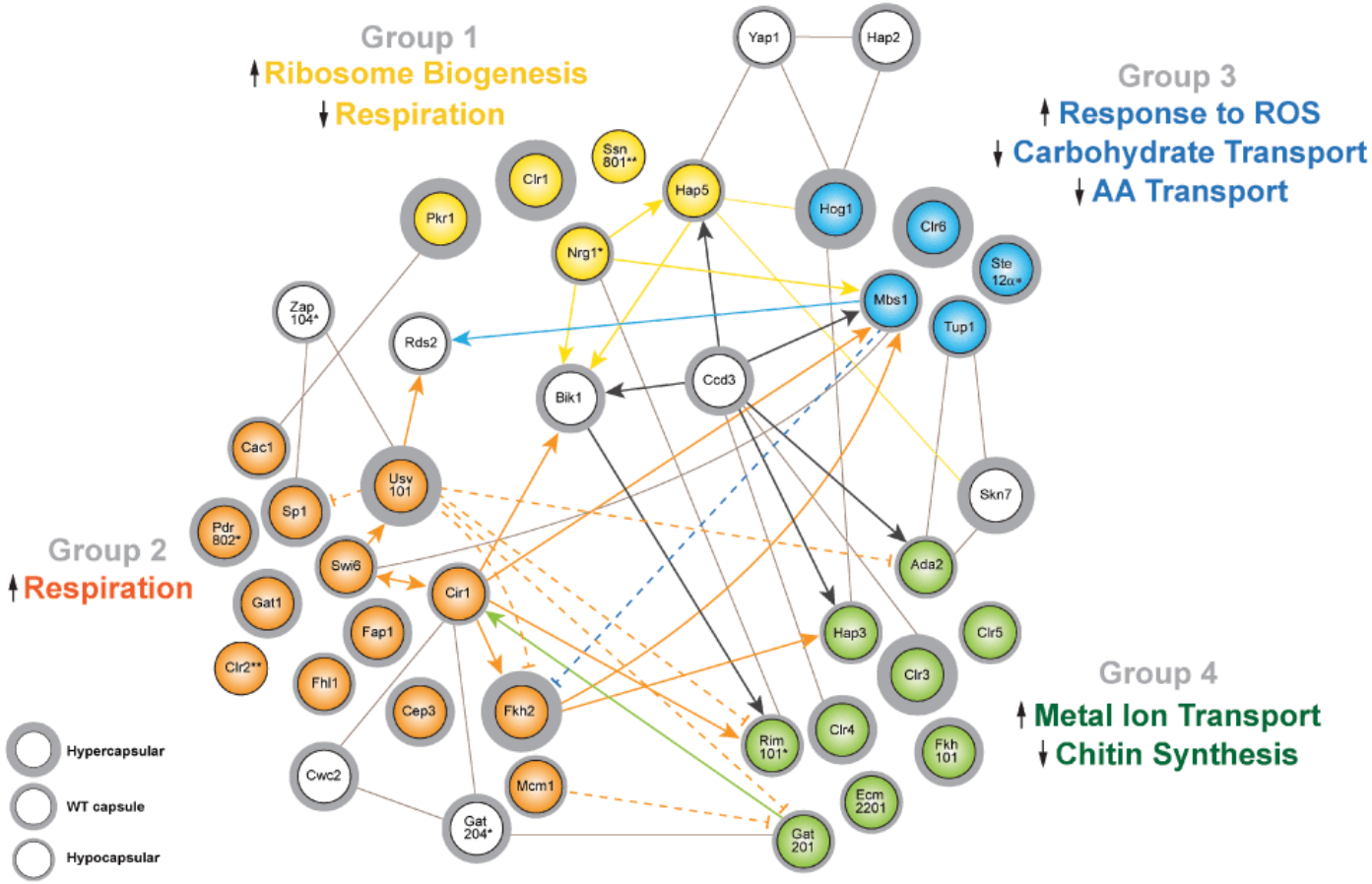

Figure 5.4-1. A network of transcription factors affecting capsule size in *Cryptococcus neoformans* (adapted from Ding *et al.*, (2016))[423].

5.4.3. Roles of differentially expressed kinases

Kinases have pivotal roles in growth, cell cycle control, differentiation, development, the stress response and many other cryptococcal cellular functions, affecting 30% of cellular proteins by phosphorylation [424]. The pathobiological networks of *C. neoformans* remains incomplete, mainly because functions of kinases which have a central role in key signaling and metabolic pathways, have not been fully characterized on a genome-wide scale.

Among pathogenicity-related kinases previously characterized, kinases involved in the cell cycle and growth control were identified most frequently. These include CDC7, MPS1, PIK1, CDC2801, MEC1, BUD32, and CKA1 [424]. These kinases didn't seem to be differentially expressed in my dataset, which should reflect the fact that ST4 and ST5 shared evolutionary conserved kinases functionalities.

Basal and stress-induced expressions of HRK1 are governed by the Hog1 MAPK. An unknown signaling component upstream of the Ssk2 MAPKKK, other than the Ssk1 response regulator, may trigger the Hog1 MAPK module (Ssk2-Pbs2-Hog1) in response to osmotic and oxidative stresses. Hrk1 is involved in intracellular glycerol synthesis upon fludioxonil treatment via the HOG pathway. However, Hrk1 appears to play several Hog1-independent roles. Independent of the HOG pathway modulating ergosterol biosynthesis, Hrk1 promotes susceptibility to polyene and azole drugs. Furthermore, Hrk1 is partly

involved in promoting resistance to oxidative damaging agents, such as diamide, and melanin biosynthesis, which is in stark contrast to Hog1. In conclusion, Hrk1 plays both Hog1-dependent and –independent roles in C. neoformans. A proposed network of kinases interaction and regulation target is summarized in **Figure 5.4-2** (adapted from Lee et al., (2016)) [424].

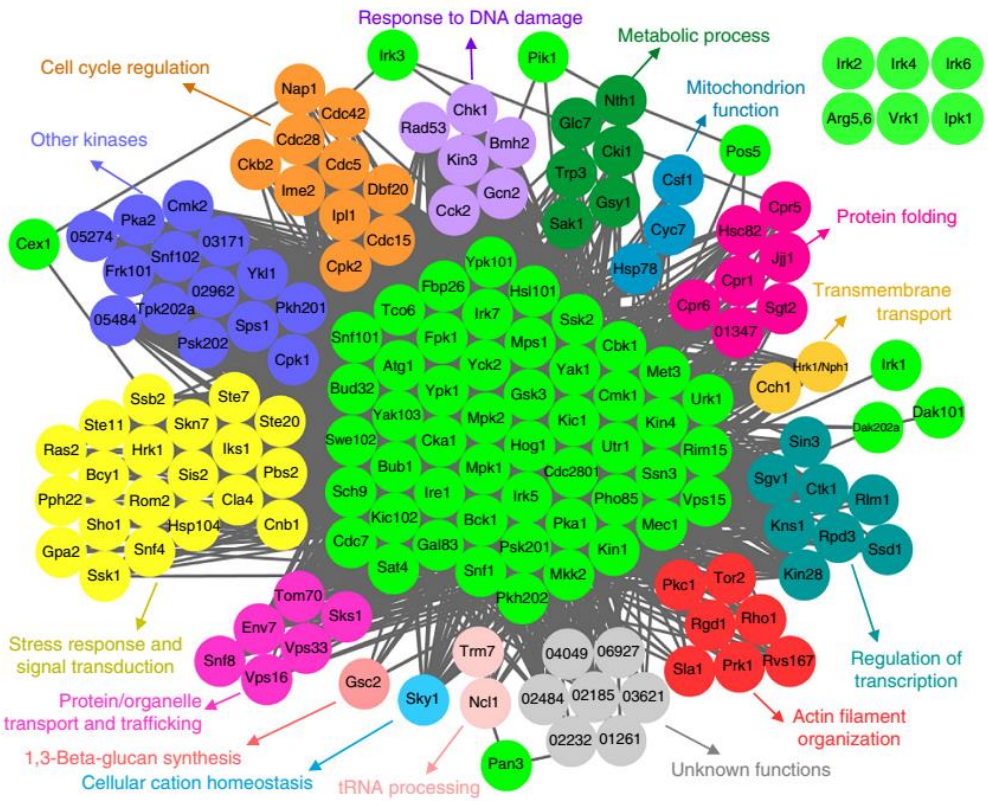

Figure 5.4-2. Network-based functional relationships among 63 pathogenicity-related kinases (adapted from Lee et al., (2016)) [424]**.**

5.4.4. The implicated roles of ST5-specific genes in virulence and adaptation

ST5 isolates possess a number of highly expressed, genotype-specific genes that were absent in ST4. These include a number of transporters, 5-oxoprolinases and a notable DEAD-box RNA helicase variant. Previously, 5-oxoprolinase was demonstrated to be required for conidiation, sexual reproduction, virulence and mycotoxin production of the phytopathogenic fungus *Fusarium graminearum* [420].

The 6 genotype-specific genes on Chromosome 5 were co-located and expressed in ST5 isolates. In fact, an intriguing aspect of co-regulated/co-expressed eukaryotic genes is that they tend to be syntenic and conserved across different taxa/genera, suggesting that they are functionally advantageous and were therefore favored by natural selection [425,426]. Furthermore, genes involved in the similar bio-chemical pathways tend to be clustered together in a number of eukaryotic genomes [427]. A correlation between gene proximity and regulation of gene expression is evident in the yeast genome [428]. For example, it was previously observed that expression of adjacent genes in *Saccharomyces cerevisiae* is frequently initiated in the same phase of the cell cycle [429]. Thus, insertions and deletions such as this in different lineages of *C. neoformans* may be related to natural selection for adaptation to one or more special environmental niches, which subsequently resulted in differential virulence potential in human hosts via a “by-stander-effect”.

The DEAD-box ATP-dependent RNA helicase (CNAG_07651), a truncated variant from the previously described DEAD-box helicase in H99 (VAD1) [430], was extremely highly expressed in ST5 isolates from Vietnam, indicating an important role in metabolism and potential pleiotropic functions in ST5-associated virulence compared with ST4. Several studies have demonstrated that DEAD-box proteins are involved in essential signaling pathways that mediate host-pathogen interactions. For example, the putative DEAD-box helicase HelTc in the parasite *Trypanosoma cruzi* that causes Chagas disease in humans, is highly up-regulated at the infective-stage of trypomastigotes [431]. The role of the first DEAD-box helicase characterized in H99 involved sensing stresses within the host during initial infection, in-host responses for survival and regulating known virulence factors [430].

Expression of a septin ring protein (CNAG_04007) was also detected specifically for ST5. There is evidence that septins in *C. neoformans* are essential for the proper development of the dikaryotic post-mating hyphae, and hyphae resulting from monokaryotic fruiting. Specifically, septins are needed for the formation of spore chains, fusion of clamp cells, and proper nuclear distribution within hyphae. In addition, septins were found to contribute directly to virulence of *C. neoformans* by being essential for the survival of the yeast cells within the host, or indirectly by being necessary for the production of spores, the presumed infectious propagules [432]. The latter may therefore be important in initiating infection in the mammalian host.

5.4.5. Hypothetical proteins and hypothetical RNAs

Most hypothetical proteins specific for ST5 possess transmembrane domains, suggesting putative involvement in transmembrane transporting. Two hypothetical proteins had DNA-binding and transcription regulating domains (CNAG_00004 and CNAG_05990), indicating their roles as putative transcription factors.

Among the 90 DEGs which were down-regulated more than 10 fold in ST5, most appeared to be genotype-specific (i.e. absent in ST4), as previously reported [325]. These included only 5 genes with annotated functions. The rest were hypothetical proteins (n=37) and hypothetical RNA (n=50). The extremely high number of hypothetical RNAs without protein coding capacity (ncRNAs) that appeared to be absent in ST5 might indicate a genotype-specific difference in ncRNA-associated transcription regulation. Most ncRNAs observed here are considered long non-coding RNAs (lncRNAs) based on their respective length (>200bp) [433]. Eukaryotic lncRNAs have a broad repertoire of regulating functions, including chromatin structure, telomere biology, subcellular structural organization as well as controlling expression of neighboring protein-coding genes [433,434]. In fact, four ncRNAs were among the ST5-specific up-regulated DEGs that appeared to be localized at the sub-telomeric regions. Specifically, except for CNAG_13142 (~485bp), the other three ncRNAs, including CNAG_12000 (~2kb), CNAG_12212 (~1kb) and CNAG_12408 (669bp), were located in the sub-telomeric regions

of 36kb from chromosome ends [18]). Since a specific class of ncRNAs in the telomeric region of *Saccharomyces cerevisiae* called "Telomeric Repeat associated cryptic ncRNAs" (TERRAs), was previously shown to be involved in controlling telomere length [435], it could be possible that these ST5-specific ncRNAs have similar roles in telomere biology. Furthermore, most functionally characterized lncRNAs in higher eukaryotes are involved in growth, development, and differentiation [436,437]. In fungi such as *Neurospora crassa* and *Aspergillus flavus*, natural antisense transcripts (NATs) and lncRNAs are found to be differentially expressed in response to specific stimuli that induce developmental changes [438,439]. ncRNAs were previously detected and characterized in *C. neoformans* var. *grubii* (H99) though their exact functions need further investigation [417]. The regulatory role of ncRNAs is demonstrated by the fact that they are mainly consist of the antisense of a coding gene or another ncRNA. For example, CNAG_12000 is antisense to the transporter CNAG_00005 on Chromosome 1, both of which are highly up-regulated in ST5 during log-phase YPD growth. While expression of CNAG_00005 could be due to other regulatory factors, it is possible that positive gene regulation through an antisense transcript is also involved, in addition to the more common negative gene regulation role of antisense RNAs. Another example is the highly overexpressed ncRNA CNAG_12019 on Chromosome 1, which was ST4-specific and was antisense to another ST4-specific and highly expressed hypothetical protein (CNAG_00128). The involvement of ncRNAs in regulating cryptococcal developmental changes has been reported, in which the ncRNA

acted as a critical morphologic switch between the yeast and hyphal form of *C. neoformans* var. *grubii* [440].

5.5. Chapter 5 Conclusion

Though closely related and morphologically similar, ST4 and ST5 *C. neoformans* var. *grubii* isolates from Vietnam with different host immune type disposition were previously shown to be genetically distinct. In this chapter I have identified and described differences in *in vitro* gene expression of key metabolic processes that are essential for growth and virulence of the two most prevailing genotypes among the *C. neoformans* var. *grubii* population from Vietnam. Future investigation of gene expression at the site of human infection would help validate current findings and provide more insight into cryptococcal pathogenesis.

Chapter 6

GENERAL DISCUSSION AND FUTURE DIRECTIONS

6.1. Introduction

The two sister species of *Cryptococcus*: *Cryptococcus neoformans*, commonly associated with disease in HIV-infected patients, and *Cryptococcus gattii*, now considered a primary human pathogen with a propensity to cause disease in apparently immunocompetent patients, are the main etiological agents responsible for the majority of cryptococcal meningitis cases globally. Intriguingly, paradoxical infection in apparently healthy, immunocompetent patients due to *C. neoformans* var. *grubii* is also reported, especially more significant from East/Southeast Asia than anywhere else. Why this variety of *C. neoformans,* traditionally considered an opportunistic pathogen in immunocompromised patients, is able to cause disease in individuals with no apparent immunosuppression in Vietnam is unclear and this thesis aimed to improve our understanding of this phenomenon.

A paradoxically higher prevalence of a subgroup of *C. neoformans* var. *grubii* yeasts in apparently immunocompetent hosts indicates has two potential explanations: either 1) increased virulence potential of the subgroup compared with other groups, or 2) an as yet unidentified host immune defect that confers increased susceptibility to the organism. In

this PhD thesis, I investigated the former hypothesis by systematically assessing the genetic composition, population structure, *in vitro* and *in vivo* virulence-associated phenotypes as well as comparative transcriptomics of *C. neoformans* var. *grubii* isolates from HIV-infected and HIV-uninfected patients in Vietnam. This is, to my knowledge, is one of the first studies to systematically tackle this issue. Findings from my study will help further the current understanding of cryptococcal disease and identify further areas for investigation.

6.2. Principal findings

1. The clinical population of *C. neoformans* var. *grubii* in Vietnam is an integrated part of the clonal Asian population, with ST4, ST5, ST6 and ST93 being the predominant genotypes.
2. AFLP-defined VNI-γ strains, which were almost entirely responsible for disease in immunocompetent patients, corresponded exactly with the single MLST sequence type: ST5; the VNI-δ cluster included a variety of different sequence types.
3. ST4/ST6 and ST5 belong to separate but closely related lineages of *C. neoformans* var. *grubii.*

4. The proportion of predominant genotypes (ST4, ST5, ST6 and ST93) changes in a geographical arc that runs South/Southwest and East/Northeast from Southeast Asia to East Asia.
5. The population structure of *C. neoformans* var. *grubii* in Vietnam is intermediate between populations from Southeast Asia and those from East Asia, and is remarkable for having more than a single dominant circulating lineage.
6. ST5 isolates tend to produce larger capsules compared to other strains when grown on capsule inducing agar and in *in vivo* models of infection. Further, they demonstrate increased heterogeneity in cell size.
7. Apart from capsular enlargement, ST5 isolates displayed similar key *in vitro* virulence-associated phenotypes with non-ST5s (i.e. melanization, urease, phospholipase, growth in *ex vivo* CSF, thermotolerance)
8. ST5 isolates induced significantly less morbidity and mortality in the murine (A/J) model of infection.
9. ST5 isolates induced significantly stronger TNF-α response at an earlier time point during murine (A/J) infection.
10. VNI-γ/ST5 strains, though appeared a genetically homogenous group, displayed remarkable heterogeneity in virulence-associated phenotypes, both *in vitro* and *in vivo*.

11. ST5 isolates from HIV-uninfected patients displayed significantly higher rates of growth inside macrophages than ST5 isolates from HIV infected patients, and from non-ST5 strains.
12. ST5s differed from ST4s in expression of key metabolic genes and processes essential for both growth/survival and virulence.

6.3. Insights into ST5 virulence potential and its implications in apparently immunocompetent hosts

The main objective of this study was to investigate whether the high prevalence of AFLP-defined VNI-γ *C. neoformans* var. *grubii* among HIV-uninfected patients in Vietnam was associated with previously identified *in vitro* and *in vivo* virulence factors. ST5 strains are closely related but genetically distinct from other STs; this must confer their unique ability to infect the immunocompetent and defines their pathogenic potential. However, my results revealed that the ability of VNI-γ *C. neoformans* var. *grubii* ST5 strains to infect and cause disease in apparently immunocompetent hosts is not necessarily associated with the capacity to cause greater in-host damage – despite stimulating an initial more robust inflammatory response, mice infected with ST5 strains had better survival than those infected with non-ST5 strains. This picture is mirrored by that seen in HIV infected patients, where the disease course resulting from ST5 infection does not appear to be more severe than that due to other sequence types . My results highlight the sheer

complexity of this ST5-related clinical phenotype. There are 3 important aspects to consider out of these findings:

First, the *in vivo* ST5-induced phenotype in A/J mice may reflect a later stage of cryptococcosis – i.e established disease rather than initial infection. Indeed, cryptococcal disease in humans is a long and complicated process that can be considered to consist of at least 6 different stages:

(1) Initial colonization of the exposed host;

(2) Establish localized infection in the lungs and other host tissues;

(3) Survival of the initial immune response and establishment of dormancy;

(4) Reactivation from dormancy;

(5) Dissemination to other host tissues including breaching the Blood-Brain-Barrier

(6) Proliferation in the CSF.

The mouse model aims to simulate and provide a brief description of cryptococcal pathogenesis through all stages, from colonization to dissemination and CSF proliferation. It necessarily involves administration of a large, concentrated infecting inoculum, which likely poorly represents what happens in nature. Moreover, it is a model of disseminated infection rather than predominant brain disease. As mentioned previously, the between lineage differences I observed somewhat model the pattern of disease seen in HIV

infected adults. Consistent with this, the immune response I observed in the A/J mice model (which is technically moderately immunocompromised due to an impaired complement response), reflected that of the later stages of HIV-infected patients with cryptococcal meningitis [386]. The lack of clear lineage specific differences in disease phenotype seen in both HIV patients and mice raises the question of whether ST5 has an advantage compared with other lineages at the earlier stages of infection, including initial host immune response evasion and establishing latency. This idea is supported by results from my macrophage model, which is a simulation of interaction with the host innate immunity. Here, I found that the ST5 isolates have increased macrophage parasitism capacity, evidence by their high intracellular proliferation rates. Furthermore, works parallel to this thesis within OUCRU have shown that ST5 strains from HIV-uninfected patients induce higher mortality in the *Galleria* model (the greater wax-moth). The *Galleria* model is another model of innate immunity.

Second, phenotypic heterogeneity observed in ST5 is potentially an evolutionary advantage. In Chapter 3 I found that ST5 strains, seemingly a genetically homogeneous phylogeny group, display marked intra-genotype variation in a number of *in vitro* and *in vivo* virulence-associated phenotypes, when compared to non-ST5 strains. Indeed, it has been demonstrated that population heterogeneity is positively related to survival of different fungi species in adverse environmental conditions [441]. From an evolutionary perspective phenotypic heterogeneity is an advantageous trait when populations face a

chronic selection pressure [442]. The results from this interaction dictate evolutionary trajectories at the genomic level and facilitate evolutionary rescue from deteriorating environmental niches [442]. It is intriguing to recall results from our previous WGS study comparing VNI-γ and VNI-δ strains in which we detected a number of VNI-γ-specific genes which appeared to be clustered at the sub-telomeric regions [325]. My RNAseq data confirmed that these genes were expressed at high levels in ST5 strains at log-phase growth in YPD but were altogether absent in ST4 strains. Chow *et al.,* (2012) reported that genes in the telomere and sub-telomere regions are linked to fungal adaptation to environmental stresses [124]; Desjardins *et al*., (2017) demonstrated that the genes in the sub-telomeric regions of VNI *C. neoformans* var. *grubii* are under significantly higher selection pressure than in the VNII or VNB lineages [90]. This observation suggests that strains from the ST5 lineage could occupy diverse and potentially adverse environmental niches, resulting in an increased likelihood of selection of strains with enhanced "virulence potential", enabling infection in immunocompetent hosts (possibly through a "by-stander" mode of action). Given that most virulence genes in *Cryptococcus* also have other pleiotropic functions, it is likely that polyploidy of such genes and pathways might actively confer to cryptococcal virulence [90].

Third, higher rates of ST5-associated disease in immunocompetent, HIV-uninfected patients may not be associated with higher in-host damage but rather better host colonization. This idea is supported by several lines of evidence:

(i) ST5 strains in my study responded better to *in vitro* capsular enlargement signals, which could potentially lead to increased sporulation as capsule biosynthesis genes are required for both efficient sexual development, spore formation and dispersal [443]. Increased number of ST5-spores at a given time means higher exposure rate to exposed and (potentially) immunocompetent hosts. Higher frequency of ST5-specific infectious propagules with better capacity to colonize and establish infection in such hosts would result in higher prevalence of ST5-related infection;

(ii) My *in vitro* macrophage model results, and works parallel to this thesis, suggest that ST5 strains seemed to be better at coping with host innate immunity at early stages of infection and dissemination. This is an interesting hypothesis that needs further investigation. Specifically, future works addressing this hypothesis should shift focus to other aspects of cryptococcal virulence not thoroughly investigated in this thesis, including: same sex mating (given the facts that all our strains were MATα) and sporulation capacity, spore virulence compared to the yeast form.

Fourth, an as-yet identified host immune defect specific for the East Asian lineage that confers increased susceptibility to cryptococcosis remains possible. The fact that the majority of reported cases of *C. neoformans* var. *grubii* infection in apparently immunocompetent, HIV-uninfected patients were reported from Southeast/East Asia raised the question of whether this lineage of human host possesses unique immune defects that are associated with increased susceptibility to infection by *C. neoformans*

var. *grubii.* For instance, IgM-producing B-cell deficiency and adult onset autoantibodies to IFN-γ and GM-CSF have been suggested as some of the possible non-HIV immunocompromising conditions associated with increased risk of acquiring active cryptococcosis [288,444,445]. However, this would not explain why it is only ST5 strains that cause disease in immunocompetent patients.

Ecological factors are implicated as the main driving forces for differential population structures in Vietnam and elsewhere in Asia

Another focus of this thesis was to study the genetic composition of the clinical *C. neoformans* var. *grubii* population in Vietnam and how it relates to other populations across the globe. Understanding the local population structure within a global context would potentially provide more insights into the origin and spread of specific lineages of interest. Populations from different countries with different geographical/ecological conditions across Asia shared a few similar predominant MLST genotypes (ST4, ST5, ST6 and ST93) albeit in different proportions. I detected a gradual change in the relative proportion of these 4 predominant STs in a South/Southwest Asia – East/Northeast Asia arc, from which the *C. neoformans* var. *grubii* population from Vietnam represents an intermediate. Ecological and human factors may have important roles in shaping the local and global cryptococcal populations. Climate and geography in Asia vary greatly, from the subtropical and tropical wet plains of Southeast Asia to the more temperate regions of

East Asia, presenting vastly different and diverse ecological niches. The different proportions of STs from each country/region, therefore, may suggest different fitness and adaptation of different STs to particular environmental niches. Human factors may not have an active role in determining population structures or dispersal of different lineages of *C. neoformans* var. *grubii*, given the fact that there is no human to human transmission of cryptococcosis. However, human activities such as irrigation, deforestation, domestication of feral pigeons and other unknown potential carriers of *Cryptococcus* may disrupt and alter traditional ecological niches of *Cryptococcus* species and may as well increase human exposure to pathogenic *C. neoformans* lineages.

6.4. ST174 as a putative most recent common ancestor of Asian *C. neoformans* var. *grubii* lineages

Maximum likelihood and goeBURST analysis suggested ST174 as the most parsimonious candidate for most recent common ancestor of all major lineages of *C. neoformans* var. *grubii* observed in Asia. ST174 and its close progenies accounted for the majority of isolates from the Middle East (Kuwait and Qatar) and South Asia (India). Interestingly, a recent study by Mathieu Vanhove and colleagues (2017) described an actively recombining cluster of VNI *C. neoformans* var. *grubii* which included a mixture of strains from Africa and India [89]. The high genetic diversity and the lack of population differentiation between this cluster and other VNI clusters could indicate that worldwide

dissemination of VNI isolates might have originate from this cluster [89]. Currently it is not known whether ST174 is related to the cluster identified in Vanhove's study. In fact, though current data suggest an "out of Africa" mode of global expansion for *C. neoformans* VNI, it is unlikely that the population in Vietnam and Asia arose from single African ancestral type but rather through various intermediate common ancestors. In essence, ST174 is potentially one of such ancestral types. Future works involving whole genome sequencing of a larger number of environmental and clinical isolates from different regions may shed more light into the complex evolutionary history of *C. neoformans* and the rise of pathogenic lineages.

6.5. Future works

This thesis has provided me with a number of possible avenues which I could explore in the future. The most important that I would be interested to take forward are:

1. **Systematic assessment of *in vitro* virulence-associated phenotypes for a larger collection of *C. neoformans* var. *grubii* isolates from Vietnam and elsewhere.**

I would be interested to understand the variability in phenotypes in the ST5 and non-ST5 strains with more precision, to ensure that the heterogeneity I saw in ST5 strains, particularly in the mouse model, is real. This would involve passaging a large number of clinical strains through these models.

2. **Investigate *C. neoformans* var. *grubii* interaction with the host at different stages of infection using different models of infection.**

The major problem with the mouse model is the mode of infection, which is likely unrealistic. Infection is believed to occur through inhalation of infectious propagules – either yeasts or spores. Aerobiology facilities, such as those at Duke University Medical College, would enable a more realistic mode if infection to be assessed by lineage, including different types of propagule. In addition, I would be interested to test the 'dose' of each lineage which can effectively establish infection. Furthermore, I would also like to investigate the interaction of different lineages of *C. neoformans* with epithelial cells (pulmonary alveolar cells, Blood-Brain-Barrier cells etc.).

3. **Making a mutants library for phenotype screening**

Using RNAseq I identified a number of genes that are differently expressed between ST5 and non-ST5 strains, some of which were genes involved in essential biological functions and virulence, the remaining were are hypothetical proteins. Charactering the phenotypic effects of knockouts on the hypothetical genes would potentially provide more insights into functionality of these genes.

4. **Investigate *in vivo C. neoformans* var. *grubii* gene expression at the site of human infection.**

The cerebrospinal fluid fungal burden in patients with cryptococcal meningitis in Vietnam is often high, which offers the potential for *in situ* RNAseq. Validating the differential expression of the genes of interest from my RNAseq data in patients would provide more insights into how different lineages of *C. neoformans* response to a potentially hostile environment in the host.

Appendices

Appendix 1. Pooled dataset for MLST analyses

Isolate ID	Specimen	Location	HIV	ST	goeBURST	Region	References
103	CSF	South Africa	Positive	4	4	Africa	Beale MA et al, Plos NTD,2015
113	CSF	South Africa	Positive	4	4	Africa	Beale MA et al, Plos NTD,2015
130	CSF	South Africa	Positive	4	4	Africa	Beale MA et al, Plos NTD,2015
134	CSF	South Africa	Positive	4	4	Africa	Beale MA et al, Plos NTD,2015
148	CSF	South Africa	Positive	4	4	Africa	Beale MA et al, Plos NTD,2015
206	CSF	South Africa	Positive	4	4	Africa	Beale MA et al, Plos NTD,2015
205	CSF	South Africa	Positive	4	4	Africa	Beale MA et al, Plos NTD,2015
264	CSF	South Africa	Positive	4	4	Africa	Beale MA et al, Plos NTD,2015
313	CSF	South Africa	Positive	4	4	Africa	Beale MA et al, Plos NTD,2015
321	CSF	South Africa	Positive	6	4	Africa	Beale MA et al, Plos NTD,2015
107	CSF	South Africa	Positive	5	5	Africa	Beale MA et al, Plos NTD,2015
101	CSF	South Africa	Positive	5	5	Africa	Beale MA et al, Plos NTD,2015
118	CSF	South Africa	Positive	5	5	Africa	Beale MA et al, Plos NTD,2015
133	CSF	South Africa	Positive	5	5	Africa	Beale MA et al, Plos NTD,2015
145	CSF	South Africa	Positive	5	5	Africa	Beale MA et al, Plos NTD,2015
229	CSF	South Africa	Positive	5	5	Africa	Beale MA et al, Plos NTD,2015
337	CSF	South Africa	Positive	5	5	Africa	Beale MA et al, Plos NTD,2015
204	CSF	South Africa	Positive	5	5	Africa	Beale MA et al, Plos NTD,2015
326	CSF	South Africa	Positive	5	5	Africa	Beale MA et al, Plos NTD,2015
339	CSF	South Africa	Positive	5	5	Africa	Beale MA et al, Plos NTD,2015
341	CSF	South Africa	Positive	5	5	Africa	Beale MA et al, Plos NTD,2015
401	CSF	South Africa	Positive	5	5	Africa	Beale MA et al, Plos NTD,2015
428	CSF	South Africa	Positive	5	5	Africa	Beale MA et al, Plos NTD,2015
437	CSF	South Africa	Positive	5	5	Africa	Beale MA et al, Plos NTD,2015
468	CSF	South	Positive	5	5	Africa	Beale MA et al, Plos

		Africa					NTD,2015
478	CSF	South Africa	Positive	5	5	Africa	Beale MA et al, Plos NTD,2015
314	CSF	South Africa	Positive	5	5	Africa	Beale MA et al, Plos NTD,2015
343	CSF	South Africa	Positive	5	5	Africa	Beale MA et al, Plos NTD,2015
425	CSF	South Africa	Positive	5	5	Africa	Beale MA et al, Plos NTD,2015
457	CSF	South Africa	Positive	5	5	Africa	Beale MA et al, Plos NTD,2015
470	CSF	South Africa	Positive	5	5	Africa	Beale MA et al, Plos NTD,2015
420	CSF	South Africa	Positive	5	5	Africa	Beale MA et al, Plos NTD,2015
424	CSF	South Africa	Positive	5	5	Africa	Beale MA et al, Plos NTD,2015
443	CSF	South Africa	Positive	5	5	Africa	Beale MA et al, Plos NTD,2015
447	CSF	South Africa	Positive	5	5	Africa	Beale MA et al, Plos NTD,2015
465	CSF	South Africa	Positive	5	5	Africa	Beale MA et al, Plos NTD,2015
475	CSF	South Africa	Positive	5	5	Africa	Beale MA et al, Plos NTD,2015
218	CSF	South Africa	Positive	202	5	Africa	Beale MA et al, Plos NTD,2015
219	CSF	South Africa	Positive	202	5	Africa	Beale MA et al, Plos NTD,2015
263	CSF	South Africa	Positive	202	5	Africa	Beale MA et al, Plos NTD,2015
257	CSF	South Africa	Positive	3	31	Africa	Beale MA et al, Plos NTD,2015
370	CSF	South Africa	Positive	31	31	Africa	Beale MA et al, Plos NTD,2015
469	CSF	South Africa	Positive	31	31	Africa	Beale MA et al, Plos NTD,2015
471	CSF	South Africa	Positive	31	31	Africa	Beale MA et al, Plos NTD,2015
106	CSF	South Africa	Positive	32	31	Africa	Beale MA et al, Plos NTD,2015
109	CSF	South Africa	Positive	32	31	Africa	Beale MA et al, Plos NTD,2015
116	CSF	South Africa	Positive	32	31	Africa	Beale MA et al, Plos NTD,2015
121	CSF	South Africa	Positive	32	31	Africa	Beale MA et al, Plos NTD,2015
122	CSF	South Africa	Positive	32	31	Africa	Beale MA et al, Plos NTD,2015
123	CSF	South Africa	Positive	32	31	Africa	Beale MA et al, Plos NTD,2015
124	CSF	South Africa	Positive	32	31	Africa	Beale MA et al, Plos NTD,2015
136	CSF	South Africa	Positive	32	31	Africa	Beale MA et al, Plos NTD,2015
137	CSF	South Africa	Positive	32	31	Africa	Beale MA et al, Plos NTD,2015
143	CSF	South	Positive	32	31	Africa	Beale MA et al, Plos

		Africa					NTD,2015
243	CSF	South Africa	Positive	32	31	Africa	Beale MA et al, Plos NTD,2015
238	CSF	South Africa	Positive	32	31	Africa	Beale MA et al, Plos NTD,2015
247	CSF	South Africa	Positive	32	31	Africa	Beale MA et al, Plos NTD,2015
252	CSF	South Africa	Positive	32	31	Africa	Beale MA et al, Plos NTD,2015
369	CSF	South Africa	Positive	32	31	Africa	Beale MA et al, Plos NTD,2015
346	CSF	South Africa	Positive	32	31	Africa	Beale MA et al, Plos NTD,2015
463	CSF	South Africa	Positive	32	31	Africa	Beale MA et al, Plos NTD,2015
360	CSF	South Africa	Positive	93	31	Africa	Beale MA et al, Plos NTD,2015
301	CSF	South Africa	Positive	93	31	Africa	Beale MA et al, Plos NTD,2015
328	CSF	South Africa	Positive	93	31	Africa	Beale MA et al, Plos NTD,2015
333	CSF	South Africa	Positive	93	31	Africa	Beale MA et al, Plos NTD,2015
367	CSF	South Africa	Positive	93	31	Africa	Beale MA et al, Plos NTD,2015
410	CSF	South Africa	Positive	93	31	Africa	Beale MA et al, Plos NTD,2015
419	CSF	South Africa	Positive	93	31	Africa	Beale MA et al, Plos NTD,2015
312	CSF	South Africa	Positive	93	31	Africa	Beale MA et al, Plos NTD,2015
319	CSF	South Africa	Positive	93	31	Africa	Beale MA et al, Plos NTD,2015
324	CSF	South Africa	Positive	93	31	Africa	Beale MA et al, Plos NTD,2015
330	CSF	South Africa	Positive	93	31	Africa	Beale MA et al, Plos NTD,2015
344	CSF	South Africa	Positive	93	31	Africa	Beale MA et al, Plos NTD,2015
345	CSF	South Africa	Positive	93	31	Africa	Beale MA et al, Plos NTD,2015
348	CSF	South Africa	Positive	93	31	Africa	Beale MA et al, Plos NTD,2015
358	CSF	South Africa	Positive	93	31	Africa	Beale MA et al, Plos NTD,2015
373	CSF	South Africa	Positive	93	31	Africa	Beale MA et al, Plos NTD,2015
304	CSF	South Africa	Positive	93	31	Africa	Beale MA et al, Plos NTD,2015
322	CSF	South Africa	Positive	93	31	Africa	Beale MA et al, Plos NTD,2015
327	CSF	South Africa	Positive	93	31	Africa	Beale MA et al, Plos NTD,2015
338	CSF	South Africa	Positive	93	31	Africa	Beale MA et al, Plos NTD,2015
342	CSF	South Africa	Positive	93	31	Africa	Beale MA et al, Plos NTD,2015
355	CSF	South	Positive	93	31	Africa	Beale MA et al, Plos

		Africa					NTD,2015
359	CSF	South Africa	Positive	93	31	Africa	Beale MA et al, Plos NTD,2015
366	CSF	South Africa	Positive	93	31	Africa	Beale MA et al, Plos NTD,2015
368	CSF	South Africa	Positive	93	31	Africa	Beale MA et al, Plos NTD,2015
380	CSF	South Africa	Positive	93	31	Africa	Beale MA et al, Plos NTD,2015
320	CSF	South Africa	Positive	93	31	Africa	Beale MA et al, Plos NTD,2015
363	CSF	South Africa	Positive	93	31	Africa	Beale MA et al, Plos NTD,2015
375	CSF	South Africa	Positive	93	31	Africa	Beale MA et al, Plos NTD,2015
417	CSF	South Africa	Positive	93	31	Africa	Beale MA et al, Plos NTD,2015
459	CSF	South Africa	Positive	93	31	Africa	Beale MA et al, Plos NTD,2015
477	CSF	South Africa	Positive	93	31	Africa	Beale MA et al, Plos NTD,2015
486	CSF	South Africa	Positive	93	31	Africa	Beale MA et al, Plos NTD,2015
444	CSF	South Africa	Positive	185	31	Africa	Beale MA et al, Plos NTD,2015
217	CSF	South Africa	Positive	199	31	Africa	Beale MA et al, Plos NTD,2015
261	CSF	South Africa	Positive	199	31	Africa	Beale MA et al, Plos NTD,2015
244	CSF	South Africa	Positive	199	31	Africa	Beale MA et al, Plos NTD,2015
141	CSF	South Africa	Positive	200	31	Africa	Beale MA et al, Plos NTD,2015
329	CSF	South Africa	Positive	236	31	Africa	Beale MA et al, Plos NTD,2015
110	CSF	South Africa	Positive	237	31	Africa	Beale MA et al, Plos NTD,2015
354	CSF	South Africa	Positive	238	31	Africa	Beale MA et al, Plos NTD,2015
406	CSF	South Africa	Positive	239	31	Africa	Beale MA et al, Plos NTD,2015
140	CSF	South Africa	Positive	240	31	Africa	Beale MA et al, Plos NTD,2015
336	CSF	South Africa	Positive	241	31	Africa	Beale MA et al, Plos NTD,2015
246	CSF	South Africa	Positive	2	63	Africa	Beale MA et al, Plos NTD,2015
308	CSF	South Africa	Positive	2	63	Africa	Beale MA et al, Plos NTD,2015
472	CSF	South Africa	Positive	2	63	Africa	Beale MA et al, Plos NTD,2015
310	CSF	South Africa	Positive	2	63	Africa	Beale MA et al, Plos NTD,2015
102	CSF	South Africa	Positive	58	63	Africa	Beale MA et al, Plos NTD,2015
256	CSF	South Africa	Positive	58	63	Africa	Beale MA et al, Plos NTD,2015
250	CSF	South	Positive	67	63	Africa	Beale MA et al, Plos

		Africa					NTD,2015
127	CSF	South Africa	Positive	234	63	Africa	Beale MA et al, Plos NTD,2015
119	CSF	South Africa	Positive	235	63	Africa	Beale MA et al, Plos NTD,2015
260	CSF	South Africa	Positive	246	63	Africa	Beale MA et al, Plos NTD,2015
154	CSF	South Africa	Positive	23	63	Africa	Beale MA et al, Plos NTD,2015
210	CSF	South Africa	Positive	23	63	Africa	Beale MA et al, Plos NTD,2015
258	CSF	South Africa	Positive	23	63	Africa	Beale MA et al, Plos NTD,2015
212	CSF	South Africa	Positive	23	63	Africa	Beale MA et al, Plos NTD,2015
223	CSF	South Africa	Positive	23	63	Africa	Beale MA et al, Plos NTD,2015
251	CSF	South Africa	Positive	23	63	Africa	Beale MA et al, Plos NTD,2015
412	CSF	South Africa	Positive	23	63	Africa	Beale MA et al, Plos NTD,2015
316	CSF	South Africa	Positive	23	63	Africa	Beale MA et al, Plos NTD,2015
357	CSF	South Africa	Positive	23	63	Africa	Beale MA et al, Plos NTD,2015
362	CSF	South Africa	Positive	23	63	Africa	Beale MA et al, Plos NTD,2015
352	CSF	South Africa	Positive	23	63	Africa	Beale MA et al, Plos NTD,2015
403	CSF	South Africa	Positive	23	63	Africa	Beale MA et al, Plos NTD,2015
415	CSF	South Africa	Positive	23	63	Africa	Beale MA et al, Plos NTD,2015
461	CSF	South Africa	Positive	23	63	Africa	Beale MA et al, Plos NTD,2015
433	CSF	South Africa	Positive	23	63	Africa	Beale MA et al, Plos NTD,2015
442	CSF	South Africa	Positive	23	63	Africa	Beale MA et al, Plos NTD,2015
481	CSF	South Africa	Positive	23	63	Africa	Beale MA et al, Plos NTD,2015
483	CSF	South Africa	Positive	23	63	Africa	Beale MA et al, Plos NTD,2015
147	CSF	South Africa	Positive	247	63	Africa	Beale MA et al, Plos NTD,2015
254	CSF	South Africa	Positive	248	63	Africa	Beale MA et al, Plos NTD,2015
216	CSF	South Africa	Positive	63	63	Africa	Beale MA et al, Plos NTD,2015
224	CSF	South Africa	Positive	63	63	Africa	Beale MA et al, Plos NTD,2015
249	CSF	South Africa	Positive	63	63	Africa	Beale MA et al, Plos NTD,2015
104	CSF	South Africa	Positive	69	63	Africa	Beale MA et al, Plos NTD,2015
146	CSF	South Africa	Positive	69	63	Africa	Beale MA et al, Plos NTD,2015
125	CSF	South	Positive	69	63	Africa	Beale MA et al, Plos

		Africa					NTD,2015
126	CSF	South Africa	Positive	69	63	Africa	Beale MA et al, Plos NTD,2015
129	CSF	South Africa	Positive	69	63	Africa	Beale MA et al, Plos NTD,2015
135	CSF	South Africa	Positive	69	63	Africa	Beale MA et al, Plos NTD,2015
139	CSF	South Africa	Positive	69	63	Africa	Beale MA et al, Plos NTD,2015
207	CSF	South Africa	Positive	69	63	Africa	Beale MA et al, Plos NTD,2015
208	CSF	South Africa	Positive	69	63	Africa	Beale MA et al, Plos NTD,2015
235	CSF	South Africa	Positive	69	63	Africa	Beale MA et al, Plos NTD,2015
241	CSF	South Africa	Positive	69	63	Africa	Beale MA et al, Plos NTD,2015
253	CSF	South Africa	Positive	69	63	Africa	Beale MA et al, Plos NTD,2015
255	CSF	South Africa	Positive	69	63	Africa	Beale MA et al, Plos NTD,2015
202	CSF	South Africa	Positive	69	63	Africa	Beale MA et al, Plos NTD,2015
203	CSF	South Africa	Positive	69	63	Africa	Beale MA et al, Plos NTD,2015
225	CSF	South Africa	Positive	69	63	Africa	Beale MA et al, Plos NTD,2015
231	CSF	South Africa	Positive	69	63	Africa	Beale MA et al, Plos NTD,2015
232	CSF	South Africa	Positive	69	63	Africa	Beale MA et al, Plos NTD,2015
233	CSF	South Africa	Positive	69	63	Africa	Beale MA et al, Plos NTD,2015
245	CSF	South Africa	Positive	69	63	Africa	Beale MA et al, Plos NTD,2015
262	CSF	South Africa	Positive	69	63	Africa	Beale MA et al, Plos NTD,2015
365	CSF	South Africa	Positive	69	63	Africa	Beale MA et al, Plos NTD,2015
371	CSF	South Africa	Positive	69	63	Africa	Beale MA et al, Plos NTD,2015
402	CSF	South Africa	Positive	69	63	Africa	Beale MA et al, Plos NTD,2015
436	CSF	South Africa	Positive	69	63	Africa	Beale MA et al, Plos NTD,2015
439	CSF	South Africa	Positive	69	63	Africa	Beale MA et al, Plos NTD,2015
318	CSF	South Africa	Positive	69	63	Africa	Beale MA et al, Plos NTD,2015
413	CSF	South Africa	Positive	69	63	Africa	Beale MA et al, Plos NTD,2015
416	CSF	South Africa	Positive	69	63	Africa	Beale MA et al, Plos NTD,2015
464	CSF	South Africa	Positive	69	63	Africa	Beale MA et al, Plos NTD,2015
405	CSF	South Africa	Positive	69	63	Africa	Beale MA et al, Plos NTD,2015
414	CSF	South	Positive	69	63	Africa	Beale MA et al, Plos

		Africa					NTD,2015
418	CSF	South Africa	Positive	69	63	Africa	Beale MA et al, Plos NTD,2015
112	CSF	South Africa	Positive	212	63	Africa	Beale MA et al, Plos NTD,2015
213	CSF	South Africa	Positive	218	63	Africa	Beale MA et al, Plos NTD,2015
227	CSF	South Africa	Positive	218	63	Africa	Beale MA et al, Plos NTD,2015
215	CSF	South Africa	Positive	218	63	Africa	Beale MA et al, Plos NTD,2015
NRHc5025.ENR.STOR	CSF	Botswana	Positive	5	5	Africa	Chen *et al.,* (2016)
NRHc5028.ENR.STOR	CSF	Botswana	Positive	3	31	Africa	Chen *et al.,* (2016)
NRHc5036.ENR	CSF	Botswana	Positive	77	31	Africa	Chen *et al.,* (2016)
NRHc5044.REL.INI.CLIN.ISO	CSF	Botswana	Positive	77	31	Africa	Chen *et al.,* (2016)
PMHc1039.ENR.STOR	CSF	Botswana	Positive	77	31	Africa	Chen *et al.,* (2016)
PMHc1018.CLIN.1	CSF	Botswana	Positive	32	31	Africa	Chen *et al.,* (2016)
PMHc1052.ENR.STOR	CSF	Botswana	Positive	9	N/A	Africa	Chen *et al.,* (2016)
PMHc1023.ENR	CSF	Botswana	Positive	40	N/A	Africa	Chen *et al.,* (2016)
NRHc5048.ENR.ISO	CSF	Botswana	Positive	80	N/A	Africa	Chen *et al.,* (2016)
PMHc1043.ENR.STOR	CSF	Botswana	Positive	80	N/A	Africa	Chen *et al.,* (2016)
PMHc1034.ENR.STOR	CSF	Botswana	Positive	89	N/A	Africa	Chen *et al.,* (2016)
NRHc5031.ENR.CLIN.ISO	CSF	Botswana	Positive	143	N/A	Africa	Chen *et al.,* (2016)
NRHc5017.ENR	CSF	Botswana	Positive	317	N/A	Africa	Chen *et al.,* (2016)
NRHc5001.ENR	CSF	Botswana	Positive	378	N/A	Africa	Chen *et al.,* (2016)
PMHc1031A.ENR.INI.LP	CSF	Botswana	Positive	379	N/A	Africa	Chen *et al.,* (2016)
PMHc1020.CLIN.1	CSF	Botswana	Positive	380	N/A	Africa	Chen *et al.,* (2016)
NRHc5041.ENR.CLIN.ISO	CSF	Botswana	Positive	384	N/A	Africa	Chen *et al.,* (2016)
PMHc1038.ENR.CLIN1	CSF	Botswana	Positive	385	N/A	Africa	Chen *et al.,* (2016)
NRHc5030.ENR.CLIN.ISO	CSF	Botswana	Positive	386	N/A	Africa	Chen *et al.,* (2016)
NRHc5013.ENR	CSF	Botswana	Positive	387	N/A	Africa	Chen *et al.,* (2016)
PMHc1001.ENR	CSF	Botswana	Positive	389	N/A	Africa	Chen *et al.,* (2016)
NRHc5009.ENR	CSF	Botswana	Positive	392	N/A	Africa	Chen *et al.,* (2016)
NRHc5037.ENR.CLIN1	CSF	Botswana	Positive	394	N/A	Africa	Chen *et al.,* (2016)
PMHc1014.ENR	CSF	Botswana	Positive	396	N/A	Africa	Chen *et al.,* (2016)
NRHc5005.ENR	CSF	Botswana	Positive	398	N/A	Africa	Chen *et al.,* (2016)
PMHc1030.ENR.CLIN.ISO	CSF	Botswana	Positive	402	N/A	Africa	Chen *et al.,* (2016)
NRHc5006.CLIN.1	CSF	Botswana	Positive	403	N/A	Africa	Chen *et al.,* (2016)
NRHc5008.ENR	CSF	Botswana	Positive	407	N/A	Africa	Chen *et al.,* (2016)
PMHc1047.ENR.CLIN1	CSF	Botswana	Positive	408	N/A	Africa	Chen *et al.,* (2016)
PMHc1024.CLIN.1	CSF	Botswana	Positive	409	N/A	Africa	Chen *et al.,* (2016)
PMHc1033.ENR	CSF	Botswana	Positive	410	N/A	Africa	Chen *et al.,* (2016)

PMHc1035.ENR.STOR	CSF	Botswana	Positive	411	N/A	Africa	Chen *et al.,* (2016)
NRHc5040.ENR.CLIN.ISO	CSF	Botswana	Positive	415	N/A	Africa	Chen *et al.,* (2016)
NRHc5026.ENR.CLIN.ISO	CSF	Botswana	Positive	416	N/A	Africa	Chen *et al.,* (2016)
PMHc1050.ENR.CLIN1	CSF	Botswana	Positive	417	N/A	Africa	Chen *et al.,* (2016)
NRHc5019.ENR	CSF	Botswana	Positive	419	N/A	Africa	Chen *et al.,* (2016)
NRHc5023.ENR	CSF	Botswana	Positive	421	N/A	Africa	Chen *et al.,* (2016)
PMHc1026.ENR	CSF	Botswana	Positive	422	N/A	Africa	Chen *et al.,* (2016)
NRHc5020.CLIN.1	CSF	Botswana	Positive	424	N/A	Africa	Chen *et al.,* (2016)
NRHc5011.ENR	CSF	Botswana	Positive	427	N/A	Africa	Chen *et al.,* (2016)
NRHc5032.ENR.CLIN.ISO	CSF	Botswana	Positive	428	N/A	Africa	Chen *et al.,* (2016)
NRHc5021.CLIN.1	CSF	Botswana	Positive	429	N/A	Africa	Chen *et al.,* (2016)
NRHc5029.ENR.CLIN.ISO	CSF	Botswana	Positive	432	N/A	Africa	Chen *et al.,* (2016)
NRHc5039.ENR.CLIN.ISO	CSF	Botswana	Positive	433	N/A	Africa	Chen *et al.,* (2016)
NRHc5024.ENR.CLIN.1	CSF	Botswana	Positive	434	N/A	Africa	Chen *et al.,* (2016)
NRHc5004.ENR	CSF	Botswana	Positive	435	N/A	Africa	Chen *et al.,* (2016)
NRHc5045.ENR.CLIN.ISO	CSF	Botswana	Positive	436	N/A	Africa	Chen *et al.,* (2016)
NRHc5035.ENR.CLIN.ISO	CSF	Botswana	Positive	438	N/A	Africa	Chen *et al.,* (2016)
NRHc5042.ENR.STOR	CSF	Botswana	Positive	447	N/A	Africa	Chen *et al.,* (2016)
NRHc5015.ENR	CSF	Botswana	Positive	449	N/A	Africa	Chen *et al.,* (2016)
PMHc1022.ENR	CSF	Botswana	Positive	449	N/A	Africa	Chen *et al.,* (2016)
PMHc1032.ENR	CSF	Botswana	Positive	449	N/A	Africa	Chen *et al.,* (2016)
NRHc5012.CLIN.1	CSF	Botswana	Positive	450	N/A	Africa	Chen *et al.,* (2016)
NRHc5014.ENR	CSF	Botswana	Positive	451	N/A	Africa	Chen *et al.,* (2016)
PMHc1049.THER1.STOR	CSF	Botswana	Positive	460	N/A	Africa	Chen *et al.,* (2016)
PMHc1011.ENR	CSF	Botswana	Positive	464	N/A	Africa	Chen *et al.,* (2016)
NRHc5027.ENR.CLIN1	CSF	Botswana	Positive	465	N/A	Africa	Chen *et al.,* (2016)
PMHc1045.ENR.STOR	CSF	Botswana	Positive	467	N/A	Africa	Chen *et al.,* (2016)
PMHc1002.ENR	CSF	Botswana	Positive	468	N/A	Africa	Chen *et al.,* (2016)
PMHc1009.ENR	CSF	Botswana	Positive	469	N/A	Africa	Chen *et al.,* (2016)
NRHc5022.ENR	CSF	Botswana	Positive	472	N/A	Africa	Chen *et al.,* (2016)
PMHc1029.ENR.STOR	CSF	Botswana	Positive	478	N/A	Africa	Chen *et al.,* (2016)
PMHc1040.ENR.STOR	CSF	Botswana	Positive	483	N/A	Africa	Chen *et al.,* (2016)
NRHc5010.ENR	CSF	Botswana	Positive	484	N/A	Africa	Chen *et al.,* (2016)
Gbc16-1	dead tree	Botswana	NA	80	N/A	Africa	Chen *et al.,* (2016)
Ftc95-3	Mopane tree	Botswana	NA	89	N/A	Africa	Chen *et al.,* (2016)
Ftc98-1	Mopane tree	Botswana	NA	377	N/A	Africa	Chen *et al.,* (2016)
Gbc51-2	Acacia sp.	Botswana	NA	378	N/A	Africa	Chen *et al.,* (2016)
Gbc42-2	Acacia sp.	Botswana	NA	381	N/A	Africa	Chen *et al.,* (2016)

Ftc321-1	Mopane tree	Botswana	NA	382	N/A	Africa	Chen *et al.,* (2016)
Gbc39-1	Acacia sp.	Botswana	NA	383	N/A	Africa	Chen *et al.,* (2016)
Ftc103-1	Mopane tree	Botswana	NA	388	N/A	Africa	Chen *et al.,* (2016)
Ftc170-1	Mopane tree	Botswana	NA	390	N/A	Africa	Chen *et al.,* (2016)
Ftc102-1	Mopane tree	Botswana	NA	391	N/A	Africa	Chen *et al.,* (2016)
Ftc322-1	Mopane tree	Botswana	NA	393	N/A	Africa	Chen *et al.,* (2016)
Ftc327-1	Mopane tree	Botswana	NA	393	N/A	Africa	Chen *et al.,* (2016)
Ftc195-1	Mopane tree	Botswana	NA	395	N/A	Africa	Chen *et al.,* (2016)
Muc525-1	soil	Botswana	NA	397	N/A	Africa	Chen *et al.,* (2016)
Ftc239-1	Mopane tree	Botswana	NA	399	N/A	Africa	Chen *et al.,* (2016)
Ftc214-1	Mopane tree	Botswana	NA	400	N/A	Africa	Chen *et al.,* (2016)
Ftc209-1	Mopane tree	Botswana	NA	401	N/A	Africa	Chen *et al.,* (2016)
Ftc241-1	Mopane tree	Botswana	NA	404	N/A	Africa	Chen *et al.,* (2016)
Ftc217-1	Mopane tree	Botswana	NA	405	N/A	Africa	Chen *et al.,* (2016)
Ftc211-1	Mopane tree	Botswana	NA	406	N/A	Africa	Chen *et al.,* (2016)
Ftc158-1	Avian guano	Botswana	NA	412	N/A	Africa	Chen *et al.,* (2016)
Ftc167-1	Mopane tree	Botswana	NA	413	N/A	Africa	Chen *et al.,* (2016)
Ftc267-1	Mopane tree	Botswana	NA	413	N/A	Africa	Chen *et al.,* (2016)
Muc402-1	Mopane tree	Botswana	NA	414	N/A	Africa	Chen *et al.,* (2016)
Gbc574-1	Ziziphus mucronata	Botswana	NA	418	N/A	Africa	Chen *et al.,* (2016)
Muc470-1	Mopane tree	Botswana	NA	418	N/A	Africa	Chen *et al.,* (2016)
Muc479-1	Mopane tree	Botswana	NA	420	N/A	Africa	Chen *et al.,* (2016)
Muc416-1	Acacia sp.	Botswana	NA	423	N/A	Africa	Chen *et al.,* (2016)
Muc468-1	Mopane tree	Botswana	NA	423	N/A	Africa	Chen *et al.,* (2016)
Ftc200-1	Mopane tree	Botswana	NA	425	N/A	Africa	Chen *et al.,* (2016)
Ftc192-1	Mopane tree	Botswana	NA	426	N/A	Africa	Chen *et al.,* (2016)
Ftc222-1	Mopane tree	Botswana	NA	430	N/A	Africa	Chen *et al.,* (2016)
Ftc257-1	Mopane tree	Botswana	NA	431	N/A	Africa	Chen *et al.,* (2016)
Gbc44-1	Acacia sp.	Botswana	NA	437	N/A	Africa	Chen *et al.,* (2016)
Ftc168-1	Mopane tree	Botswana	NA	439	N/A	Africa	Chen *et al.,* (2016)
Gbc573-1	Ziziphus mucronata	Botswana	NA	440	N/A	Africa	Chen *et al.,* (2016)
Muc449-1	Ziziphus mucronata	Botswana	NA	441	N/A	Africa	Chen *et al.,* (2016)
Muc498-1	Mopane tree	Botswana	NA	441	N/A	Africa	Chen *et al.,* (2016)
Muc499-1	Mopane tree	Botswana	NA	441	N/A	Africa	Chen *et al.,* (2016)
Ftc555-1	Mopane tree	Botswana	NA	442	N/A	Africa	Chen *et al.,* (2016)
Muc418-1	Acacia sp.	Botswana	NA	443	N/A	Africa	Chen *et al.,* (2016)
Muc421-3	Acacia sp.	Botswana	NA	443	N/A	Africa	Chen *et al.,* (2016)

Muc460-1	Mopane tree	Botswana	NA	443	N/A	Africa	Chen *et al.,* (2016)
Ftc146-1	Mopane tree	Botswana	NA	444	N/A	Africa	Chen *et al.,* (2016)
Muc364-1	Mopane tree	Botswana	NA	445	N/A	Africa	Chen *et al.,* (2016)
Ftc109-1	Mopane tree	Botswana	NA	446	N/A	Africa	Chen *et al.,* (2016)
Ftc260-1	Mopane tree	Botswana	NA	448	N/A	Africa	Chen *et al.,* (2016)
Ftc151-1	Mopane tree	Botswana	NA	452	N/A	Africa	Chen *et al.,* (2016)
Ftc153-1	Mopane tree	Botswana	NA	453	N/A	Africa	Chen *et al.,* (2016)
Ftc132-1	Mopane tree	Botswana	NA	454	N/A	Africa	Chen *et al.,* (2016)
Ftc134-1	Mopane tree	Botswana	NA	454	N/A	Africa	Chen *et al.,* (2016)
Ftc225-1	Mopane tree	Botswana	NA	455	N/A	Africa	Chen *et al.,* (2016)
Muc451-1	Mopane tree	Botswana	NA	456	N/A	Africa	Chen *et al.,* (2016)
Ftc137-1	Mopane tree	Botswana	NA	457	N/A	Africa	Chen *et al.,* (2016)
Ftc152-2	Mopane tree	Botswana	NA	457	N/A	Africa	Chen *et al.,* (2016)
Ftc111-1	Mopane tree	Botswana	NA	458	N/A	Africa	Chen *et al.,* (2016)
Ftc173-1	Mopane tree	Botswana	NA	459	N/A	Africa	Chen *et al.,* (2016)
Muc387-1	Mopane tree	Botswana	NA	461	N/A	Africa	Chen *et al.,* (2016)
Muc437-1	Ziziphus mucronata	Botswana	NA	462	N/A	Africa	Chen *et al.,* (2016)
Muc367-1	Mopane tree	Botswana	NA	463	N/A	Africa	Chen *et al.,* (2016)
Muc466-1	Mopane tree	Botswana	NA	466	N/A	Africa	Chen *et al.,* (2016)
Muc415-1	Mopane tree	Botswana	NA	470	N/A	Africa	Chen *et al.,* (2016)
Muc450-1	Mopane tree	Botswana	NA	471	N/A	Africa	Chen *et al.,* (2016)
Muc489-1	Mopane tree	Botswana	NA	471	N/A	Africa	Chen *et al.,* (2016)
Muc504-1	Mopane tree	Botswana	NA	471	N/A	Africa	Chen *et al.,* (2016)
Muc529-1	Mopane tree	Botswana	NA	471	N/A	Africa	Chen *et al.,* (2016)
Ftc207-1	Mopane tree	Botswana	NA	473	N/A	Africa	Chen *et al.,* (2016)
Ftc236-1	Mopane tree	Botswana	NA	474	N/A	Africa	Chen *et al.,* (2016)
Muc463-2	Mopane tree	Botswana	NA	475	N/A	Africa	Chen *et al.,* (2016)
Muc507-1	Mopane tree	Botswana	NA	476	N/A	Africa	Chen *et al.,* (2016)
Ftc154-1	Mopane tree	Botswana	NA	477	N/A	Africa	Chen *et al.,* (2016)
Muc503-1	Mopane tree	Botswana	NA	479	N/A	Africa	Chen *et al.,* (2016)
Muc433-1	Acacia sp.	Botswana	NA	480	N/A	Africa	Chen *et al.,* (2016)
Muc457-1	Mopane tree	Botswana	NA	480	N/A	Africa	Chen *et al.,* (2016)
Muc458-1	Mopane tree	Botswana	NA	480	N/A	Africa	Chen *et al.,* (2016)
Muc516-1	Mopane tree	Botswana	NA	481	N/A	Africa	Chen *et al.,* (2016)
Ftc202-1	Mopane tree	Botswana	NA	482	N/A	Africa	Chen *et al.,* (2016)
mal 104	Blood	Malawi	Positive	4	4	Africa	Litvintseva et al. Genetics. 2006
Tn148	Blood	Tanzania	Positive	4	4	Africa	Litvintseva et al. Genetics. 2006

ug2463	CSF	Uganda	Positive	6	4	Africa	Litvintseva et al. Genetics. 2006
bt134	CSF	Botswana	Positive	25	5	Africa	Litvintseva et al. Genetics. 2006
bt130	CSF	Botswana	Positive	13	31	Africa	Litvintseva et al. Genetics. 2006
bt104	CSF	Botswana	Positive	22	31	Africa	Litvintseva et al. Genetics. 2006
JH125.91	Clinical	Tanzania	Unknown	3	31	Africa	Litvintseva et al. Genetics. 2006
mal 9	Blood	Malawi	Positive	30	31	Africa	Litvintseva et al. Genetics. 2006
Tn10	Blood	Tanzania	Positive	32	31	Africa	Litvintseva et al. Genetics. 2006
ug2458	CSF	Uganda	Positive	32	31	Africa	Litvintseva et al. Genetics. 2006
za1346	CSF	Zaire	Positive	32	31	Africa	Litvintseva et al. Genetics. 2006
mal 120	Blood	Malawi	Positive	2	63	Africa	Litvintseva et al. Genetics. 2006
Tn470	Blood	Tanzania	Positive	2	63	Africa	Litvintseva et al. Genetics. 2006
ug2459	CSF	Uganda	Positive	23	63	Africa	Litvintseva et al. Genetics. 2006
bt150	CSF	Botswana	Positive	21	N/A	Africa	Litvintseva et al. Genetics. 2006 Litvintseva et al. PlosOne. 2011
bt121	CSF	Botswana	Positive	34	N/A	Africa	Litvintseva et al. Genetics. 2006 Litvintseva et al. PlosOne. 2011
bt9	CSF	Botswana	Positive	36	N/A	Africa	Litvintseva et al. Genetics. 2006 Litvintseva et al. PlosOne. 2011
UgCl018	CSF	Uganda	Positive	4	4	Africa	Wiesner et al. mBio. 2012
UgCl021	CSF	Uganda	Positive	5	5	Africa	Wiesner et al. mBio. 2012
UgCl076	CSF	Uganda	Positive	31	31	Africa	Wiesner et al. mBio. 2012
UgCl037	CSF	Uganda	Positive	39	31	Africa	Wiesner et al. mBio. 2012
UgCl040	CSF	Uganda	Positive	78	31	Africa	Wiesner et al. mBio. 2012
UgCl107	CSF	Uganda	Positive	91	31	Africa	Wiesner et al. mBio. 2012
UgCl122	CSF	Uganda	Positive	92	31	Africa	Wiesner et al. mBio. 2012
UgCl001	CSF	Uganda	Positive	93	31	Africa	Wiesner et al. mBio. 2012
UgCl011	CSF	Uganda	Positive	77	31	Africa	Wiesner et al. mBio. 2012
UgCl036	CSF	Uganda	Positive	94	31	Africa	Wiesner et al. mBio. 2012
UgCl074	CSF	Uganda	Positive	95	31	Africa	Wiesner et al. mBio. 2012
UgCl057	CSF	Uganda	Positive	63	63	Africa	Wiesner et al. mBio. 2012
UgCl030	CSF	Uganda	Positive	69	63	Africa	Wiesner et al. mBio. 2012
WM 148	CSF	Australia	Unknown	63	63	Australasia	Litvintseva et al. Genetics. 2006
K30	Blood	Korea	Positive	4	4	East Asia	Choi et al. FEMS Yeast Res. 2010,10
K1	Urine	Korea	Unknown	5	5	East Asia	Choi et al. FEMS Yeast Res. 2010,10

K54	CSF	Korea	Positive	312	31	East Asia	Choi et al. FEMS Yeast Res. 2010,10
K37	CSF	Korea	Positive	23	63	East Asia	Choi et al. FEMS Yeast Res. 2010,10
WH098	CSF	China	Positive	5	5	East Asia	Dou *et al.,* (2014)
WH121	Blood	China	Positive	5	5	East Asia	Dou *et al.,* (2014)
WH122	CSF	China	Positive	5	5	East Asia	Dou *et al.,* (2014)
WH124	CSF	China	Positive	5	5	East Asia	Dou *et al.,* (2014)
WH126	CSF	China	Positive	5	5	East Asia	Dou *et al.,* (2014)
PU27		China	Positive	5	5	East Asia	Dou *et al.,* (2014)
PU64		China	Positive	5	5	East Asia	Dou *et al.,* (2014)
PU65		China	Positive	5	5	East Asia	Dou *et al.,* (2014)
PU147		China	Positive	5	5	East Asia	Dou *et al.,* (2014)
PU148		China	Positive	5	5	East Asia	Dou *et al.,* (2014)
PU149		China	Positive	5	5	East Asia	Dou *et al.,* (2014)
PU150		China	Positive	5	5	East Asia	Dou *et al.,* (2014)
PU151		China	Positive	5	5	East Asia	Dou *et al.,* (2014)
PU152		China	Positive	5	5	East Asia	Dou *et al.,* (2014)
PU153		China	Positive	5	5	East Asia	Dou *et al.,* (2014)
PU154		China	Positive	5	5	East Asia	Dou *et al.,* (2014)
PU155		China	Positive	5	5	East Asia	Dou *et al.,* (2014)
PU156		China	Positive	5	5	East Asia	Dou *et al.,* (2014)
PU158		China	Positive	5	5	East Asia	Dou *et al.,* (2014)
PU159		China	Positive	5	5	East Asia	Dou *et al.,* (2014)
PU160		China	Positive	5	5	East Asia	Dou *et al.,* (2014)
PU163		China	Positive	5	5	East Asia	Dou *et al.,* (2014)
PU164		China	Positive	5	5	East Asia	Dou *et al.,* (2014)
PU167		China	Positive	5	5	East Asia	Dou *et al.,* (2014)
PU1		China	Negative	5	5	East Asia	Dou *et al.,* (2014)
PU16		China	Negative	5	5	East Asia	Dou *et al.,* (2014)
PU18		China	Negative	5	5	East Asia	Dou *et al.,* (2014)
PU30		China	Negative	5	5	East Asia	Dou *et al.,* (2014)
PU33		China	Negative	5	5	East Asia	Dou *et al.,* (2014)
PU38		China	Negative	5	5	East Asia	Dou *et al.,* (2014)
PU44		China	Negative	5	5	East Asia	Dou *et al.,* (2014)
PU47		China	Negative	5	5	East Asia	Dou *et al.,* (2014)
PU49		China	Negative	5	5	East Asia	Dou *et al.,* (2014)
PU67		China	Negative	5	5	East Asia	Dou *et al.,* (2014)
PU145		China	Negative	5	5	East Asia	Dou *et al.,* (2014)
HK_02	Clinical	China	Unknown	4	4	East Asia	Khayhan et al., (2013)

HK_01	Clinical	China	Unknown	6	4	East Asia	Khayhan et al., (2013)
WH003	Sputum	China	Negative	5	5	East Asia	Khayhan et al., (2013)
WH004	CSF	China	Negative	5	5	East Asia	Khayhan et al., (2013)
WH005	CSF	China	Negative	5	5	East Asia	Khayhan et al., (2013)
WH006	CSF	China	Negative	5	5	East Asia	Khayhan et al., (2013)
WH007	CSF	China	Negative	5	5	East Asia	Khayhan et al., (2013)
WH008	CSF	China	Negative	5	5	East Asia	Khayhan et al., (2013)
WH011	CSF	China	Negative	5	5	East Asia	Khayhan et al., (2013)
WH012	CSF	China	Negative	5	5	East Asia	Khayhan et al., (2013)
WH013	CSF	China	Negative	5	5	East Asia	Khayhan et al., (2013)
WH014	CSF	China	Negative	5	5	East Asia	Khayhan et al., (2013)
WH015	Sputum	China	Negative	5	5	East Asia	Khayhan et al., (2013)
WH016	CSF	China	Negative	5	5	East Asia	Khayhan et al., (2013)
WH017	CSF	China	Negative	5	5	East Asia	Khayhan et al., (2013)
WH019	CSF	China	Negative	5	5	East Asia	Khayhan et al., (2013)
WH020	Blood	China	Negative	5	5	East Asia	Khayhan et al., (2013)
WH022	CSF	China	Negative	5	5	East Asia	Khayhan et al., (2013)
WH023	CSF	China	Negative	5	5	East Asia	Khayhan et al., (2013)
WH025	CSF	China	Negative	5	5	East Asia	Khayhan et al., (2013)
WH026	CSF	China	Negative	5	5	East Asia	Khayhan et al., (2013)
WH027	CSF	China	Negative	5	5	East Asia	Khayhan et al., (2013)
WH028	CSF	China	Negative	5	5	East Asia	Khayhan et al., (2013)
WH030	CSF	China	Negative	5	5	East Asia	Khayhan et al., (2013)
WH031	Lung	China	Negative	5	5	East Asia	Khayhan et al., (2013)
WH033	Skin	China	Negative	5	5	East Asia	Khayhan et al., (2013)
WH034	CSF	China	Negative	5	5	East Asia	Khayhan et al., (2013)
WH035	CSF	China	Negative	5	5	East Asia	Khayhan et al., (2013)
WH036	CSF	China	Negative	5	5	East Asia	Khayhan et al., (2013)
WH040	CSF	China	Negative	5	5	East Asia	Khayhan et al., (2013)
WH041	CSF	China	Negative	5	5	East Asia	Khayhan et al., (2013)
WH042	CSF	China	Negative	5	5	East Asia	Khayhan et al., (2013)
WH044	CSF	China	Negative	5	5	East Asia	Khayhan et al., (2013)
WH047	CSF	China	Negative	5	5	East Asia	Khayhan et al., (2013)
WH050	CSF	China	Negative	5	5	East Asia	Khayhan et al., (2013)
WH051	CSF	China	Negative	5	5	East Asia	Khayhan et al., (2013)
WH054	CSF	China	Negative	5	5	East Asia	Khayhan et al., (2013)
WH055	CSF	China	Negative	5	5	East Asia	Khayhan et al., (2013)
WH057	CSF	China	Negative	5	5	East Asia	Khayhan et al., (2013)

WH058	Skin	China	Negative	5	5	East Asia	Khayhan et al., (2013)
WH061	CSF	China	Negative	5	5	East Asia	Khayhan et al., (2013)
WH062	Skin	China	Negative	5	5	East Asia	Khayhan et al., (2013)
WH063	CSF	China	Negative	5	5	East Asia	Khayhan et al., (2013)
WH066	CSF	China	Negative	5	5	East Asia	Khayhan et al., (2013)
WH067	CSF	China	Negative	5	5	East Asia	Khayhan et al., (2013)
WH068	CSF	China	Negative	5	5	East Asia	Khayhan et al., (2013)
WH072	CSF	China	Negative	5	5	East Asia	Khayhan et al., (2013)
WH075	CSF	China	Negative	5	5	East Asia	Khayhan et al., (2013)
WH076	CSF	China	Negative	5	5	East Asia	Khayhan et al., (2013)
WH077	CSF	China	Negative	5	5	East Asia	Khayhan et al., (2013)
WH078	CSF	China	Negative	5	5	East Asia	Khayhan et al., (2013)
WH079	CSF	China	Negative	5	5	East Asia	Khayhan et al., (2013)
WH080	CSF	China	Negative	5	5	East Asia	Khayhan et al., (2013)
WH082	CSF	China	Negative	5	5	East Asia	Khayhan et al., (2013)
WH083	Blood	China	Negative	5	5	East Asia	Khayhan et al., (2013)
WH091	CSF	China	Negative	5	5	East Asia	Khayhan et al., (2013)
WH093	CSF	China	Negative	5	5	East Asia	Khayhan et al., (2013)
WH094	CSF	China	Negative	5	5	East Asia	Khayhan et al., (2013)
WH096	CSF	China	Negative	5	5	East Asia	Khayhan et al., (2013)
WH101	CSF	China	Negative	5	5	East Asia	Khayhan et al., (2013)
WH102	CSF	China	Negative	5	5	East Asia	Khayhan et al., (2013)
WH104	CSF	China	Negative	5	5	East Asia	Khayhan et al., (2013)
WH105	CSF	China	Negative	5	5	East Asia	Khayhan et al., (2013)
WH106	CSF	China	Negative	5	5	East Asia	Khayhan et al., (2013)
WH108	CSF	China	Negative	5	5	East Asia	Khayhan et al., (2013)
WH114	CSF	China	Negative	5	5	East Asia	Khayhan et al., (2013)
WH115	CSF	China	Negative	5	5	East Asia	Khayhan et al., (2013)
WH117	CSF	China	Negative	5	5	East Asia	Khayhan et al., (2013)
WH118	CSF	China	Negative	5	5	East Asia	Khayhan et al., (2013)
WH119	CSF	China	Negative	5	5	East Asia	Khayhan et al., (2013)
WH120	CSF	China	Negative	5	5	East Asia	Khayhan et al., (2013)
HK_03	Clinical	China	Unknown	5	5	East Asia	Khayhan et al., (2013)
HK_04	Clinical	China	Unknown	5	5	East Asia	Khayhan et al., (2013)
HK_05	Clinical	China	Unknown	5	5	East Asia	Khayhan et al., (2013)
HK_06	Clinical	China	Unknown	5	5	East Asia	Khayhan et al., (2013)
HK_07	Clinical	China	Unknown	5	5	East Asia	Khayhan et al., (2013)
HK_08	Clinical	China	Unknown	5	5	East Asia	Khayhan et al., (2013)

HK_09	Clinical	China	Unknown	5	5	East Asia	Khayhan et al., (2013)
HK_10	Clinical	China	Unknown	5	5	East Asia	Khayhan et al., (2013)
HK_11	Clinical	China	Unknown	5	5	East Asia	Khayhan et al., (2013)
HK_12	Clinical	China	Unknown	5	5	East Asia	Khayhan et al., (2013)
HK_13	Clinical	China	Unknown	5	5	East Asia	Khayhan et al., (2013)
HK_14	Clinical	China	Unknown	5	5	East Asia	Khayhan et al., (2013)
9104	Skin	Japan	Negative	5	5	East Asia	Khayhan et al., (2013)
9106	CSF	Japan	Negative	5	5	East Asia	Khayhan et al., (2013)
9107	Unknown	Japan	Negative	5	5	East Asia	Khayhan et al., (2013)
9108	Skin	Japan	Negative	5	5	East Asia	Khayhan et al., (2013)
9111	CSF	Japan	Negative	5	5	East Asia	Khayhan et al., (2013)
9114	Unknown	Japan	Negative	5	5	East Asia	Khayhan et al., (2013)
9165	CSF	Japan	Negative	5	5	East Asia	Khayhan et al., (2013)
9166	Skin	Japan	Negative	5	5	East Asia	Khayhan et al., (2013)
9167	CSF	Japan	Negative	5	5	East Asia	Khayhan et al., (2013)
9170	Skin	Japan	Negative	5	5	East Asia	Khayhan et al., (2013)
9172	CSF	Japan	Unknown	5	5	East Asia	Khayhan et al., (2013)
9173	CSF	Japan	Negative	5	5	East Asia	Khayhan et al., (2013)
9174	CSF	Japan	Negative	5	5	East Asia	Khayhan et al., (2013)
9179	Unknown	Japan	Negative	5	5	East Asia	Khayhan et al., (2013)
9197	Unknown	Japan	Unknown	5	5	East Asia	Khayhan et al., (2013)
9198	Unknown	Japan	Unknown	5	5	East Asia	Khayhan et al., (2013)
9199	Unknown	Japan	Unknown	5	5	East Asia	Khayhan et al., (2013)
9204	Unknown	Japan	Unknown	5	5	East Asia	Khayhan et al., (2013)
9205	Unknown	Japan	Unknown	5	5	East Asia	Khayhan et al., (2013)
9211	Avian guano	Japan	NA	5	5	East Asia	Khayhan et al., (2013)
9212	Avian guano	Japan	NA	5	5	East Asia	Khayhan et al., (2013)
9213	Unknown	Japan	Unknown	5	5	East Asia	Khayhan et al., (2013)
9217	Unknown	Japan	Unknown	5	5	East Asia	Khayhan et al., (2013)
9237	Skin	Japan	Negative	5	5	East Asia	Khayhan et al., (2013)
9238	CSF	Japan	Negative	5	5	East Asia	Khayhan et al., (2013)
9239	Skin	Japan	Negative	5	5	East Asia	Khayhan et al., (2013)
9251	Skin	Japan	Negative	5	5	East Asia	Khayhan et al., (2013)
9254	Avian guano	Japan	NA	5	5	East Asia	Khayhan et al., (2013)
9255	Avian guano	Japan	NA	5	5	East Asia	Khayhan et al., (2013)
9258	Avian guano	Japan	NA	5	5	East Asia	Khayhan et al., (2013)
9259	Avian guano	Japan	NA	5	5	East Asia	Khayhan et al., (2013)
9260	Avian guano	Japan	NA	5	5	East Asia	Khayhan et al., (2013)

9261	Avian guano	Japan	NA	5	5	East Asia	Khayhan et al., (2013)
9263	Skin	Japan	Negative	5	5	East Asia	Khayhan et al., (2013)
9264	Skin	Japan	Negative	5	5	East Asia	Khayhan et al., (2013)
9265	Skin	Japan	Negative	5	5	East Asia	Khayhan et al., (2013)
WH123	CSF	China	Positive	194	5	East Asia	Khayhan et al., (2013)
PU161		China	Positive	296	5	East Asia	Khayhan et al., (2013)
WH095	Ure	China	Negative	186	5	East Asia	Khayhan et al., (2013)
WH071	CSF	China	Negative	194	5	East Asia	Khayhan et al., (2013)
WH037	CSF	China	Negative	31	31	East Asia	Khayhan et al., (2013)
9256	Avian guano	Japan	NA	31	31	East Asia	Khayhan et al., (2013)
WH001	CSF	China	Negative	93	31	East Asia	Khayhan et al., (2013)
WH069	CSF	China	Negative	191	31	East Asia	Khayhan et al., (2013)
PU162		China	Positive	63	63	East Asia	Khayhan et al., (2013)
9257	Avian guano	Japan	NA	23	63	East Asia	Khayhan et al., (2013)
WH125	CSF	China	Positive	53	174	East Asia	Khayhan et al., (2013)
WH018	CSF	China	Negative	53	174	East Asia	Khayhan et al., (2013)
WH070	CSF	China	Negative	53	174	East Asia	Khayhan et al., (2013)
WH073	CSF	China	Negative	53	174	East Asia	Khayhan et al., (2013)
WH113	CSF	China	Negative	53	174	East Asia	Khayhan et al., (2013)
WH132	CSF	China	Positive	195	N/A	East Asia	Khayhan et al., (2013)
NIIDCr0013	Clinical	Japan	Unknown	4	4	East Asia	Umeyama et al. Jpn. J. Infect. Dis. 2013
NIIDCr0012	Clinical	Japan	Unknown	85	5	East Asia	Umeyama et al. Jpn. J. Infect. Dis. 2013
NIIDCr0036	Clinical	Japan	Unknown	230	63	East Asia	Umeyama et al. Jpn. J. Infect. Dis. 2013
NIIDCr0029	Clinical	Japan	Unknown	63	63	East Asia	Umeyama et al. Jpn. J. Infect. Dis. 2013
C5	CSF	China	Unknown	31	31	East Asia	Wu et al. Mycoses. 2015
HLJ2	Blood	China	Unknown	63	63	East Asia	Wu et al. Mycoses. 2015
IUM 01-2006	Blood	Italy	Positive	84	5	Europe	Cogliati et al. Medical Mycology. 2013
IUM 99-5690	CSF	Italy	Positive	59	31	Europe	Cogliati et al. Medical Mycology. 2013
IUM 02-2304	CSF	Italy	Positive	75	31	Europe	Cogliati et al. Medical Mycology. 2013
IUM 01-3463	Blood	Italy	Positive	56	63	Europe	Cogliati et al. Medical Mycology. 2013
IUM 99-5716	CSF	Italy	Positive	61	63	Europe	Cogliati et al. Medical Mycology. 2013
IUM 98-3890	CSF	Italy	Positive	62	63	Europe	Cogliati et al. Medical Mycology. 2013
IUM 97-4634	Blood	Italy	Positive	65	63	Europe	Cogliati et al. Medical Mycology. 2013
IUM 97-4874	CSF	Italy	Positive	68	63	Europe	Cogliati et al. Medical Mycology. 2013
IUM 99-5673	CSF	Italy	Positive	69	63	Europe	Cogliati et al. Medical

							Mycology. 2013
IUM 99-5719	CSF	Italy	Positive	138	63	Europe	Cogliati et al. Medical Mycology. 2013
IUM 97-4877	CSF	Italy	Positive	55	174	Europe	Cogliati et al. Medical Mycology. 2013
IUM 00-1072	CSF	Italy	Positive	81	174	Europe	Cogliati et al. Medical Mycology. 2013
AD1-76	CSF	France	Unknown	5	5	Europe	Desnos-Ollivier et al. mBio. 2010
AD4-27A	CSF	France	Unknown	75	31	Europe	Desnos-Ollivier et al. mBio. 2010
AD4-5	CSF	France	Unknown	23	63	Europe	Desnos-Ollivier et al. mBio. 2010
AD1-12	Blood	France	Unknown	324	63	Europe	Desnos-Ollivier et al. mBio. 2010
Isolate1	Unknown	France	Unknown	320	31	Europe	http://mlst.mycologylab.org/
Isolate2	Unknown	France	Unknown	321	63	Europe	http://mlst.mycologylab.org/
Isolate4	Unknown	France	Unknown	323	63	Europe	http://mlst.mycologylab.org/
Isolate3	Unknown	France	Unknown	322	63	Europe	http://mlst.mycologylab.org/
blg7	Avian guano	Belgium	NA	5	5	Europe	Litvintseva et al. Genetics. 2006
blg11	Avian guano	Belgium	NA	32	31	Europe	Litvintseva et al. Genetics. 2006
blg12	Air in zoo	Belgium	NA	23	63	Europe	Litvintseva et al. Genetics. 2006
fr1	Avian guano	France	NA	1	63	Europe	Litvintseva et al. Genetics. 2006
05-0006	CSF	Germany	Positive	4	4	Europe	Sanchini et al. Med Microbiol Immunol. 2014
04-0059	CSF	Germany	Positive	6	4	Europe	Sanchini et al. Med Microbiol Immunol. 2014
09-0007	CSF	Germany	Positive	288	5	Europe	Sanchini et al. Med Microbiol Immunol. 2014
04-0106	CSF	Germany	#N/A	5	5	Europe	Sanchini et al. Med Microbiol Immunol. 2014
09-0552	CSF	Germany	Positive	32	31	Europe	Sanchini et al. Med Microbiol Immunol. 2014
10-0493	CSF	Germany	Positive	23	63	Europe	Sanchini et al. Med Microbiol Immunol. 2014
10-0457	CSF	Germany	Positive	69	63	Europe	Sanchini et al. Med Microbiol Immunol. 2014
07-0325	CSF	Germany	Positive	71	63	Europe	Sanchini et al. Med Microbiol Immunol. 2014
04-0202	CSF	Germany	Negative	2	63	Europe	Sanchini et al. Med Microbiol Immunol. 2014
10-0484	CSF	Germany	Unknown	58	63	Europe	Sanchini et al. Med Microbiol Immunol. 2014
10-0603	CSF	Germany	#N/A	63	63	Europe	Sanchini et al. Med Microbiol Immunol. 2014
08-0251	CSF	Germany	#N/A	67	63	Europe	Sanchini et al. Med Microbiol Immunol. 2014
09-0829	CSF	Germany	#N/A	289	63	Europe	Sanchini et al. Med Microbiol Immunol. 2014
08-0445	CSF	Germany	Negative	290	63	Europe	Sanchini et al. Med Microbiol Immunol. 2014
05-0070	CSF	Germany	Positive	174	174	Europe	Sanchini et al. Med Microbiol

							Immunol. 2014
194_96	Lym node biopsy	Kuwait	Positive	4	4	Middle East	Khayhan et al., (2013)
1608000894	CSF	Qatar	Positive	4	4	Middle East	Khayhan et al., (2013)
1185_04	Endotracheal secretion	Kuwait	Negative	5	5	Middle East	Khayhan et al., (2013)
201_95	Lumbar aspirate	Kuwait	Negative	5	5	Middle East	Khayhan et al., (2013)
1609290340	CSF	Qatar	Negative	5	5	Middle East	Khayhan et al., (2013)
1607001262	CSF	Qatar	Positive	5	5	Middle East	Khayhan et al., (2013)
481_03	CSF	Kuwait	Positive	93	31	Middle East	Khayhan et al., (2013)
1605202443	CSF	Qatar	Negative	31	31	Middle East	Khayhan et al., (2013)
1608000352	CSF	Qatar	Negative	31	31	Middle East	Khayhan et al., (2013)
177_02	Wound swab	Kuwait	Negative	185	31	Middle East	Khayhan et al., (2013)
8_92	CSF	Kuwait	Negative	23	63	Middle East	Khayhan et al., (2013)
110_99	Blood	Kuwait	Negative	69	63	Middle East	Khayhan et al., (2013)
200_16	Lym node biopsy	Kuwait	Positive	175	174	Middle East	Khayhan et al., (2013)
2365_08	CSF	Kuwait	Negative	174	174	Middle East	Khayhan et al., (2013)
1589_04	CSF	Kuwait	Negative	192	174	Middle East	Khayhan et al., (2013)
A3 38-20	Avian guano	USA	NA	1	63	North America	Litvintseva et al. Genetics. 2006
A5 35-17	Avian guano	USA	NA	5	5	North America	Litvintseva et al. Genetics. 2006 Litvintseva et al. PlosOne. 2011
A2 102-5	Avian guano	USA	NA	15	31	North America	Litvintseva et al. Genetics. 2006 Litvintseva et al. PlosOne. 2011
A3 1-1	Avian guano	USA	NA	23	63	North America	Litvintseva et al. Genetics. 2006 Litvintseva et al. PlosOne. 2011
A4 1-12	Avian guano	USA	NA	58	63	North America	Litvintseva et al. Genetics. 2006 Litvintseva et al. PlosOne. 2011
A1	Avian guano	USA	NA	2	63	North America	Litvintseva et al. Genetics. 2006 Simwami et al. PLoS Pathogens. 2011
JS18	Veterinay	USA	NA	39	31	North America	Singer et al. J Clin Microbiol. 2014
JS71	Veterinay	USA	NA	32	31	North America	Singer et al. J Clin Microbiol. 2014
JS25	Veterinay	USA	NA	64	63	North America	Singer et al. J Clin Microbiol. 2014
UFTM 14.48	Urine	Brazil	Positive	5	5	South America	Ferreira-Paim et al, PlosNTD,2017
UFTM 14.153	CSF	Brazil	Positive	5	5	South America	Ferreira-Paim et al, PlosNTD,2017

UFTM 14.32	Enviromental	Brazil	NA	5	5	South America	Ferreira-Paim et al, PlosNTD,2017
UFTM 14.132	CSF	Brazil	Positive	31	31	South America	Ferreira-Paim et al, PlosNTD,2017
UFTM 14.133	CSF	Brazil	Positive	31	31	South America	Ferreira-Paim et al, PlosNTD,2017
UFTM 14.113	CSF	Brazil	Positive	39	31	South America	Ferreira-Paim et al, PlosNTD,2017
UFTM 14.96	CSF	Brazil	Positive	32	31	South America	Ferreira-Paim et al, PlosNTD,2017
UFTM 14.140	CSF	Brazil	Positive	32	31	South America	Ferreira-Paim et al, PlosNTD,2017
UFTM 14.46	Urine	Brazil	Positive	93	31	South America	Ferreira-Paim et al, PlosNTD,2017
UFTM 14.47	Urine	Brazil	Positive	93	31	South America	Ferreira-Paim et al, PlosNTD,2017
UFTM 14.49	Urine	Brazil	Positive	93	31	South America	Ferreira-Paim et al, PlosNTD,2017
UFTM 14.50	Urine	Brazil	Positive	93	31	South America	Ferreira-Paim et al, PlosNTD,2017
UFTM 14.51	Urine	Brazil	Positive	93	31	South America	Ferreira-Paim et al, PlosNTD,2017
UFTM 14.52	Urine	Brazil	Positive	93	31	South America	Ferreira-Paim et al, PlosNTD,2017
UFTM 14.55	Urine	Brazil	Positive	93	31	South America	Ferreira-Paim et al, PlosNTD,2017
UFTM 14.61	Blood	Brazil	Positive	93	31	South America	Ferreira-Paim et al, PlosNTD,2017
UFTM 14.62	Blood	Brazil	Positive	93	31	South America	Ferreira-Paim et al, PlosNTD,2017
UFTM 14.64	Blood	Brazil	Positive	93	31	South America	Ferreira-Paim et al, PlosNTD,2017
UFTM 14.66	Blood	Brazil	Positive	93	31	South America	Ferreira-Paim et al, PlosNTD,2017
UFTM 14.67	Blood	Brazil	Positive	93	31	South America	Ferreira-Paim et al, PlosNTD,2017
UFTM 14.68	Blood	Brazil	Positive	93	31	South America	Ferreira-Paim et al, PlosNTD,2017
UFTM 14.69	Blood	Brazil	Positive	93	31	South America	Ferreira-Paim et al, PlosNTD,2017
UFTM 14.71	Blood	Brazil	Positive	93	31	South America	Ferreira-Paim et al, PlosNTD,2017
UFTM 14.73	Blood	Brazil	Positive	93	31	South America	Ferreira-Paim et al, PlosNTD,2017
UFTM 14.77	CSF	Brazil	Positive	93	31	South America	Ferreira-Paim et al, PlosNTD,2017
UFTM 14.80	CSF	Brazil	Positive	93	31	South America	Ferreira-Paim et al, PlosNTD,2017
UFTM 14.81	CSF	Brazil	Positive	93	31	South America	Ferreira-Paim et al, PlosNTD,2017
UFTM 14.84	CSF	Brazil	Positive	93	31	South America	Ferreira-Paim et al, PlosNTD,2017
UFTM 14.85	CSF	Brazil	Positive	93	31	South America	Ferreira-Paim et al, PlosNTD,2017
UFTM 14.89	CSF	Brazil	Positive	93	31	South America	Ferreira-Paim et al, PlosNTD,2017
UFTM 14.92	CSF	Brazil	Positive	93	31	South America	Ferreira-Paim et al, PlosNTD,2017

UFTM 14.93	CSF	Brazil	Positive	93	31	South America	Ferreira-Paim et al, PlosNTD,2017
UFTM 14.95	CSF	Brazil	Positive	93	31	South America	Ferreira-Paim et al, PlosNTD,2017
UFTM 14.97	CSF	Brazil	Positive	93	31	South America	Ferreira-Paim et al, PlosNTD,2017
UFTM 14.99	CSF	Brazil	Positive	93	31	South America	Ferreira-Paim et al, PlosNTD,2017
UFTM 14.100	CSF	Brazil	Positive	93	31	South America	Ferreira-Paim et al, PlosNTD,2017
UFTM 14.102	CSF	Brazil	Positive	93	31	South America	Ferreira-Paim et al, PlosNTD,2017
UFTM 14.104	CSF	Brazil	Positive	93	31	South America	Ferreira-Paim et al, PlosNTD,2017
UFTM 14.106	CSF	Brazil	Positive	93	31	South America	Ferreira-Paim et al, PlosNTD,2017
UFTM 14.107	CSF	Brazil	Positive	93	31	South America	Ferreira-Paim et al, PlosNTD,2017
UFTM 14.108	CSF	Brazil	Positive	93	31	South America	Ferreira-Paim et al, PlosNTD,2017
UFTM 14.115	CSF	Brazil	Positive	93	31	South America	Ferreira-Paim et al, PlosNTD,2017
UFTM 14.116	CSF	Brazil	Positive	93	31	South America	Ferreira-Paim et al, PlosNTD,2017
UFTM 14.119	CSF	Brazil	Positive	93	31	South America	Ferreira-Paim et al, PlosNTD,2017
UFTM 14.122	CSF	Brazil	Positive	93	31	South America	Ferreira-Paim et al, PlosNTD,2017
UFTM 14.123	CSF	Brazil	Positive	93	31	South America	Ferreira-Paim et al, PlosNTD,2017
UFTM 14.125	CSF	Brazil	Positive	93	31	South America	Ferreira-Paim et al, PlosNTD,2017
UFTM 14.126	CSF	Brazil	Positive	93	31	South America	Ferreira-Paim et al, PlosNTD,2017
UFTM 14.127	CSF	Brazil	Positive	93	31	South America	Ferreira-Paim et al, PlosNTD,2017
UFTM 14.128	CSF	Brazil	Positive	93	31	South America	Ferreira-Paim et al, PlosNTD,2017
UFTM 14.129	CSF	Brazil	Positive	93	31	South America	Ferreira-Paim et al, PlosNTD,2017
UFTM 14.131	CSF	Brazil	Positive	93	31	South America	Ferreira-Paim et al, PlosNTD,2017
UFTM 14.137	CSF	Brazil	Positive	93	31	South America	Ferreira-Paim et al, PlosNTD,2017
UFTM 14.138	CSF	Brazil	Positive	93	31	South America	Ferreira-Paim et al, PlosNTD,2017
UFTM 14.139	CSF	Brazil	Positive	93	31	South America	Ferreira-Paim et al, PlosNTD,2017
UFTM 14.142	CSF	Brazil	Positive	93	31	South America	Ferreira-Paim et al, PlosNTD,2017
UFTM 14.143	CSF	Brazil	Positive	93	31	South America	Ferreira-Paim et al, PlosNTD,2017
UFTM 14.144	CSF	Brazil	Positive	93	31	South America	Ferreira-Paim et al, PlosNTD,2017
UFTM 14.145	CSF	Brazil	Positive	93	31	South America	Ferreira-Paim et al, PlosNTD,2017
UFTM 14.146	CSF	Brazil	Positive	93	31	South America	Ferreira-Paim et al, PlosNTD,2017

UFTM 14.148	CSF	Brazil	Positive	93	31	South America	Ferreira-Paim et al, PlosNTD,2017
UFTM 14.149	CSF	Brazil	Positive	93	31	South America	Ferreira-Paim et al, PlosNTD,2017
UFTM 14.150	CSF	Brazil	Positive	93	31	South America	Ferreira-Paim et al, PlosNTD,2017
UFTM 14.151	CSF	Brazil	Positive	93	31	South America	Ferreira-Paim et al, PlosNTD,2017
UFTM 14.152	CSF	Brazil	Positive	93	31	South America	Ferreira-Paim et al, PlosNTD,2017
UFTM 14.156	CSF	Brazil	Positive	93	31	South America	Ferreira-Paim et al, PlosNTD,2017
UFTM 14.157	CSF	Brazil	Positive	93	31	South America	Ferreira-Paim et al, PlosNTD,2017
UFTM 14.158	CSF	Brazil	Positive	93	31	South America	Ferreira-Paim et al, PlosNTD,2017
UFTM 14.160	CSF	Brazil	Positive	93	31	South America	Ferreira-Paim et al, PlosNTD,2017
UFTM 14.162	CSF	Brazil	Positive	93	31	South America	Ferreira-Paim et al, PlosNTD,2017
UFTM 14.76	CSF	Brazil	Positive	540	31	South America	Ferreira-Paim et al, PlosNTD,2017
UFTM 14.44	Enviromental	Brazil	NA	15	31	South America	Ferreira-Paim et al, PlosNTD,2017
UFTM 14.94	CSF	Brazil	Kidney transplant/Diabets mellitus	39	31	South America	Ferreira-Paim et al, PlosNTD,2017
UFTM 14.130	CSF	Brazil	Crohn's disease	39	31	South America	Ferreira-Paim et al, PlosNTD,2017
UFTM 14.15	Enviromental	Brazil	NA	93	31	South America	Ferreira-Paim et al, PlosNTD,2017
UFTM 14.16	Enviromental	Brazil	NA	93	31	South America	Ferreira-Paim et al, PlosNTD,2017
UFTM 14.25	Enviromental	Brazil	NA	93	31	South America	Ferreira-Paim et al, PlosNTD,2017
UFTM 14.27	Enviromental	Brazil	NA	93	31	South America	Ferreira-Paim et al, PlosNTD,2017
UFTM 14.29	Enviromental	Brazil	NA	93	31	South America	Ferreira-Paim et al, PlosNTD,2017
UFTM 14.39	Enviromental	Brazil	NA	93	31	South America	Ferreira-Paim et al, PlosNTD,2017
UFTM 14.58	Skin	Brazil	Kidney transplant	93	31	South America	Ferreira-Paim et al, PlosNTD,2017
UFTM 14.65	Blood	Brazil	Diabets mellitus	93	31	South America	Ferreira-Paim et al, PlosNTD,2017
UFTM 14.91	CSF	Brazil	Unknown	93	31	South America	Ferreira-Paim et al, PlosNTD,2017
UFTM 14.101	CSF	Brazil	Systemic Lupus Erythematosus	93	31	South America	Ferreira-Paim et al, PlosNTD,2017
UFTM 14.110	CSF	Brazil	Unknown	93	31	South America	Ferreira-Paim et al, PlosNTD,2017
UFTM 14.111	CSF	Brazil	Diabets mellitus/Nefritis	93	31	South America	Ferreira-Paim et al, PlosNTD,2017
UFTM 14.134	CSF	Brazil	Unknown	93	31	South America	Ferreira-Paim et al, PlosNTD,2017
UFTM 14.135	CSF	Brazil	Unknown	93	31	South America	Ferreira-Paim et al, PlosNTD,2017
UFTM 14.154	CSF	Brazil	Unknown	93	31	South America	Ferreira-Paim et al, PlosNTD,2017

UFTM 14.17	Enviromental	Brazil	NA	77	31	South America	Ferreira-Paim et al, PlosNTD,2017
UFTM 14.18	Enviromental	Brazil	NA	77	31	South America	Ferreira-Paim et al, PlosNTD,2017
UFTM 14.19	Enviromental	Brazil	NA	77	31	South America	Ferreira-Paim et al, PlosNTD,2017
UFTM 14.22	Enviromental	Brazil	NA	77	31	South America	Ferreira-Paim et al, PlosNTD,2017
UFTM 14.23	Enviromental	Brazil	NA	77	31	South America	Ferreira-Paim et al, PlosNTD,2017
UFTM 14.24	Enviromental	Brazil	NA	77	31	South America	Ferreira-Paim et al, PlosNTD,2017
UFTM 14.26	Enviromental	Brazil	NA	77	31	South America	Ferreira-Paim et al, PlosNTD,2017
UFTM 14.30	Enviromental	Brazil	NA	77	31	South America	Ferreira-Paim et al, PlosNTD,2017
UFTM 14.31	Enviromental	Brazil	NA	77	31	South America	Ferreira-Paim et al, PlosNTD,2017
UFTM 14.33	Enviromental	Brazil	NA	77	31	South America	Ferreira-Paim et al, PlosNTD,2017
UFTM 14.34	Enviromental	Brazil	NA	77	31	South America	Ferreira-Paim et al, PlosNTD,2017
UFTM 14.36	Enviromental	Brazil	NA	77	31	South America	Ferreira-Paim et al, PlosNTD,2017
UFTM 14.37	Enviromental	Brazil	NA	77	31	South America	Ferreira-Paim et al, PlosNTD,2017
UFTM 14.63	CSF	Brazil	Positive	23	63	South America	Ferreira-Paim et al, PlosNTD,2017
UFTM 14.70	Blood	Brazil	Positive	23	63	South America	Ferreira-Paim et al, PlosNTD,2017
UFTM 14.72	Blood	Brazil	Positive	23	63	South America	Ferreira-Paim et al, PlosNTD,2017
UFTM 14.87	CSF	Brazil	Positive	23	63	South America	Ferreira-Paim et al, PlosNTD,2017
UFTM 14.103	CSF	Brazil	Positive	23	63	South America	Ferreira-Paim et al, PlosNTD,2017
UFTM 14.117	CSF	Brazil	Positive	23	63	South America	Ferreira-Paim et al, PlosNTD,2017
UFTM 14.45	Urine	Brazil	Positive	63	63	South America	Ferreira-Paim et al, PlosNTD,2017
UFTM 14.57	BAL	Brazil	Positive	63	63	South America	Ferreira-Paim et al, PlosNTD,2017
UFTM 14.79	CSF	Brazil	Positive	63	63	South America	Ferreira-Paim et al, PlosNTD,2017
UFTM 14.83	CSF	Brazil	Positive	63	63	South America	Ferreira-Paim et al, PlosNTD,2017
UFTM 14.121	CSF	Brazil	Positive	63	63	South America	Ferreira-Paim et al, PlosNTD,2017
UFTM 14.159	CSF	Brazil	Positive	63	63	South America	Ferreira-Paim et al, PlosNTD,2017
UFTM 14.53	Urine	Brazil	Positive	71	63	South America	Ferreira-Paim et al, PlosNTD,2017
UFTM 14.98	CSF	Brazil	Positive	71	63	South America	Ferreira-Paim et al, PlosNTD,2017
UFTM 14.161	CSF	Brazil	Positive	71	63	South America	Ferreira-Paim et al, PlosNTD,2017
UFTM 14.147	CSF	Brazil	Positive	289	63	South America	Ferreira-Paim et al, PlosNTD,2017

UFTM 14.90	CSF	Brazil	Kidney transplant	23	63	South America	Ferreira-Paim et al, PlosNTD,2017
UFTM 14.43	Enviromental	Brazil	NA	71	63	South America	Ferreira-Paim et al, PlosNTD,2017
UFTM 14.20	Enviromental	Brazil	NA	2	63	South America	Ferreira-Paim et al, PlosNTD,2017
UFTM 14.09	Enviromental	Brazil	NA	15	31	South America	Ferreira-paim et. al. Mycoses. 2011
UFTM 14.10	Enviromental	Brazil	NA	31	31	South America	Ferreira-paim et. al. Mycoses. 2011
UFTM 14.02	Enviromental	Brazil	NA	93	31	South America	Ferreira-paim et. al. Mycoses. 2011
UFTM 14.03	Enviromental	Brazil	NA	93	31	South America	Ferreira-paim et. al. Mycoses. 2011
UFTM 14.04	Enviromental	Brazil	NA	93	31	South America	Ferreira-paim et. al. Mycoses. 2011
UFTM 14.07	Enviromental	Brazil	NA	93	31	South America	Ferreira-paim et. al. Mycoses. 2011
UFTM 14.06	Enviromental	Brazil	NA	77	31	South America	Ferreira-paim et. al. Mycoses. 2011
UFTM 14.08	Enviromental	Brazil	NA	77	31	South America	Ferreira-paim et. al. Mycoses. 2011
UFTM 14.11	Enviromental	Brazil	NA	77	31	South America	Ferreira-paim et. al. Mycoses. 2011
UFTM 14.13	Enviromental	Brazil	NA	77	31	South America	Ferreira-paim et. al. Mycoses. 2011
br2362	Unknown	Brazil	Unknown	32	31	South America	Litvintseva et al. Genetics. 2006
arg1366	Unknown	Argentina	Unknown	2	63	South America	Litvintseva et al. Genetics. 2006
25_316	CSF	India	Negative	4	4	South Asia	Khayhan et al., (2013)
25_372	CSF	India	Positive	6	4	South Asia	Khayhan et al., (2013)
25_373	CSF	India	Positive	6	4	South Asia	Khayhan et al., (2013)
25_311	CSF	India	Negative	189	4	South Asia	Khayhan et al., (2013)
25_104	CSF	India	Positive	77	31	South Asia	Khayhan et al., (2013)
25_244	CSF	India	Positive	77	31	South Asia	Khayhan et al., (2013)
25_365	CSF	India	Positive	77	31	South Asia	Khayhan et al., (2013)
25_369	CSF	India	Positive	77	31	South Asia	Khayhan et al., (2013)
25_61	CSF	India	Positive	77	31	South Asia	Khayhan et al., (2013)
25_63	CSF	India	Positive	77	31	South Asia	Khayhan et al., (2013)
25_229	CSF	India	Positive	31	31	South Asia	Khayhan et al., (2013)
25_357	CSF	India	Positive	31	31	South Asia	Khayhan et al., (2013)
25_370	CSF	India	Positive	31	31	South Asia	Khayhan et al., (2013)
25_228	CSF	India	Positive	93	31	South Asia	Khayhan et al., (2013)
25_237	CSF	India	Positive	93	31	South Asia	Khayhan et al., (2013)
25_239	CSF	India	Positive	93	31	South Asia	Khayhan et al., (2013)
25_261	CSF	India	Positive	93	31	South Asia	Khayhan et al., (2013)
25_272	BAL	India	Positive	93	31	South Asia	Khayhan et al., (2013)
25_277	CSF	India	Positive	93	31	South Asia	Khayhan et al., (2013)

25_290	CSF	India	Positive	93	31	South Asia	Khayhan et al., (2013)
25_292	CSF	India	Positive	93	31	South Asia	Khayhan et al., (2013)
25_302	CSF	India	Positive	93	31	South Asia	Khayhan et al., (2013)
25_304	CSF	India	Positive	93	31	South Asia	Khayhan et al., (2013)
25_308	CSF	India	Positive	93	31	South Asia	Khayhan et al., (2013)
25_312	CSF	India	Positive	93	31	South Asia	Khayhan et al., (2013)
25_313	CSF	India	Positive	93	31	South Asia	Khayhan et al., (2013)
25_334	CSF	India	Positive	93	31	South Asia	Khayhan et al., (2013)
25_336	CSF	India	Positive	93	31	South Asia	Khayhan et al., (2013)
25_337	CSF	India	Positive	93	31	South Asia	Khayhan et al., (2013)
25_341	CSF	India	Positive	93	31	South Asia	Khayhan et al., (2013)
25_344	BAL	India	Positive	93	31	South Asia	Khayhan et al., (2013)
25_356	CSF	India	Positive	93	31	South Asia	Khayhan et al., (2013)
25_358	CSF	India	Positive	93	31	South Asia	Khayhan et al., (2013)
25_367	CSF	India	Positive	93	31	South Asia	Khayhan et al., (2013)
25_368	CSF	India	Positive	93	31	South Asia	Khayhan et al., (2013)
25_105	CSF	India	Negative	77	31	South Asia	Khayhan et al., (2013)
25_110	CSF	India	Negative	77	31	South Asia	Khayhan et al., (2013)
25_52	CSF	India	Negative	77	31	South Asia	Khayhan et al., (2013)
25_53	CSF	India	Negative	77	31	South Asia	Khayhan et al., (2013)
25_62	CSF	India	Negative	77	31	South Asia	Khayhan et al., (2013)
25_84	Blood	India	Negative	77	31	South Asia	Khayhan et al., (2013)
25_14	Clinical	India	Unknown	77	31	South Asia	Khayhan et al., (2013)
25_40	Unknown	India	Unknown	77	31	South Asia	Khayhan et al., (2013)
25_18	CSF	India	Negative	31	31	South Asia	Khayhan et al., (2013)
25_266	CSF	India	Negative	31	31	South Asia	Khayhan et al., (2013)
25_298	CSF	India	Negative	31	31	South Asia	Khayhan et al., (2013)
25_355	CSF	India	Negative	31	31	South Asia	Khayhan et al., (2013)
25_299	CSF	India	Negative	93	31	South Asia	Khayhan et al., (2013)
25_339	CSF	India	Negative	93	31	South Asia	Khayhan et al., (2013)
25_371	CSF	India	Negative	93	31	South Asia	Khayhan et al., (2013)
25_49	CSF	India	Negative	93	31	South Asia	Khayhan et al., (2013)
25_50	CSF	India	Negative	93	31	South Asia	Khayhan et al., (2013)
25_86	CSF	India	Negative	93	31	South Asia	Khayhan et al., (2013)
25_78	Unknown	India	Unknown	93	31	South Asia	Khayhan et al., (2013)
25_33	CSF	India	Negative	177	31	South Asia	Khayhan et al., (2013)
25_340	CSF	India	Negative	187	31	South Asia	Khayhan et al., (2013)
25_328	CSF	India	Positive	71	63	South Asia	Khayhan et al., (2013)

25_296	CSF	India	Positive	174	174	South Asia	Khayhan et al., (2013)
25_17	Blood	India	Negative	174	174	South Asia	Khayhan et al., (2013)
25_240	CSF	India	Negative	174	174	South Asia	Khayhan et al., (2013)
25_291	CSF	India	Negative	40	N/A	South Asia	Khayhan et al., (2013)
in2629	CSF	India	Positive	38	31	South Asia	Litvintseva et al. Genetics. 2006
11109	Clinical	Thailand	Unknown	4	4	Southeast Asia	Khayhan et al., (2013)
11112	Clinical	Thailand	Unknown	4	4	Southeast Asia	Khayhan et al., (2013)
109A	Avian guano	Thailand	NA	4	4	Southeast Asia	Khayhan et al., (2013)
109C	Avian guano	Thailand	NA	4	4	Southeast Asia	Khayhan et al., (2013)
110C	Avian guano	Thailand	NA	4	4	Southeast Asia	Khayhan et al., (2013)
110D	Avian guano	Thailand	NA	4	4	Southeast Asia	Khayhan et al., (2013)
130C	Avian guano	Thailand	NA	4	4	Southeast Asia	Khayhan et al., (2013)
4_231	Clinical	Thailand	Unknown	4	4	Southeast Asia	Khayhan et al., (2013)
4_253	Clinical	Thailand	Unknown	4	4	Southeast Asia	Khayhan et al., (2013)
4_319	Clinical	Thailand	Unknown	4	4	Southeast Asia	Khayhan et al., (2013)
4_381	Clinical	Thailand	Unknown	4	4	Southeast Asia	Khayhan et al., (2013)
96B	Avian guano	Thailand	NA	4	4	Southeast Asia	Khayhan et al., (2013)
1111I_08	Blood	Thailand	Negative	4	4	Southeast Asia	Khayhan et al., (2013)
D12	Avian guano	Thailand	NA	4	4	Southeast Asia	Khayhan et al., (2013)
D14	Avian guano	Thailand	NA	4	4	Southeast Asia	Khayhan et al., (2013)
D2	Avian guano	Thailand	NA	4	4	Southeast Asia	Khayhan et al., (2013)
D27	Avian guano	Thailand	NA	4	4	Southeast Asia	Khayhan et al., (2013)
D28	Avian guano	Thailand	NA	4	4	Southeast Asia	Khayhan et al., (2013)
D3	Avian guano	Thailand	NA	4	4	Southeast Asia	Khayhan et al., (2013)
D31	Avian guano	Thailand	NA	4	4	Southeast Asia	Khayhan et al., (2013)
D43	Avian guano	Thailand	NA	4	4	Southeast Asia	Khayhan et al., (2013)
D46	Avian guano	Thailand	NA	4	4	Southeast Asia	Khayhan et al., (2013)
D69	Avian guano	Thailand	NA	4	4	Southeast Asia	Khayhan et al., (2013)
D71	Avian guano	Thailand	NA	4	4	Southeast Asia	Khayhan et al., (2013)
D73	Avian guano	Thailand	NA	4	4	Southeast Asia	Khayhan et al., (2013)

P6	Clinical	Thailand	Unknown	4	4	Southeast Asia	Khayhan et al., (2013)
PG21	Avian guano	Thailand	NA	4	4	Southeast Asia	Khayhan et al., (2013)
PG26	Avian guano	Thailand	NA	4	4	Southeast Asia	Khayhan et al., (2013)
PG3	Avian guano	Thailand	NA	4	4	Southeast Asia	Khayhan et al., (2013)
PG46	Avian guano	Thailand	NA	4	4	Southeast Asia	Khayhan et al., (2013)
2895I_08	Blood	Thailand	Negative	4	4	Southeast Asia	Khayhan et al., (2013)
268	CSF	Indonesia	Positive	4	4	Southeast Asia	Khayhan et al., (2013)
328	CSF	Indonesia	Positive	4	4	Southeast Asia	Khayhan et al., (2013)
544	CSF	Indonesia	Positive	4	4	Southeast Asia	Khayhan et al., (2013)
612	CSF	Indonesia	Positive	4	4	Southeast Asia	Khayhan et al., (2013)
778	CSF	Indonesia	Positive	4	4	Southeast Asia	Khayhan et al., (2013)
2597	CSF	Indonesia	Positive	4	4	Southeast Asia	Khayhan et al., (2013)
2606	CSF	Indonesia	Positive	4	4	Southeast Asia	Khayhan et al., (2013)
Jakarta	CSF	Indonesia	Positive	4	4	Southeast Asia	Khayhan et al., (2013)
267	CSF	Indonesia	Positive	6	4	Southeast Asia	Khayhan et al., (2013)
2339	CSF	Indonesia	Positive	6	4	Southeast Asia	Khayhan et al., (2013)
2594	CSF	Indonesia	Positive	6	4	Southeast Asia	Khayhan et al., (2013)
3187	CSF	Indonesia	Positive	6	4	Southeast Asia	Khayhan et al., (2013)
Jakarta (H)	Blood	Indonesia	Positive	6	4	Southeast Asia	Khayhan et al., (2013)
Jakarta (KT)	Skin	Indonesia	Positive	6	4	Southeast Asia	Khayhan et al., (2013)
Jakarta (KT)	Skin	Indonesia	Positive	6	4	Southeast Asia	Khayhan et al., (2013)
Jakarta (P)	Blood	Indonesia	Positive	6	4	Southeast Asia	Khayhan et al., (2013)
Jakarta KLT	Skin	Indonesia	Positive	6	4	Southeast Asia	Khayhan et al., (2013)
Jakarta RTL	Skin	Indonesia	Positive	6	4	Southeast Asia	Khayhan et al., (2013)
44	Avian guano	Thailand	NA	6	4	Southeast Asia	Khayhan et al., (2013)
269	Clinical	Thailand	Unknown	6	4	Southeast Asia	Khayhan et al., (2013)
1219	Clinical	Thailand	Unknown	6	4	Southeast Asia	Khayhan et al., (2013)
1_587	Clinical	Thailand	Unknown	6	4	Southeast Asia	Khayhan et al., (2013)
1_588	Clinical	Thailand	Unknown	6	4	Southeast Asia	Khayhan et al., (2013)

1_846	Clinical	Thailand	Unknown	6	4	Southeast Asia	Khayhan et al., (2013)
2551_07	Avian guano	Thailand	NA	6	4	Southeast Asia	Khayhan et al., (2013)
4_187	Clinical	Thailand	Unknown	6	4	Southeast Asia	Khayhan et al., (2013)
4_202	Clinical	Thailand	Unknown	6	4	Southeast Asia	Khayhan et al., (2013)
4_315	Clinical	Thailand	Unknown	6	4	Southeast Asia	Khayhan et al., (2013)
4_83	Clinical	Thailand	Unknown	6	4	Southeast Asia	Khayhan et al., (2013)
D1	Avian guano	Thailand	NA	6	4	Southeast Asia	Khayhan et al., (2013)
D18	Avian guano	Thailand	NA	6	4	Southeast Asia	Khayhan et al., (2013)
D21	Avian guano	Thailand	NA	6	4	Southeast Asia	Khayhan et al., (2013)
D22	Avian guano	Thailand	NA	6	4	Southeast Asia	Khayhan et al., (2013)
D26	Avian guano	Thailand	NA	6	4	Southeast Asia	Khayhan et al., (2013)
D30	Avian guano	Thailand	NA	6	4	Southeast Asia	Khayhan et al., (2013)
D33	Avian guano	Thailand	NA	6	4	Southeast Asia	Khayhan et al., (2013)
D34	Avian guano	Thailand	NA	6	4	Southeast Asia	Khayhan et al., (2013)
D35	Avian guano	Thailand	NA	6	4	Southeast Asia	Khayhan et al., (2013)
D36	Avian guano	Thailand	NA	6	4	Southeast Asia	Khayhan et al., (2013)
D41	Avian guano	Thailand	NA	6	4	Southeast Asia	Khayhan et al., (2013)
D64	Avian guano	Thailand	NA	6	4	Southeast Asia	Khayhan et al., (2013)
D76	Avian guano	Thailand	NA	6	4	Southeast Asia	Khayhan et al., (2013)
PG1	Avian guano	Thailand	NA	6	4	Southeast Asia	Khayhan et al., (2013)
PG2	Avian guano	Thailand	NA	6	4	Southeast Asia	Khayhan et al., (2013)
PG32	Avian guano	Thailand	NA	6	4	Southeast Asia	Khayhan et al., (2013)
20662_07	Blood	Thailand	Positive	4	4	Southeast Asia	Khayhan et al., (2013)
28170_07	CSF	Thailand	Positive	4	4	Southeast Asia	Khayhan et al., (2013)
4500_07	Blood	Thailand	Positive	4	4	Southeast Asia	Khayhan et al., (2013)
50NC2	CSF	Thailand	Positive	4	4	Southeast Asia	Khayhan et al., (2013)
50NC5	CSF	Thailand	Positive	4	4	Southeast Asia	Khayhan et al., (2013)
CM10	CSF	Thailand	Positive	4	4	Southeast Asia	Khayhan et al., (2013)
CM11	CSF	Thailand	Positive	4	4	Southeast Asia	Khayhan et al., (2013)

CM14	CSF	Thailand	Positive	4	4	Southeast Asia	Khayhan et al., (2013)
CM15	CSF	Thailand	Positive	4	4	Southeast Asia	Khayhan et al., (2013)
CM16	CSF	Thailand	Positive	4	4	Southeast Asia	Khayhan et al., (2013)
CM2	CSF	Thailand	Positive	4	4	Southeast Asia	Khayhan et al., (2013)
CM20	CSF	Thailand	Positive	4	4	Southeast Asia	Khayhan et al., (2013)
CM24	CSF	Thailand	Positive	4	4	Southeast Asia	Khayhan et al., (2013)
CM27	CSF	Thailand	Positive	4	4	Southeast Asia	Khayhan et al., (2013)
CM28	CSF	Thailand	Positive	4	4	Southeast Asia	Khayhan et al., (2013)
CM29	CSF	Thailand	Positive	4	4	Southeast Asia	Khayhan et al., (2013)
CM3	CSF	Thailand	Positive	4	4	Southeast Asia	Khayhan et al., (2013)
CM32	CSF	Thailand	Positive	4	4	Southeast Asia	Khayhan et al., (2013)
CM34	CSF	Thailand	Positive	4	4	Southeast Asia	Khayhan et al., (2013)
CM36	CSF	Thailand	Positive	4	4	Southeast Asia	Khayhan et al., (2013)
CM4	CSF	Thailand	Positive	4	4	Southeast Asia	Khayhan et al., (2013)
CM45	CSF	Thailand	Positive	4	4	Southeast Asia	Khayhan et al., (2013)
CM5	CSF	Thailand	Positive	4	4	Southeast Asia	Khayhan et al., (2013)
CM50	CSF	Thailand	Positive	4	4	Southeast Asia	Khayhan et al., (2013)
CM52	CSF	Thailand	Positive	4	4	Southeast Asia	Khayhan et al., (2013)
CM60	CSF	Thailand	Positive	4	4	Southeast Asia	Khayhan et al., (2013)
CM64	CSF	Thailand	Positive	4	4	Southeast Asia	Khayhan et al., (2013)
CN49008	CSF	Thailand	Positive	4	4	Southeast Asia	Khayhan et al., (2013)
CN4902	CSF	Thailand	Positive	4	4	Southeast Asia	Khayhan et al., (2013)
CN4904	CSF	Thailand	Positive	4	4	Southeast Asia	Khayhan et al., (2013)
CN4905	CSF	Thailand	Positive	4	4	Southeast Asia	Khayhan et al., (2013)
CN4907	CSF	Thailand	Positive	4	4	Southeast Asia	Khayhan et al., (2013)
CN4909	CSF	Thailand	Positive	4	4	Southeast Asia	Khayhan et al., (2013)
CN4914	CSF	Thailand	Positive	4	4	Southeast Asia	Khayhan et al., (2013)
CN4915	CSF	Thailand	Positive	4	4	Southeast Asia	Khayhan et al., (2013)
CN4927	CSF	Thailand	Positive	4	4	Southeast Asia	Khayhan et al., (2013)

CN4931	CSF	Thailand	Positive	4	4	Southeast Asia	Khayhan et al., (2013)
CN4932	CSF	Thailand	Positive	4	4	Southeast Asia	Khayhan et al., (2013)
CN4933	CSF	Thailand	Positive	4	4	Southeast Asia	Khayhan et al., (2013)
CN4934	CSF	Thailand	Positive	4	4	Southeast Asia	Khayhan et al., (2013)
CN4936	CSF	Thailand	Positive	4	4	Southeast Asia	Khayhan et al., (2013)
CN4937	CSF	Thailand	Positive	4	4	Southeast Asia	Khayhan et al., (2013)
CN4938	CSF	Thailand	Positive	4	4	Southeast Asia	Khayhan et al., (2013)
CN4949	CSF	Thailand	Positive	4	4	Southeast Asia	Khayhan et al., (2013)
CN4950	CSF	Thailand	Positive	4	4	Southeast Asia	Khayhan et al., (2013)
4_9	Clinical	Thailand	Unknown	82	4	Southeast Asia	Khayhan et al., (2013)
CN4952	CSF	Thailand	Positive	4	4	Southeast Asia	Khayhan et al., (2013)
CN4954	CSF	Thailand	Positive	4	4	Southeast Asia	Khayhan et al., (2013)
CN4955	BAL	Thailand	Positive	4	4	Southeast Asia	Khayhan et al., (2013)
CN4956	CSF	Thailand	Positive	4	4	Southeast Asia	Khayhan et al., (2013)
CN4957	CSF	Thailand	Positive	4	4	Southeast Asia	Khayhan et al., (2013)
CN4968	CSF	Thailand	Positive	4	4	Southeast Asia	Khayhan et al., (2013)
CN4970	CSF	Thailand	Positive	4	4	Southeast Asia	Khayhan et al., (2013)
CN5001	CSF	Thailand	Positive	4	4	Southeast Asia	Khayhan et al., (2013)
CN5002	Blood	Thailand	Positive	4	4	Southeast Asia	Khayhan et al., (2013)
CN5003	Blood	Thailand	Positive	4	4	Southeast Asia	Khayhan et al., (2013)
CN5005	Blood	Thailand	Positive	4	4	Southeast Asia	Khayhan et al., (2013)
CN5009	Blood	Thailand	Positive	4	4	Southeast Asia	Khayhan et al., (2013)
CN5011	Blood	Thailand	Positive	4	4	Southeast Asia	Khayhan et al., (2013)
CN5013	CSF	Thailand	Positive	4	4	Southeast Asia	Khayhan et al., (2013)
CN5014	Blood	Thailand	Positive	4	4	Southeast Asia	Khayhan et al., (2013)
CN5017	CSF	Thailand	Positive	4	4	Southeast Asia	Khayhan et al., (2013)
CN5019	Blood	Thailand	Positive	4	4	Southeast Asia	Khayhan et al., (2013)
2461_07	CSF	Thailand	Positive	6	4	Southeast Asia	Khayhan et al., (2013)
2550II_07	Blood	Thailand	Positive	6	4	Southeast Asia	Khayhan et al., (2013)

2551_07_CM	CSF	Thailand	Positive	6	4	Southeast Asia	Khayhan et al., (2013)
CM1	CSF	Thailand	Positive	6	4	Southeast Asia	Khayhan et al., (2013)
CM12	CSF	Thailand	Positive	6	4	Southeast Asia	Khayhan et al., (2013)
CM13	CSF	Thailand	Positive	6	4	Southeast Asia	Khayhan et al., (2013)
CM17	CSF	Thailand	Positive	6	4	Southeast Asia	Khayhan et al., (2013)
CM18	CSF	Thailand	Positive	6	4	Southeast Asia	Khayhan et al., (2013)
CM22	CSF	Thailand	Positive	6	4	Southeast Asia	Khayhan et al., (2013)
CM23	CSF	Thailand	Positive	6	4	Southeast Asia	Khayhan et al., (2013)
CM25	CSF	Thailand	Positive	6	4	Southeast Asia	Khayhan et al., (2013)
CM26	CSF	Thailand	Positive	6	4	Southeast Asia	Khayhan et al., (2013)
CM33	CSF	Thailand	Positive	6	4	Southeast Asia	Khayhan et al., (2013)
CM37	CSF	Thailand	Positive	6	4	Southeast Asia	Khayhan et al., (2013)
CM38	CSF	Thailand	Positive	6	4	Southeast Asia	Khayhan et al., (2013)
CM39	CSF	Thailand	Positive	6	4	Southeast Asia	Khayhan et al., (2013)
CM40	CSF	Thailand	Positive	6	4	Southeast Asia	Khayhan et al., (2013)
CM41	CSF	Thailand	Positive	6	4	Southeast Asia	Khayhan et al., (2013)
CM42	CSF	Thailand	Positive	6	4	Southeast Asia	Khayhan et al., (2013)
CM43	CSF	Thailand	Positive	6	4	Southeast Asia	Khayhan et al., (2013)
CM44	CSF	Thailand	Positive	6	4	Southeast Asia	Khayhan et al., (2013)
CM46	CSF	Thailand	Positive	6	4	Southeast Asia	Khayhan et al., (2013)
CM47	CSF	Thailand	Positive	6	4	Southeast Asia	Khayhan et al., (2013)
CM48	CSF	Thailand	Positive	6	4	Southeast Asia	Khayhan et al., (2013)
CM49	CSF	Thailand	Positive	6	4	Southeast Asia	Khayhan et al., (2013)
CM51	CSF	Thailand	Positive	6	4	Southeast Asia	Khayhan et al., (2013)
CM55	CSF	Thailand	Positive	6	4	Southeast Asia	Khayhan et al., (2013)
CM56	CSF	Thailand	Positive	6	4	Southeast Asia	Khayhan et al., (2013)
CM57	CSF	Thailand	Positive	6	4	Southeast Asia	Khayhan et al., (2013)
CM58	CSF	Thailand	Positive	6	4	Southeast Asia	Khayhan et al., (2013)
CM59	CSF	Thailand	Positive	6	4	Southeast Asia	Khayhan et al., (2013)

CM6	CSF	Thailand	Positive	6	4	Southeast Asia	Khayhan et al., (2013)
CM61	CSF	Thailand	Positive	6	4	Southeast Asia	Khayhan et al., (2013)
CM63	CSF	Thailand	Positive	6	4	Southeast Asia	Khayhan et al., (2013)
CM7	CSF	Thailand	Positive	6	4	Southeast Asia	Khayhan et al., (2013)
CM8	CSF	Thailand	Positive	6	4	Southeast Asia	Khayhan et al., (2013)
CN49005	CSF	Thailand	Positive	6	4	Southeast Asia	Khayhan et al., (2013)
CN4901	CSF	Thailand	Positive	6	4	Southeast Asia	Khayhan et al., (2013)
CN4903	CSF	Thailand	Positive	6	4	Southeast Asia	Khayhan et al., (2013)
CN4917	CSF	Thailand	Positive	6	4	Southeast Asia	Khayhan et al., (2013)
CN4918	CSF	Thailand	Positive	6	4	Southeast Asia	Khayhan et al., (2013)
CN4919	CSF	Thailand	Positive	6	4	Southeast Asia	Khayhan et al., (2013)
CN4926	CSF	Thailand	Positive	6	4	Southeast Asia	Khayhan et al., (2013)
CN4940	CSF	Thailand	Positive	6	4	Southeast Asia	Khayhan et al., (2013)
CN4941	CSF	Thailand	Positive	6	4	Southeast Asia	Khayhan et al., (2013)
CN4942	CSF	Thailand	Positive	6	4	Southeast Asia	Khayhan et al., (2013)
CN4943	CSF	Thailand	Positive	6	4	Southeast Asia	Khayhan et al., (2013)
CN4944	CSF	Thailand	Positive	6	4	Southeast Asia	Khayhan et al., (2013)
CN4945	CSF	Thailand	Positive	6	4	Southeast Asia	Khayhan et al., (2013)
CN4947	CSF	Thailand	Positive	6	4	Southeast Asia	Khayhan et al., (2013)
CN4964	CSF	Thailand	Positive	6	4	Southeast Asia	Khayhan et al., (2013)
CN4987	CSF	Thailand	Positive	6	4	Southeast Asia	Khayhan et al., (2013)
CN4988	CSF	Thailand	Positive	6	4	Southeast Asia	Khayhan et al., (2013)
CN4989	CSF	Thailand	Positive	6	4	Southeast Asia	Khayhan et al., (2013)
CN4995	CSF	Thailand	Positive	6	4	Southeast Asia	Khayhan et al., (2013)
CN4998	CSF	Thailand	Positive	6	4	Southeast Asia	Khayhan et al., (2013)
CN5010	Blood	Thailand	Positive	6	4	Southeast Asia	Khayhan et al., (2013)
D9	Avian guano	Thailand	NA	141	4	Southeast Asia	Khayhan et al., (2013)
D42	Avian guano	Thailand	NA	176	4	Southeast Asia	Khayhan et al., (2013)
110E	Avian guano	Thailand	NA	188	4	Southeast Asia	Khayhan et al., (2013)

130D	Avian guano	Thailand	NA	190	4	Southeast Asia	Khayhan et al., (2013)
40	Avian guano	Thailand	NA	5	5	Southeast Asia	Khayhan et al., (2013)
1_488	Clinical	Thailand	Unknown	5	5	Southeast Asia	Khayhan et al., (2013)
1_489	Clinical	Thailand	Unknown	5	5	Southeast Asia	Khayhan et al., (2013)
189E	Avian guano	Thailand	NA	5	5	Southeast Asia	Khayhan et al., (2013)
CN48	Clinical	Thailand	Unknown	5	5	Southeast Asia	Khayhan et al., (2013)
D16	Avian guano	Thailand	NA	5	5	Southeast Asia	Khayhan et al., (2013)
D4	Avian guano	Thailand	NA	5	5	Southeast Asia	Khayhan et al., (2013)
D6	Avian guano	Thailand	NA	5	5	Southeast Asia	Khayhan et al., (2013)
PG37	Avian guano	Thailand	NA	5	5	Southeast Asia	Khayhan et al., (2013)
CM30	CSF	Thailand	Positive	5	5	Southeast Asia	Khayhan et al., (2013)
CN49004	CSF	Thailand	Positive	5	5	Southeast Asia	Khayhan et al., (2013)
CN49006	CSF	Thailand	Positive	5	5	Southeast Asia	Khayhan et al., (2013)
CN4906	CSF	Thailand	Positive	5	5	Southeast Asia	Khayhan et al., (2013)
CN4916	CSF	Thailand	Positive	5	5	Southeast Asia	Khayhan et al., (2013)
CN4920	CSF	Thailand	Positive	5	5	Southeast Asia	Khayhan et al., (2013)
CN4921	CSF	Thailand	Positive	5	5	Southeast Asia	Khayhan et al., (2013)
CN4924	CSF	Thailand	Positive	5	5	Southeast Asia	Khayhan et al., (2013)
CN4946	CSF	Thailand	Positive	5	5	Southeast Asia	Khayhan et al., (2013)
CN4948	CSF	Thailand	Positive	5	5	Southeast Asia	Khayhan et al., (2013)
CN4960	CSF	Thailand	Positive	5	5	Southeast Asia	Khayhan et al., (2013)
CN4967	CSF	Thailand	Positive	5	5	Southeast Asia	Khayhan et al., (2013)
CN4977	CSF	Thailand	Positive	5	5	Southeast Asia	Khayhan et al., (2013)
CN4980	CSF	Thailand	Positive	5	5	Southeast Asia	Khayhan et al., (2013)
CN4983	CSF	Thailand	Positive	5	5	Southeast Asia	Khayhan et al., (2013)
CN4993	CSF	Thailand	Positive	5	5	Southeast Asia	Khayhan et al., (2013)
CN5008	CSF	Thailand	Positive	5	5	Southeast Asia	Khayhan et al., (2013)
CN5012	CSF	Thailand	Positive	5	5	Southeast Asia	Khayhan et al., (2013)
CN5015	CSF	Thailand	Positive	5	5	Southeast Asia	Khayhan et al., (2013)

CN5018	Blood	Thailand	Positive	5	5	Southeast Asia	Khayhan et al., (2013)
D44	Avian guano	Thailand	NA	193	5	Southeast Asia	Khayhan et al., (2013)
132	CSF	Indonesia	Positive	93	31	Southeast Asia	Khayhan et al., (2013)
597	CSF	Indonesia	Positive	93	31	Southeast Asia	Khayhan et al., (2013)
676	CSF	Indonesia	Positive	93	31	Southeast Asia	Khayhan et al., (2013)
1019	CSF	Indonesia	Positive	93	31	Southeast Asia	Khayhan et al., (2013)
1051	CSF	Indonesia	Positive	93	31	Southeast Asia	Khayhan et al., (2013)
1116	CSF	Indonesia	Positive	93	31	Southeast Asia	Khayhan et al., (2013)
1200	CSF	Indonesia	Positive	93	31	Southeast Asia	Khayhan et al., (2013)
1206	CSF	Indonesia	Positive	93	31	Southeast Asia	Khayhan et al., (2013)
1336	CSF	Indonesia	Positive	93	31	Southeast Asia	Khayhan et al., (2013)
1462	CSF	Indonesia	Positive	93	31	Southeast Asia	Khayhan et al., (2013)
1571	CSF	Indonesia	Positive	93	31	Southeast Asia	Khayhan et al., (2013)
2126	CSF	Indonesia	Positive	93	31	Southeast Asia	Khayhan et al., (2013)
3400	CSF	Indonesia	Positive	93	31	Southeast Asia	Khayhan et al., (2013)
3594	CSF	Indonesia	Positive	93	31	Southeast Asia	Khayhan et al., (2013)
3634	CSF	Indonesia	Positive	93	31	Southeast Asia	Khayhan et al., (2013)
Jakarta 1051	CSF	Indonesia	Positive	93	31	Southeast Asia	Khayhan et al., (2013)
CR2231	CSF	Indonesia	Positive	177	31	Southeast Asia	Khayhan et al., (2013)
CR755	CSF	Indonesia	Positive	177	31	Southeast Asia	Khayhan et al., (2013)
CM35	CSF	Thailand	Positive	93	31	Southeast Asia	Khayhan et al., (2013)
CN5007	CSF	Thailand	Positive	93	31	Southeast Asia	Khayhan et al., (2013)
D15	Avian guano	Thailand	NA	31	31	Southeast Asia	Khayhan et al., (2013)
D17	Avian guano	Thailand	NA	31	31	Southeast Asia	Khayhan et al., (2013)
D19	Avian guano	Thailand	NA	31	31	Southeast Asia	Khayhan et al., (2013)
1048	Unknown	Indonesia	Unknown	93	31	Southeast Asia	Khayhan et al., (2013)
3281	Unknown	Indonesia	Unknown	93	31	Southeast Asia	Khayhan et al., (2013)
1291_09	Blood	Thailand	Negative	93	31	Southeast Asia	Khayhan et al., (2013)
CR0E	CSF	Indonesia	Negative	177	31	Southeast Asia	Khayhan et al., (2013)

110A	Avian guano	Thailand	NA	185	31	Southeast Asia	Khayhan et al., (2013)
264	CSF	Indonesia	Positive	69	63	Southeast Asia	Khayhan et al., (2013)
2478	CSF	Indonesia	Positive	69	63	Southeast Asia	Khayhan et al., (2013)
34	Avian guano	Thailand	NA	53	174	Southeast Asia	Khayhan et al., (2013)
D45	Avian guano	Thailand	NA	175	174	Southeast Asia	Khayhan et al., (2013)
CNS1553	CSF	Laos	Negative	4	4	Southeast Asia	This study
FS4256/ CNS1444	CSF	Laos	Negative	4	4	Southeast Asia	This study
UI_16721	CSF	Laos	Negative	4	4	Southeast Asia	This study
CNS456	CSF	Laos	Negative	6	4	Southeast Asia	This study
UI_16771	CSF	Laos	Negative	6	4	Southeast Asia	This study
BK1	CSF	Vietnam	Positive	4	4	Southeast Asia	This study
BK111	CSF	Vietnam	Positive	4	4	Southeast Asia	This study
BK120	CSF	Vietnam	Positive	4	4	Southeast Asia	This study
CNS1017	CSF	Laos	Positive	4	4	Southeast Asia	This study
CNS1047	CSF	Laos	Positive	4	4	Southeast Asia	This study
CNS1110	CSF	Laos	Positive	4	4	Southeast Asia	This study
CNS1129	CSF	Laos	Positive	4	4	Southeast Asia	This study
CNS1179	CSF	Laos	Positive	4	4	Southeast Asia	This study
CNS1181	CSF	Laos	Positive	4	4	Southeast Asia	This study
CNS133_2	CSF	Laos	Positive	4	4	Southeast Asia	This study
CNS1379	CSF	Laos	Positive	4	4	Southeast Asia	This study
CNS1394	CSF	Laos	Positive	4	4	Southeast Asia	This study
CNS199	CSF	Laos	Positive	4	4	Southeast Asia	This study
CNS289	CSF	Laos	Positive	4	4	Southeast Asia	This study
CNS360	CSF	Laos	Positive	4	4	Southeast Asia	This study
CNS365	CSF	Laos	Positive	4	4	Southeast Asia	This study
CNS447	CSF	Laos	Positive	4	4	Southeast Asia	This study
CNS625	CSF	Laos	Positive	4	4	Southeast Asia	This study
CNS681	CSF	Laos	Positive	4	4	Southeast Asia	This study

CNS806	CSF	Laos	Positive	4	4	Southeast Asia	This study
CNS814	CSF	Laos	Positive	4	4	Southeast Asia	This study
CNS897	CSF	Laos	Positive	4	4	Southeast Asia	This study
CNS929	CSF	Laos	Positive	4	4	Southeast Asia	This study
CNS955	CSF	Laos	Positive	4	4	Southeast Asia	This study
CNS978	CSF	Laos	Positive	4	4	Southeast Asia	This study
CNS999	CSF	Laos	Positive	4	4	Southeast Asia	This study
HC_ST2296	CSF	Laos	Positive	4	4	Southeast Asia	This study
HC_ST352	CSF	Laos	Positive	4	4	Southeast Asia	This study
UI_11199	CSF	Laos	Positive	4	4	Southeast Asia	This study
UI_29674	CSF	Laos	Positive	4	4	Southeast Asia	This study
UI31647_2	CSF	Laos	Positive	4	4	Southeast Asia	This study
UI32312	CSF	Laos	Positive	4	4	Southeast Asia	This study
CNS245	CSF	Laos	Unknown	4	4	Southeast Asia	This study
CNS57	CSF	Laos	Unknown	4	4	Southeast Asia	This study
04CN30_001/ UI24618/ CNS1285	CSF	Laos	Positive	6	4	Southeast Asia	This study
04CN30_008 / UI21923 / CNS1143_2	CSF	Laos	Positive	6	4	Southeast Asia	This study
CNS_ST1930	CSF	Laos	Positive	6	4	Southeast Asia	This study
CNS1026	CSF	Laos	Positive	6	4	Southeast Asia	This study
CNS1085	CSF	Laos	Positive	6	4	Southeast Asia	This study
CNS1087	CSF	Laos	Positive	6	4	Southeast Asia	This study
CNS1089	CSF	Laos	Positive	6	4	Southeast Asia	This study
CNS1125	CSF	Laos	Positive	6	4	Southeast Asia	This study
CNS1156	CSF	Laos	Positive	6	4	Southeast Asia	This study
CNS1285	CSF	Laos	Positive	6	4	Southeast Asia	This study
CNS1302	CSF	Laos	Positive	6	4	Southeast Asia	This study
CNS1385	CSF	Laos	Positive	6	4	Southeast Asia	This study
CNS1403	CSF	Laos	Positive	6	4	Southeast Asia	This study
CNS1413	CSF	Laos	Positive	6	4	Southeast Asia	This study

CNS1419	CSF	Laos	Positive	6	4	Southeast Asia	This study
CNS1420	CSF	Laos	Positive	6	4	Southeast Asia	This study
CNS1453	CSF	Laos	Positive	6	4	Southeast Asia	This study
CNS1474	CSF	Laos	Positive	6	4	Southeast Asia	This study
CNS1589	CSF	Laos	Positive	6	4	Southeast Asia	This study
CNS198	CSF	Laos	Positive	6	4	Southeast Asia	This study
CNS445	CSF	Laos	Positive	6	4	Southeast Asia	This study
CNS569	CSF	Laos	Positive	6	4	Southeast Asia	This study
CNS573	CSF	Laos	Positive	6	4	Southeast Asia	This study
CNS863	CSF	Laos	Positive	6	4	Southeast Asia	This study
CNS984	CSF	Laos	Positive	6	4	Southeast Asia	This study
ST1931	CSF	Laos	Positive	6	4	Southeast Asia	This study
UI_12808	CSF	Laos	Positive	6	4	Southeast Asia	This study
UI_14167	CSF	Laos	Positive	6	4	Southeast Asia	This study
UI_14344	CSF	Laos	Positive	6	4	Southeast Asia	This study
UI_21616	CSF	Laos	Positive	6	4	Southeast Asia	This study
CNS626	CSF	Laos	Positive	306	4	Southeast Asia	This study
BK14	CSF	Vietnam	Positive	4	4	Southeast Asia	This study
BK151	CSF	Vietnam	Positive	4	4	Southeast Asia	This study
BK156	CSF	Vietnam	Positive	4	4	Southeast Asia	This study
BK163	CSF	Vietnam	Positive	4	4	Southeast Asia	This study
BK182	CSF	Vietnam	Positive	4	4	Southeast Asia	This study
BK192	CSF	Vietnam	Positive	4	4	Southeast Asia	This study
BK193	CSF	Vietnam	Positive	4	4	Southeast Asia	This study
BK2	CSF	Vietnam	Positive	4	4	Southeast Asia	This study
BK224	CSF	Vietnam	Positive	4	4	Southeast Asia	This study
BK225	CSF	Vietnam	Positive	4	4	Southeast Asia	This study
BK23	CSF	Vietnam	Positive	4	4	Southeast Asia	This study
BK30	CSF	Vietnam	Positive	4	4	Southeast Asia	This study

BK35	CSF	Vietnam	Positive	4	4	Southeast Asia	This study
BK48	CSF	Vietnam	Positive	4	4	Southeast Asia	This study
BK56	CSF	Vietnam	Positive	4	4	Southeast Asia	This study
BK57	CSF	Vietnam	Positive	4	4	Southeast Asia	This study
BK59	CSF	Vietnam	Positive	4	4	Southeast Asia	This study
BK69	CSF	Vietnam	Positive	4	4	Southeast Asia	This study
CNS595	CSF	Laos	Unknown	4	4	Southeast Asia	This study
BK73	CSF	Vietnam	Positive	4	4	Southeast Asia	This study
BK74	CSF	Vietnam	Positive	4	4	Southeast Asia	This study
BK80	CSF	Vietnam	Positive	4	4	Southeast Asia	This study
BK87	CSF	Vietnam	Positive	4	4	Southeast Asia	This study
BK88	CSF	Vietnam	Positive	4	4	Southeast Asia	This study
BK89	CSF	Vietnam	Positive	4	4	Southeast Asia	This study
BK90	CSF	Vietnam	Positive	4	4	Southeast Asia	This study
BMD1392	CSF	Vietnam	Negative	4	4	Southeast Asia	This study
BMD1415	CSF	Vietnam	Negative	4	4	Southeast Asia	This study
BMD1879	CSF	Vietnam	Positive	4	4	Southeast Asia	This study
BMD394	CSF	Vietnam	Negative	4	4	Southeast Asia	This study
BK115	CSF	Vietnam	Positive	5	5	Southeast Asia	This study
CNS430	CSF	Laos	Unknown	6	4	Southeast Asia	This study
BK116	CSF	Vietnam	Positive	5	5	Southeast Asia	This study
BK117	CSF	Vietnam	Positive	5	5	Southeast Asia	This study
BK119	CSF	Vietnam	Positive	5	5	Southeast Asia	This study
BK124	CSF	Vietnam	Positive	5	5	Southeast Asia	This study
BK139	CSF	Vietnam	Positive	5	5	Southeast Asia	This study
BK147	CSF	Vietnam	Positive	5	5	Southeast Asia	This study
BK15	CSF	Vietnam	Positive	5	5	Southeast Asia	This study
BK160	CSF	Vietnam	Positive	5	5	Southeast Asia	This study
BK169	CSF	Vietnam	Positive	5	5	Southeast Asia	This study

BK171	CSF	Vietnam	Positive	5	5	Southeast Asia	This study
BK175	CSF	Vietnam	Positive	5	5	Southeast Asia	This study
BK185	CSF	Vietnam	Positive	5	5	Southeast Asia	This study
BK190	CSF	Vietnam	Positive	5	5	Southeast Asia	This study
BK20	CSF	Vietnam	Positive	5	5	Southeast Asia	This study
BK241	CSF	Vietnam	Positive	5	5	Southeast Asia	This study
CNS128	CSF	Laos	Negative	5	5	Southeast Asia	This study
CNS1569	CSF	Laos	Negative	5	5	Southeast Asia	This study
BK25	CSF	Vietnam	Positive	5	5	Southeast Asia	This study
BK26	CSF	Vietnam	Positive	5	5	Southeast Asia	This study
BK28	CSF	Vietnam	Positive	5	5	Southeast Asia	This study
BK34	CSF	Vietnam	Positive	5	5	Southeast Asia	This study
BK38	CSF	Vietnam	Positive	5	5	Southeast Asia	This study
BK4	CSF	Vietnam	Positive	5	5	Southeast Asia	This study
BK41	CSF	Vietnam	Positive	5	5	Southeast Asia	This study
BK42	CSF	Vietnam	Positive	5	5	Southeast Asia	This study
BK44	CSF	Vietnam	Positive	5	5	Southeast Asia	This study
BK45	CSF	Vietnam	Positive	5	5	Southeast Asia	This study
BK49	CSF	Vietnam	Positive	5	5	Southeast Asia	This study
BK50	CSF	Vietnam	Positive	5	5	Southeast Asia	This study
BK54	CSF	Vietnam	Positive	5	5	Southeast Asia	This study
BK58	CSF	Vietnam	Positive	5	5	Southeast Asia	This study
BK62	CSF	Vietnam	Positive	5	5	Southeast Asia	This study
BK63	CSF	Vietnam	Positive	5	5	Southeast Asia	This study
BK76	CSF	Vietnam	Positive	5	5	Southeast Asia	This study
BK78	CSF	Vietnam	Positive	5	5	Southeast Asia	This study
BK94	CSF	Vietnam	Positive	5	5	Southeast Asia	This study
BMD101	CSF	Vietnam	Negative	5	5	Southeast Asia	This study
BMD1198	CSF	Vietnam	Negative	5	5	Southeast Asia	This study

BMD1228	CSF	Vietnam	Negative	5	5	Southeast Asia	This study
BMD1232	CSF	Vietnam	Negative	5	5	Southeast Asia	This study
BMD1291	CSF	Vietnam	Negative	5	5	Southeast Asia	This study
BMD1338	CSF	Vietnam	Negative	5	5	Southeast Asia	This study
BMD1353	CSF	Vietnam	Negative	5	5	Southeast Asia	This study
BMD1452	CSF	Vietnam	Negative	5	5	Southeast Asia	This study
BMD1465	CSF	Vietnam	Negative	5	5	Southeast Asia	This study
BMD1534	CSF	Vietnam	Negative	5	5	Southeast Asia	This study
BMD1592	CSF	Vietnam	Negative	5	5	Southeast Asia	This study
BMD1646	CSF	Vietnam	Negative	5	5	Southeast Asia	This study
04CN30_002 / UI24734/ CNS1292_3	CSF	Laos	Positive	5	5	Southeast Asia	This study
04CN30_016/ UI14893/ CNS605_2	CSF	Laos	Positive	5	5	Southeast Asia	This study
04CN30_019/ UI29069/ CNS1415_2	CSF	Laos	Positive	5	5	Southeast Asia	This study
CNS121	CSF	Laos	Positive	5	5	Southeast Asia	This study
CNS1396_2	CSF	Laos	Positive	5	5	Southeast Asia	This study
CNS517	CSF	Laos	Positive	5	5	Southeast Asia	This study
CNS936	CSF	Laos	Unknown	5	5	Southeast Asia	This study
BMD1713	CSF	Vietnam	Negative	5	5	Southeast Asia	This study
BMD1716	CSF	Vietnam	Negative	5	5	Southeast Asia	This study
BMD1828	CSF	Vietnam	Negative	5	5	Southeast Asia	This study
BMD367	CSF	Vietnam	Negative	5	5	Southeast Asia	This study
BMD368	CSF	Vietnam	Negative	5	5	Southeast Asia	This study
BMD494	CSF	Vietnam	Negative	5	5	Southeast Asia	This study
BMD534	CSF	Vietnam	Negative	5	5	Southeast Asia	This study
BMD673	CSF	Vietnam	Negative	5	5	Southeast Asia	This study
BMD700	CSF	Vietnam	Negative	5	5	Southeast Asia	This study
BMD732	CSF	Vietnam	Negative	5	5	Southeast Asia	This study
BMD761	CSF	Vietnam	Negative	5	5	Southeast Asia	This study
BMD852	CSF	Vietnam	Negative	5	5	Southeast Asia	This study

BMD854	CSF	Vietnam	Negative	5	5	Southeast Asia	This study
BMD865	CSF	Vietnam	Negative	5	5	Southeast Asia	This study
BMD894	CSF	Vietnam	Negative	5	5	Southeast Asia	This study
BMD899	CSF	Vietnam	Negative	5	5	Southeast Asia	This study
BMD903	CSF	Vietnam	Negative	5	5	Southeast Asia	This study
BMD910	CSF	Vietnam	Negative	5	5	Southeast Asia	This study
BMD973	CSF	Vietnam	Negative	5	5	Southeast Asia	This study
BK18	CSF	Vietnam	Positive	6	4	Southeast Asia	This study
BK188	CSF	Vietnam	Positive	6	4	Southeast Asia	This study
BK189	CSF	Vietnam	Positive	6	4	Southeast Asia	This study
BK205	CSF	Vietnam	Positive	6	4	Southeast Asia	This study
BK218	CSF	Vietnam	Positive	6	4	Southeast Asia	This study
BK219	CSF	Vietnam	Positive	6	4	Southeast Asia	This study
BK234	CSF	Vietnam	Positive	6	4	Southeast Asia	This study
BK52	CSF	Vietnam	Positive	6	4	Southeast Asia	This study
BK71	CSF	Vietnam	Positive	6	4	Southeast Asia	This study
BK75	CSF	Vietnam	Positive	6	4	Southeast Asia	This study
BK96	CSF	Vietnam	Positive	6	4	Southeast Asia	This study
BMD745	CSF	Vietnam	Negative	6	4	Southeast Asia	This study
BK11	CSF	Vietnam	Positive	32	31	Southeast Asia	This study
BK17	CSF	Vietnam	Positive	32	31	Southeast Asia	This study
BK27	CSF	Vietnam	Positive	32	31	Southeast Asia	This study
BK46	CSF	Vietnam	Positive	32	31	Southeast Asia	This study
CNS487	CSF	Laos	Negative	93	31	Southeast Asia	This study
CNS1465	CSF	Laos	Positive	187	31	Southeast Asia	This study
BK68	CSF	Vietnam	Positive	32	31	Southeast Asia	This study
BMD915	CSF	Vietnam	Negative	32	31	Southeast Asia	This study
CNS811	CSF	Laos	Unknown	93	31	Southeast Asia	This study
BMD942	CSF	Vietnam	Negative	32	31	Southeast Asia	This study

BK154	CSF	Vietnam	Positive	39	31	Southeast Asia	This study
BK167	CSF	Vietnam	Positive	39	31	Southeast Asia	This study
BK209	CSF	Vietnam	Positive	39	31	Southeast Asia	This study
BK12	CSF	Vietnam	Positive	93	31	Southeast Asia	This study
BK157	CSF	Vietnam	Positive	93	31	Southeast Asia	This study
BK179	CSF	Vietnam	Positive	93	31	Southeast Asia	This study
BK213	CSF	Vietnam	Positive	93	31	Southeast Asia	This study
BK228	CSF	Vietnam	Positive	93	31	Southeast Asia	This study
BK24	CSF	Vietnam	Positive	93	31	Southeast Asia	This study
BK33	CSF	Vietnam	Positive	93	31	Southeast Asia	This study
BK85	CSF	Vietnam	Positive	93	31	Southeast Asia	This study
BK109	CSF	Vietnam	Positive	137	4	Southeast Asia	This study
BK172	CSF	Vietnam	Positive	188	4	Southeast Asia	This study
BK64	CSF	Vietnam	Positive	188	4	Southeast Asia	This study
BK129	CSF	Vietnam	Positive	195	N/A	Southeast Asia	This study
BMD1367	CSF	Vietnam	Negative	306	4	Southeast Asia	This study
BK150	CSF	Vietnam	Positive	338	31	Southeast Asia	This study
BK153	CSF	Vietnam	Positive	339	31	Southeast Asia	This study
BK55	CSF	Vietnam	Positive	340	31	Southeast Asia	This study

Publications

Parts of this thesis have been included in publications:

Chapter 1 (Introduction) was included in a review:

> Beardsley, J., **Thanh, L.T**. & Day, J (2017) A Model CNS Fungal Infection: Cryptococcal Meningitis. J. Curr Clin Micro Rpt 2:96. (https://doi.org/10.1007/s40588-015-0016-0)

Preliminary MLST data from Chapter 2 (MLST) was published in this PlosNTD paper in 2017:

> Day JN, Qihui S, **Thanh LT**, Trieu PH, Van AD, Thu NH, et al. (2017) Comparative genomics of Cryptococcus neoformans var. grubii associated with meningitis in HIV infected and uninfected patients in Vietnam. PLoS Negl Trop Dis 11(6): e0005628. https://doi.org/10.1371/journal.pntd.0005628

Manuscripts for additional MLST data (Chapter 2) and mouse data (Chapter 3) are being prepared for publication.

Bibliography

1. Park BJ, Wannemuehler KA, Marston BJ, Govender N, Pappas PG, Chiller TM. Estimation of the current global burden of cryptococcal meningitis among persons living with HIV/AIDS. AIDS. 2009;23: 525–30. doi:10.1097/QAD.0b013e328322ffac
2. Rajasingham R, Smith RM, Park BJ, Jarvis JN, Govender NP, Chiller TM, et al. Global burden of disease of HIV-associated cryptococcal meningitis: an updated analysis. Lancet Infect Dis. 2017;17: 873–881. doi:10.1016/S1473-3099(17)30243-8
3. Pasquier E, Kunda J, De Beaudrap P, Loyse A, Temfack E, Molloy SF, et al. Long term mortality and disability in Cryptococcal Meningitis: a systematic literature review. Clin Infect Dis. 2017;66: 1122–1132. doi:10.1093/cid/cix870
4. George IA, Spec A, Powderly WG, Santos CAQ. Comparative epidemiology and outcomes of Human Immunodeficiency virus (HIV), non-HIV, non-transplant, and solid organ transplant associated cryptococcosis: A population-based study. Clin Infect Dis. 2018;66: 608–611. doi:10.1093/cid/cix867
5. Williamson PR, Jarvis JN, Panackal AA, Fisher MC, Molloy SF, Loyse A, et al. Cryptococcal meningitis: epidemiology, immunology, diagnosis and therapy. Nat Rev Neurol. 2016;13: 13–24. doi:10.1038/nrneurol.2016.167
6. Kwon-Chung KJ, Fraser JA, Doering TL, Wang ZA, Janbon G, Idnurm A, et al. *Cryptococcus neoformans* and *Cryptococcus gattii*, the Etiologic Agents of Cryptococcosis. Cold Spring Harb Perspect Med. 2014;4: a019760–a019760. doi:10.1101/cshperspect.a019760
7. Chaturvedi V, Chaturvedi S. *Cryptococcus gattii*: a resurgent fungal pathogen. Trends Microbiol. 2011;19: 564–71. doi:10.1016/j.tim.2011.07.010
8. Kidd SE, Hagen F, Tscharke RL, Huynh M, Bartlett KH, Fyfe M, et al. A rare genotype of *Cryptococcus gattii* caused the cryptococcosis outbreak on Vancouver Island

(British Columbia, Canada). Proc Natl Acad Sci U S A. 2004;101: 17258–63. doi:10.1073/pnas.0402981101

9. Frange P, Assoumou L, Descamps D, Chéret A, Goujard C, Tran L, et al. HIV-1 subtype B-infected MSM may have driven the spread of transmitted resistant strains in France in 2007-12: impact on susceptibility to first-line strategies. J Antimicrob Chemother. 2015;70: 2084–9. doi:10.1093/jac/dkv049
10. WHO | Guidelines for the diagnosis, prevention and management of cryptococcal disease in HIV-infected adults, adolescents and children. WHO. World Health Organization; 2018;
11. Busse O. Uber Saccharomycosis hominis. Virchows Arch A Pathol Anat Histol. 1895;140: 23–46.
12. Busse O. Uber parasite Zelleinschlusse und ihre Zuchtung. Zentralbl Bakteriol. 1894;16: 175–180.
13. Sanfelice F. Contributo alla morfologia e biologia dei blastomiceti che si sviluppano nei succhili alcuni frutti. Ann Igen. 1894;4: 463–495.
14. Heitman J et al H, Kozel TR, Kwon-Chung KJ, Perfect JR, Casadevall A. *Cryptococcus*: From human pathogen to model yeast. ASM press. Washington DC: ASM Press; 2011. doi:10.1016/S1473-3099(11)70140-2
15. Vuillemin JP. Les blastomyces pathogenes. Rev Gen Sci. 1901;12: 732–751.
16. Casadevall A, Perfect JR. *Cryptococcus neoformans*. Washington DC: ASM Press; 1998.
17. Franzot SP, Salkin IF, Casadevall A. *Cryptococcus neoformans* var. *grubii*: separate varietal status for *Cryptococcus neoformans* serotype A isolates. J Clin Microbiol. 1999;37: 838–40.
18. Belay, T., R. Cherniak, E. B. O'Neill and TRK. Serotyping of *Cryptococcus neoformans* by dot enzyme assay. J Clin Microbiol. 1996;34: 466–470.

19. Levitz SM. The ecology of *Cryptococcus neoformans* and the epidemiology of cryptococcosis. Rev Infect Dis. 1991;13: 1163–1169.
20. Ngamskulrungroj, P., Y. Chang, J. Roh and KJK-C. Differences in nitrogen metabolism between *Cryptococcus neoformans* and C. *gattii*, the two etiologic agents of cryptococcosis. PLoS One. 2012;7:e34258.
21. Ngamskulrungroj, P., Y. Chang, E. Sionov and KJK-C. The primary target organ of *Cryptococcus gattii* is different from that of *Cryptococcus neoformans* in a murine model. MBio. 2012;3.
22. Ngamskulrungroj P, Gilgado F, Faganello J, Litvintseva AP, Leal AL, Tsui KM, et al. Genetic diversity of the *Cryptococcus* species complex suggests that *Cryptococcus gattii* deserves to have varieties. PLoS One. 2009;4: e5862. doi:10.1371/journal.pone.0005862
23. Xu J, Vilgalys R, Mitchell TG. Multiple gene genealogies reveal recent dispersion and hybridization in the human pathogenic fungus *Cryptococcus neoformans*. Mol Ecol. 2000;9: 1471–81. doi:10.1046/j.1365-294X.2000.01021.x
24. Fan M, Currie BP, Gutell RR, Ragan MA, Casadevall A. The 16S-like, 5.8S and 23S-like rRNAs of the two varieties of *Cryptococcus neoformans*: sequence, secondary structure, phylogenetic analysis and restriction fragment polymorphisms. J Med Vet Mycol. 1994;32: 163–180. doi:10.1080/02681219480000231
25. Bovers M, Hagen F, Kuramae EE, Boekhout T. Six monophyletic lineages identified within *Cryptococcus neoformans* and *Cryptococcus gattii* by multi-locus sequence typing. Fungal Genet Biol. 2008;45: 400–21. doi:10.1016/j.fgb.2007.12.004
26. Kavanaugh L a, Fraser J a, Dietrich FS. Recent evolution of the human pathogen *Cryptococcus neoformans* by intervarietal transfer of a 14-gene fragment. Mol Biol Evol. 2006;23: 1879–90. doi:10.1093/molbev/msl070
27. Sorrell TC, Chen SC, Ruma P, Meyer W, Pfeiffer TJ, Ellis DH, et al. Concordance of

clinical and environmental isolates of *Cryptococcus neoformans* var. *gattii* by random amplification of polymorphic DNA analysis and PCR fingerprinting. J Clin Microbiol. 1996;34: 1253–60.

28. Meyer W, Castañeda A, Jackson S, Huynh M, Castañeda E, IberoAmerican Cryptococcal Study Group. Molecular typing of IberoAmerican *Cryptococcus neoformans* isolates. Emerg Infect Dis. 2003;9: 189–95. doi:10.3201/eid0902.020246
29. Litvintseva AP, Thakur R, Vilgalys R, Mitchell TG. Multilocus sequence typing reveals three genetic subpopulations of *Cryptococcus neoformans* var. *grubii* (serotype A), including a unique population in Botswana. Genetics. 2006;172: 2223–38. doi:10.1534/genetics.105.046672
30. Meyer W, Aanensen DM, Boekhout T, Cogliati M, Diaz MR, Esposto MC, et al. Consensus multi-locus sequence typing scheme for *Cryptococcus neoformans* and *Cryptococcus gattii*. Med Mycol. 2009;47: 561–70. doi:10.1080/13693780902953886
31. Meyer W, Marszewska K, Amirmostofian M, Igreja RP, Hardtke C, Methling K, et al. Molecular typing of global isolates of *Cryptococcus neoformans* var. *neoformans* by polymerase chain reaction fingerprinting and randomly amplified polymorphic DNA-a pilot study to standardize techniques on which to base a detailed epidemiological survey. Electrophoresis. 1999;20: 1790–9. doi:10.1002/(SICI)1522-2683(19990101)20:8<1790::AID-ELPS1790>3.0.CO;2-2
32. Yilmaz A, Göral G, Helvaci S, Kiliçturgay K, Gökirmak F, Töre O, et al. Distribution of *Cryptococcus neoformans* in pigeon feces. Mikrobiyol Bul. 1989;23: 121–6.
33. Hubalek Z. Distribution of *Cryptococcus neoformans* in a pigeon habitat. Folia Parasitol (Praha). 1975;22: 73–79.
34. Emmons CW. Prevalence of *Cryptococcus neoformans* in pigeon habitats. Public

Health Rep. 1960;75: 362–4.

35. Ellis D, Pfeiffer T. The ecology of *Cryptococcus neoformans*. Eur J Epidemiol. 1992;8: 321–325. doi:10.1007/BF00158562

36. Fiskin AM, Zalles MC, Garrison RG. Electron cytochemical studies of *Cryptococcus neoformans* grown on uric acid and related sources of nitrogen. J Med Vet Mycol. 1990;28: 197–207.

37. Criseo G, Gallo M, Pernice A. Killer activity at different pHs against *Cryptococcus neoformans* var. *neoformans* serotype A by environmental yeast isolates. Mycoses. 1999;42: 601–608.

38. Lin X, Heitman J. The biology of the *Cryptococcus neoformans* species complex. Annu Rev Microbiol. 2006;60: 69–105. doi:10.1146/annurev.micro.60.080805.142102

39. Littman ML, Borok R. Relation of the pigeon to cryptococcosis: Natural carrier state, heat resistance and survival of *Cryptococcus neoformans*. Mycopathol Mycol Appl. Kluwer Academic Publishers; 1968;35: 329–345. doi:10.1007/BF02050749

40. Lazera MS, Salmito Cavalcanti M a, Londero a T, Trilles L, Nishikawa MM, Wanke B. Possible primary ecological niche of *Cryptococcus neoformans*. Med Mycol. 2000;38: 379–383.

41. Gugnani HC, Mitchell TG, Litvintseva AP, Lengeler KB, Heitman J, Kumar A, et al. Isolation of *Cryptococcus gattii* and *Cryptococcus neoformans* var. *grubii* from the flowers and bark of Eucalyptus trees in India. Med Mycol. 2005;43: 565–569. doi:10.1080/13693780500160785

42. Sorrell TC, Ellis DH. Ecology of *Cryptococcus neoformans*. Rev Iberoam Micol. 1997;14: 42–43. doi:19971442 [pii]

43. Littman ML, Borok R. Relation of the pigeon to cryptococcosis: natural carrier state, heat resistance and survival of *Cryptococcus neoformans*. Mycopathol Mycol Appl.

1968;35: 329–45.

44. Kuroki M, Phichaichumpon C, Yasuoka A, Chiranairadul P, Chosa T, Sirinirund P, et al. Environmental isolation of *Cryptococcus neoformans* from an endemic region of HIV-associated cryptococcosis in Thailand. Yeast. 2004;21: 809–812. doi:10.1002/yea.1112

45. Imwidthaya P, Dithaprasop P, Egtasaeng C. Clinical and environmental isolates of *Cryptococcus neoformans* in Bangkok (Thailand). Mycopathologia. 1989;108: 65–67.

46. Grover N, Nawange SR, Naidu J, Singh SM, Sharma A. Ecological niche of *Cryptococcus neoformans* var. *grubii* and *Cryptococcus gattii* in decaying wood of trunk hollows of living trees in Jabalpur City of Central India. Mycopathologia. 2007;164: 159–170. doi:10.1007/s11046-007-9039-2

47. Refojo N, Perrotta D, Brudny M, Abrantes R, Hevia a I, Davel G. Isolation of *Cryptococcus neoformans* and *Cryptococcus gattii* from trunk hollows of living trees in Buenos Aires City, Argentina. Med Mycol. 2009;47: 177–84. doi:10.1080/13693780802227290

48. Chowdhary A, Rhandhawa HS, Prakash A, Meis JF. Environmental prevalence of *Cryptococcus neoformans* and *Cryptococcus gattii* in India: an update. Crit Rev Microbiol. 2012;38: 1–16. doi:10.3109/1040841X.2011.606426

49. Kwon-Chung KJ. A New Genus, Filobasidiella, the Perfect State of *Cryptococcus neoformans*. Mycologia. 1975;67: 1197. doi:10.2307/3758842

50. Kwon-Chung KJ. Morphogenesis of Filobasidiella *neoformans*, the sexual state of *Cryptococcus neoformans*. Mycologia. 1976;68: 821–833. doi:10.2307/3758800

51. Metin B, Findley K, Heitman J. The mating type locus (MAT) and sexual reproduction of *Cryptococcus* heveanensis: Insights into the evolution of sex and sex-determining chromosomal regions in fungi. PLoS Genet. 2010;6: 14.

doi:10.1371/journal.pgen.1000961

52. Karos M, Chang YC, McClelland CM, Clarke DL, Fu J, Wickes BL, et al. Mapping of the *Cryptococcus neoformans* MATalpha Locus: Presence of Mating Type-Specific Mitogen-Activated Protein Kinase Cascade Homologs. J Bacteriol. 2000;182: 6222–6227. doi:10.1128/JB.182.21.6222-6227.2000
53. Lengeler KB, Fox DS, Fraser JA, Allen A, Forrester K, Dietrich FS, et al. Mating-type locus of *Cryptococcus neoformans*: A step in the evolution of sex chromosomes. Eukaryot Cell. 2002;1: 704–718. doi:10.1128/EC.1.5.704-718.2002
54. Hull CM, Heitman J. Genetics of *Cryptococcus neoformans*. Annu Rev Genet. 2002;36: 557–615. doi:10.1146/annurev.genet.36.052402.152652
55. Sukroongreung S, Kitiniyom K, Nilakul C, Tantimavanich S. Pathogenicity of basidiospores of Filobasidiella *neoformans* var. *neoformans*. Med Mycol. 1998;36: 419–424. doi:10.1046/j.1365-280X.1998.00181.x
56. Kwon-Chung KJ, Bennett JE. Distribution of α and a mating types of *Cryptococcus neoformans* among natural and clinical isolates. Am J Epidemiol. 1978;108: 337–40.
57. Litvintseva AP, Marra RE, Nielsen K, Heitman J, Vilgalys R, Mitchell TG. Evidence of Sexual Recombination among *Cryptococcus neoformans* Serotype A Isolates in Sub-Saharan Africa. Eukaryot Cell. 2003;2: 1162–1168. doi:10.1128/EC.2.6.1162-1168.2003
58. Wickes BL, Mayorga ME, Edman U, Edman JC. Dimorphism and haploid fruiting in *Cryptococcus neoformans*: association with the alpha-mating type. Proc Natl Acad Sci U S A. 1996;93: 7327–7331. doi:10.1073/pnas.93.14.7327
59. Tscharke RL, Lazera M, Chang YC, Wickes BL, Kwon-Chung KJ. Haploid fruiting in *Cryptococcus neoformans* is not mating type α-specific. Fungal Genet Biol. 2003;39: 230–237. doi:10.1016/S1087-1845(03)00046-X
60. Lin X, Hull CM, Heitman J. Sexual reproduction between partners of the same

mating type in *Cryptococcus neoformans*. Nature. 2005;434: 1017–1021. doi:10.1038/nature03448

61. Fraser J a, Giles SS, Wenink EC, Geunes-Boyer SG, Wright JR, Diezmann S, et al. Same-sex mating and the origin of the Vancouver Island *Cryptococcus gattii* outbreak. Nature. 2005;437: 1360–1364. doi:10.1038/nature04220
62. Kwon-Chung KJ, Edman JC, Wickes BL. Genetic association of mating types and virulence in *Cryptococcus neoformans*. Infect Immun. 1991;60: 602–605.
63. Nielsen K, Cox GM, Litvintseva AP, Mylonakis E, Malliaris SD, Benjamin DK, et al. *Cryptococcus neoformans* α strains preferentially disseminate to the central nervous system during coinfection. Infect Immun. 2005;73: 4922–4933. doi:10.1128/IAI.73.8.4922-4933.2005
64. Fu C, Sun S, Billmyre RB, Roach KC, Heitman J. Unisexual versus bisexual mating in *Cryptococcus neoformans*: Consequences and biological impacts. Fungal Genet Biol. 2014;78: 65–75. doi:10.1016/j.fgb.2014.08.008
65. Hu G, Wang J, Choi J, Jung WH, Liu I, Litvintseva AP, et al. Variation in chromosome copy number influences the virulence of *Cryptococcus neoformans* and occurs in isolates from AIDS patients. BMC Genomics. 2011;12: 526. doi:10.1186/1471-2164-12-526
66. Sionov E, Lee H, Chang YC, Kwon-Chung KJ. *Cryptococcus neoformans* overcomes stress of azole drugs by formation of disomy in specific multiple chromosomes. PLoS Pathog. 2010;6: e1000848. doi:10.1371/journal.ppat.1000848
67. Ni M, Feretzaki M, Li W, Floyd-Averette A, Mieczkowski P, Dietrich FS, et al. Unisexual and heterosexual meiotic reproduction generate aneuploidy and phenotypic diversity de novo in the yeast *Cryptococcus neoformans*. PLoS Biol. 2013;11: e1001653. doi:10.1371/journal.pbio.1001653
68. Fan W, Kraus PR, Boily M-J, Heitman J. *Cryptococcus neoformans* gene expression

during murine macrophage infection. Eukaryot Cell; 2005;4: 1420–1433. doi:10.1128/EC.4.8.1420-1433.2005

69. d'Enfert C. Fungal spore germination: Insights from the molecular genetics of *Aspergillus nidulans* and *Neurospora crassa*. Fungal Genet Biol. 1997;21: 163–172. doi:10.1006/fgbi.1997.0975

70. Giles SS, Dagenais TRT, Botts MR, Keller NP, Hull CM. Elucidating the pathogenesis of spores from the human fungal pathogen *Cryptococcus neoformans*. Infect Immun. 2009;77: 3491–3500. doi:10.1128/IAI.00334-09

71. Hatch TF. Distribution and deposition of inhaled particles in respiratory tract. Bacteriol Rev. 1961;25: 237–40.

72. Zimmer BL, Hempel HO, Goodman NL. Pathogenicity of the basidiospores of Filobasidiella *neoformans*. Mycopathologia. 1984;85: 149–153. doi:10.1007/BF00440944

73. Velagapudi R, Hsueh Y-P, Geunes-Boyer S, Wright JR, Heitman J. Spores as infectious propagules of *Cryptococcus neoformans*. Infect Immun. 2009;77: 4345–4355. doi:10.1128/IAI.00542-09

74. Wang L, Lin X. Mechanisms of unisexual mating in *Cryptococcus neoformans*. Fungal Genet Biol. 2011;48: 651–60. doi:10.1016/j.fgb.2011.02.001

75. McClelland CM, Chang YC, Varma A, Kwon-Chung KJ. Uniqueness of the mating system in *Cryptococcus neoformans*. Trends in Microbiology. 2004. pp. 208–212. doi:10.1016/j.tim.2004.03.003

76. Laguna L, Disturbance PB, Design MJE. Sexual reproduction between partners of the same mating type in *Cryptococcus neoformans*. 2005; 1017–1021. doi:10.1038/nature03450.1.

77. Chaturvedi V, Fan J, Stein B, Behr MJ, Samsonoff WA, Wickes BL, et al. Molecular genetic analyses of mating pheromones reveal intervariety mating or hybridization

in *Cryptococcus neoformans*. Infect Immun. 2002;70: 5225–5235. doi:10.1128/IAI.70.9.5225-5235.2002

78. Mitchell TG, Perfect JR. Cryptococcosis in the era of AIDS--100 years after the discovery of *Cryptococcus neoformans*. Clin Microbiol Rev. 1995;8: 515–48.
79. Bovers M, Hagen F, Boekhout T. Diversity of the *Cryptococcus neoformans-Cryptococcus gattii* species complex. Rev Iberoam Micol. 2008;25: S4–12.
80. Cogliati M. Global molecular epidemiology of *Cryptococcus neoformans* and *Cryptococcus gattii* : An Atlas of the molecular types. Scientifica (Cairo). 2013;2013: 1–23. doi:10.1155/2013/675213
81. Litvintseva AP, Carbone I, Rossouw J, Thakur R, Govender NP, Mitchell TG. Evidence that the human pathogenic fungus *Cryptococcus neoformans* var. *grubii* may have evolved in Africa. Nielsen K, editor. PLoS One. 2011;6: e19688. doi:10.1371/journal.pone.0019688
82. Chen Y, Litvintseva AP, Frazzitta AE, Haverkamp MR, Wang L, Fang C, et al. Comparative analyses of clinical and environmental populations of *Cryptococcus neoformans* in Botswana. Mol Ecol. 2015;24: 3559–3571. doi:10.1111/mec.13260
83. Litvintseva AP, Kestenbaum L, Vilgalys R, Mitchell TG. Comparative Analysis of Environmental and Clinical Populations of *Cryptococcus neoformans*. J Clin Microbiol. 2005;43: 556–564. doi:10.1128/JCM.43.2.556
84. Yan Z, Li X, Xu J. Geographic Distribution of Mating Type Alleles of *Cryptococcus neoformans* in Four Areas of the United States. 2002;40: 965–972. doi:10.1128/JCM.40.3.965
85. Boekhout T, Theelen B, Diaz M, Fell JW, Hop WCJ, Abeln ECA, et al. Hybrid genotypes in the pathogenic yeast *Cryptococcus neoformans*. Microbiology. 2001;147: 891–907.
86. Rhodes J, Desjardins CA, Sykes SM, Beale MA, Vanhove M, Sakthikumar S, et al.

Tracing Genetic Exchange and Biogeography of *Cryptococcus neoformans* var. *grubii* at the Global Population Level. Genetics. Genetics; 2017;207: 327–346. doi:10.1534/genetics.117.203836

87. Litvintseva AP, Lin X, Templeton I, Heitman J, Mitchell TG. Many globally isolated AD hybrid strains of *Cryptococcus neoformans* originated in Africa. PLoS Pathog. 2007;3: 1109–1117. doi:10.1371/journal.ppat.0030114
88. Nielsen K, De Obaldia AL, Heitman J. *Cryptococcus neoformans* mates on pigeon guano: implications for the realized ecological niche and globalization. Eukaryot Cell. 2007;6: 949–59. doi:10.1128/EC.00097-07
89. Vanhove M, Beale MA, Rhodes J, Chanda D, Lakhi S, Kwenda G, et al. Genomic epidemiology of *Cryptococcus* yeasts identifies adaptation to environmental niches underpinning infection across an African HIV/AIDS cohort. Mol Ecol. Wiley-Blackwell; 2017;26: 1991–2005. doi:10.1111/mec.13891
90. Desjardins CA, Giamberardino C, Sykes SM, Yu C-H, Tenor JL, Chen Y, et al. Population genomics and the evolution of virulence in the fungal pathogen *Cryptococcus neoformans*. Genome Res. 2017;27: 1207–1219. doi:10.1101/gr.218727.116
91. Litvintseva… AP. Population Genetic Analyses Reveal the African Origin and Strain Variation of *Cryptococcus neoformans* var. *grubii*. PLoS Pathog. 2012;
92. Simwami SP, Khayhan K, Henk D a, Aanensen DM, Boekhout T, Hagen F, et al. Low diversity *Cryptococcus neoformans* variety *grubii* multilocus sequence types from Thailand are consistent with an ancestral African origin. PLoS Pathog. 2011;7: e1001343. doi:10.1371/journal.ppat.1001343
93. Cox GM, Harrison TS, Mcdade HC, Taborda CP, Heinrich G, Casadevall A, et al. Superoxide Dismutase Influences the Virulence of *Cryptococcus neoformans* by Affecting Growth within Macrophages. Infect Immun. 2003;71: 173–180.

doi:10.1128/IAI.71.1.173

94. Steenbergen JN, Casadevall A. The origin and maintenance of virulence for the human pathogenic fungus *Cryptococcus neoformans*. Microbes Infect. 2003;5: 667–675.

95. Xue C. *Cryptococcus* and Beyond-Inositol Utilization and Its Implications for the Emergence of Fungal Virulence. PLoS Pathog. 2012;8. doi:10.1371/journal.ppat.1002869

96. Xue C, Liu T, Chen L, Li W, Liu I, Kronstad JW, et al. Role of an expanded inositol transporter repertoire in *Cryptococcus neoformans* sexual reproduction and virulence. MBio. 2010;1. doi:10.1128/mBio.00084-10

97. Fisher SK, Novak JE, Agranoff BW. Inositol and higher inositol phosphates in neural tissues: homeostasis, metabolism and functional significance. J Neurochem. 2002;82: 736–54.

98. Liu T-B, Kim J-C, Wang Y, Toffaletti DL, Eugenin E, Perfect JR, et al. Brain inositol is a novel stimulator for promoting *Cryptococcus* penetration of the blood-brain barrier. PLoS Pathog. Public Library of Science; 2013;9: e1003247. doi:10.1371/journal.ppat.1003247

99. Jain N, Wickes BL, Keller SM, Fu J, Casadevall A, Jain P, et al. Molecular epidemiology of clinical *Cryptococcus neoformans* strains from India. J Clin Microbiol. 2005;43: 5733–42. doi:10.1128/JCM.43.11.5733-5742.2005

100. Hiremath SS, Chowdhary A, Kowshik T, Randhawa HS, Sun S, Xu J. Long-distance dispersal and recombination in environmental populations of *Cryptococcus neoformans* var. *grubii* from India. Microbiology. 2008;154: 1513–24. doi:10.1099/mic.0.2007/015594-0

101. Khayhan K, Hagen F, Pan W, Simwami S, Fisher MC, Wahyuningsih R, et al. Geographically structured populations of *Cryptococcus neoformans* Variety *grubii*

in Asia correlate with HIV status and show a clonal population structure. Zaragoza O, editor. PLoS One. 2013;8: e72222. doi:10.1371/journal.pone.0072222

102. Kaocharoen S, Ngamskulrungroj P, Firacative C, Trilles L, Piyabongkarn D, Banlunara W, et al. Molecular epidemiology reveals genetic diversity amongst isolates of the *Cryptococcus neoformans*/C. *gattii* species complex in Thailand. Wanke B, editor. PLoS Negl Trop Dis. 2013;7: e2297. doi:10.1371/journal.pntd.0002297

103. Day JN, Hoang TN, Duong A V, Hong CTT, Diep PT, Campbell JI, et al. Most cases of cryptococcal meningitis in HIV-uninfected patients in Vietnam are due to a distinct amplified fragment length polymorphism-defined cluster of *Cryptococcus neoformans* var. *grubii* VN1. J Clin Microbiol. 2011;49: 658–64. doi:10.1128/JCM.01985-10

104. Dou H, Wang H, Xie S, Chen X, Xu Z, Xu Y. Molecular characterization of *Cryptococcus neoformans* isolated from the environment in Beijing, China. Med Mycol. 2017;38: 1–11. doi:10.1093/mmy/myx026

105. Dou H-T, Xu Y-C, Wang H-Z, Li T-S. Molecular epidemiology of *Cryptococcus neoformans* and *Cryptococcus gattii* in China between 2007 and 2013 using multilocus sequence typing and the DiversiLab system. Eur J Clin Microbiol Infect Dis. 2014;34: 753–62. doi:10.1007/s10096-014-2289-2

106. Fan X, Xiao M, Chen S-L, Kong F, Dou H-T, Wang H, et al. Predominance of *Cryptococcus neoformans* var. *grubii* multilocus sequence type 5 and emergence of isolates with non-wild-type minimum inhibitory concentrations to fluconazole: a multi-centre study in China. Clin Microbiol Infect.; 2016;22: 887.e1–887.e9. doi:10.1016/j.cmi.2016.07.008

107. Mihara T, Izumikawa K, Kakeya H, Ngamskulrungroj P, Umeyama T, Takazono T, et al. Multilocus sequence typing of *Cryptococcus neoformans* in non-HIV associated cryptococcosis in Nagasaki, Japan. Med Mycol. 2013;51: 252–60.

doi:10.3109/13693786.2012.708883

108. Tibayrenc M, Ayala FJ. Reproductive clonality of pathogens: A perspective on pathogenic viruses, bacteria, fungi, and parasitic protozoa. Proc Natl Acad Sci. 2012;109: E3305–E3313. doi:10.1073/pnas.1212452109
109. Chen J, Varma A, Diaz M. *Cryptococcus neoformans* strains and infection in apparently immunocompetent patients, China. Emerg Infect Dis. 2008;14.
110. Wu S-Y, Lei Y, Kang M, Xiao Y-L, Chen Z-X. Molecular characterisation of clinical *Cryptococcus neoformans* and *Cryptococcus gattii* isolates from Sichuan province, China. Mycoses. 2015;58: 280–287. doi:10.1111/myc.12312
111. Choi YH, Ngamskulrungroj P, Varma A, Sionov E, Hwang M, Carriconde F, et al. Prevalence of the VNIc genotype of *Cryptococcus neoformans* in non-HIV associated cryptococcosis in the Republic of Korea. FEMS Yeast Res. 2010;10: 769–778. doi:10.1111/j.1567-1364.2010.00648.x.Prevalence
112. Casadevall A, Steenbergen JN, Nosanchuk JD. “Ready made” virulence and “dual use” virulence factors in pathogenic environmental fungi — the *Cryptococcus neoformans* paradigm. Curr Opin Microbiol. 2003;6: 332–337. doi:10.1016/S1369-5274(03)00082-1
113. Kronstad JW, Attarian R, Cadieux B, Choi J, D’Souza C a, Griffiths EJ, et al. Expanding fungal pathogenesis: *Cryptococcus* breaks out of the opportunistic box. Nat Rev Microbiol. Nature Publishing Group; 2011;9: 193–203. doi:10.1038/nrmicro2522
114. Aksenov, Babyeva, Golubev. On the mechanism of adaptation of micro-organisms to conditions of extreme low humidity. Life Sci Sp Res. 1973;11: 55–61.
115. Steenbergen JN, Shuman H a, Casadevall A. *Cryptococcus neoformans* interactions with amoebae suggest an explanation for its virulence and intracellular pathogenic strategy in macrophages. Proc Natl Acad Sci U S A. 2001;98: 15245–50. doi:10.1073/pnas.261418798

116. Garcia-solache MA, Casadevall A. Global Warming Will Bring New Fungal Diseases for Mammals. MBio. 2010;1. doi:10.1128/mBio.00061-10.Updated
117. Shuman EK. Global climate change and infectious diseases. Int J Occup Environ Med. 2011;2: 11–9.
118. Wang Y, Casadevall A. Decreased susceptibility of melanized *Cryptococcus neoformans* to UV light. Appl Environ Microbiol. 1994;60: 3864–3866.
119. Liu L, Tewari RP, Williamson PR. Laccase protects *Cryptococcus neoformans* from antifungal activity of alveolar macrophages. Infect Immun. 1999;67: 6034–9.
120. Chrisman CJ, Alvarez M, Casadevall A. Phagocytosis of *Cryptococcus neoformans* by, and nonlytic exocytosis from, Acanthamoeba castellanii. Appl Environ Microbiol. 2010;76: 6056–62. doi:10.1128/AEM.00812-10
121. Zaragoza O, Rocío GR, Nosanchuk JD, Cuenca-Estrella M, Rodríguez-Tudela JL, Casadevall A. Fungal cell gigantism during mammalian infection. PLoS Pathog. 2010;6. doi:10.1371/journal.ppat.1000945
122. Fu MS, Casadevall A. Divalent metal cations potentiate the predatory capacity of amoeba for *Cryptococcus neoformans*. Appl Environ Microbiol. 2018;84. doi:10.1128/AEM.01717-17
123. Hu G, Chen SH, Qiu J, Bennett JE, Myers TG, Williamson PR. Microevolution during serial mouse passage demonstrates FRE3 as a virulence adaptation gene in *Cryptococcus neoformans*. MBio. 2014;5. doi:10.1128/mBio.00941-14
124. Chow EWL, Morrow CA, Djordjevic JT, Wood IA, Fraser JA. Microevolution of *Cryptococcus neoformans* driven by massive tandem gene amplification. Mol Biol Evol. 2012;29: 1987–2000. doi:10.1093/molbev/mss066
125. Rhodes J, Beale M, Vanhove M, Jarvis JN, Kannambath S, Simpson JA, et al. A population genomics approach to assessing the genetic basis of within-host microevolution underlying recurrent cryptococcal meningitis infection. bioRxiv.

2016; 083469. doi:10.1101/083469

126. Voelz K. Macrophage-*Cryptococcus* interaction during Cryptococcosis. University of Birmingham. 2010.

127. Nicola AM, Robertson EJ, Albuquerque P, Casadevall A. Nonlytic Exocytosis of *Cryptococcus neoformans* from Macrophages Occurs In Vivo and Is Influenced by Phagosomal pH. 2011;2: 1–9. doi:10.1128/mBio.00167-11.Editor

128. Johnston S a, May RC. The human fungal pathogen *Cryptococcus neoformans* escapes macrophages by a phagosome emptying mechanism that is inhibited by Arp2/3 complex-mediated actin polymerisation. PLoS Pathog. 2010;6: e1001041. doi:10.1371/journal.ppat.1001041

129. Feldmesser M, Tucker S, Casadevall a. Intracellular parasitism of macrophages by *Cryptococcus neoformans*. Trends Microbiol. 2001;9: 273–8.

130. Ma H. Intracellular parasitism of macrophages by *Cryptococcus*. University of Birmingham. 2009.

131. Ma H, Croudace JE, Lammas D a, May RC. Expulsion of live pathogenic yeast by macrophages. Curr Biol. 2006;16: 2156–60. doi:10.1016/j.cub.2006.09.032

132. Charlier C, Nielsen K, Daou S, Brigitte M, Chretien F, Dromer F. Evidence of a role for monocytes in dissemination and brain invasion by *Cryptococcus neoformans*. Infect Immun. 2009;77: 120–7. doi:10.1128/IAI.01065-08

133. Alvarez M, Burn T, Luo Y, Pirofski L, Casadevall A. The outcome of *Cryptococcus neoformans* intracellular pathogenesis in human monocytes. BMC Microbiol. 2009;9: 1–9. doi:10.1186/1471-2180-9-51

134. Poeta M Del. Role of Phagocytosis in the Virulence of *Cryptococcus neoformans*. Eukaryot Cell. 2004;3: 1067. doi:10.1128/EC.3.5.1067

135. Sabiiti W, Robertson E, Beale MA, Johnston SA, Brouwer AE, Loyse A, et al. Efficient phagocytosis and laccase activity affect the outcome of HIV-associated

cryptococcosis. J Clin Invest. 2014;124. doi:10.1172/JCI72950.2000

136. Alanio A, Desnos-Ollivier M, Dromer F. Dynamics of *Cryptococcus neoformans*-macrophage interactions reveal that fungal background influences outcome during cryptococcal meningoencephalitis in humans. MBio. 2011;2: e00158–11. doi:10.1128/mBio.00158-11.Editor

137. Mansour MK, Vyas JM, Levitz SM. Dynamic virulence: Real-time assessment of intracellular pathogenesis links *Cryptococcus neoformans* phenotype with clinical outcome. mBio. 2011. doi:10.1128/mBio.00217-11

138. Voelz K, Johnston SA, Smith LM, Hall RA, Idnurm A, May RC. "Division of labour" in response to host oxidative burst drives a fatal *Cryptococcus gattii* outbreak. Nat Commun. Nature Publishing Group; 2014;5: 5194. doi:10.1038/ncomms6194

139. Wang C-Y, Wu H-D, Hsueh P-R. Nosocomial Transmission of Cryptococcosis. N Engl J Med. 2005;352: 1271–1272. doi:10.1056/NEJM200503243521225

140. Miozzo I, Aquino VR, Duarte M, Santos RP, Goldani LZ. *Cryptococcus neoformans* as a rare cause of hospital infection. Infect Control Hosp Epidemiol. 2010;31: 315–7. doi:10.1086/651064

141. Henderson DK, Bennett JE, Huber MA. Long-lasting, specific immunologic unresponsiveness associated with cryptococcal meningitis. J Clin Invest. 1982;69: 1185–1190. doi:10.1172/JCI110555

142. Deshaw M, Pirofski LA. Antibodies to the *Cryptococcus neoformans* capsular glucuronoxylomannan are ubiquitous in serum from HIV+ and HIV- individuals. Clin Exp Immunol. Wiley-Blackwell; 1995;99: 425–32.

143. Dromer F, Aucouturier P, Clauvel JP, Saimot G, Yeni P. *Cryptococcus neoformans* antibody levels in patients with AIDS. Scand J Infect Dis. 1988;20: 283–5.

144. Goldman DL, Khine H, Abadi J, Lindenberg DJ, Pirofski L -a., Niang R, et al. Serologic Evidence for *Cryptococcus neoformans* Infection in Early Childhood. Pediatrics.

2001;107: e66–e66. doi:10.1542/peds.107.5.e66

145. Davis J, Zheng WY, Glatman-Freedman A, Ng JAN, Pagcatipunan MR, Lessin H, et al. Serologic evidence for regional differences in pediatric cryptococcal infection. Pediatr Infect Dis J. 2007;26: 549–51. doi:10.1097/INF.0b013e318047e073

146. Garcia-Hermoso D, Janbon G, Dromer F. Epidemiological evidence for dormant *Cryptococcus neoformans* infection. J Clin Microbiol. 1999;37: 3204–9.

147. Singh N, Dromer F, Perfect JR, Lortholary O. Cryptococcosis in solid organ transplant recipients: current state of the science. Clin Infect Dis. 2008;47: 1321–7. doi:10.1086/592690

148. Chow WLE, Fraser J. Microevolution in the Human Fungal Pathogen *Cryptococcus neoformans*. Gene. 2010;41: 8–11.

149. Sullivan D, Haynes K, Moran G, Shanley D, Coleman D. Persistence, replacement, and microevolution of *Cryptococcus neoformans* strains in recurrent meningitis in AIDS patients. J Clin Microbiol. 1996;34: 1739–1744.

150. Desnos-Ollivier M, Patel S, Spaulding AR, Charlier C, Garcia-Hermoso D, Nielsen K, et al. Mixed infections and in vivo evolution in the human fungal pathogen *Cryptococcus neoformans*. MBio. 2010;1. doi:10.1128/mBio.00091-10

151. Ferreira-Paim K, Andrade-Silva L, Fonseca FM, Ferreira TB, Mora DJ, Andrade-Silva J, et al. MLST-based population genetic analysis in a global context reveals clonality amongst *Cryptococcus neoformans* var. *grubii* VNI isolates from HIV patients in Southeastern Brazil. Vinetz JM, editor. PLoS Negl Trop Dis. 2017;11: e0005223. doi:10.1371/journal.pntd.0005223

152. Cogliati M, Zamfirova RR, Tortorano AM, Viviani MA. Molecular epidemiology of Italian clinical *Cryptococcus neoformans* var. *grubii* isolates. Med Mycol. 2013;51: 499–506. doi:10.3109/13693786.2012.751642

153. Zaragoza O, Rodrigues ML, Jesus M De, Frases S, Casadevall A, Micología S De, et al.

The capsule of the fungal pathogen *Cryptococcus neoformans*. Adv Appl Microbiol. 2010;2164: 1–64. doi:10.1016/S0065-2164(09)01204-0.The

154. Feldmesser M, Kress Y, Casadevall a. Dynamic changes in the morphology of *Cryptococcus neoformans* during murine pulmonary infection. Microbiology. 2001;147: 2355–65.
155. García-Rivera J, Chang YC, Kwon-Chung KJ, Casadevall A. *Cryptococcus neoformans* CAP59 (or Cap59p) is involved in the extracellular trafficking of capsular glucuronoxylomannan. Eukaryot Cell. 2004;3: 385–392. doi:10.1128/EC.3.2.385-392.2004
156. Yoneda A, Doering TL. A eukaryotic capsular polysaccharide is synthesized intracellularly and secreted via exocytosis. Mol Biol Cell. 2006;17: 5131–5140. doi:10.1091/mbc.E06-08-0701
157. Rodrigues ML, Nimrichter L, Oliveira DL, Frases S, Miranda K, Zaragoza O, et al. Vesicular polysaccharide export in *Cryptococcus neoformans* is a eukaryotic solution to the problem of fungal trans-cell wall transport. Eukaryot Cell. 2007;6: 48–59. doi:10.1128/EC.00318-06
158. Cordero RJB, Frases S, Guimaräes AJ, Rivera J, Casadevall A. Evidence for branching in cryptococcal capsular polysaccharides and consequences on its biological activity. Mol Microbiol. 2011;79: 1101–17. doi:10.1111/j.1365-2958.2010.07511.x
159. Cherniak R, Morris LC, Belay T, Spitzer ED, Casadevall A. Variation in the structure of glucuronoxylomannan in isolates from patients with recurrent cryptococcal meningitis. Infect Immun. 1995;63: 1899–1905.
160. Gates M a, Thorkildson P, Kozel TR. Molecular architecture of the *Cryptococcus neoformans* capsule. Mol Microbiol. 2004;52: 13–24. doi:10.1111/j.1365-2958.2003.03957.x
161. Bryan R a., Zaragoza O, Zhang T, Ortiz G, Casadevall a., Dadachova E. Radiological

studies reveal radial differences in the architecture of the polysaccharide capsule of *Cryptococcus neoformans*. Eukaryot Cell. 2005;4: 465–475. doi:10.1128/EC.4.2.465-475.2005

162. Frases S, Pontes B, Nimrichter L, Viana NB, Rodrigues ML, Casadevall A. Capsule of *Cryptococcus neoformans* grows by enlargement of polysaccharide molecules. Proc Natl Acad Sci U S A. 2009;106: 1228–1233. doi:10.1073/pnas.0808995106
163. Gates M a., Kozel TR. Differential localization of complement component 3 within the capsular matrix of *Cryptococcus neoformans*. Infect Immun. 2006;74: 3096–3106. doi:10.1128/IAI.01213-05
164. Robertson EJ, Najjuka G, Rolfes M a, Akampurira A, Jain N, Anantharanjit J, et al. *Cryptococcus neoformans* ex vivo capsule size is associated with intracranial pressure and host immune response in HIV-associated cryptococcal meningitis. J Infect Dis. 2014;209: 74–82. doi:10.1093/infdis/jit435
165. Fromtling RA, Shadomy HJ, Jacobson ES. Decreased virulence in stable, acapsular mutants of *Cryptococcus neoformans*. Mycopathologia. 1982;79: 23–29. doi:10.1007/BF00636177
166. Wilder JA, Olson GK, Chang YC, Kwon-chung KJ, Lipscomb MF. Complementation of a Capsule Deficient *Cryptococcus neoformans* with Cap64 Restores Virulence in a Murine Lung Infection.
167. Casadevall A, Perfect J. *Cryptococcus neoformans*. Washington DC: ASM Press; 1998.
168. Frases S, Nimrichter L, Viana NB, Nakouzi A, Casadevall A. *Cryptococcus neoformans* capsular polysaccharide and exopolysaccharide fractions manifest physical, chemical, and antigenic differences. Eukaryot Cell. 2008;7: 319–27. doi:10.1128/EC.00378-07
169. Vecchiarelli A. Immunoregulation by capsular components of *Cryptococcus*

neoformans. Med Mycol. 2000;38: 407–417.

170. Feldmesser M, Kress Y, Novikoff P, Casadevall a. *Cryptococcus neoformans* is a facultative intracellular pathogen in murine pulmonary infection. Infect Immun. 2000;68: 4225–37.
171. Tucker SC, Casadevall A. Replication of *Cryptococcus neoformans* in macrophages is accompanied by phagosomal permeabilization and accumulation of vesicles containing polysaccharide in the cytoplasm. Proc Natl Acad Sci U S A. 2002;99: 3165–70. doi:10.1073/pnas.052702799
172. Almeida GM, Andrade RM, Bento C a. M. The Capsular Polysaccharides of *Cryptococcus neoformans* Activate Normal CD4+ T Cells in a Dominant Th2 Pattern. J Immunol. 2001;167: 5845–5851. doi:10.4049/jimmunol.167.10.5845
173. Denning DW, Armstrong RW, Lewis BH, Stevens DA. Elevated cerebrospinal fluid pressures in patients with cryptococcal meningitis and acquired immunodeficiency syndrome. Am J Med. 1991;91: 267–72. doi:10.1016/0002-9343(91)90126-I
174. Rocha JDB, Nascimento MTC, Decote-Ricardo D, Côrte-Real S, Morrot A, Heise N, et al. Capsular polysaccharides from *Cryptococcus neoformans* modulate production of neutrophil extracellular traps (NETs) by human neutrophils. Sci Rep. Nature Publishing Group; 2015;5: 8008. doi:10.1038/srep08008
175. Chiapello L, Iribarren P, Cervi L, Rubinstein H, Masih D. Mechanisms for Induction of Immunosuppression during Experimental Cryptococcosis: Role of Glucuronoxylomannan. Clin Immunol. 2001;100: 96–106. doi:10.1006/clim.2001.5046
176. Blackstock R. Cryptococcal capsular polysaccharide utilizes an antigen-presenting cell to induce a T-suppressor cell to secrete TsF. Med Mycol. 1996;34: 19–30. doi:10.1080/02681219680000041
177. Blackstock R, McElwee N, Neller E, Shaddix-White J. Regulation of cytokine

expression in mice immunized with cryptococcal polysaccharide, a glucuronoxylomannan (GXM), associated with peritoneal antigen-presenting cells (APC): requirements for GXM, APC activation, and interleukin-12. Infect Immun.; 2000;68: 5146–53.

178. Blackstock R, Murphy JW. Secretion of the C3 component of complement by peritoneal cells cultured with encapsulated *Cryptococcus neoformans*. Infect Immun.; 1997;65: 4114–21.
179. Syme RM, Bruno TF, Kozel TR, Mody CH. The capsule of *Cryptococcus neoformans* reduces T-lymphocyte proliferation by reducing phagocytosis, which can be restored with anticapsular antibody. Infect Immun.; 1999;67: 4620–7.
180. Villena SN, Pinheiro RO, Pinheiro CS, Nunes MP, Takiya CM, DosReis GA, et al. Capsular polysaccharides galactoxylomannan and glucuronoxylomannan from *Cryptococcus neoformans* induce macrophage apoptosis mediated by Fas ligand. Cell Microbiol. 2008;10: 1274–1285. doi:10.1111/j.1462-5822.2008.01125.x
181. Lupo P, Chang YC, Kelsall BL, Farber JM, Pietrella D, Vecchiarelli A, et al. The presence of capsule in *Cryptococcus neoformans* influences the gene expression profile in dendritic cells during interaction with the fungus. Infect Immun.; 2008;76: 1581–9. doi:10.1128/IAI.01184-07
182. Casadevall A. Fungal virulence, vertebrate endothermy, and dinosaur extinction: is there a connection? Fungal Genet Biol. 2005;42: 98–106. doi:10.1016/j.fgb.2004.11.008
183. Leach MD, Cowen LE. Surviving the heat of the moment: a fungal pathogens perspective. PLoS Pathog. 2013;9: e1003163. doi:10.1371/journal.ppat.1003163
184. Gow N a R. Fungal morphogenesis: some like it hot. Curr Biol. ; 2009;19: R333–4. doi:10.1016/j.cub.2009.03.027
185. Perfect JR. *Cryptococcus neoformans*: the yeast that likes it hot. FEMS Yeast Res.

2006;6: 463–8. doi:10.1111/j.1567-1364.2006.00051.x

186. Martinez LR, Garcia-Rivera J, Casadevall A. *Cryptococcus neoformans* var. *neoformans* (serotype D) strains are more susceptible to heat than C. *neoformans* var. *grubii* (serotype A) strains. J Clin Microbiol. 2001;39: 3365–3367. doi:10.1128/JCM.39.9.3365-3367.2001

187. Williamson PR, Wakamatsu K, Ito S. Melanin biosynthesis in *Cryptococcus neoformans*. J Bacteriol. 1998;180: 1570–1572.

188. Eisenman HC, Mues M, Weber SE, Frases S, Chaskes S, Gerfen G, et al. *Cryptococcus neoformans* laccase catalyses melanin synthesis from both D- and L-DOPA. Microbiology. 2007;153: 3954–3962. doi:10.1099/mic.0.2007/011049-0

189. Williamson PR. Laccase and melanin in the pathogenesis of *Cryptococcus neoformans*. Front Biosci. 1997;2: e99–e107.

190. Rosas ÁL, Casadevall A. Melanization affects susceptibility of *Cryptococcus neoformans* to heat and cold. FEMS Microbiol Lett. 1997;153: 265–272. doi:10.1016/S0378-1097(97)00239-5

191. Nosanchuk JD, Rudolph J, Rosas AL, Casadevall A. Evidence that *Cryptococcus neoformans* is melanized in pigeon excreta: implications for pathogenesis. Infect Immun. 1999;67: 5477–9.

192. Rosas ÁL, Casadevall A. Melanization decreases the susceptibility of *Cryptococcus neoformans* to enzymatic degradation. Mycopathologia. 2001;151: 53–56. doi:10.1023/A:1010977107089

193. García-Rivera J, Casadevall A. Melanization of *Cryptococcus neoformans* reduces its susceptibility to the antimicrobial effects of silver nitrate. Med Mycol. 2001;39: 353–357. doi:10.1080/mmy.39.4.353.357

194. Ikeda R, Sugita T, Jacobson ES, Shinoda T. Effects of melanin upon susceptibility of *Cryptococcus* to antifungals. Microbiol Immunol. 2003;47: 271–7.

195. Feldmesser M, Kress Y, Casadevall a. Dynamic changes in the morphology of *Cryptococcus neoformans* during murine pulmonary infection. Microbiology. 2001;147: 2355–65.

196. Okagaki LH, Strain AK, Nielsen JN, Charlier C, Baltes NJ, Chr??tien F, et al. Cryptococcal cell morphology affects host cell interactions and pathogenicity. PLoS Pathog. 2010;6. doi:10.1371/journal.ppat.1000953

197. Okagaki LH, Strain AK, Nielsen JN, Charlier C, Baltes NJ, Chrétien F, et al. Cryptococcal cell morphology affects host cell interactions and pathogenicity. PLoS Pathog. 2010;6: e1000953. doi:10.1371/journal.ppat.1000953

198. Idnurm A, Bahn Y-S, Nielsen K, Lin X, Fraser J a, Heitman J. Deciphering the model pathogenic fungus *Cryptococcus neoformans*. Nat Rev Microbiol. 2005;3: 753–764. doi:10.1038/nrmicro1245

199. Hsueh YP, Heitman J. Orchestration of sexual reproduction and virulence by the fungal mating-type locus. Current Opinion in Microbiology. 2008. pp. 517–524. doi:10.1016/j.mib.2008.09.014

200. D'Souza CA, Alspaugh JA, Yue C, Harashima T, Cox GM, Perfect JR, et al. Cyclic AMP-dependent protein kinase controls virulence of the fungal pathogen *Cryptococcus neoformans*. Mol Cell Biol. 2001;21: 3179–91. doi:10.1128/MCB.21.9.3179-3191.2001

201. Love GL, Boyd GD, Greer DL. Large *Cryptococcus neoformans* isolated from brain abscess. J Clin Microbiol. 1985;22: 1068–1070.

202. Zaragoza O, García-Rodas R, Nosanchuk JD, Cuenca-Estrella M, Rodríguez-Tudela JL, Casadevall A. Fungal cell gigantism during mammalian infection. PLoS Pathog. 2010;6: e1000945. doi:10.1371/journal.ppat.1000945

203. Polacheck I, Lebens GA. Electrophoretic karyotype of the pathogenic yeast *Cryptococcus neoformans*. J Gen Microbiol. 1989;135: 65–71.

doi:10.1099/00221287-135-1-65

204. Perfect JR, Ketabchi N, Cox GM, Ingram CW, Beiser CL. Karyotyping of *Cryptococcus neoformans* as an epidemiological tool. J Clin Microbiol. 1993;31: 3305–3309.

205. Boekhout T, Van Belkum A. Variability of karyotypes and RAPD types in genetically related strains of *Cryptococcus neoformans*. Curr Genet. 1997;32: 203–208. doi:10.1007/s002940050267

206. Boekhout T, van Belkum A, Leenders AC, Verbrugh HA, Mukamurangwa P, Swinne D, et al. Molecular typing of *Cryptococcus neoformans*: taxonomic and epidemiological aspects. Int J Syst Bacteriol. 1997;47: 432–442. doi:10.1099/00207713-47-2-432

207. Fries BC, Chen F, Currie BP, Casadevall A. Karyotype instability in *Cryptococcus neoformans* infection. J Clin Microbiol. 1996;34: 1531–1534.

208. Ormerod KL, Fraser J a. Balancing Stability and Flexibility within the Genome of the Pathogen *Cryptococcus neoformans*. Goldman WE, editor. PLoS Pathog. 2013;9: e1003764. doi:10.1371/journal.ppat.1003764

209. Currie B, Sanati H, Ibrahim AS, Edwards JE, Casadevall A, Ghannoum MA. Sterol compositions and susceptibilities to amphotericin B of environmental *Cryptococcus neoformans* isolates are changed by murine passage. Antimicrob Agents Chemother. 1995;39: 1934–1937. doi:10.1128/AAC.39.9.1934

210. Sionov E, Chang YC, Garraffo HM, Kwon-Chung KJ. Heteroresistance to fluconazole in *Cryptococcus neoformans* is intrinsic and associated with virulence. Antimicrob Agents Chemother. 2009;53: 2804–15. doi:10.1128/AAC.00295-09

211. Hu G, Liu I, Sham A, Stajich JE, Dietrich FS, Kronstad JW. Comparative hybridization reveals extensive genome variation in the AIDS-associated pathogen *Cryptococcus neoformans*. Genome Biol. 2008;9: R41. doi:10.1186/gb-2008-9-2-r41

212. Selmecki A, Forche A, Berman J. Genomic plasticity of the human fungal pathogen

Candida albicans. Eukaryot Cell. 2010;9: 991–1008. doi:10.1128/EC.00060-10

213. Kwon-Chung KJ, Chang YC. Aneuploidy and drug resistance in pathogenic fungi. PLoS Pathog. 2012;8: e1003022. doi:10.1371/journal.ppat.1003022

214. Ngamskulrungroj P, Chang Y, Hansen B, Bugge C, Fischer E, Kwon-Chung KJ. Characterization of the chromosome 4 genes that affect fluconazole-induced disomy formation in *Cryptococcus neoformans*. PLoS One. 2012;7: e33022. doi:10.1371/journal.pone.0033022

215. Desjardins C, Giamberardino C, Sykes S, Yu C-H, Tenor J, Chen Y, et al. Population genomics and the evolution of virulence in the fungal pathogen *Cryptococcus neoformans*. bioRxiv. 2017; 118323. doi:10.1101/gr.218727.116.Freely

216. Jung K-W, Yang D-H, Maeng S, Lee K-T, So Y-S, Hong J, et al. Systematic functional profiling of transcription factor networks in *Cryptococcus neoformans*. Nat Commun. 2015;6: 6757. doi:10.1038/ncomms7757

217. Liu TB, Kim JC, Wang Y, Toffaletti DL, Eugenin E, Perfect JR, et al. Brain Inositol Is a Novel Stimulator for Promoting *Cryptococcus* Penetration of the Blood-Brain Barrier. PLoS Pathog. 2013;9. doi:10.1371/journal.ppat.1003247

218. Shea JM, Henry JL, Del Poeta M. Lipid metabolism in *Cryptococcus neoformans*. FEMS Yeast Research. 2006. pp. 469–479. doi:10.1111/j.1567-1364.2006.00080.x

219. Fisher SK, Novak JE, Agranoff BW. Inositol and higher inositol phosphates in neural tissues: Homeostasis, metabolism and functional significance. Journal of Neurochemistry. 2002. pp. 736–754. doi:10.1046/j.1471-4159.2002.01041.x

220. Rosa e Silva LK, Staats CC, Goulart LS, Morello LG, Pelegrinelli Fungaro MH, Schrank A, et al. Identification of novel temperature-regulated genes in the human pathogen *Cryptococcus neoformans* using representational difference analysis. Res Microbiol. 2008;159: 221–229. doi:10.1016/j.resmic.2007.12.006

221. Steen BR, Lian T, Zuyderduyn S, MacDonald WK, Marra M, Jones SJM, et al.

Temperature-regulated transcription in the pathogenic fungus *Cryptococcus neoformans*. Genome Res. Cold Spring Harbor Laboratory Press; 2002;12: 1386–400. doi:10.1101/gr.80202

222. Kraus PR, Boily MJ, Giles SS, Stajich JE, Allen A, Cox GM, et al. Identification of *Cryptococcus neoformans* temperature-regulated genes with a genomic-DNA microarray. Eukaryot Cell.; 2004;3: 1249–1260. doi:10.1128/EC.3.5.1249-1260.2004
223. Upadhya R, Campbell LT, Donlin MJ, Aurora R, Lodge JK. Global transcriptome profile of *Cryptococcus neoformans* during exposure to hydrogen peroxide induced oxidative stress. PLoS One. 2013;8: e55110. doi:10.1371/journal.pone.0055110
224. Haynes BC, Skowyra ML, Spencer SJ, Gish SR, Williams M, Held EP, et al. Toward an integrated model of capsule regulation in *Cryptococcus neoformans*. Mitchell AP, editor. PLoS Pathog. Public Library of Science; 2011;7: e1002411. doi:10.1371/journal.ppat.1002411
225. Lian T, Simmer MI, D'Souza C a., Steen BR, Zuyderduyn SD, Jones SJM, et al. Iron-regulated transcription and capsule formation in the fungal pathogen *Cryptococcus neoformans*. Mol Microbiol. 2005;55: 1452–1472. doi:10.1111/j.1365-2958.2004.04474.x
226. Goulart L, Rosa e Silva LK, Chiapello L, Silveira C, Crestani J, Masih D, et al. *Cryptococcus neoformans* and *Cryptococcus gattii* genes preferentially expressed during rat macrophage infection. Med Mycol. 2010;48: 932–41. doi:10.3109/13693781003677494
227. Fan W, Kraus PR, Boily M-J, Heitman J. *Cryptococcus neoformans* gene expression during murine macrophage infection. Eukaryot Cell. 2005;4: 1420–33. doi:10.1128/EC.4.8.1420-1433.2005
228. Hu G, Cheng P-Y, Sham A, Perfect JR, Kronstad JW. Metabolic adaptation in

Cryptococcus neoformans during early murine pulmonary infection. Mol Microbiol. Blackwell Publishing Ltd; 2008;69: 1456–75. doi:10.1111/j.1365-2958.2008.06374.x

229. Garcia-Rivera J, Tucker SC, Feldmesser M, Williamson PR, Casadevall A. Laccase expression in murine pulmonary *Cryptococcus neoformans* infection. Infect Immun. 2005;73: 3124–3127. doi:10.1128/IAI.73.5.3124-3127.2005
230. Steen BR, Zuyderduyn S, Toffaletti DL, Marra M, Jones SJM, Perfect JR, et al. *Cryptococcus neoformans* Gene Expression during Experimental Cryptococcal Meningitis. 2003;2: 1336–1349. doi:10.1128/EC.2.6.1336
231. Erickson T, Liu L, Gueyikian A, Zhu X, Gibbons J, Williamson PR. Multiple virulence factors of *Cryptococcus neoformans* are dependent on VPH1. Mol Microbiol. 2001;42: 1121–1131. doi:10.1046/j.1365-2958.2001.02712.x
232. Giles SS, Batinic I, Perfect JR, Cox GM. *Cryptococcus neoformans* Mitochondrial Superoxide Dismutase : an Essential Link between Antioxidant Function and High-Temperature Growth. Eukaryot Cell. 2005;4: 46–54. doi:10.1128/EC.4.1.46
233. Kraus PR, Fox DS, Cox GM, Heitman J. The *Cryptococcus neoformans* MAP kinase Mpk1 regulates cell integrity in response to antifungal drugs and loss of calcineurin function. Mol Microbiol. 2003;48: 1377–1387. doi:10.1046/j.1365-2958.2003.03508.x
234. Akhter S, McDade HC, Gorlach JM, Heinrich G, Cox GM, Perfect JR. Role of alternative oxidase gene in pathogenesis of *Cryptococcus neoformans*. Infect Immun. 2003;71: 5794–5802. doi:10.1128/IAI.71.10.5794-5802.2003
235. Görlach J, Fox DS, Cutler NS, Cox GM, Perfect JR, Heitman J. Identification and characterization of a highly conserved calcineurin binding protein, CBP1/calcipressin, in *Cryptococcus neoformans*. EMBO J. 2000;19: 3618–3629. doi:10.1093/emboj/19.14.3618
236. Odom a, Muir S, Lim E, Toffaletti DL, Perfect J, Heitman J. Calcineurin is required

for virulence of *Cryptococcus neoformans*. EMBO J. 1997;16: 2576–2589. doi:10.1093/emboj/16.10.2576

237. Toffaletti DL, Del Poeta M, Rude TH, Dietrich F, Perfect JR. Regulation of cytochrome c oxidase subunit 1 (COX1) expression in *Cryptococcus neoformans* by temperature and host environment. Microbiology. 2003;149: 1041–9. doi:10.1099/mic.0.26021-0
238. Wang Y, Aisen P, Casadevall A. *Cryptococcus neoformans* melanin and virulence: mechanism of action. Infect Immun. 1995;63: 3131–6.
239. Giles SS, Perfect JR, Cox GM. Cytochrome c peroxidase contributes to the antioxidant defense of *Cryptococcus neoformans*. Fungal Genet Biol. 2005;42: 20–9. doi:10.1016/j.fgb.2004.09.003
240. Giles SS, Stajich JE, Nichols C, Gerrald QD, Alspaugh JA, Dietrich F, et al. The *Cryptococcus neoformans* catalase gene family and its role in antioxidant defense. Eukaryot Cell. 2006;5: 1447–59. doi:10.1128/EC.00098-06
241. Tesfa-Selase F, Hay RJ. Superoxide dismutase of *Cryptococcus neoformans*: purification and characterization. J Med Vet Mycol. 1995;33: 253–259.
242. Missall TA, Pusateri ME, Lodge JK. Thiol peroxidase is critical for virulence and resistance to nitric oxide and peroxide in the fungal pathogen , *Cryptococcus neoformans*. 2004;51: 1447–1458. doi:10.1046/j.1365-2958.2003.03921.x
243. Missall TA, Lodge JK. Function of the thioredoxin proteins in *Cryptococcus neoformans* during stress or virulence and regulation by putative transcriptional modulators. Mol Microbiol. 2005;57: 847–858. doi:10.1111/j.1365-2958.2005.04735.x
244. Missall TA, Cherry-Harris JF, Lodge JK. Two glutathione peroxidases in the fungal pathogen *Cryptococcus neoformans* are expressed in the presence of specific substrates. Microbiology. 2005;151: 2573–2581. doi:10.1099/mic.0.28132-0

245. Feldmesser M, Kress Y, Novikoff P. *Cryptococcus neoformans* Is a Facultative Intracellular Pathogen in Murine Pulmonary Infection. Infect Immun. 2000;68: 4225. doi:10.1128/IAI.68.7.4225-4237.2000.Updated

246. Feldmesser M, Tucker S, Casadevall A. Intracellular parasitism of macrophages by *Cryptococcus neoformans*. Trends in Microbiology. 2001. pp. 273–278. doi:10.1016/S0966-842X(01)02035-2

247. García-Rodas R, Zaragoza O. Catch me if you can: phagocytosis and killing avoidance by *Cryptococcus neoformans*. FEMS Immunol Med Microbiol. 2012;64: 147–61. doi:10.1111/j.1574-695X.2011.00871.x

248. Johnston SA, May RC. *Cryptococcus* interactions with macrophages : evasion and manipulation of the phagosome by a fungal pathogen. Cell microbiol. 2012; doi:10.1111/cmi.12067

249. Casadevall A. *Cryptococcus neoformans* : intracellular or extracellular ? TRENDS Microbiol. 2001;9: 417–418.

250. Ko YJ, Yu YM, Kim GB, Lee GW, Maeng PJ, Kim S, et al. Remodeling of global transcription patterns of *Cryptococcus neoformans* genes mediated by the stress-activated HOG signaling pathways. Eukaryot Cell. 2009;8: 1197–1217. doi:10.1128/EC.00120-09

251. Derengowski L da S, Paes HC, Albuquerque P, Tavares AHFP, Fernandes L, Silva-Pereira I, et al. The transcriptional response of *Cryptococcus neoformans* to ingestion by Acanthamoeba castellanii and macrophages provides insights into the evolutionary adaptation to the mammalian host. Eukaryot Cell. 2013;12: 761–774. doi:10.1128/EC.00073-13

252. De Jesús-Berríos M, Liu L, Nussbaum JC, Cox GM, Stamler JS, Heitman J. Enzymes that Counteract Nitrosative Stress Promote Fungal Virulence. Curr Biol. 2003;13: 1963–1968. doi:10.1016/j.cub.2003.10.029

253. Chen Y, Toffaletti DL, Tenor JL, Litvintseva AP, Fang C, Mitchell TG, et al. The *Cryptococcus neoformans* transcriptome at the site of human meningitis. MBio. 2014;5: e01087–13. doi:10.1128/mBio.01087-13

254. Upadhya R, Kim H, Jung KW, Park G, Lam W, Lodge JK, et al. Sulphiredoxin plays peroxiredoxin-dependent and -independent roles via the HOG signalling pathway in *Cryptococcus neoformans* and contributes to fungal virulence. Mol Microbiol. 2013;90: 630–648. doi:10.1111/mmi.12388

255. Kwang-Woo Jung, Anna K Strain, Kirsten Nielsen K-HJ. Two cation transporters Ena1 and Nha1 cooperatively modulate ion homeostasis, antifungal drug resistance, and virulence of *Cryptococcus neoformans* via the HOG pathway. Fungal Genet Biol. 2012;49: 332–345. doi:10.1016/j.fgb.2012.02.001.Two

256. Meara TRO, Holmer SM, Selvig K, Dietrich F, Alspaugh JA. *Cryptococcus neoformans* Rim101 Is Associated with Cell Wall Remodeling and Evasion of the Host Immune Responses. MBio. 2013;4. doi:10.1128/mBio.00522-12.Editor

257. O'Meara TR, Xu W, Selvig KM, O'Meara MJ, Mitchell AP, Alspaugh JA. The *Cryptococcus neoformans* Rim101 Transcription Factor Directly Regulates Genes Required for Adaptation to the Host. Mol Cell Biol. 2014;34: 673–684. doi:10.1128/MCB.01359-13

258. Chun FZ, Ling LM, Jones GJ, Gill MJ, Krensky AM, Kubes P, et al. Cytotoxic CD4+ T cells use granulysin to kill *Cryptococcus neoformans*, and activation of this pathway is defective in HIV patients. Blood. 2007;109: 2049–2057. doi:10.1182/blood-2006-03-009720

259. Lindell DM, Ballinger MN, McDonald R a, Toews GB, Huffnagle GB. Diversity of the T-cell response to pulmonary *Cryptococcus neoformans* infection. Infect Immun. 2006;74: 4538–48. doi:10.1128/IAI.00080-06

260. Mody CH, Lipscomb MF, Street NE, Toews GB. Depletion of CD4+ (L3T4+)

lymphocytes in vivo impairs murine host defense to *Cryptococcus neoformans*. J Immunol. 1990;144: 1472–7.

261. Buchanan KL, Doyle HA. Requirement for CD4+ T lymphocytes in host resistance against *Cryptococcus neoformans* in the central nervous system of immunized mice. Infect Immun. 2000;68: 456–462. doi:10.1128/IAI.68.2.456-462.2000
262. Ma LL, Spurrell JCL, Wang JF, Neely GG, Epelman S, Krensky a. M, et al. CD8 T Cell-Mediated Killing of *Cryptococcus neoformans* Requires Granulysin and Is Dependent on CD4 T Cells and IL-15. J Immunol. 2002;169: 5787–5795. doi:10.4049/jimmunol.169.10.5787
263. Hill JO, Aguirre KM. CD4+ T cell-dependent acquired state of immunity that protects the brain against *Cryptococcus neoformans*. J Immunol. 1994;152: 2344–50.
264. Huffnagle GB. Immunity to a pulmonary *Cryptococcus neoformans* infection requires both CD4+ and CD8+ T cells. J Exp Med. 1991;173: 793–800. doi:10.1084/jem.173.4.793
265. Syme RM, Wood CJ, Wong H, Mody CH. Both CD4+ and CD8+ human lymphocytes are activated and proliferate in response to *Cryptococcus neoformans*. Immunology. 1997;92: 194–200. doi:10.1046/j.1365-2567.1997.00345.x
266. Marr KJ, Jones GJ, Zheng C, Huston SM, Timm-McCann M, Islam A, et al. *Cryptococcus neoformans* directly stimulates perforin production and rearms NK cells for enhanced anticryptococcal microbicidal activity. Infect Immun. 2009;77: 2436–2446. doi:10.1128/IAI.01232-08
267. Oykhman P, Timm-McCann M, Xiang RF, Islam A, Li SS, Stack D, et al. Requirement and redundancy of the Src family kinases Fyn and Lyn in perforin-dependent killing of *Cryptococcus neoformans* by NK cells. Infect Immun. 2013;81: 3912–3922. doi:10.1128/IAI.00533-13

268. Ma LL, Wang CLC, Neely GG, Epelman S, Krensky AM, Mody CH. NK Cells Use Perforin Rather than Granulysin for Anticryptococcal Activity. J Immunol. 2004;173: 3357–3365. doi:10.4049/jimmunol.173.5.3357

269. Jarvis JN, Casazza JP, Stone HH, Meintjes G, Lawn SD, Levitz SM, et al. The phenotype of the *Cryptococcus*-specific CD4+ memory T-cell response is associated with disease severity and outcome in HIV-associated cryptococcal meningitis. J Infect Dis. 2013;207: 1817–28. doi:10.1093/infdis/jit099

270. Beenhouwer DO, Shapiro S, Feldmesser M, Casadevall A, Scharff MD. Both Th1 and Th2 cytokines affect the ability of monoclonal antibodies to protect mice against *Cryptococcus neoformans*. Infect Immun.; 2001;69: 6445–55. doi:10.1128/IAI.69.10.6445-6455.2001

271. Jain A V, Zhang Y, Fields WB, McNamara D a, Choe MY, Chen G-H, et al. Th2 but not Th1 immune bias results in altered lung functions in a murine model of pulmonary *Cryptococcus neoformans* infection. Infect Immun. 2009;77: 5389–99. doi:10.1128/IAI.00809-09

272. Voelz K, Lammas D a, May RC. Cytokine signaling regulates the outcome of intracellular macrophage parasitism by *Cryptococcus neoformans*. Infect Immun. 2009;77: 3450–7. doi:10.1128/IAI.00297-09

273. Abe K, Kadota J, Ishimatsu Y, Iwashita T, Tomono K, Kawakami K, et al. Th1-Th2 Cytokine Kinetics in the Bronchoalveolar Lavage Fluid of Mice Infected with *Cryptococcus neoformans* of Different Virulences. Microbiol Immunol. 2000;44: 849–855. doi:10.1111/j.1348-0421.2000.tb02573.x

274. Decken K, Köhler G, Palmer-Lehmann K, Wunderlin A, Mattner F, Magram J, et al. Interleukin-12 is essential for a protective Th1 response in mice infected with *Cryptococcus neoformans*. Infect Immun. 1998;66: 4994–5000.

275. Kawakami K, Qifeng X, Tohyama M, Qureshi MH, Saito a. Contribution of tumour

necrosis factor-alpha (TNF-alpha) in host defence mechanism against *Cryptococcus neoformans*. Clin Exp Immunol. 1996;106: 468–474.

276. Kawakami K, Qureshi MH, Zhang T, Koguchi Y, Shibuya K, Naoe S, et al. Interferon-gamma (IFN-γ)-dependent protection and synthesis of chemoattractants for mononuclear leucocytes caused by IL-12 in the lungs of mice infected with *Cryptococcus neoformans*. Clin Exp Immunol. 1999;117: 113–122. doi:10.1046/j.1365-2249.1999.00955.x
277. Zhang T, Kawakami K, Qureshi MH, Okamura H, Kurimoto M, Saito A. Interleukin-12 (IL-12) and IL-18 synergistically induce the fungicidal activity of murine peritoneal exudate cells against *Cryptococcus neoformans* through production of gamma interferon by natural killer cells. Infect Immun. 1997;65: 3594–9.
278. Arora S, Olszewski M a, Tsang TM, McDonald R a, Toews GB, Huffnagle GB. Effect of cytokine interplay on macrophage polarization during chronic pulmonary infection with *Cryptococcus neoformans*. Infect Immun. 2011;79: 1915–26. doi:10.1128/IAI.01270-10
279. Levitz SM, Tabuni A, Nong SH, Golenbock DT. Effects of interleukin-10 on human peripheral blood mononuclear cell responses to *Cryptococcus neoformans*, Candida albicans, and lipopolysaccharide. Infect Immun. 1996;64: 945–51.
280. Holmer SM, Evans KS, Asfaw YG, Saini D, Schell WA, Ledford JG, et al. Impact of surfactant protein D, interleukin-5, and eosinophilia on Cryptococcosis. Infect Immun.; 2014;82: 683–93. doi:10.1128/IAI.00855-13
281. Blackstock R, Murphy JW. Role of Interleukin-4 in Resistance to *Cryptococcus neoformans* Infection. Am J Respir Cell Mol Biol. American Thoracic Society; 2004;30: 109–117. doi:10.1165/rcmb.2003-0156OC
282. Koguchi Y, Kawakami K. Cryptococcal infection and Th1-Th2 cytokine balance. Int Rev Immunol. 21: 423–38.

283. Muller U, Stenzel W, Kohler G, Werner C, Polte T, Hansen G, et al. IL-13 induces disease-promoting type 2 cytokines, alternatively activated macrophages and allergic inflammation during pulmonary infection of mice with *Cryptococcus neoformans*. J Immunol. 2007;179: 5367–5377. doi:179/8/5367 [pii]

284. Hardison SE, Ravi S, Wozniak K, Young ML, Olszewski MA, Wormley F, et al. Pulmonary infection with an interferon-gamma-producing *Cryptococcus neoformans* strain results in classical macrophage activation and protection. Am J Pathol. 2010;176: 774–85. doi:10.2353/ajpath.2010.090634

285. Arora S, Olszewski MA, Tsang TM, McDonald RA, Toews GB, Huffnagle GB. Effect of cytokine interplay on macrophage polarization during chronic pulmonary infection with *Cryptococcus neoformans*. Infect Immun. 2011;79: 1915–1926. doi:10.1128/IAI.01270-10

286. Wozniak KL, Hardison SE, Kolls JK, Wormley FL. Role of IL-17A on Resolution of Pulmonary C. *neoformans* Infection. Unutmaz D, editor. PLoS One. 2011;6: e17204. doi:10.1371/journal.pone.0017204

287. Murdock BJ, Huffnagle GB, Olszewski MA, Osterholzer JJ. Interleukin-17A Enhances Host Defense against Cryptococcal Lung Infection through Effects Mediated by Leukocyte Recruitment, Activation, and Gamma Interferon Production. Infect Immun. 2014;82: 937–948. doi:10.1128/IAI.01477-13

288. Aguirre KM, Johnson LL. A role for B cells in resistance to *Cryptococcus neoformans* in mice. Infect Immun. 1997;65: 525–30.

289. Feldmesser M, Mednick A, Casadevall A. Antibody-mediated protection in murine *Cryptococcus neoformans* infection is associated with pleotrophic effects on cytokine and leukocyte responses. Infect Immun. 2002;70: 1571–1580. doi:10.1128/IAI.70.3.1571-1580.2002

290. Rivera J, Zaragoza O, Casadevall A. Antibody-mediated protection against

Cryptococcus neoformans pulmonary infection is dependent on B cells. Infect Immun. 2005;73: 1141–1150. doi:10.1128/IAI.73.2.1141-1150.2005

291. Rapaka RR, Ricks DM, Alcorn JF, Chen K, Khader SA, Zheng M, et al. Conserved natural IgM antibodies mediate innate and adaptive immunity against the opportunistic fungus *Pneumocystis murina*. J Exp Med. 2010;207: 2907–2919. doi:10.1084/jem.20100034
292. Subramaniam K, Metzger B, Hanau LH, Guh A, Rucker L, Badri S, et al. IgM+ Memory B Cell Expression Predicts HIV-Associated Cryptococcosis status. J Infect Dis. 2010;200: 244–251. doi:10.1086/599318.IgM
293. Fleuridor R, Lyles RH, Pirofski L. Quantitative and qualitative differences in the serum antibody profiles of human immunodeficiency virus-infected persons with and without *Cryptococcus neoformans* meningitis. J Infect Dis. 1999;180: 1526–35. doi:10.1086/315102
294. Day JN, Chau TTH, Wolbers M, Mai PP, Dung NT, Mai NH, et al. Combination antifungal therapy for cryptococcal meningitis. N Engl J Med. 2013;368: 1291–1302. doi:10.1056/NEJMoa1110404
295. Beardsley J, Wolbers M, Kibengo FM, Ggayi A-BM, Kamali A, Cuc NTK, et al. Adjunctive Dexamethasone in HIV-Associated Cryptococcal Meningitis. N Engl J Med. 2016;374: 542–554. doi:10.1056/NEJMoa1509024
296. Siddiqui AA, Brouwer AE, Wuthiekanun V, Jaffar S, Shattock R, Irving D, et al. IFN-gamma at the site of infection determines rate of clearance of infection in cryptococcal meningitis. J Immunol. 2005;174: 1746–1750. doi:10.4049/jimmunol.174.3.1746
297. Altfeld M, Addo MM, Kreuzer KA, Rockstroh JK, Dumoulin FL, Schliefer K, et al. T(H)1 to T(H)2 shift of cytokines in peripheral blood of HIV-infected patients is detectable by reverse transcriptase polymerase chain reaction but not by enzyme-

linked immunosorbent assay under nonstimulated conditions. J Acquir Immune Defic Syndr. 2000;23: 287–94.

298. Singh N, Alexander BD, Lortholary O, Dromer F, Gupta KL, John GT, et al. Pulmonary cryptococcosis in solid organ transplant recipients: clinical relevance of serum cryptococcal antigen. Clin Infect Dis. 2008;46: e12–e18. doi:10.1086/524738
299. Day J. Cryptococcal meningitis. Pract Neurol. 2004; doi:10.1093/bmb/ldh043
300. Fang W, Chen M, Liu J, Hagen F, MS A, Al-Hatmi, et al. Cryptococcal meningitis in systemic lupus erythematosus patients: pooled analysis and systematic review. Emerg Microbes Infect. 2016;5: e95. doi:10.1038/emi.2016.93
301. Chen S, Sorrell T, Nimmo G, Speed B, Currie B, Ellis D, et al. Epidemiology and Host- and Variety-Dependent Characteristics of Infection Due to *Cryptococcus neoformans* in Australia and New Zealand. Clin Infect Dis. 2000;31: 499–508. doi:10.1086/313992
302. Rozenbaum R, Gonçalves AJR. Clinical epidemiological study of 171 cases of cryptococcosis. Clin Infect Dis. 1994;18: 369–380. doi:10.1093/clinids/18.3.369
303. Sorrell TC. *Cryptococcus neoformans* variety *gattii*. Med Mycol. 2001;39: 155–68. doi:10.1080/714031012
304. Speed B, Dunt D. Clinical and host differences between infections with the two varieties of *Cryptococcus neoformans*. Clin Infect Dis. 1995;21: 28–34; discussion 35–6. doi:10.1093/clinids/21.1.28
305. Lalloo D, Fisher D, Naraqi S, Laurenson I, Temu P, Sinha A, et al. Cryptococcal meningitis (C. *Neoformans* var. *Gattii*) leading to blindness in previously healthy melanesian adults in Papua New Guinea. QJM. 1994;87: 343–349. doi:10.1093/oxfordjournals.qjmed.a068939
306. Rinaldi MG, Drutz DJ, Howell A, Sande MA, Wofsy CB, Keith Hadley W. Serotypes of *Cryptococcus neoformans* in Patients with AIDS. J Infect Dis. 1986;153: 642.

307. Chau TT, Mai NH, Phu NH, Nghia HD, Chuong L V, Sinh DX, et al. A prospective descriptive study of cryptococcal meningitis in HIV uninfected patients in Vietnam - high prevalence of *Cryptococcus neoformans* var. *grubii* in the absence of underlying disease. BMC Infect Dis. 2010;10: 199. doi:10.1186/1471-2334-10-199

308. Fang W, Fa Z, Liao W. Epidemiology of *Cryptococcus* and cryptococcosis in China. Fungal Genet Biol.; 2014; doi:10.1016/j.fgb.2014.10.017

309. Feng X, Yao Z, Ren D, Liao W, Wu J. Genotype and mating type analysis of *Cryptococcus neoformans* and *Cryptococcus gattii* isolates from China that mainly originated from non-HIV-infected patients. FEMS Yeast Res. 2008;8: 930–8. doi:10.1111/j.1567-1364.2008.00422.x

310. Li Z, Liu Y, Cao H, Huang S, Long M. Epidemiology and Clinical Characteristics of Cryptococcal Meningitis in China (1981-2013): A Review of the Literature. Med Mycol Open Access. 2017;3: 1–6. doi:10.4172/2471-8521.100022

311. Liu Y, Kang M, Wu S-Y, Ma Y, Chen Z-X, Xie Y, et al. Different characteristics of cryptococcal meningitis between HIV-infected and HIV-uninfected patients in the Southwest of China. Med Mycol. 2016;0: myw075. doi:10.1093/mmy/myw075

312. Chen M, Li XR, Wu SX, Tang XP, Feng BW, Yao ZR, et al. Molecular epidemiology of *Cryptococcus neoformans* species complex isolates from HIV-positive and HIV-negative patients in southeast China. Front Med China. 2010;4: 117–126. doi:10.1007/s11684-010-0011-z

313. Pappas PG. Cryptococcal infections in non-HIV-infected patients. Trans Am Clin Climatol Assoc. 2013;124: 61–79.

314. Ma H, May RC. Mitochondria and the regulation of hypervirulence in the fatal fungal outbreak on Vancouver Island. Virulence. 2010;1: 197–201.

315. Ma H, May R. Intracellular parasitism of *Cryptococcus neoformans*. School of Biosciences. University of Birmingham. 2009.

316. Ngamskulrungroj P, Price J, Sorrell T, Perfect JR, Meyer W. *Cryptococcus gattii* virulence composite: candidate genes revealed by microarray analysis of high and less virulent Vancouver island outbreak strains. PLoS One. 2011;6: e16076. doi:10.1371/journal.pone.0016076

317. Bovers M, Hagen F, Kuramae EE, Diaz MR, Spanjaard L, Dromer F, et al. Unique hybrids between the fungal pathogens *Cryptococcus neoformans* and *Cryptococcus gattii*. FEMS Yeast Res. 2006;6: 599–607. doi:10.1111/j.1567-1364.2006.00082.x

318. Bovers M, Hagen F, Kuramae EE, Hoogveld HL, Dromer F, St-Germain G, et al. AIDS patient death caused by novel *Cryptococcus neoformans* x C. *gattii* hybrid. Emerg Infect Dis. 2008;14: 1105–1108. doi:10.3201/eid1407.080122

319. Aminnejad M, Diaz M, Arabatzis M, Castañeda E, Lazera M, Velegraki A, et al. Identification of novel hybrids between *Cryptococcus neoformans* var. *grubii* VNI and *Cryptococcus gattii* VGII. Mycopathologia. 2012;173: 337–46. doi:10.1007/s11046-011-9491-x

320. Aminnejad M, Diaz M, Arabatzis M, Castañeda E, Lazera M, Velegraki A, et al. Identification of Novel Hybrids Between *Cryptococcus neoformans* var. *grubii* VNI and *Cryptococcus gattii* VGII. Mycopathologia. 2012;173: 337–346. doi:10.1007/s11046-011-9491-x

321. Souza CAD, Hagen ÆF, Boekhout ÆT, Cox GM, Heitman ÆJ, D'Souza C a, et al. Investigation of the basis of virulence in serotype A strains of *Cryptococcus neoformans* from apparently immunocompetent individuals. Curr Genet. 2004;46: 92–102. doi:10.1007/s00294-004-0511-y

322. Alspaugh JA, Perfect JR, Heitman J. *Cryptococcus neoformans* mating and virulence are regulated by the G-protein alpha subunit GPA1 and cAMP. Genes Dev. 1997;11: 3206–3217. doi:10.1101/gad.11.23.3206

323. Alspaugh JA, Pukkila-Worley R, Harashima T, Cavallo LM, Funnell D, Cox GM, et al.

Adenylyl cyclase functions downstream of the Galpha protein Gpa1 and controls mating and pathogenicity of *Cryptococcus neoformans*. Eukaryot Cell. 2002;1: 75–84. doi:10.1128/EC.1.1.75-84.2002

324. Kozubowski L, Heitman J. Profiling a killer, the development of *Cryptococcus neoformans*. FEMS Microbiol Rev. 2012;36: 78–94. doi:10.1111/j.1574-6976.2011.00286.x
325. Day JN, Qihui S, Thanh LT, Trieu PH, Van AD, Thu NH, et al. Comparative genomics of *Cryptococcus neoformans* var. *grubii* associated with meningitis in HIV infected and uninfected patients in Vietnam. Vinetz JM, editor. PLoS Negl Trop Dis. 2017;11: e0005628. doi:10.1371/journal.pntd.0005628
326. Boyce KJ, Wang Y, Verma S, Shakya VPS, Xue C, Idnurm A. Mismatch Repair of DNA Replication Errors Contributes to Microevolution in the Pathogenic Fungus *Cryptococcus neoformans*. MBio.; 2017;8. doi:10.1128/mBio.00595-17
327. Goodwin TJ, Poulter RT. The diversity of retrotransposons in the yeast *Cryptococcus neoformans*. Yeast. 2001;18: 865–80. doi:10.1002/yea.733
328. Goldman DL, Fries BC, Franzot SP, Montella L, Casadevall a. Phenotypic switching in the human pathogenic fungus *Cryptococcus neoformans* is associated with changes in virulence and pulmonary inflammatory response in rodents. Proc Natl Acad Sci U S A. 1998;95: 14967–14972. doi:10.1073/pnas.95.25.14967
329. Fries BC, Taborda CP, Serfass E, Casadevall a. Phenotypic switching of *Cryptococcus neoformans* occurs in vivo and influences the outcome of infection. J Clin Invest. 2001;108: 1639–1648. doi:10.1172/JCI200113407
330. Gupta G, Fries BC. Variability of phenotypic traits in *Cryptococcus* varieties and species and the resulting implications for pathogenesis. Futur Microbiol. 2011;5: 775–787. doi:10.2217/fmb.10.44.Variability
331. Alanio A, Desnos-Ollivier M, Dromer F. Dynamics of *Cryptococcus neoformans*-

Macrophage Interactions Reveal that Fungal Background Influences Outcome during Cryptococcal Meningoencephalitis in Humans. MBio. 2011;2: e00158–11–e00158–11. doi:10.1128/mBio.00158-11

332. Mitchell TG, Litvintseva AP. Pathogenic Yeasts. Ashbee R, Bignell EM, editors. Pathogenic Yeasts. Berlin, Heidelberg: Springer Berlin Heidelberg; 2010. doi:10.1007/978-3-642-03150-2

333. Pedroso RS, Lavrador MA, Ferreira JC, Candido RC, Maffei CM. *Cryptococcus neoformans* var. *grubii* - Pathogenicity of environmental isolates correlated to virulence factors, susceptibility to fluconazole and molecular profile. Mem Inst Oswaldo Cruz. 2010;105: 993–1000.

334. Liaw S-J, Wu H-C, Hsueh P-R. Microbiological characteristics of clinical isolates of *Cryptococcus neoformans* in Taiwan: serotypes, mating types, molecular types, virulence factors, and antifungal susceptibility. Clin Microbiol Infect. 2010;16: 696–703. doi:10.1111/j.1469-0691.2009.02930.x

335. Kumar P, Yang M, Haynes BC, Skowyra ML, Doering TL. Emerging themes in cryptococcal capsule synthesis. Curr Opin Struct Biol. 2011;21: 597–602. doi:10.1016/j.sbi.2011.08.006

336. Luberto C, Martinez-mariño B, Taraskiewicz D, Bolaños B, Chitano P, Toffaletti DL, et al. Identification of App1 as a regulator of phagocytosis and virulence of *Cryptococcus neoformans*. J Clin Invest. 2003;112: 1080–1094. doi:10.1172/JCI200318309.Introduction

337. Miglia KJ, Govender NP, Rossouw J, Meiring S, Mitchell TG, Group for Enteric, Respiratory and Meningeal Disease Surveillance in South Africa and the G for, et al. Analyses of pediatric isolates of *Cryptococcus neoformans* from South Africa. J Clin Microbiol.; 2011;49: 307–14. doi:10.1128/JCM.01277-10

338. Wiesner DL, Moskalenko O, Jennifer M, Corcoran JM, Mcdonald T, Rolfes MA, et al.

Cryptococcal Genotype Influences Immunologic Response and Human Clinical Outcome after Meningitis. MBio. 2012;3: 1–10. doi:10.1128/mBio.00196-12.Updated

339. Litvintseva AP, Mitchell TG. Most environmental isolates of *Cryptococcus neoformans* var. *grubii* (serotype A) are not lethal for mice. Infect Immun. 2009;77: 3188–95. doi:10.1128/IAI.00296-09

340. Casadevall A. Determinants of virulence in the pathogenic fungi. Fungal Biology Reviews. 2007. pp. 130–132. doi:10.1016/j.fbr.2007.02.007

341. Casadevall A, Pirofski L. Accidental virulence, cryptic pathogenesis, martians, lost hosts, and the pathogenicity of environmental microbes. Eukaryot Cell. 2007;6: 2169–74. doi:10.1128/EC.00308-07

342. Ngamskulrungroj P. A Non-HIV Specific ST5 Genotype of *Cryptococcus neoformans-gattii* Species Complex. Siriraj Med J. 2013;67: 301–305. doi:10.1111/head.12009

343. Meyer W, Castañeda A, Jackson S, Huynh M, Castañeda E, IberoAmerican Cryptococcal Study Group. Molecular typing of Ibero American *Cryptococcus neoformans* isolates. Emerg Infect Dis. 2003;9: 189–95. doi:10.3201/eid0902.020246

344. Lu G, Moriyama EN. Vector NTI, a balanced all-in-one sequence analysis suite. Brief Bioinform. 2004;5: 378–388. doi:10.1093/bib/5.4.378

345. Beale MA, Sabiiti W, Robertson EJ, Fuentes-Cabrejo KM, O'Hanlon SJ, Jarvis JN, et al. Genotypic diversity is associated with clinical outcome and phenotype in cryptococcal meningitis across Southern Africa. Vinetz JM, editor. PLoS Negl Trop Dis. Cambridge University Press; 2015;9: e0003847. doi:10.1371/journal.pntd.0003847

346. Tamura K, Stecher G, Peterson D, Filipski A, Kumar S. MEGA6: Molecular Evolutionary Genetics Analysis version 6.0. Mol Biol Evol. 2013;30: 2725–9.

doi:10.1093/molbev/mst197

347. Francisco AP, Vaz C, Monteiro PT, Melo-Cristino J, Ramirez M, Carriço JA. PHYLOViZ: phylogenetic inference and data visualization for sequence based typing methods. BMC Bioinformatics. 2012;13: 87. doi:10.1186/1471-2105-13-87
348. Nascimento M, Sousa A, Ramirez M, Francisco AP, Carriço JA, Vaz C. PHYLOViZ 2.0: providing scalable data integration and visualization for multiple phylogenetic inference methods. Bioinformatics. 2016; btw582. doi:10.1093/bioinformatics/btw582
349. Librado P, Rozas J. DnaSP v5: A software for comprehensive analysis of DNA polymorphism data. Bioinformatics. 2009;25: 1451–1452. doi:10.1093/bioinformatics/btp187
350. Day JN, Hoang TN, Duong A V, Hong CTT, Diep PT, Campbell JI, et al. Most cases of cryptococcal meningitis in HIV-uninfected patients in Vietnam are due to a distinct amplified fragment length polymorphism-defined cluster of *Cryptococcus neoformans* var. *grubii* VN1. J Clin Microbiol. 2011;49: 658–64. doi:10.1128/JCM.01985-10
351. Shen YZ, Qi TK, Ma JX, Jiang XY, Wang JR, Xu QN, et al. Invasive fungal infections among inpatients with acquired immune deficiency syndrome at a Chinese university hospital. Mycoses. 2007;50: 475–480. doi:10.1111/j.1439-0507.2007.01421.x
352. Tseng H-K, Liu C-P, Ho M-W, Lu P-L, Lo H-J, Lin Y-H, et al. Microbiological, epidemiological, and clinical characteristics and outcomes of patients with cryptococcosis in Taiwan, 1997-2010. PLoS One. 2013;8: e61921. doi:10.1371/journal.pone.0061921
353. Chan M, Lye D, Win MK, Chow A, Barkham T. Clinical and microbiological characteristics of cryptococcosis in Singapore: Predominance of *Cryptococcus*

neoformans compared with *Cryptococcus gattii*. Int J Infect Dis. 2014;26. doi:10.1016/j.ijid.2014.05.019

354. Tay ST, Rohani MY, Soo Hoo TS, Hamimah H. Epidemiology of cryptococcosis in Malaysia. Mycoses. 2010;53: 509–514. doi:10.1111/j.1439-0507.2009.01750.x
355. Pan W, Khayhan K, Hagen F, Wahyuningsih R, Chakrabarti A, Chowdhary A, et al. Resistance of Asian *Cryptococcus neoformans* serotype A is confined to few microsatellite genotypes. PLoS One. 2012;7: e32868. doi:10.1371/journal.pone.0032868
356. UNAIDS. HIV in Asia and the Pacific. UNAIDS. 2013; doi:10.1128/AAC.03728-14
357. Chen Y-H, Yu F, Bian Z-Y, Hong J-M, Zhang N, Zhong Q-S, et al. Multilocus Sequence Typing reveals both shared and unique genotypes of *Cryptococcus neoformans* in Jiangxi province, China. Sci Rep. Springer US; 2018;8: 1495. doi:10.1038/s41598-018-20054-4
358. Hughes AC. Understanding the drivers of Southeast Asian biodiversity loss. Ecosphere. 2017;8. doi:10.1002/ecs2.1624
359. Sodhi NS, Koh LP, Brook BW, Ng PKL. Southeast Asian biodiversity: An impending disaster. Trends in Ecology and Evolution. 2004. pp. 654–660. doi:10.1016/j.tree.2004.09.006
360. Rodríguez-Lado L, Sun G, Berg M, Zhang Q, Xue H, Zheng Q, et al. Groundwater arsenic contamination throughout China. Science. 2013;341: 866–8. doi:10.1126/science.1237484
361. Kim K-W, Chanpiwat P, Hanh HT, Phan K, Sthiannopkao S. Arsenic geochemistry of groundwater in Southeast Asia. Front Med. 2011;5: 420–433. doi:10.1007/s11684-011-0158-2
362. Tobin DM, Vary JC, Ray JP, Walsh GS, Dunstan SJ, Bang ND, et al. The lta4h locus modulates susceptibility to mycobacterial infection in zebrafish and humans. Cell.

2010;140: 717–30. doi:10.1016/j.cell.2010.02.013

363. Lu D, Xu S. Principal component analysis reveals the 1000 Genomes Project does not sufficiently cover the human genetic diversity in Asia. Front Genet. 2013;4. doi:10.3389/fgene.2013.00127

364. Sanchini A, Smith IMC, Sedlacek L, Schwarz R, Tintelnot K, Rickerts V. Molecular typing of clinical *Cryptococcus neoformans* isolates collected in Germany from 2004 to 2010. Med Microbiol Immunol. Springer Berlin Heidelberg; 2014;203: 333–340. doi:10.1007/s00430-014-0341-6

365. Bogaerts J, Rouvroy D, Taelman H, Kagame A, Aziz MA, Swinne D, et al. AIDS-associated cryptococcal meningitis in Rwanda (1983-1992): epidemiologic and diagnostic features. J Infect. 1999;39: 32–7. doi:10.1016/S0163-4453(99)90099-3

366. Litvintseva AP, Thakur R, Reller LB, Mitchell TG. Prevalence of clinical isolates of *Cryptococcus gattii* serotype C among patients with AIDS in Sub-Saharan Africa. J Infect Dis. 2005;192: 888–892. doi:10.1086/432486

367. Shih CC, Chen YC, Chang SC, Luh KT, Hsieh WC. Cryptococcal meningitis in non-HIV-infected patients. QJM. 2000;93: 245–251. doi:10.1093/qjmed/93.4.245

368. Mitchell DH, Sorrell TC, Allworth AM, Heath CH, McGregor AR, Papanaoum K, et al. Cryptococcal disease of the CNS in immunocompetent hosts: Influence of cryptococcal variety on clinical manifestations and outcome. Clin Infect Dis. 1995;20: 611–616. doi:10.1093/clinids/20.3.611

369. Chen S, Sorrell T, Nimmo G, Speed B, Currie B, Ellis D, et al. Epidemiology and Host- and Variety-Dependent Characteristics of Infection Due to *Cryptococcus neoformans* in Australia and New Zealand. Clin Infect Dis. 1996;31: 499–508. doi:10.1086/313992

370. Brandt ME, Pfaller MA, Hajjeh RA, Hamill RJ, Pappas PG, Reingold AL, et al. Trends in Antifungal Drug Susceptibility of *Cryptococcus neoformans* Isolates in the United

States : 1992 to 1994 and 1996 to 1998. 2001;45: 3065–3069. doi:10.1128/AAC.45.11.3065

371. Chaturvedi S, Rodeghier B, Fan J, McClelland CM, Wickes BL, Chaturvedi V. Direct PCR of *Cryptococcus neoformans* MATalpha and MATa pheromones to determine mating type, ploidy, and variety: a tool for epidemiological and molecular pathogenesis studies. J Clin Microbiol. 2000;38: 2007–9.
372. Lee A, Toffaletti DL, Tenor J, Soderblom EJ, Thompson JW, Moseley MA, et al. Survival defects of *Cryptococcus neoformans* mutants exposed to human cerebrospinal fluid result in attenuated virulence in an experimental model of meningitis. Infect Immun. 2010;78: 4213–25. doi:10.1128/IAI.00551-10
373. Idnurm A, Walton FJ, Floyd A, Reedy JL, Heitman J. Identification of ENA1 as a virulence gene of the human pathogenic fungus *Cryptococcus neoformans* through signature-tagged insertional mutagenesis. Eukaryot Cell. 2009;8: 315–26. doi:10.1128/EC.00375-08
374. Salas SD, Bennett JE, Kwon-Chung KJ, Perfect JR, Williamson PR. Effect of the laccase gene CNLAC1, on virulence of *Cryptococcus neoformans*. J Exp Med. 1996;184: 377–386. doi:10.1084/jem.184.2.377
375. Eisenman HC, Mues M, Weber SE, Frases S, Chaskes S, Gerfen G, et al. *Cryptococcus neoformans* laccase catalyses melanin synthesis from both D- and L-DOPA. Microbiology. 2007;153: 3954–3962. doi:10.1099/mic.0.2007/011049-0
376. Chen SC, Muller M, Zhou JZ, Wright LC, Sorrell TC. Phospholipase activity in *Cryptococcus neoformans*: a new virulence factor? J Infect Dis. 1997;175: 414–420. doi:10.1093/infdis/175.2.414
377. Zaragoza O, Casadevall A. Experimental modulation of capsule size in *Cryptococcus neoformans*. Biol Proced Online. BioMed Central; 2004;6: 10–15. doi:10.1251/bpo68

378. Levitz SM, Tabuni A, Nong SH, Golenbock DT. Effects of interleukin-10 on human peripheral blood mononuclear cell responses to *Cryptococcus neoformans*, Candida albicans, and lipopolysaccharide. Infect Immun. 1996;64: 945–51.

379. García-Rodas R, Casadevall A, Rodríguez-Tudela JL, Cuenca-Estrella M, Zaragoza O. *Cryptococcus neoformans* capsular enlargement and cellular gigantism during *Galleria mellonella* infection. PLoS One. 2011;6: e24485. doi:10.1371/journal.pone.0024485

380. Zaragoza O, Chrisman CJ, Castelli MV, Frases S, Cuenca-Estrella M, Rodríguez-Tudela JL, et al. Capsule enlargement in *Cryptococcus neoformans* confers resistance to oxidative stress suggesting a mechanism for intracellular survival. Cell Microbiol. 2008;10: 2043–2057. doi:10.1111/j.1462-5822.2008.01186.x

381. Vecchiarelli A, Pericolini E, Gabrielli E, Chow S-K, Bistoni F, Cenci E, et al. *Cryptococcus neoformans* galactoxylomannan is a potent negative immunomodulator, inspiring new approaches in anti-inflammatory immunotherapy. Immunotherapy. 2011;3: 997–1005. doi:10.2217/imt.11.86

382. McClelland EE, Bernhardt P, Casadevall A. Estimating the relative contributions of virulence factors for pathogenic microbes. Infect Immun. 2006;74: 1500–1504. doi:10.1128/IAI.74.3.1500-1504.2006

383. Zaragoza O, Alvarez M, Telzak A, Rivera J, Casadevall A. The relative susceptibility of mouse strains to pulmonary *Cryptococcus neoformans* infection is associated with pleiotropic differences in the immune response. Infect Immun. American Society for Microbiology; 2007;75: 2729–39. doi:10.1128/IAI.00094-07

384. Cheng P-Y, Sham A, Kronstad JW. *Cryptococcus gattii* isolates from the British Columbia cryptococcosis outbreak induce less protective inflammation in a murine model of infection than *Cryptococcus neoformans*. Infect Immun. 2009;77: 4284–94. doi:10.1128/IAI.00628-09

385. Sellers RS, Clifford CB, Treuting PM, Brayton C. Immunological Variation Between Inbred Laboratory Mouse Strains: Points to Consider in Phenotyping Genetically Immunomodified Mice. Vet Pathol. 2012;49: 32–43. doi:10.1177/0300985811429314

386. Lortholary O, Improvisi L, Rayhane N, Gray F, Fitting C, Cavaillon JM, et al. Cytokine Profiles of AIDS Patients Are Similar to Those of Mice with Disseminated *Cryptococcus neoformans*Infection. Infect Immun. 1999;67: 6314–20.

387. Verheul FM, Vaishnav V V, Cherniak R, Chaka W, Scharringa J, Verhoef JAN, et al. *Cryptococcus neoformans* and Cryptococcal Glucuronoxylomannan , Galactoxylomannan , and Mannoprotein Induce Different Levels of Tumor Necrosis Factor Alpha in Human Peripheral Blood Mononuclear Cells. 1997;65: 272–278.

388. Levitz SM, Tabuni A, Kornfeld H, Reardon CC, Golenbock DT. Production of Tumor Necrosis Factor Alpha in Human Leukocytes Stimulated by *Cryptococcus neoformans*. 1994;62: 1975–1981.

389. Gibson JF, Johnston SA. Immunity to *Cryptococcus neoformans* and C. *gattii* during cryptococcosis. Fungal Genet Biol.; 2015;78: 76–86. doi:10.1016/j.fgb.2014.11.006

390. Rohatgi S, Pirofski L-A. Host immunity to *Cryptococcus neoformans*. Future Microbiol. 2015;10: 565–81. doi:10.2217/fmb.14.132

391. Hole C, Wormley FL. Innate host defenses against *Cryptococcus neoformans*. Journal of Microbiology. 2016. pp. 202–211. doi:10.1007/s12275-016-5625-7

392. Coelho C, Bocca AL, Casadevall A. The intracellular life of *Cryptococcus neoformans*. Annu Rev Pathol. 2014;9: 219–38. doi:10.1146/annurev-pathol-012513-104653

393. Ma H, Croudace JE, Lammas D a, May RC. Direct cell-to-cell spread of a pathogenic yeast. BMC Immunol. 2007;8: 15. doi:10.1186/1471-2172-8-15

394. Diamond RD, Bennett JE. Growth of *Cryptococcus neoformans* within human macrophages in vitro. Infect Immun. 1973;7: 231–236.

395. Saha DC, Goldman DL, Shao X, Casadevall A, Husain S, Limaye AP, et al. Serologic evidence for reactivation of cryptococcosis in solid-organ transplant recipients. Clin Vaccine Immunol. 2007;14: 1550–1554. doi:10.1128/CVI.00242-07

396. Da Silva EG, Baroni FDA, Viani FC, Ruiz LDS, Gandra RF, Auler ME, et al. Virulence profile of strains of *Cryptococcus neoformans* var. *grubii* evaluated by experimental infection in BALB/c mice and correlation with exoenzyme activity. J Med Microbiol. 2006;55: 139–142. doi:10.1099/jmm.0.46206-0

397. Leys C, Ley C, Klein O, Bernard P, Licata L. Detecting outliers: Do not use standard deviation around the mean, use absolute deviation around the median. J Exp Soc Psychol. Academic Press; 2013;49: 764–766. doi:10.1016/J.JESP.2013.03.013

398. Voelz K, Johnston S a, Rutherford JC, May RC. Automated analysis of cryptococcal macrophage parasitism using GFP-tagged cryptococci. PLoS One. 2010;5: e15968. doi:10.1371/journal.pone.0015968

399. Bojarczuk A, Miller KA, Hotham R, Lewis A, Ogryzko N V., Kamuyango AA, et al. *Cryptococcus neoformans* Intracellular Proliferation and Capsule Size Determines Early Macrophage Control of Infection. Sci Rep. Nature Publishing Group; 2016;6: 21489. doi:10.1038/srep21489

400. Zaragoza O, Taborda CP, Casadevall A. The efficacy of complement-mediated phagocytosis of *Cryptococcus neoformans* is dependent on the location of C3 in the polysaccharide capsule and involves both direct and indirect C3-mediated interactions. Eur J Immunol. 2003;33: 1957–1967. doi:10.1002/eji.200323848

401. Schurch NJ, Schofield P, Gierliński M, Cole C, Sherstnev A, Singh V, et al. How many biological replicates are needed in an RNA-seq experiment and which differential expression tool should you use? RNA. 2016;22: 839–51. doi:10.1261/rna.053959.115

402. Kim D, Langmead B, Salzberg SL. HISAT: A fast spliced aligner with low memory

requirements. Nat Methods. Nature Publishing Group; 2015;12: 357–360. doi:10.1038/nmeth.3317

403. Li H, Handsaker B, Wysoker A, Fennell T, Ruan J, Homer N, et al. The Sequence Alignment/Map format and SAMtools. Bioinformatics. Oxford University Press; 2009;25: 2078–2079. doi:10.1093/bioinformatics/btp352
404. Liao Y, Smyth GK, Shi W. FeatureCounts: An efficient general purpose program for assigning sequence reads to genomic features. Bioinformatics. 2014;30: 923–930. doi:10.1093/bioinformatics/btt656
405. Love MI, Huber W, Anders S. Moderated estimation of fold change and dispersion for RNA-seq data with DESeq2. Genome Biol. BioMed Central; 2014;15: 550. doi:10.1186/s13059-014-0550-8
406. John D. Storey with contributions from Andrew J. Bass AD and DR. qvalue: Q-value estimation for false discovery rate control. 2015.
407. Ashburner M, Ball CA, Blake JA, Botstein D, Butler H, Cherry JM, et al. Gene ontology: Tool for the unification of biology. Nature Genetics. NIH Public Access; 2000. pp. 25–29. doi:10.1038/75556
408. Love MI, Huber W, Anders S. Moderated estimation of fold change and dispersion for RNA-seq data with DESeq2. Genome Biol. 2014;15. doi:10.1186/s13059-014-0550-8
409. Liu OW, Chun CD, Chow ED, Chen C, Madhani HD, Noble SM. Systematic genetic analysis of virulence in the human fungal pathogen *Cryptococcus neoformans*. Cell. 2008;135: 174–188. doi:10.1016/j.cell.2008.07.046.Systematic
410. Kronstad J, Jung WH, Hu G. Beyond the Big Three: Systematic Analysis of Virulence Factors in *Cryptococcus neoformans*. Cell Host Microbe. 2008;4: 308–310. doi:10.1016/j.chom.2008.09.003
411. Kelliher CM, Haase SB. Connecting virulence pathways to cell-cycle progression in

the fungal pathogen *Cryptococcus neoformans*. Current Genetics. 2017. pp. 803–811. doi:10.1007/s00294-017-0688-5

412. Fraser JA. Nitrogen Metabolite Repression of Metabolism and Virulence in the Human Fungal Pathogen *Cryptococcus neoformans*. 2011; doi:10.1534/genetics.111.128538
413. Fernandes JDS, Martho K, Tofik V, Vallim MA, Pascon RC. The Role of Amino Acid Permeases and Tryptophan Biosynthesis in *Cryptococcus neoformans* Survival. Bahn Y-S, editor. PLoS One. 2015;10: e0132369. doi:10.1371/journal.pone.0132369
414. Nazi I, Scott A, Sham A, Rossi L, Williamson PR, Kronstad JW, et al. Role of homoserine transacetylase as a new target for antifungal agents. Antimicrob Agents Chemother. 2007;51: 1731–1736. doi:10.1128/AAC.01400-06
415. Coelho C, Bocca AL, Casadevall A. The Tools for Virulence of *Cryptococcus neoformans*. 1st ed. Advances in Applied Microbiology.; 2014. doi:10.1016/B978-0-12-800261-2.00001-3
416. Liu OW, Chun CD, Chow ED, Chen C, Madhani HD, Noble SM. Systematic genetic analysis of virulence in the human fungal pathogen *Cryptococcus neoformans*. Cell. 2008;135: 174–88. doi:10.1016/j.cell.2008.07.046
417. Janbon G, Ormerod KL, Paulet D, Byrnes EJ, Yadav V, Chatterjee G, et al. Analysis of the genome and transcriptome of *Cryptococcus neoformans* var. *grubii* reveals complex RNA expression and microevolution leading to virulence attenuation. PLoS Genet. 2014;10: e1004261. doi:10.1371/journal.pgen.1004261
418. Jung K-W, Yang D-H, Maeng S, Lee K-T, So Y-S, Hong J, et al. Systematic functional profiling of transcription factor networks in *Cryptococcus neoformans*. Nat Commun. Nature Publishing Group; 2015;6: 6757. doi:10.1038/ncomms7757
419. MacPherson S, Larochelle M, Turcotte B. A fungal family of transcriptional regulators: the zinc cluster proteins. Microbiol Mol Biol Rev.; 2006;70: 583–604.

doi:10.1128/MMBR.00015-06

420. Lu J, Cao H, Zhang L, Huang P, Lin F. Systematic analysis of Zn2Cys6 transcription factors required for development and pathogenicity by high-throughput gene knockout in the rice blast fungus. PLoS Pathog. Public Library of Science; 2014;10: e1004432. doi:10.1371/journal.ppat.1004432
421. Zhang J. The potential of a new fungicide fludioxonil for stem-end rot and green mold control on Florida citrus fruit. Postharvest Biol Technol.; 2007;46: 262–270. doi:10.1016/j.postharvbio.2007.05.016
422. Desjardins C, Giamberardino C, Sykes S, Yu C-H, Tenor J, Chen Y, et al. Population Genomics And The Evolution Of Virulence In The Fungal Pathogen *Cryptococcus neoformans*. bioRxiv. 2017; 118323. doi:10.1101/gr.218727.116.Freely
423. Ding H, Mayer FL, Sánchez-León E, de S Araújo GR, Frases S, Kronstad JW. Networks of fibers and factors: regulation of capsule formation in *Cryptococcus neoformans*. F1000Research. 2016;5: 1786. doi:10.12688/f1000research.8854.1
424. Lee K-T, So Y-S, Yang D-H, Jung K-W, Choi J, Lee D-G, et al. Systematic functional analysis of kinases in the fungal pathogen *Cryptococcus neoformans*. Nat Commun. Nature Publishing Group; 2016;7: 12766. doi:10.1038/ncomms12766
425. Stolc V, Gauhar Z, Mason C, Halasz G, Van Batenburg MF, Rifkin SA, et al. A gene expression map for the euchromatic genome of Drosophila melanogaster. Science (80-). 2004;306: 655–660. doi:10.1126/science.1101312
426. Singer GAC, Lloyd AT, Huminiecki LB, Wolfe KH. Clusters of co-expressed genes in mammalian genomes are conserved by natural selection. Mol Biol Evol. 2005;22: 767–775. doi:10.1093/molbev/msi062
427. Lee JM, Sonnhammer ELL. Genomic gene clustering analysis of pathways in eukaryotes. Genome Res. 2003;13: 875–882. doi:10.1101/gr.737703
428. Zhang X, Smith TF. Yeast “operons”. Microb Comp Genomics. 1998;3: 133–40.

doi:10.1089/omi.1.1998.3.133

429. Cho RJ, Campbell MJ, Winzeler EA, Steinmetz L, Conway A, Wodicka L, et al. A genome-wide transcriptional analysis of the mitotic cell cycle. Mol Cell. 1998;2: 65–73. doi:10.1016/S1097-2765(00)80114-8

430. Panepinto J, Liu L, Ramos J, Zhu X, Valyi-Nagy T, Eksi S, et al. The DEAD-box RNA helicase Vad1 regulates multiple virulence-associated genes in *Cryptococcus neoformans*. J Clin Invest. 2005;115: 632–641. doi:10.1172/JCI200523048

431. Díaz Añel AM, Rossi MS, Espinosa JM, Güida C, Freitas FA, Kornblihtt AR, et al. mRNA encoding a putative RNA helicase of the DEAD-box gene family is up-regulated in trypomastigotes of Trypanosoma cruzi. J Eukaryot Microbiol. 2000;47: 555–560. doi:10.1111/j.1550-7408.2000.tb00089.x

432. Kozubowski L, Heitman J. Septins enforce morphogenetic events during sexual reproduction and contribute to virulence of *Cryptococcus neoformans*. Mol Microbiol. 2010;75: 658–675. doi:10.1111/j.1365-2958.2009.06983.x

433. Mercer TR, Dinger ME, Mattick JS. Long non-coding RNAs: Insights into functions. Nat Rev Genet. 2009;10: 155–159. doi:10.1038/nrg2521

434. Amaral PP, Mattick JS. Noncoding RNA in development. Mammalian Genome. 2008. pp. 454–492. doi:10.1007/s00335-008-9136-7

435. Luke B, Panza A, Redon S, Iglesias N, Li Z, Lingner J. The Rat1p 5′ to 3′ Exonuclease Degrades Telomeric Repeat-Containing RNA and Promotes Telomere Elongation in Saccharomyces cerevisiae. Mol Cell. 2008;32: 465–477. doi:10.1016/j.molcel.2008.10.019

436. Loewer S, Cabili MN, Guttman M, Loh YH, Thomas K, Park IH, et al. Large intergenic non-coding RNA-RoR modulates reprogramming of human induced pluripotent stem cells. Nat Genet. 2010;42: 1113–1117. doi:10.1038/ng.710

437. Cesana M, Cacchiarelli D, Legnini I, Santini T, Sthandier O, Chinappi M, et al. A long

noncoding RNA controls muscle differentiation by functioning as a competing endogenous RNA. Cell. 2011;147: 358–369. doi:10.1016/j.cell.2011.09.028

438. Arthanari Y, Heintzen C, Griffiths-Jones S, Crosthwaite SK. Natural antisense transcripts and long non-coding RNA in Neurospora crassa. PLoS One. 2014;9. doi:10.1371/journal.pone.0091353

439. Smith CA, Robertson D, Yates B, Nielsen DM, Brown D, Dean RA, et al. The effect of temperature on Natural Antisense Transcript (NAT) expression in Aspergillus flavus. Curr Genet. 2008;54: 241–269. doi:10.1007/s00294-008-0215-9

440. Chacko N, Zhao Y, Yang E, Wang L, Cai JJ, Lin X. The lncRNA RZE1 Controls Cryptococcal Morphological Transition. Butler G, editor. PLOS Genet. 2015;11: e1005692. doi:10.1371/journal.pgen.1005692

441. Holland SL, Reader T, Dyer PS, Avery S V. Phenotypic heterogeneity is a selected trait in natural yeast populations subject to environmental stress. Environ Microbiol. 2014;16: 1729–40. doi:10.1111/1462-2920.12243

442. Bódi Z, Farkas Z, Nevozhay D, Kalapis D, Lázár V, Csörgő B, et al. Phenotypic heterogeneity promotes adaptive evolution. PLoS Biol. 2017;15: e2000644. doi:10.1371/journal.pbio.2000644

443. Botts MR, Giles SS, Gates MA, Kozel TR, Hull CM. Isolation and characterization of *Cryptococcus neoformans* spores reveal a critical role for capsule biosynthesis genes in spore biogenesis. Eukaryot Cell. 2009;8: 595–605. doi:10.1128/EC.00352-08

444. Wozniak KL, Olszewski M a, Wormley FL. Molecules at the interface of *Cryptococcus* and the host that determine disease susceptibility. Fungal Genet Biol. 2014; 1–6. doi:10.1016/j.fgb.2014.10.013

445. Browne SK, Burbelo PD, Chetchotisakd P, Suputtamongkol Y, Kiertiburanakul S, Shaw P a, et al. Adult-onset Immunodeficiency in Thailand and Taiwan. N Engl J

Med. 2012;367: 725–734. doi:10.1056/NEJMoa1111160